C.1

PHYTOPLANKTON-ZOOPLANKTON INTERACTIONS : DATA ANALYSIS AND MODELLING (WITH PARTICULAR REFERENCE TO OCEAN STATION P (50°N, 145°W) AND CONTROLLED ECOSYSTEM EXPERIMENTS).

By

JOHN STANLEY PARSLOW

B.Sc., University of Queensland, 1974

A THESIS SUBMITTED IN PARTIAL FULFILMENT OF

THE REQUIREMENTS FOR THE DEGREE OF

DOCTOR OF PHILOSOPHY

in

THE FACULTY OF GRADUATE STUDIES

(DEPARTMENT OF MATHEMATICS)

We accept this thesis as conforming

to the required standard

THE UNIVERSITY OF BRITISH COLUMBIA

January 1981

In presenting this thesis in partial fulfilment of the requirements for an advanced degree at the University of British Columbia, I agree that the Library shall make it freely available for reference and study. I further agree that permission for extensive copying of this thesis for scholarly purposes may be granted by the head of my department or by his or her representatives. It is understood that copying or publication of this thesis for financial gain shall not be allowed without my written permission.

Department of MATHEMATICS

The University of British Columbia
2075 Wesbrook Place
Vancouver, Canada
V6T 1W5

Date 23rd. April, 1981.

ABSTRACT

The anomalous phytoplankton seasonal cycle in the Subarctic Pacific has been attributed to grazing control. In simple classical models of the phytoplankton-zooplankton interaction, grazing thresholds are found to be necessary to obtain this type of control. Weathership observations at O.S.P. are analysed to provide a basis for a more realistic model. Phytoplankton are present at O.S.P. in almost uniformly low concentrations (about 0.4 mg Chla.m^{-3}), have low photosynthetic efficiency (<0.5 mg C.mg $Chla^{-1}.ly^{-1}$), adapt to seasonal changes in solar radiation and show most surface inhibition in the spring. A numerical production model based on these results and driven by physical time series from the weatherships yields low annual production levels compared with previous estimates. Predicted production levels are sensitive to the choice of respiration rate, and introduction of a rapid light response or 'Marra' effect results in a doubling of net production. Predicted year to year variation is low and might be higher if variation in Secchi depth could be accounted for.

In a phytoplankton-zooplankton (biomass) model based on the production model, grazing thresholds and over-wintering strategies are both necessary for grazing control. Systems identification techniques are adapted to estimate population parameters for cohorts of the dominant grazers. Cohort structure is introduced into the phytoplankton-zooplankton model using these estimates. As a result, attention is shifted from the spring to late summer and fall where sensitivity and stability problems are associated with the over-wintering departure of the

dominant grazers.

An approximate mathematical analysis of Steele's (1974) nutrient-phytoplankton-zooplankton model allows the explanation and elaboration of previous authors' numerical results. Stable cyclic solutions are shown to exist under nutrient limitation for constant mortality rates in the absence of grazing thresholds. Attention is focused on the transient (spring bloom) approach to the nutrient-limited cycle and a broader (physiological and behavioural) framework for zooplankton response to declining food concentrations is proposed. Systems identification techniques are also used to estimate zooplankton feeding and growth parameters from CEPEX copepod time series. The estimates are compared with literature values and the statistical and deterministic limitations of the time series discussed with a mind to future experiments. A nutrient-phytoplankton-zooplankton model, based on the parameter estimates, provides a consistent explanation of the observed phytoplankton persistence at low densities as a stable nutrient-limited equilibrium.

A mathematical solution in terms of Bessel functions is found for phytoplankton populations undergoing diffusion and sinking in the case of an exponential growth profile. Non-dimensionalization allows a relatively complete discussion of the effects of varying physical and biological parameters on profiles and population growth rates. Subsurface maxima for constant diffusivity and sinking rate, previously reported for an idealised step-function growth profile, are also obtained for the exponential growth profile. Solutions to coupled non-linear phytoplankton-nutrient equations corresponding to subsurface

maxima of the nutrient-trap type are also obtained using boundary-layer techniques. The dependence of the depth, shape and magnitude of these maxima on parameters is explored. The approximate theory agrees well with previously published results from a complex simulation model.

CONTENTS

ABSTRACT ii

LIST OF TABLES ix

LIST OF FIGURES xi

ACKNOWLEDGEMENTS xxi

PREFACE xxii

CHAPTER 1. INTRODUCTION AND ANALYSIS OF SIMPLE GRAZING MODELS.

1.1 General Introduction. 1

1.2 Physical Oceanography of the Subarctic Pacific. 2

1.3 Biology of the Subarctic Pacific. 8

1.4 Simple Phytoplankton-Zooplankton Models for the Subarctic Pacific 14

1.5 Preview of Chapters 2-4. 33

CHAPTER 2. QUALITATIVE ANALYSIS OF A COMPLEX SIMULATION MODEL.

2.1 Introduction. 38

2.2 Model and Analysis 40

2.3 Simulation Results. 47

2.4 Conclusions. 59

CHAPTER 3. PHYTOPLANKTON AT O.S.P.: DATA ANALYSIS AND MODELLING.

3.1 Introduction. 68

3.2 Data Analysis. 68
3.2.1 Description of the Data Set. 68
3.2.2 Chlorophyll Data. 69
3.2.3 ^{14}C Data. 75
3.2.4 Nitrate Data 101
3.2.5 Nitrate Concentration and Production. 104
3.3 A Phytoplankton Growth Model. 111
3.3.1 Introduction. 111
3.3.2 Physical Structure and Driving Variables. 113
3.3.3 Biological Basis for the Model. 117
3.3.4 Simulation Results. 124
3.3.5 Primary Production and Nitrate Depletion. 148

CHAPTER 4. HERBIVOROUS ZOOPLANKTON AT O.S.P.: DATA ANALYSIS AND MODELLING.

4.1 Parameter Estimation. 150
4.1.1 Description of Data. 150
4.1.2 Review of Parameter Estimation Techniques. 151
4.1.3 Application to O.S.P. Data. 156
4.1.4 Statistical Considerations. 160
4.1.5 Results for Calanus plumchrus. 161
4.1.6 Results for Calanus cristatus. 168
4.1.7 Other Species 174
4.1.8 Secondary Production Estimates. 175
4.2 Biomass Model for Zooplankton. 180
4.2.1 Introduction. 180
4.2.2 Formulation of a Biomass Grazing Model 181
4.2.3 Choice of Zooplankton Parameters. 183

4.2.4 Simulation Results and Discussion. 187
4.3 A Cohort Model for Zooplankton. 198
4.3.1 Introduction. 198
4.3.2 Model Formulation. 200
4.3.3 Parameters. 201
4.3.4 Simulation Results and Discussion. 202
4.4 Conclusions. 224

CHAPTER 5. PARAMETER ESTIMATION AND STABILITY FOR A CEPEX ENCLOSURE.
5.1 Introduction 250
5.2 Estimation of Parameters in a Zooplankton Growth Model.253
5.3 Estimation Results. 261
5.4 Stability of the Phytoplankton-Zooplankton Interaction.298
5.5 Conclusions 303

CHAPTER 6. DIFFUSION, SINKING AND GROWTH OF PHYTOPLANKTON.
6.1 Introduction. 310
6.2 Review of a Simple Model. 312
6.3 A More Realistic Model. 321
6.4 Effect of a Mixed Layer. 327
6.5 A General Necessary Condition For Growth. 336
6.6 Discussion 337

CHAPTER 7. MATHEMATICAL ANALYSIS OF DEEP CHLOROPHYLL MAXIMA.
7.1 Introduction. 342
7.2 A Phytoplankton-Nutrient Model. 344

7.3 Effect of a Mixed Layer. 354

7.4 Effect of Nutrient Dependent Sinking Rates. 356

7.5 Discussion. 358

CHAPTER 8. CONCLUDING REMARKS. 373

BIBLIOGRAPHY. 377

LIST OF TABLES.

Table I. Parameters used in Steele's Model (2.1). 42

Table II. Predicted annual primary production at O.S.P., 1964 to 1976. 128

Table III. Monthly means of predicted daily net primary production at O.S.P. using three light adaptation time scales. 134

Table IV. Parameter estimates for Calanus plumchrus. 163

Table V. Parameter estimates for Calanus cristatus. 169

Table VI. Secondary production estimates. 179

Table VII. Average relative seasonal abundance of microzooplankton. 233

Table VIII. Final parameter estimates and SSQ errors for Pseudocalanus. 269

Table IX. Exponential growth rates for Calanus. 275

Table X. Final parameter estimates and SSQ errors for Calanus. 278

Table XI. Final parameter estimates and SSQ errors for *Paracalanus*. 291

LIST OF FIGURES.

Figure 1. Seasonal cycle in vertical structure at O.S.P. 5

Figure 2. Schematic diagram of surface currents and domains in the Subarctic Pacific. 6

Figure 3. Seasonal cycle in chlorophyll a at O.S.P. and Departure Bay, Strait of Georgia. 16

Figure 4. Seasonal cycle at O.S.P. in primary production and zooplankton standing stock. 17

Figure 5. Phase plane portraits for the system 1.2. 21

Figure 6. Type III functional responses. 28

Figure 7. Phase plane portraits for the system 1.6. 29

Figure 8. Phase plane portraits for the system 2.3. 45

Figure 9. Comparison of generation times from equation 2.4 and those obtained in numerical solutions of 2.2. 48

Figure 10. Stable cyclic solutions of the system 2.2 for GX=0.05 and (a) F=0.4. (b) F=0.2 49
(c) F=0.6 51

Figure 11. Behaviour of the system 2.1 for GX=0.05 and B=10. with: (a) F=0.4, D=100. (stable cycle) 52
(b) F=0.2, D=100. (unstable oscillations). (c) F=0.2, D=175. (stable cycle) 53

Figure 12. Simulation of spring and summer using the system 2.1 with: (a) B=10., F=0.4, D=100. and GX=0.05 58
(b) B=10., F=0.4, D=175. and GX=0.05 60
(c) B=10., F=0.4, D=175. and GX=0.04 61
(d) B=10., F=0.2, D=250., GX=0.05 and E=0.3 62

Figure 13. Surface observations of chlorophyll a from the weatherships at O.S.P. 70

Figure 14. Surface chlorophyll a (cruise medians, annual smooth, seasonal fit plus residuals) for:
(a) and (b) 1964-68 72
(c) and (d) 1969-76 73

Figure 15. Observations of Chl b/Chl a and Chl c/Chl a from the weatherships at O.S.P. 76

Figure 16. Surface Chl b/Chl a (cruise medians, annual smooth, seasonal fit plus residuals) 1969-76 77

Figure 17. Surface Chl c/Chl a (cruise medians, annual smooth, seasonal fit plus residuals) 1969-76 78

Figure 18. Surface observations of productivity per unit Chl a from the weatherships at O.S.P. 80

Figure 19. Frequency histograms for P(0). 81

Figure 20. P(0) (cruise medians, annual smooth, seasonal fit plus residuals) for: (a) and (b) 1964-68 82
(c) and (d) 1969-76 83

Figure 21. Scatter plot of P(0) vs I for 1964-68. 85

Figure 22. Scatter plot of $\hat{A}$ vs I for 1964-68. 91

Figure 23. Depth profiles of P. 92

Figure 24. Monthly averages of $\hat{\alpha}$. 94

Figure 25. Scatter plot of $\hat{B}$ vs I_o for 1964-68. 96

Figure 26. Scatter plot of P_{MAX} vs I_o for 1964-68. 98

Figure 27. Monthly averages of estimates of light adaptation parameters: (a) B 99
(b) B_s 100

Figure 28. Surface observations of nitrate concentration from the weatherships at O.S.P. 102

Figure 29. Surface nitrate concentrations (cruise medians, annual smooth, seasonal fit plus residuals) 103

Figure 30. Nitrate concentrations from depth profiles (layer averages, annual smooths, seasonal fits plus residuals) 105
(a) 0 - 20m 106
(b) 20 - 40m 107
(c) 40 - 80m 108
(d) 80 - 130m 109
(e) 130 - 200m 110

Figure 31. P(0) vs low surface nitrate values, May to October, 1964-68. 112

Figure 32. Time series of total solar radiation, surface temperature and mixed layer depth used to drive simulation model. 125

Figure 33. Predicted daily net production using standard parameter set. 127

Figure 34. Predicted net production, mixed layer Chl a and mixed layer C:Chl a ratio for 1976 using standard parameter set and seasonal light adaptation. 130

Figure 35. As for Fig 34, but with 'instantaneous' light adaptation. 131

Figure 36. As for Fig 34, but with 3-day adaptation. 133

Figure 37. Predicted C:Chl a ratio in the mixed layer for 1976 using α=0.5 and B =2.0. 136

Figure 38. Predicted daily net production on increasing ν to 0.1. 139

Figure 39. Predicted daily net production and mixed layer C:Chl a ratio for α=1.0, B =2.0 with constraint V≤100. ..140

Figure 40. Predicted daily net production for standard parameter set with Marra effect introduced. 142

Figure 41. Observed Secchi depths at O.S.P. vs time of year. 143

Figure 42. Predicted daily net production using standard parameter set and (a) upper envelope to Secchi depths. ...144
(b) lower envelope to Secchi depths. 145

Figure 43. Predicted seasonal cycle in mixed layer C:Chl a ratio using optimality criterion. 147

Figure 44. Projection of approximate 95% confidence regions for Calanus plumchrus parameter estimates on
(a) (θ, R^T) plane 164
(b) (γ, θ) plane 165

Figure 45. Projection of approximate 95% confidence regions for Calanus cristatus parameter estimates 171
on (a) (θ,R^T) plane 172
(b) (γ,θ) plane 173

Figure 46. Regression coefficients W_i vs corresponding lengths l_i on log-log scale. 177

Figure 47. Predicted mixed layer Chl a and herbivore biomass for 1976 using standard parameter set. 188

Figure 48. Effect of decreasing D on Fig 47. 191

Figure 49. Effect of introducing over-wintering strategy in Fig 47. 194

Figure 50. Effect of reducing spring recruitment to 25 mg $C.m^{-3}$ on Fig 49. 195

Figure 51. Predicted Chl a and grazer standing stock for biomass model with Type I functional response and spring recruitment. 199

Figure 52. Predicted Chl a and zooplankton biomass for 1976, using weight thresholds for departure in cohort model 203

Figure 53. As for Fig 52, but with fixed residence times

and lower growth and mortality rates for C. Cristatus. ..209

Figure 54. Effect of quadrupling spring recruitment in Fig 53. 211

Figure 55. Effect of halving spring recruitment in Fig 53. 213

Figure 56. Effect of increasing mortality rates for Calanus in Fig 53. 214

Figure 57. Effect of decreasing grazing parameters C0 and D in Fig 53. 216

Figure 58. Effect of increasing metabolic rates in Fig 57. 217

Figure 59. Predicted mixed layer Chl a and total zooplankton carbon for 1964-76, using the parameters and fixed recruitment levels of Fig 53. 219

Figure 60. Observed zooplankton wet weights (10 day means) at O.S.P. 1956-78. 221

Figure 61. Predicted mixed layer Chl a and zooplankton carbon for 1964-76 using coupled recruitment. 223

Figure 62. Average seasonal cycles in (a) observed

zooplankton wet weights (10 day means, 1956-78) 228
(b) ingestion variable V1 (10 day means, 1969-78) 229
(c) ingestion variable V2 (10 day means, 1969-78) 230

Figure 63. Annual variation (10 day means) in
(a) ingestion variable V1 237
(b) ingestion variable V2 238

Figure 64. Phytoplankton carbon (0-20m average) in CEE5 ..257

Figure 65. $\phi_J(W)$, $\psi_J(W)$ for W_J=0.4 μg C, W_{J+1} =2.0 μg C ...262

Figure 66. Functional response data for Pseusocalanus 264

Figure 67. Observed densities of Pseudocalanus in CEE5 ...266

Figure 68. Comparison of predictions and observations for
Pseudocalanus (a) trial 1 270
(b) trial 6 271

Figure 69. Observed densities of Calanus in CEE5. 276

Figure 70. Comparison of predictions and observations for
Calanus. (a) trial 1 279
(b) trial 4 281
(c) trial 6 283
(d) trial 7 284

Figure 71. Observed densities of Paracalanus in CEE5. ...288

Figure 72. Observed densities of total nauplii in CEE5 ...289

Figure 73. Comparison of predictions and observations for Paracalanus (a) trial 1 292
(b) trial 2 293
(c) trial 3 295
(d) trial 4 297

Figure 74. Predicted phytoplankton concentrations in CEE5 after day 30. 302

Figure 75. An illustration of the eigencondition 6.6. ...316

Figure 76. Contour plot of the function $\Lambda(\omega, \delta_g)$. 317

Figure 77. Characteristic profiles p(δ). 319

Figure 78. An illustration of the eigencondition 6.9. ...324

Figure 79. Contour plot of the function $\Lambda^1(\omega,\beta)$. 325

Figure 80. Characteristic phytoplankton profile for ω=0.7, β=20. 328

Figure 81. Contour plot of the function $\Lambda^3(\Omega,\xi)$ for (a) β=0. 332

(b) β=1. 333

(c) β=3. 334

(d) β=10. 335

Figure 82. Contour plot of S_T/β vs ω,β for δ=0.1. 359

Figure 83. Characteristic profiles P($\S$) vs $\S/\beta$. 361

Figure 84. Phytoplankton profiles P(φ) vs φ for θ=1. and θ=0.1 365

Figure 85. Contour plots of $\varphi_T - \varphi_c$ vs β^*,ω^* for δ^*=0.1 and θ=1. and 0.1 366

Figure 86. Contour plots of φ_T vs β^*,ω^* for w_1=w and w_1=5.w 368

Figure 87. Comparison of phytoplankton profiles predicted by complex simulation model and by asymptotic analysis. ..372

ACKNOWLEDGEMENTS

I would like to acknowledge the encouragement, support and advice of my thesis supervisor, Dr T.R.Parsons, and also the other members of my thesis committee for helpful discussions. I have to thank Mr J.D.Fulton and Mr O.D.Kennedy of the Pacific Biological station, Nanaimo, for kindly providing much of the raw data used in this study and assisting in its interpretation. The study of parameter estimation owes much to an initial, stimulating collaboration with Dr J.B.L.Matthews and Mr N.C.Sonntag. My studies in Canada were supported by a post-graduate studentship from CSIRO, Australia.

PREFACE

Ecology has been variously called a soft science, an immature science, or even a pre-science (Kuhn,1970) by comparison with the classical fields of physics and chemistry. The latter disciplines have acquired a theoretical core which is rigorously (and usually mathematically) formulated. A mathematician working in these fields is essentially concerned with deducing the implications of this theory according to the principles of mathematics and logic. He can, for the most part, face this task without nervous backward glances to see if the theory has just changed.

This is not to say that the 'real world' does not intrude upon him. The mathematical problem usually corresponds to a question about the real system involving experiment and/or observation. Moreover, in many interesting cases, an exact general solution to the appropriate mathematical problem cannot be found and the derivation of an approximate, tractable problem is necessary (applied mathematics has been called in part 'the art of judicious approximation' (Greenspan,1969)). It is this procedure which demands of successful applied mathematicians a familiarity with the science, or 'physical intuition', as well as technical mathematical ability.

A soft science such as ecology is distinguished by its lack of an accepted theoretical core. For any particular real system, there is no universally accepted, mathematically formulated model. An applied mathematician venturing into such a field has two choices. He can take a previously published model and analyze its mathematical properties, paying little attention to

the (sensitive) issue of its biological accuracy. A theory can develop which is increasingly divorced from reality. There is a large body of ecological theory, often of considerable mathematical elegance, concerning traditional idealised models which do not correspond in detail to any real system. This theory can be useful in the study of a particular, real system (it is used in this thesis), but the gap between theory and reality may overwhelm the field biologist lacking formal mathematical training.

The mathematician's alternative is to plunge into the biological controversy and become a modeller; that is, someone who formulates his own mathematical version of reality. While familiarity with the biological science is a prerequisite for modelling, sophisticated mathematical ability is not. With the advent of the computer, very large, complex simulation models can be constructed and studied with little advanced mathematics. One might wonder then if biologists, who presumably have more familiarity with their science, need applied mathematicians at all.

The answer to this question is yes, for the same reason that computers have not eliminated all mathematicians except numerical analysts in the physical sciences. A simulation model is a clumsy tool which produces a particular outcome for a specific set of parameter values. Particularly in the case of complicated simulation models, involving many parameters and interactions, the usual consideration of a small number of simulations (sensitivity analysis) can give a very misleading picture of the model's properties. It is the task of the applied mathematician

to uncover the general dependence of a model's behaviour on both parameter values and the assumptions which are implicit in its mathematical structure. This is especially important in a field such as ecology, where uncertainty regarding both parameter values and the appropriate model structure is very high. As in the physical sciences, exact general solutions to model equations are not usually available and techniques of approximation and qualitative analysis are important.

Some of the sections of this thesis involve the analysis of simulation models constructed by others (Chapter 2), or of simple idealised models (Chapters 1,6,7). Others involve the formulation and analysis of original models with considerable new biological input (Chapter 4). In each case, a clear picture has been sought of the relationship between the model's mathematical output (behaviour) and input (structure and parameter values), both interpreted biologically.

In an interesting discussion of the notion of intelligence, Weizenbaum(1976) observes that being given a blueprint of the human mind, or of a complex computer system, which allowed us to construct an exact, working copy, would not be at all the same thing as understanding the human mind or the computer. The concept of 'understanding' is a difficult one to define rigorously and may be a highly personal one. I share Weizenbaum's notion of understanding sufficiently to agree with his statement and would make the same point about complex simulation models in ecology : an ability to construct a large, complicated model from component pieces and even to have it mimic the natural system perfectly (an unlikely event) is not the same

thing as an understanding of the ecosystem. I find that the qualitative, approximate analyses described above and carried out in this thesis, by uncovering relationships between assumptions and predictions at a simple, often graphical level, provide that sense of understanding which a complex simulation model lacks.

In addition to the construction and analysis of models, a number of types of data analysis are presented in this thesis. These range from relatively conventional descriptive techniques to the rather ambitious model-fitting procedures of Chapter 5. All techniques of data analysis are based on an underlying statistical model. In many of the classical techniques, the underlying model was kept deliberately simple, usually linear, to facilitate the computation of parameter estimates and the analysis of their statistical properties. The development of computers and numerical model-fitting algorithms (Benson,1978) now offers the possibility of estimating biologically meaningful parameters in more complex models from observations on complicated natural or experimental systems. Much of the data analysis in this thesis represents an exploration of the potential of this approach.

CHAPTER 1

INTRODUCTION AND ANALYSIS OF SIMPLE GRAZING MODELS.

1.1 General Introduction.

The problems discussed in this thesis have all arisen out of an initial interest in the marine planktonic ecosystem of the Subarctic Pacific. The general introduction given in this section is intended as a brief survey of the problems treated and their interrelationships. A detailed introduction to the physical and biological oceanography of the Subarctic Pacific is given in Sections 1.2 and 1.3 respectively. Comprehensive introductions to the derived problems are left to the corresponding chapters.

At the time this study commenced, in 1976, modelling of seasonal cycles in planktonic nutrient-plant-herbivore systems, particularly the phenomena of spring and fall phytoplankton blooms, was well established. Against this background of empirical knowledge and theoretical understanding, the observed seasonal cycle in the Subarctic Pacific, showing little or no variation in phytoplankton standing stock, stood out as an anomaly. A number of simple verbal hypotheses had been proposed to account for this cycle (McAllister et al,1960; Heinrich,1962) and the time seemed ripe for a more rigorous examination of the problem via modelling, especially in view of the existence of a long time series of biological observations from the weatherships at Ocean Station "P" (henceforth abbreviated O.S.P.) at 50°N, 145°W in the Subarctic Pacific.

Preliminary considerations, using some classical population-

interaction models (Chapter 1) suggested that grazing thresholds could be important at O.S.P. This result prompted an approximate qualitative analysis of a complex numerical model (Steele,1974; Landry,1976) whose behaviour in computer simulation had provoked some discussion of thresholds. The insights obtained from this analysis proved useful in a more quantitative, detailed modelling investigation of ecosystem dynamics at O.S.P. (Chapters 3,4). Analysis of the time series of biological observations from the weatherships, conducted as part of this investigation, involved some novel statistical problems, including the adaptation of a systems identification technique for estimating population parameters from zooplankton time series (Parslow et al ,1979) (Chapter 4) to overcome inconsistencies in the zooplankton time series from O.S.P. A variant of the parameter estimation technique was applied to phytoplankton and zooplankton time series from a controlled ecosystem enclosure studied during the CEPEX programme (Chapter 5), in an attempt to estimate functional response parameters relevant to biological questions which arose in the theoretical analysis of chapter two.

Chapters 6 and 7 involve a theoretical analysis of phytoplankton populations undergoing growth, diffusion, sinking and nutrient limitation. While originally motivated by consideration of light-limited growth at O.S.P. , the results proved to be of more interest in cases of low-turbulence environments and sub-surface chlorophyll maxima.

1.2 Physical Oceanography of the Subarctic Pacific.

This introduction to the physical oceanography of the

Subarctic Pacific is intended as background to the ecological models considered later. Two aspects are considered here. The seasonal cycle in water column structure at O.S.P. is important in the modelling of primary production there. The location of O.S.P. relative to the broad circulation patterns of the Subarctic Pacific is discussed in an assessment of horizontal advective effects on biological processes.

The weatherships' observations of temperature and salinity profiles, as well as meteorological variables, have provided a basis for a number of theoretical and empirical studies of seasonal cycles at O.S.P. , particularly the heat budget associated with formation and breakdown of the seasonal thermocline (Tabata,1965; Denman,1972). This cycle will be presented quantitatively with a model of primary production at O.S.P. in Chapter 3; a brief description is given here.

On the basis of salinity, Dodimead et al (1963) distinguish three permanent zones : an upper zone from 0 to 100m, a halocline from 100 to 200m in which salinity increases from 32.8‰ to 33.8‰, and a lower zone, in which salinity increases slowly to 34.4‰ at 1000m. The top of the halocline corresponds to the maximum depth of the surface mixed layer, attained in March at the end of the period of net heat loss through the surface. A seasonal thermocline is established over the period of net heat gain, from April to September, with the mixed layer being typically about 30m deep at the end of this period. Surface temperatures increase from about 5°C to 13°C over this period. The seasonal thermocline and an associated seasonal halocline are eroded over the cooling period, from October to March, by convective overturn

and storm activity. This seasonal cycle (Fig 1) is qualitatively characteristic of the oceanic Subarctic Pacific although there is some geographical variation in the magnitude and timing of the cycle.

Two reviews of the physical oceanography of the Subarctic Pacific have been published as part of investigations into the ocean environment of salmon by the International North Pacific Fisheries Commission (Dodimead et al ,1963; Favorite et al ,1976). In the earlier review, the principal current systems and domains were summarized as in Fig 2. The southern limit of the Subarctic region was defined by an almost vertical isohaline surface of 34‰ at about 42°N latitude. Immediately to the north a body of warmer water formed by mixing of the Kuroshio and Oyashio currents and moving eastward at 2 to 4 nautical miles/day was identified as the transition domain. To the north again, the Subarctic current was described as moving east at about 2 nautical miles/day and consisting of that part of the Oyashio which does not mix with the Kuroshio. These eastward flowing currents divide off the coast of North America, part travelling south to form the California current and part flowing northward around the Gulf of Alaska, forming a relatively intense boundary current (the Alaskan Steam). Part of the Alaskan Stream turns south to form the Alaskan Gyre, while part moves north into the Bering Sea to eventually join the East Kamchatka current or the Oyashio. The circulation time for the entire system is given as about 4-6 years.

O.S.P. is located north of the transition zone, on the south-easterly edge of the Alaskan Gyre. The following quote is

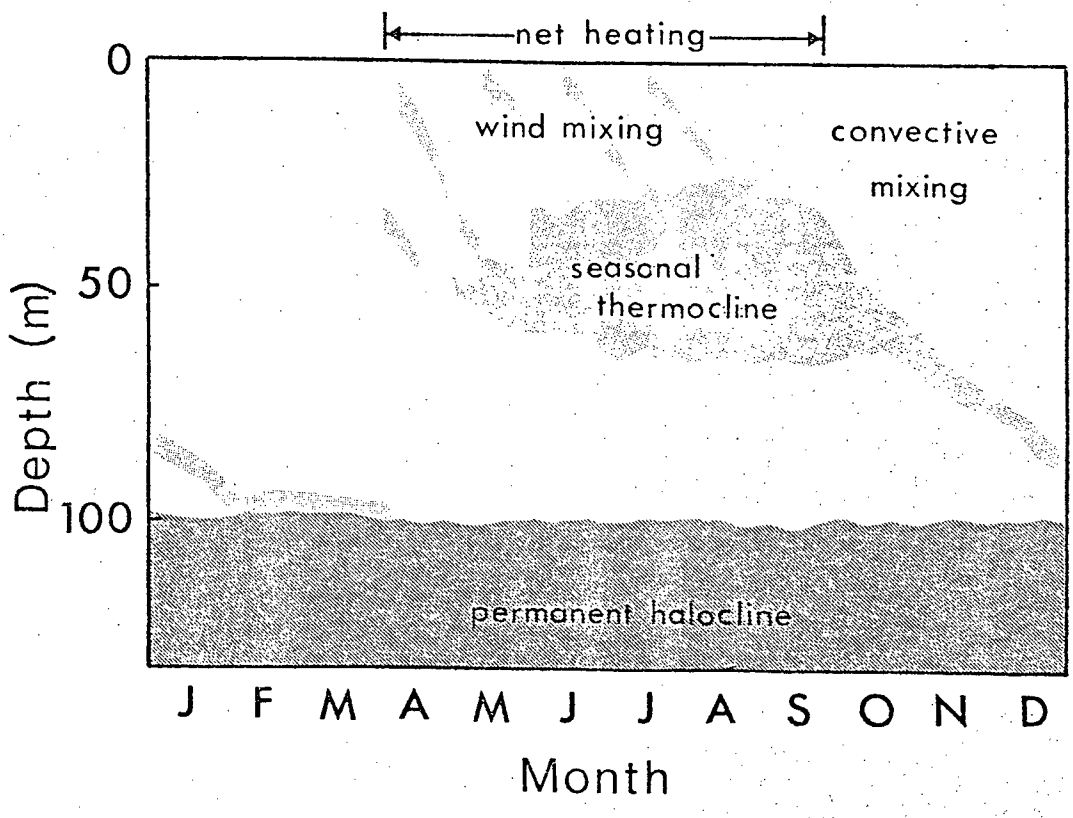

Figure 1. Seasonal cycle in vertical structure at O.S.P. (Adapted from Tabata, 1965).

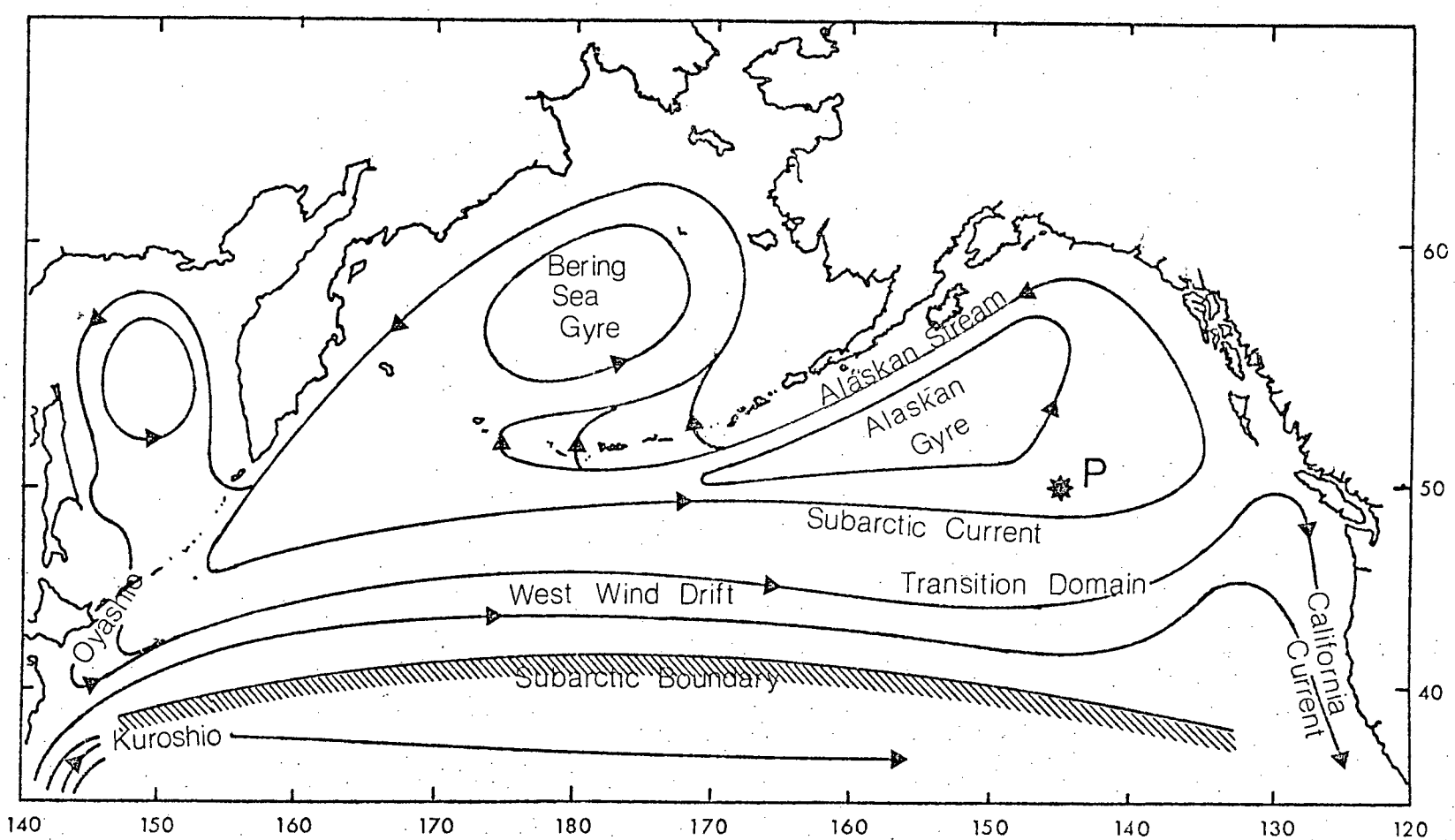

Figure 2. Schematic diagram of surface currents and domains in the Subarctic Pacific. (Adapted from Dodimead et al, 1963.)

particularly relevant for modelling the planktonic ecosystem at O.S.P. although it was prompted by considerations of seasonal salinity and temperature cycles there :

'. . . the geostrophic flow in the vicinity of Ocean Station "P" is generally zonal, but, more importantly, slow (2 miles/day). Hence, within the time period considered here, ' (seasonal) ' the waters in the area are subjected to climatic conditions similar to those at Ocean Station "P"; thus, they can be regarded as having resided there. . . ' (Dodimead et al ,1963).

The second review (Favorite et al ,1976) presents a similar pattern for the general circulation, with further elaboration of the current and domain structures. There is, however, a new feature presented which may affect biological modelling and data-interpretation for O.S.P. The dynamic topography for July shows a small clockwise gyre in the surface circulation off the Queen Charlotte Islands, east of the north-south branching of the Subarctic Current. Associated with this gyre is a 'Dilute Domain' of water showing the effects of coastal runoff. The review is ambiguous as to the westward extent of this domain . Circulation patterns suggested by dynamic topography, integrated total wind-stress transport and numerical model results all indicate that the coastal gyre lies well to the east of O.S.P. and that the flow at O.S.P. is essentially as described above from the earlier review. However, the Dilute Domain defined on the basis of the 33‰ isohaline contour at 100m extends westward to almost 160°W and includes O.S.P. In Fig 41 of Favorite et al (1976), the Subarctic Current is portrayed as dividing to the

west of the Dilute Domain and O.S.P.

The Dilute Domain is dilute by comparison with the higher salinity waters of the Ridge Domain to the northwest (due to upwelling in the Alaskan Gyre), the coastal upwelling domains to the southeast and the transition domain to the south. It is not clear to what extent the lower salinity at O.S.P. may be due to the annual excess of precipitation over evaporation which occurs throughout the eastern Subarctic (Dodimead et al,1963), superimposed on a zonal flow. If the flow through O.S.P. is predominantly zonal and part of the eastward-flowing Subarctic current, then as indicated by the quote above, a model of seasonal changes either in the physical structure of the water column or in the planktonic community may reasonably be constructed without taking large-scale horizontal advection into account. The models presented in this thesis have been created on this basis. If O.S.P. really lies within a small-scale coastal circulation, which seems unlikely for reasons cited above and others (for example, the nitrate seasonal cycle at O.S.P. is characteristic of Subarctic oceanic rather than coastal waters), a more explicit treatment of advective effects may be required.

1.3 Biology of the Subarctic Pacific.

A very considerable literature exists on the biology of the Subarctic Pacific and this brief survey makes no pretence at an exhaustive review. The following information is presented partly as an introduction to the questions addressed here using a modelling approach. It is also intended partly as an overview of the current state of biological knowledge, so that a reader

unfamiliar with this literature can place the models considered here, with their necessary limitations and rather narrow focus, in broader perspective. Much of the review will be concerned with studies at O.S.P. which is by far the most intensively sampled ocean station in the region. Relevant information from surrounding areas will be mentioned where appropriate.

Probably the best-known feature of the planktonic ecosystem in the sub-Arctic Pacific is the absence of a spring increase in phytoplankton abundance. This was reported for the Bering Sea over 20 years ago (Semina,1958), and confirmed by the weathership observations at O.S.P. (Parsons,1965). During a cruise in July and August of 1959, macronutrients (nitrate, silicate, phosphate), phytoplankton (chlorophyll a) and particulate organic carbon were measured (McAllister et al ,1960). Nutrient levels were consistently high (>6 $\mu gat.l^{-1}$ NO_3^-, >16 $\mu gat.l^{-1}$ SiO_2, >1.2 $\mu gat.l^{-1}$ PO_4^{3-}), at a time of year when nutrient depletion might normally be expected. This observation, together with the observed exponential increase of phytoplankton in batch culture to some 40 times the initial concentration once grazers were removed, supported the argument, advanced by Semina (1960), that zooplankton grazing is responsible for the constancy of phytoplankton concentration in the Subarctic. The seasonal cycle in the Subarctic Pacific was contrasted with the 'spring bloom' cycles of coastal areas and the North Atlantic by Heinrich (1962). He attributed the difference to the life history strategies of the dominant herbivorous copepods, Calanus plumchrus and Calanus cristatus, in the Subarctic Pacific.

A preliminary picture of zooplankton abundance, composition

and vertical distribution at O.S.P. was given by McAllister (1961), based on surface trawls and vertical hauls made from the weatherships from 1956 to 1958. He described a winter minimum in zooplankton biomass from December to March and a summer maximum from April to July. Surface trawls were dominated by copepods in April and May and by amphipods in June and July and in November and December. Vertical hauls (150m to surface) were predominantly copepods (ca 75%) and chaetognaths (15%) at all times. Two layers of maximum abundance of zooplankton were found, above and below the permanent halocline. Zooplankton wet weight in the top 150m ranged from ca 10 $mg.m^{-3}$ in winter to 80 $mg.m^{-3}$ in May, 1957.

Perhaps the single most comprehensive study of the biology of the Subarctic Pacific to date is that of LeBrasseur (1969). This study of predator-prey relationships in the Gulf of Alaska included a detailed analysis of nine years (1956-64) of zooplankton data from O.S.P. The life histories of the dominant zooplankton species were discussed, based on average seasonal patterns of abundance by stage as reflected in vertical hauls and surface tows. Next to the two species mentioned above, a third large herbivorous copepod, Eucalanus bungi, makes a significant contribution to biomass, as noted for other locations in the Subarctic Pacific (Heinrich,1962; Sekiguchi,1975). Smaller copepods (Pseudocalanus, Calanus pacificus, Metridia pacifica) are important in fall and winter. A mixed collection of planktonic primary carnivores, including chaetognaths (Sagitta elegans, Eukrohnia hamata) and the trachymedusa Aglantha digitale were also discussed. An attempt was made to estimate the

standing stocks of forage organisms (myctophid and squid) and the annual carbon flux through a simplified food web leading up to the tertiary consumers (salmon, baleen whales and pomfret).

Due to the nature of the sampling program at O.S.P. , much more is known of the herbivorous and carnivorous zooplankton than of the trophic levels above or below. For example, the population dynamics of squid, an important primary/secondary carnivore, are virtually unknown. The seasonal pattern in species composition of phytoplankton at O.S.P. is also comparatively poorly known. Weathership phytoplankton samples have not yet been analysed quantitatively. Information on abundance of net phytoplankton is available from the ships of opportunity program (Venrick,1971) and from weathership micro-zooplankton data (discussed later). Observations at O.S.P. in July, August, 1959 (McAllister et al,1960), during the Transpac cruise of 1969 (Parsons,1972) and preliminary analysis of Line P stations (R. Waters, pers. comm.) suggest that phytoplankton are dominated in biomass by small flagellates, less than 10 μm in diameter.

There have been a number of theoretical analyses of primary and secondary production at O.S.P. or in its vicinity. The seasonal cycle of chlorophyll a and primary production at O.S.P. (based on ^{14}C uptake measurements) was described by Parsons (1965). In that paper, Sverdrup's critical depth model (Sverdrup,1953) was used to explore the interaction of secchi depth, mixed layer depth and surface irradiance. All macro-nutrients were described as non-limiting throughout the Gulf of Alaska and an annual primary production of ca 60 g $C.m^{-2}$ was

estimated, based on ^{14}C measurements and the seasonal decrease in nitrate and phosphate. The critical depth approach was later expanded to cover the full Gulf of Alaska by Parsons and LeBrasseur (1968). The large-scale pattern in the timing of the spring increase in zooplankton standing stock was predicted in this study.

Results of primary production studies on the Transpac cruise and a ships of opportunity program conducted from American Mail Line cruises between Seattle and Yokohama were reported by Parsons and Anderson (1970). A depth-integrated form of Steele and Menzel's (1962) equation was found to overestimate production on the Transpac cruise. Reducing the photosynthetic efficiency parameter from 0.24 to 0.17 ($\mu g\ C.\mu g\ Chl\ a^{-1}.ly^{-1}$) in this equation provided a better fit for the Transpac data, but values ranging from 0.07 to 3.1 ($\mu g\ C.\mu g\ Chl\ a^{-1}.ly^{-1}$) were necessary to obtain agreement with data from the AML cruises.

The conversion of primary production to secondary production at O.S.P. has been studied by McAllister (1969,1972). Daily phytoplankton production (estimated from ^{14}C measurements), minus estimated dark respiration, was assumed to be ingested by zooplankton. Zooplankton respiration was calculated as a fraction of zooplankton standing stock. Assimilated ration minus respiration was taken as secondary production. Because of uncertainty in zooplankton respiration rates (eg Steele,1974), estimates of secondary production represented the difference of two large, uncertain quantities and ranged from negative values to a maximum of 23g $C.m^{-2}.yr^{-1}$. An estimate of 13 g $C.m^{-2}.yr^{-1}$ was chosen as most likely.

For the purposes of this thesis, an interesting summary of the current state of biological knowledge for this location can be obtained by assessing its strengths and weaknesses as a basis for a detailed, rational mechanistic model (Platt et al ,1975) of the ecosystem there. Whether a model of this kind is a desirable goal, particularly if we wish to make successful quantitative predictions, is debatable (Platt et al ,1975), but it does provide a useful way to structure an approach to existing data.

There is a long time series of observations of chlorophyll a, ^{14}C productivity and macronutrients at O.S.P. However, for a model of phytoplankton dynamics, a knowledge of variations in phytoplankton carbon and carbon:chlorophyll ratios, in the photosynthesis vs light relationship (on short and long time scales), in phytoplankton respiration rates and in limiting effects of micronutrients, if any, would all be desirable. An attempt will be made to infer some of these indirectly from the available observations in Chapter 3. Investigation of size and/or species dependent effects in biological interactions would require observations at a comparable level of detail.

The long time series of 150m vertical hauls is the principal zooplankton data source, providing information on total wet weight, species composition and some stage and/or size structure. These data are supported by studies on seasonal and diurnal patterns of vertical migration (Vinogradov,1968; Frost and McCrone,1974; Sekiguchi,1975; Marlowe and Miller,1975). Some measurements have been made of grazing rates, chemical composition and respiration of the dominant herbivores primarily in coastal locations far from O.S.P. (Parsons et al ,1969;

Ikeda,1972; Taguchi and Ishii,1972; Fulton,1973; Ikeda,1977). However, information on the functional and numerical responses of these dominant copepods is poor compared with better studied coastal species such as Calanus pacificus (Paffenhoffer,1970; Frost,1972,1975) or Pseudocalanus (Paffenhoffer and Harris,1976). The average seasonal pattern of microzooplankton (retained by 44 μm mesh) at O.S.P. has been reported (LeBrasseur and Kennedy,1972), but the autecology of most of these organisms is very poorly known. A similar state of ignorance exists for most of the primary carnivores mentioned above, while even the abundance of forage organisms such as squid is poorly known. The study of forage organisms is complicated by their very large diurnal and seasonal migrations and long (multi-year) generation times. For such long-lived organisms, and of course for wide-ranging predators such as whales, salmon and pomfret, a model of conditions at O.S.P. becomes meaningless and the large-scale variability and circulation of the Subarctic Pacific would have to be modelled.

1.4 Simple Phytoplankton-Zooplankton Models for the Subarctic Pacific.

As the summary of Section 1.3 demonstates, an attempt to construct a detailed, complete ecosystem model for O.S.P. , or rather for the Gulf of Alaska or the whole Subarctic Pacific, would be premature, to say the least. For multiple trophic levels and large horizontal scales, the simpler tropho-dynamic arguments of LeBrasseur (1969) and Sanger (1972) are more appropriate at present. A much narrower range of questions is

addressed here, centering on the observed constancy of chlorophyll a concentrations at O.S.P. These questions can be addressed using simplified simulation models which are more commensurate with the present state of biological knowledge.

The seasonal cycle of Chl a at O.S.P. is presented in Fig 3. The cycle in the Strait of Georgia is also presented for contrast. While the decrease in mixed layer depth and increase in solar radiation at O.S.P. in the spring does result in an increase in primary productivity (Parsons,1965) this is not reflected in an increase in phytoplankton standing stock (as measured by Chl a). Instead, the biomass (wet weight) of zooplankton above 150m varies seasonally in a similar manner to primary productivity (Fig 4). This seems to be consistent with the hypothesis that zooplankton grazing results in a phytoplankton mortality rate which balances phytoplankton growth throughout the year.

This hypothesis of grazing control in turn raises other questions. Why should it occur in the oceanic Subarctic Pacific and not in coastal areas, nor in the oceanic North Atlantic? Perhaps even more troublesome, in view of the rapid growth rate of phytoplankton, seasonal and daily variations in this growth rate, and the observed variability in zooplankton standing stock, is the tight balance required between grazing and phytoplankton growth by this hypothesis.

The first question was answered by Heinrich (1962) as follows. The dominant grazers in the North Atlantic and in many coastal areas, copepods such as Calanus finmarchicus and Calanus pacificus, over-winter as late copepodite stages or adults and

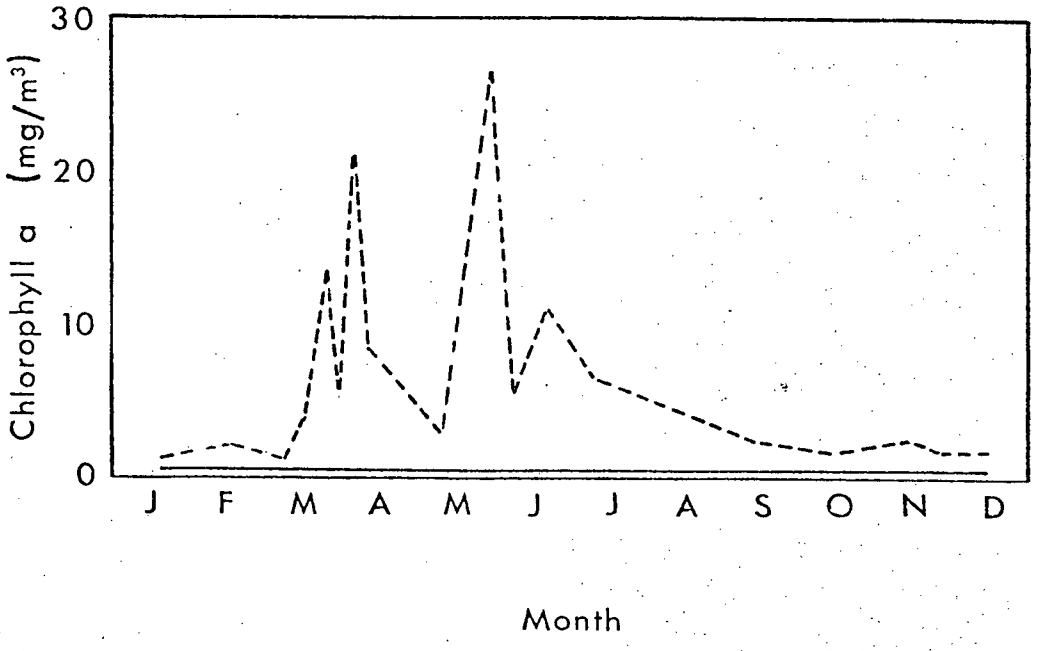

Figure 3. Seasonal cycle in chlorophyll a at O.S.P. (solid line) and in Departure Bay, Strait of Georgia (dashed line). (Adapted from Parsons, 1965).

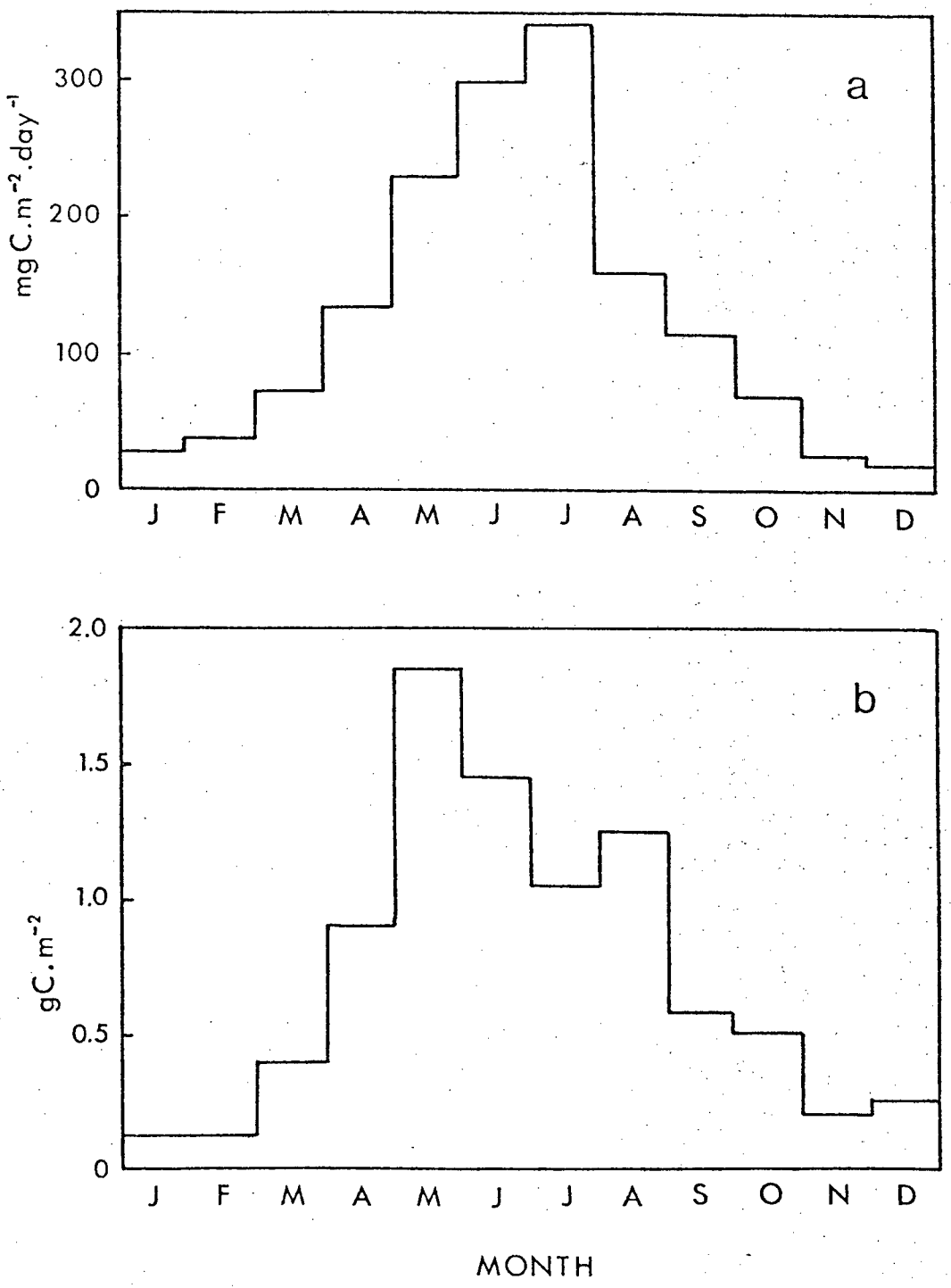

Figure 4. Seasonal cycle at O.S.P. in (a) primary production and (b) zooplankton standing stock. (from McAllister, 1969).

cannot reproduce in the spring until they have accumulated egg tissue by feeding on adequate phytoplankton concentrations. A further period in which nauplii do not feed follows reproduction, so that a sizeable lag occurs in the numerical response of zooplankton to the spring increase in phytoplankton growth. The dominant copepods in the Subarctic, C. plumchrus and C. cristatus, reproduce at depth in the spring, using fat stores laid down the previous summer. An actively-growing population is thereby recruited to the surface in the spring without any lag in response to increasing phytoplankton growth rates. There are some coastal areas such as the Strait of Georgia (Parsons,1965) and the Sea of Japan (Heinrich,1962) where C. plumchrus and/or C. cristatus dominate but a phytoplankton spring bloom does occur. Heinrich attributed this to an earlier increase in phytoplankton growth rate in stratified coastal waters and a consequent failure in timing of the spring recruitment of these copepods.

While this argument seems to offer a solution to the first question (a sufficient lag in zooplankton response in the spring will clearly ensure a spring phytoplankton bloom), it does not address the second question. In the remainder of this section, this question of balance is addressed by considering the stability properties of some simple biomass models of phytoplankton-zooplankton interactions. These should not be regarded as realistic or predictive models but rather as statements of paradigm, in the sense of Kuhn(1970). Their consideration will allow us to relate the question of balancing grazing loss and phytoplankton growth to some important current

issues in marine ecology.

A classical starting point for simple models of predator-prey interactions (as the zooplankton-phytoplankton interaction will be regarded for the rest of this section) is the differential equation model :

$$\dot{x} = r.x - a.x.y \qquad 1.1a$$

$$\dot{y} = e.a.x.y - m.y \qquad 1.1b$$

(Lotka,1925). In this model, the parameter r represents an intrinsic rate of growth of prey, x; the parameter a is the successful encounter rate by a single predator per unit prey density so that a.x.y is the total rate of consumption of prey by predators; e is the efficiency of conversion of consumed prey to predator so that e.a.x.y represents the consequent rate of increase in predator, y, while m is a constant per capita loss rate for predators in the absence of food. The oscillatory solutions of system 1.1 originally attracted some interest, but their neutral stability properties and consequent lack of robustness under small structural changes in the model led to its replacement.

The model can be improved by introducing further non-linearities to account for resource-limitation of prey and saturation of predators (Holling,1959). One possible form for such a model is

$$\dot{x} = r.x.(1-x/K) - i_M.x.y/(D+x) \qquad 1.2a$$

$$\dot{y} = e.i_M.x.y/(D+x) - m.y \qquad 1.2b$$

Here, K is a carrying capacity for prey in the absence of predators, i_M is the maximum rate of consumption of prey per predator and D is the prey density at which prey consumption reaches half its maximum value. The ratio i_M/D is comparable to the parameter a in equation 1.1. The qualitative behaviour of this model has seen much discussion (for a review,see May,1974). Two types of phase plane portraits are shown in Fig 5. The prey isocline always forms a quadratic 'hump' and the predator isocline a vertical line. Their intersection $(\bar{x},\bar{y})$ is a critical point of the system and a simple geometric rule determines its stability properties. When the predator isocline $(x = \bar{x})$ lies to the right of the 'hump', (Fig 5a), $(\bar{x},\bar{y})$ is asymptotically stable and trajectories spiral into it. When the predator isocline lies to the left of the hump, trajectories spiral outward to a stable limit cycle solution.

To relate these results to the O.S.P. seasonal cycle, a way must be found to incorporate seasonal effects into this presently homogeneous model. The obvious approach is to allow the phytoplankton growth parameters r and K to be functions of time, t, reflecting the seasonal cycle in primary productivity (Fig 4). The resulting system is no longer homogeneous and consequently difficult to treat analytically. Suppose for the moment that the parameters in 1.2 at any particular time t are such that a stable non-trivial equilibrium $(\bar{x}(t),\bar{y}(t))$ exists for the corresponding homogeneous system. If the time scale for approach to this equilibrium is sufficiently fast compared with the (seasonal) time scales over which r and K change, it seems reasonable that the solution to the non-homogeneous system, if it starts near

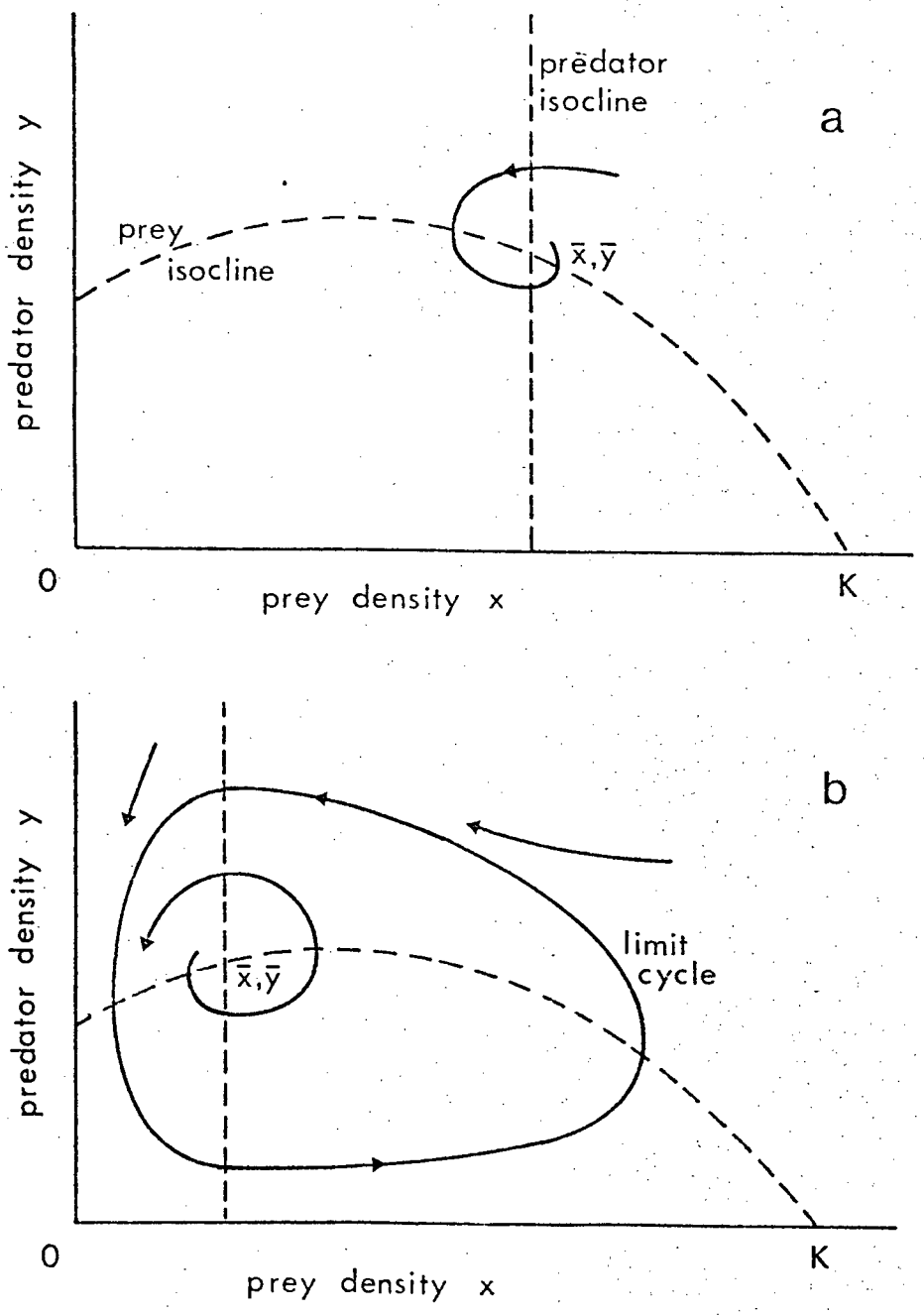

Figure 5. Phase plane portraits for system 1.2. (a) equilibrium stable. (b) equilibrium unstable.

$(x(t),y(t))$, will remain close to this quasi-equilibrium solution. By this separation of time scales (Ludwig *et al*, 1978), a seasonal cycle can be envisaged which is closely approximated by the quasi-equilibrium solution. Now $\bar{x}(t)$, $\bar{y}(t)$ are determined by

$$e.i_M.\bar{x}/(D+\bar{x}) = m \qquad 1.3a$$

$$\bar{y}(t) = r(t).(1-\bar{x}/K(t)).(D+\bar{x})/i_M \qquad 1.3b$$

There are two immediately encouraging aspects of these expressions. The quasi-equilibrium phytoplankton concentration is constant over time, depending only on zooplankton parameters. The quasi-equilibrium zooplankton concentration is proportional to the phytoplankton growth rate. Phytoplankton and zooplankton standing stocks which followed $(\bar{x}(t),\bar{y}(t))$ closely would behave as observed at O.S.P. , with phytoplankton concentration approximately constant and zooplankton concentration varying with primary productivity.

There is however a serious problem with this 'explanation'. The stability criterion given above can be written as

$$D > K - 2.\bar{x} \qquad 1.4$$

K represents the standing stock of phytoplankton at which resource limitation causes the growth rate to drop to zero. There are two obvious potentially limiting resources for phytoplankton, namely nutrient supply and available light. In section 1.3, nutrient concentrations at O.S.P. were described as

non-limiting. The value of K reached in the culture experiment of McAllister et al (1960) was about 40 times $\bar{x}$. In fact, the usual non-linear Michaelis-Menten relationship between growth and nutrient concentration means that any negative feedback on growth rate of small increases in x above $\bar{x}$ will be much smaller than a value of x/K of 1/40 in the logistic model would suggest.

Increases in phytoplankton density can decrease phytoplankton growth rates through self-shading. This effect can be quantified for a homogeneous mixed-layer population by employing a relationship between extinction coefficient, k, and chlorophyll, x,

$$k = k_o + k_1 . x$$

(adapted from Parsons et al, 1977), combined with a photosynthesis (P) vs light (I) relationship (eg $P = \alpha . I . \exp(-I/I_{MAX})$; Steele,1962). Integrating over depth gives an expression for growth in the mixed layer as a function of mixed layer depth, z_M, surface light intensity I_o, P vs I parameters α and I_{MAX}, the parameters k_o and k_1 and the Chl a concentration, x. Differentiating this expression with respect to x and substituting for $x = \bar{x}$ yields a value suitable for insertion as 1/K in 1.2. For z_M = 30m (late summer), k_1 = .02 $m^2 . mg\ Chl\ a^{-1}$, (Lorenzen,1980;Megard et al ,1980), k_o = .1 m^{-1}, and I_o/I_{MAX} = 2. (Steele,1962), this yields a value of K_{light} = 8 mg Chl $a . m^{-3}$ or about 20 times $\bar{x}$. This value agrees with the results of Takahashi and Parsons(1972).

Both considerations of nutrient limitation and self-shading

suggest that ,at O.S.P. , the phytoplankton population is being maintained at concentrations about one-twentieth of its carrying capacity or less. According to the condition 1.4, for this equilibrium to be stable, D must be about 20 times x which would imply that zooplankton at O.S.P. are growing and reproducing at phytoplankton concentrations sufficient to supply 1/40 of their maximum ration. While large values of the grazing half-saturation constant of this order have been reported, such a low relative ingestion rate seems unlikely to cover even the basal metabolic requirements of the zooplankton. Of course, the particular value 1/40 can be questioned as it depends on the specific form of the grazers' functional response, as well as the assumptions underlying the estimate of K. However, the problem is more fundamental than the stability criterion alone would suggest. For example, a piecewise linear, or Type I (Holling,1965) functional response on the part of zooplankton grazers has received support (Mullin and Brooks,1975). If a functional response of this type is substituted into 1.2, the equilibrium is always asymptotically stable, no matter how small $\bar{x}/K$ may be. The local rate of approach to equilibrium, on the other hand, is then given by $r.\bar{x}/K$, and the quasi-equilibrium explanation depends not only on $(\bar{x},\bar{y})$ being stable, but on the further condition that approach to equilibrium occurs on a fast time scale compared with changes in $(\bar{x}(t),\bar{y}(t))$. Values of $\bar{x}/K$ of order 1/20th and a value of r of 0.2 day^{-1}, estimated from McAllister et al (1960), give a characteristic time of approach to equilibrium of order 50 days. This is not short compared with the seasonal time scale of changes in phytoplankton growth rate

and $\bar{y}(t)$. Large oscillations in phytoplankton and zooplankton abundance would occur if such a weakly-stable system was subjected to seasonal cycles in productivity. Although the homogeneous system with a type I functional response is stable, when $\bar{x}/K$ is very small, it is little better than neutrally stable in terms of its ability to track a seasonally varying equilibrium.

The system 1.2 cannot provide a consistent explanation of observations at O.S.P. However, the quasi-equilibrium approach seems promising and one might try to proceed by modifying the system so as to overcome the stability time scale problem, while retaining the qualitative behaviour of the quasi-equilibrium solution $(\bar{x},\bar{y}(t))$.

One approach which doesn't work is mentioned here for interest sake. Introducing a quadratic loss term for predators is known to bring about asymptotic stability in simple predator-prey models (Bazykin,1974) and has been suggested in other phytoplankton-zooplankton models (Landry,1976). A model of this kind, with type I functional response, can be written as

$$\dot{x} = r.x - a.x.y \qquad 1.5a$$

$$\dot{y} = e.a.x.y - u.y^2 \qquad 1.5b$$

for x at sub-maximal ration levels. (An increase in per capita loss rate (u.y) with predator density could result from intraspecific competition for resources other than food, or from switching or aggregative responses in higher carnivores.) This model can be rejected, without considering its stability

properties, as the quasi-equilibrium solution for seasonally varying r(t) is

$$\bar{y}(t) = r(t)/a$$
$$\bar{x}(t) = u.\bar{y}(t)/(e.a)$$

The quasi-equilibrium phytoplankton concentration $\bar{x}(t)$ is not constant but varies with $\bar{y}(t)$ in this model. This is certainly not consistent with observations at O.S.P.

Two possible functional responses have already been considered in 1.2 : a hyperbolic (Type II) and piecewise linear (Type I) response (Holling,1965). Within the context of simple biomass models such as 1.2, these can be characterized as destabilizing and neutrally stable respectively. A third form of functional response discussed by Holling (1965) is the sigmoid or Type III functional response, incorporating a reduced clearance rate by copepods at low food densities. This type of functional response has a stabilising effect in simple biomass models.

A number of studies of pelagic copepods have suggested grazing responses of this type, involving either a cessation of feeding below some threshold food density (Parsons et al ,1969; Frost,1972), or a reduction in filtering rate at low food densities (Frost,1975). Theoretical considerations suggest that a copepod trying to optimize energy intake should reduce its filtering activity at low food densities (Lam and Frost,1976; Steele and Frost,1977).

The effect of allowing a type III grazing response can be seen in a phase plane analysis of the system

$$\dot{x} = r.x - f(x).y \qquad 1.6a$$

$$\dot{y} = e.f(x).y - m.y \qquad 1.6b$$

where the grazing function f(x) has the threshold form (Fig 6a) or sigmoid form (Fig 6b). (The phytoplankton self-limiting term (-x/K) has been dropped as it is negligible under the conditions prevailing at O.S.P.).

Phase plane portraits for the system 1.6 are given in Fig 7. For the case of a grazing threshold at $x=x_o$, the prey isocline asymptotes to the vertical line $x=x_o$ at the left, has a minimum at some point x^*, and asymptotes to the line $y=r.x/i_M$ as x approaches ∞. (The parameter i_M represents the maximum zooplankton ration.) The zooplankton isocline is a vertical line as for system 1.2. These intersect at the equilibrium given by

$$f(\bar{x}) = m/(e.a) \qquad 1.7a$$

$$\bar{y} = r.\bar{x}.e/m \qquad 1.7b$$

By linearizing in the neighbourhood of $(\bar{x},\bar{y})$, it can be shown that this equilibrium is asymptotically stable if and only if $\bar{x} < x^*$; that is, the zooplankton isocline must lie to the left of the minimum in the phytoplankton isocline. Given that this condition is satisfied, there are still two qualitatively distinct phase portraits. When x is very large, the system 1.6 becomes approximately

$$\dot{x} = r.x - i_M.y \qquad 1.8a$$

$$\dot{y} = (e.i_M - m).y \qquad 1.8b$$

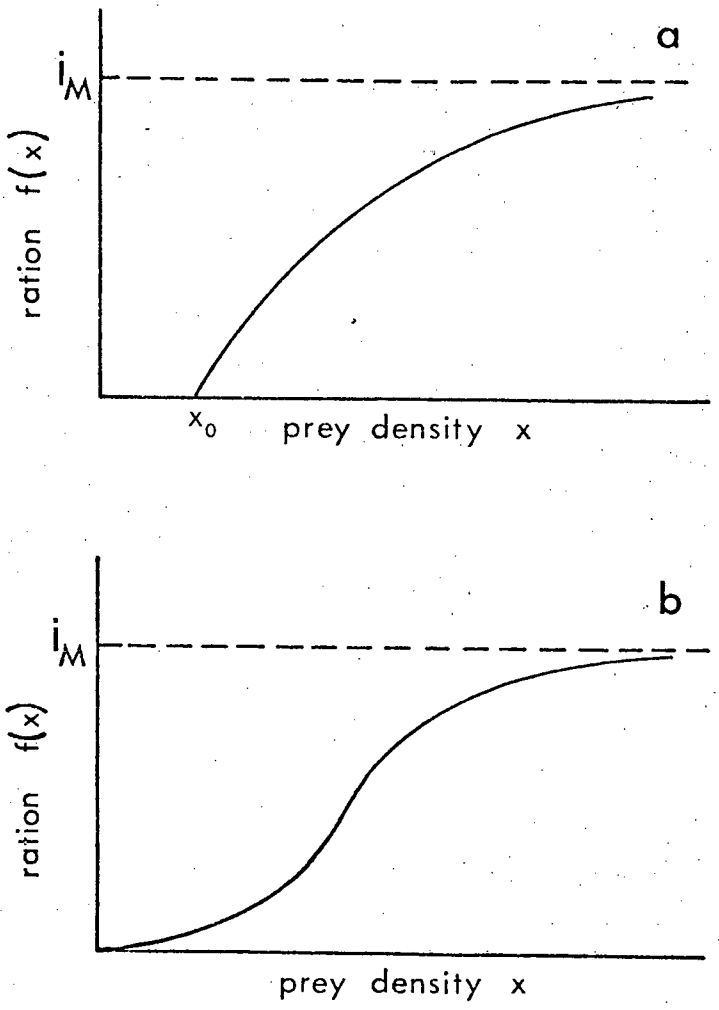

Figure 6. Type III functional responses: (a) threshold. (b) sigmoid.

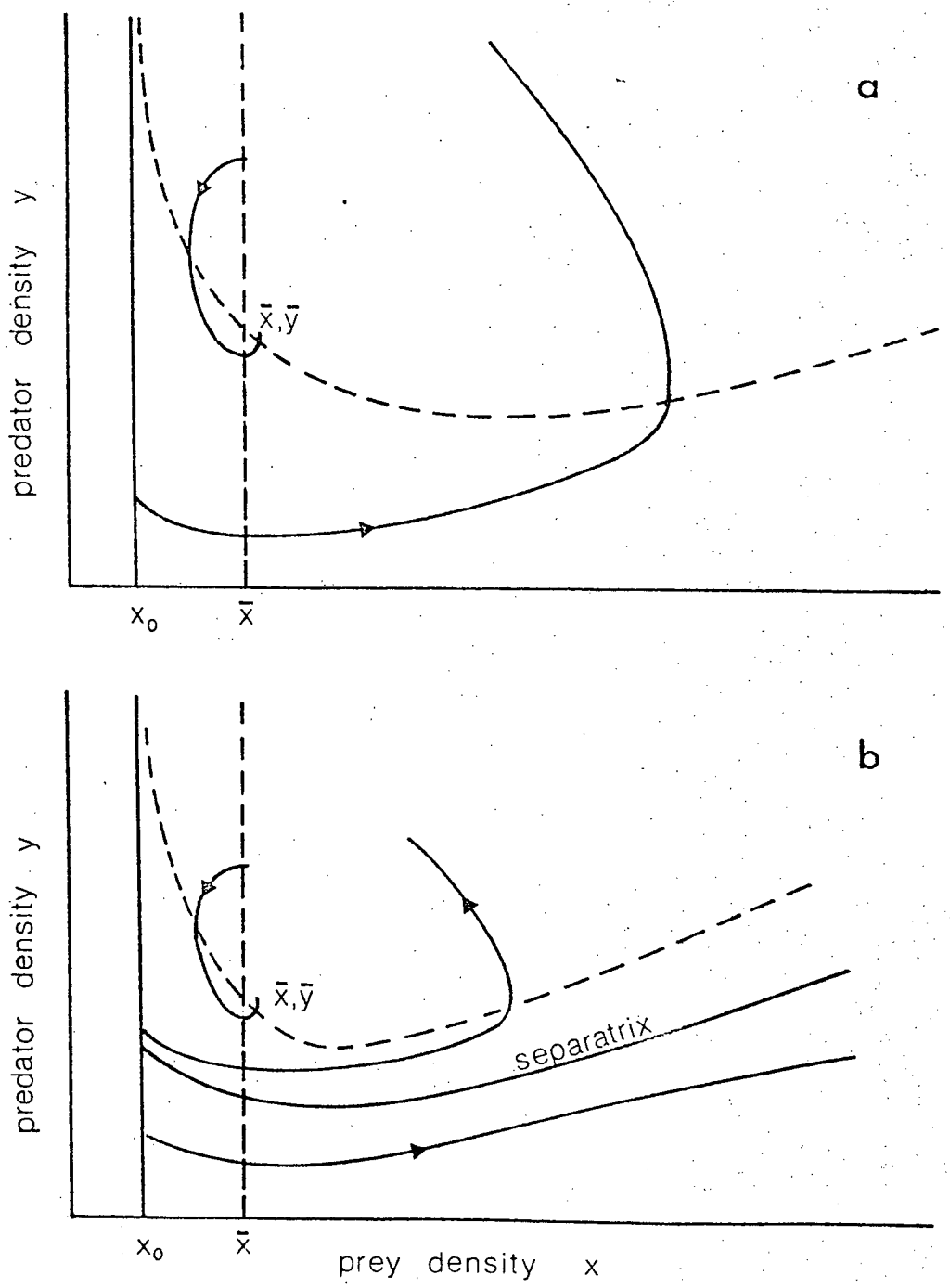

Figure 7. Phase plane portraits for system 1.6.

(a) $e.i_M - m > r$. (b) $e.i_M - m < r$.

If $e.i_M - m > r$, or, equivalently, if the maximum growth rate of zooplankton exceeds that of phytoplankton, trajectories starting from large x and small y will always cycle back to low phytoplankton concentrations (Fig 7a). In this sense, it is impossible for phytoplankton to escape zooplankton control permanently. If $e.i_M - m < r$, (as seems more likely), the behaviour of trajectories for large x depends on initial conditions, (x_i, y_i). If y_i is large enough, the trajectory will cycle, but otherwise, x will increase indefinitely and the trajectory will approach $(+\infty, +\infty)$. In the corresponding phase plane portrait (Fig 7b) there is a separatrix which divides trajectories which cycle from those which don't. The phase plane portraits for sigmoid functional responses are qualitatively similar, the principal difference being that the phytoplankton isocline asymptotes to x=0.

The local rate of approach of trajectories to equilibrium can be found by linearizing about $(\bar{x},\bar{y})$. In fact, if h(x) is the clearance rate of zooplankton (given by f(x)/x), the local rate of approach to equilibrium is given by

$$r.\bar{x}.h'(\bar{x})/h(\bar{x})$$

The stability criterion $x < x^*$ is simply equivalent to a positive rate of approach, x^* being given by $h'(x^*)=0$. That is, the equilibrium $(\bar{x},\bar{y})$ is locally stable provided the clearance rate increases with x at $x=\bar{x}$.

In the case of a threshold, hyperbolic functional response as used by Steele (1974),

$$f(x) = i_M.(x-x_o)^+ /(D+(x-x_o)^+) \ ,$$

and explicit formulae can be written for x^* and for the rate of approach:

$$x^*-x_o = \sqrt{D.x_o}$$

$$\text{rate of approach} = r.((x^*-x_o)^2-(\bar{x}-x_o)^2) \ / \ ((\bar{x}-x_o).D+(\bar{x}-x_o)^2)$$

That is, the clearance rate is a maximum at a density x^* which is greater than the threshold by the geometric mean of the half-saturation constant, D, and the threshold x_o. Provided the equilibrium $\bar{x}$ does not lie too close to x^*, the rate of approach to equilibrium is of the same order as the phytoplankton growth rate, r.

It is possible then for the approach to equilibrium in 1.6 to occur on relatively fast time scales, of the same order as phytoplankton growth, and consequently for the quasi-equilibrium assumption to be valid for seasonal variation in phytoplankton growth rate, r. Note that the quasi-equilibrium cycle given by 1.7 predicts, as before, a constant phytoplankton standing stock and a zooplankton standing stock which varies with primary production. The simple biomass model 1.6, according to this approximate argument based on separation of time scales, should be capable of qualitatively reproducing the observed seasonal cycle at O.S.P.

Reflection on time scales allows an interesting, intuitive perspective on the development so far. The time scales one traditionally associates with phytoplankton growth are short and

one would expect an agent which regulates phytoplankton density tightly to operate on a similar time scale. The time scales one traditionally associates with copepod dynamics are much longer and this appears to be a problem with a grazing control hypothesis at O.S.P. Where nutrients are limiting, feedback effects on phytoplankton growth can tightly regulate phytoplankton density, as discussed in Chapter 2, but this is apparently not the case at O.S.P. The sigmoid or threshold functional response in 1.6 essentially introduces a new fast time scale, a zooplankton behavioural time scale, into the problem.

This development augments rather neatly Heinrich's(1962) explanation of the differences between seasonal cycles in the Subarctic and elsewhere, based on the life-history strategies of the dominant grazers. He attributed the spring bloom in the North Atlantic to a delay in the numerical response of the dominant grazer to the spring increase in phytoplankton growth and abundance. If the maximum growth rate of phytoplankton exceeds that of zooplankton biomass, a phase plane portrait as in Fig 7b is appropriate. The spring increase in phytoplankton growth rate is equivalent to a vertical shift in the phytoplankton isocline. A delay in zooplankton response can then easily result in the system being overtaken by the separatrix, leaving the local stability domain about $(\bar{x},\bar{y})$ and entering a region in which phytoplankton have escaped zooplankton control. According to 1.6, the trajectory will approach $(+\infty,+\infty)$. In practice, of course, nutrients are depleted and the spring bloom terminates.

Heinrich(1962) attributed the occurrence of spring blooms in

coastal regions of the Subarctic where C. plumchrus is present to a failure in timing of recruitment. Although the spring bloom does occur earlier in the Strait of Georgia than in oceanic locations (Parsons,1965), the nauplii of C. plumchrus reach the surface waters of the Strait of Georgia in February and March (Fulton,1973) and it is not clear that the timing is inappropriate. The phase plane portrait in Fig 7b suggests another explanation. In coastal waters subject to run-off, stratification and a consequent increase in phytoplankton growth rate can occur very rapidly. This may result in the system state $(x(t),y(t))$ failing to track the rapidly shifting quasi-equilibrium cycle $(\bar{x},\bar{y}(t))$ and again being overtaken by the separatrix, resulting in a spring bloom.

The observations of Fulton (1973) suggest a simpler and perhaps more convincing explanation : namely, that recruitment of C. plumchrus in the strait fails to coincide in space, rather than time, with the spring bloom. Successful over-wintering of C. plumchrus occurs only in water deeper than 300m, which occupies only one-fourth of the area of the strait. Arrival of C. plumchrus in the remaining areas is presumably delayed, subject to horizontal advection.

1.5 Preview of Chapters 2-4.

Each of the simple models considered above can be regarded as a composite hypothesis concerning trophic interactions at O.S.P. There is clearly a need for independent experimental tests of aspects of these hypotheses. For example, the functional responses of the dominant copepods at O.S.P. are not well-known and the existence of zero or reduced clearance rates

at low phytoplankton densities is an essential part of the model 1.6.

The theoretical possibilities have hardly been exhausted by the above analysis. Given the comparative wealth of information in the long time series of observations at O.S.P. , more than rough qualitative agreement of a model with average seasonal cycles can be demanded. A quantitative comparison of prediction and observation requires a more carefully constructed, more detailed model. For example, the state variables x and y above have been used rather loosely to represent phytoplankton and zooplankton standing stock, although they have been implicitly identified with Chl a in $mg.m^{-3}$ and zooplankton wet weight in $mg.m^{-2}$ respectively. As the phytoplankton population at O.S.P. varies seasonally in vertical distribution and (hypothetically) in C:Chl a ratio (McAllister,1969), the use of Chl a in $mg.m^{-3}$ as a state variable clearly needs careful examination. Zooplankton wet weight is a rough summary variable, representing contributions from carnivores as well as herbivores, although dominated by herbivorous copepods at most times (LeBrasseur,1969). More detailed size and species information is available for O.S.P. and this certainly deserves attention in view of recent theoretical results (Steele,1974; Steele and Frost,1977).

These problems are addressed in Chapter 3 and Chapter 4. In Chapter 3, an attempt is made at a more realistic quantitative simulation model of phytoplankton growth at O.S.P. The model is partly based on an original analysis of the phytoplankton data, particularly ^{14}C uptake rates, obtained from the weatherships.

In Chapter 4, a parameter estimation technique developed for copepod time series is applied to estimate population parameters for the dominant herbivores at O.S.P. Two more elaborate models of the phytoplankton-zooplankton interaction are constructed, using these results and those of Chapter 3. Some effect of herbivore size-structure and species composition is considered in the second model. The models are studied using simulation and the qualitative techniques and results of this chapter and Chapter 2.

Three hypotheses concerning the phytoplankton-zooplankton interaction at O.S.P. have been considered in Section 1.4. All explain the seasonal cycles in phytoplankton and zooplankton standing stock as the result of the system's ability to closely track a quasi-equilibrium seasonal cycle. The hypotheses differ in the mechanisms responsible for the short term stabilising feedback necessary for this tracking of a seasonally shifting equilibrium. The model 1.2, involving resource-limitation of phytoplankton growth, is certainly capable of the appropriate qualitative behaviour, but has been rejected on the basis of independent experimental evidence. The model 1.5, involving a quadratic loss rate for grazers, cannot reproduce the observed seasonal cycle. The model 1.6, which assumes a reduction in grazing rate at low phytoplankton densities, is capable of reproducing the observed seasonal cycle qualitatively. As noted earlier, the actual functional responses of grazers at O.S.P. are not known.

The simulations considered in Chapter 4 will be primarily based upon the system 1.6 and the assumption of grazing

thresholds. However, the composite hypothesis implicit in 1.6 will become modified in the process of model elaboration. In particular, an explicit treatment of copepod life-history strategies will show that the spring recruitment of nauplii over an extended period can stabilise the phytoplankton-zooplankton interaction and prevent a spring bloom, even in the absence of grazing thresholds. As a result, attention will focus on the problem of maintaining grazing control in the summer and fall against the destabilising effect of over-wintering departure by the dominant copepods. A lack of model robustness during this period and discrepancies in detail between model predictions and observations will force a re-evaluation of the grazing threshold hypothesis and a search for alternatives. The possibility of nutrient limitation of phytoplankton growth in late summer and fall will be reconsidered and the potential importance of spatial variation in maintaining grazing control will be discussed.

Chapter 2 is not directly concerned with events at O.S.P. but is of more general theoretical interest. The idea that feeding thresholds may be important in plankton ecosystems is not a new one. In a numerical model of phytoplankton-zooplankton interactions in the North Sea, Steele(1974) found that thresholds were necessary to obtain realistic behaviour. An alternative was proposed by Landry(1976), who found that inserting a quadratic loss term for herbivores into Steele's model eliminated the need for thresholds. Both authors based their theoretical conclusions on simulation results. A qualitative mathematical analysis of these models, based on separation of time scales, is give in Chapter 2. The analysis provides insights into the results of

Steele and Landry which appear to have interesting implications for marine ecosystem models in general, and the models considered here for O.S.P. in particular.

CHAPTER 2

QUALITATIVE ANAYLSIS OF A COMPLEX SIMULATION MODEL

2.1 Introduction.

In a theoretical treatise on the planktonic ecosystem of the North Sea, Steele (1974) examined the relative importance of interactions between different trophic levels as 'control mechanisms for the whole system'. His conclusions were based on a simulation model of a simplified nutrient-phytoplankton-copepod food chain which continues to be of theoretical interest, both as a basis for more complex realistic models (Steele and Frost,1977) and as a first step in complexity and realism above the highly simplified predator-prey models of the Lotka-Volterra type (Lotka,1925;May,1974).

Steele's conclusions were based primarily on comparisons of a number of computer simulations of the model involving various assumptions concerning the form and magnitude of trophic interactions. A key finding was that the model could not predict timestreams which agreed qualitatively with observations of the North Sea unless a threshold-feeding mechanism, or type III functional response (Holling,1959), was invoked for herbivorous copepods. Landry (1976) obtained realistic behaviour from Steele's model without thresholds by introducing a per capita predation rate on herbivores which increased in proportion to herbivore numbers at low densities. This was partly introduced by Landry as a size-dependent term (smaller copepods being more abundant) but its significance seemed to lie in the resulting quadratic loss term for herbivores (Steele,1976); the

introduction of such a loss term is well-known to produce stable equilibria in otherwise unstable simple Lotka-Volterra models (Bazykin,1974).

Both Steele and Landry presented their results as at least suggestive evidence for the existence and importance of thresholds and density-dependent per-capita predation rates respectively in real ecosystems. This focusing of attention on particular biological questions is recognised as a valuable potential contribution of modelling studies in general, and it appears to have been successful here in view of the discussion aroused concerning the experimental observation of feeding thresholds (Mullin et al ,1975; Frost,1975). However, any argument that some aspect of a model is necessary if realistic results are to be obtained must always be viewed with caution. One reason for this, common to all modelling studies, is that conceptual elaboration of a model is always possible (as in the case of Landry versus Steele), so that the necessity of any particular concept can never be established.

A second reason applies particularly to studies such as Steele's and Landry's which are based on computer simulation. Given the large uncertainty in most ecological parameters, it is not clear that a model having a prescribed functional form should be judged to be incapable of satisfying a set of qualitative criteria on the basis of a small number of numerical solutions using particular parameter values. This criticism can be addressed by the theoretician, at least in principle, as qualitative mathematical analysis of the model can provide information about the behaviour of solutions over regions in

parameter space, rather than at points within them. Analysis of this type can also lead to a better understanding of the behaviour of the model and its dependence on parameters and thereby allow useful biological insights.

Additional motivation for a qualitative analysis of Steele's model is provided by the study of simple Lotka-Volterra models in Chapter 1 which suggested that grazing thresholds are important in the Subarctic Pacific ecosystem. While this is superficially consistent with Steele's conclusion for the North Sea, a puzzling discrepancy exists. It was necessary to invoke thresholds in simple models of the Subarctic Pacific only because phytoplankton there are not nutrient-limited. In the North Sea simulation model, phytoplankton are nutrient-limited throughout much of the summer, and it is not clear why thresholds should be needed for stability. An explanation of this discrepancy is sought here through the qualitative analysis of Steele's model.

2.2 Model and Analysis

The model developed by Steele (1974) and used, with certain alterations, by Landry(1976) is:

$$\dot{R} = V.(R0-R) + U.(E.(P-P1)/(D+P) + F).Z.W^{0.7} - A.R.P/(B+R) \quad 2.1a$$

(rate of change of nutrient equals mixing through thermocline + zooplankton excretion - phytoplankton uptake)

$$\dot{P} = A.R.P/(B+R) - V.P - C.Z.W^{0.7}.(P-P1)/(D+P) \quad 2.1b$$

(rate of change of phytoplankton = growth - mixing - grazing)

$$\dot{W} = ((0.7.C-E).(P-P1)/(D+P) - F).W^{0.7} \qquad 2.1c$$

(rate of individual growth = net assimilation - active and basal metabolism)

$$\dot{Z} = -GW.(W-W1).(Z-Z1)/(H+Z.W) - GX.Z \qquad 2.1d$$

(zooplankton mortality rate = nonlinear, weight-dependent term + linear term).

When copepods reach adult weight, W2, growth is diverted to reproductive store, S, for a period of J days, after which ZO naupli are released, ZO being given by

$$ZO = X.S/WO \qquad 2.1e$$

where X is efficiency and WO the initial naupliar weight. The notation here (Table I) follows that of Steele(1974), except that GW is used in 2.1d to allow G to be reserved for zooplankton biomass. The reader is referred to Steele for a detailed derivation of the model.

The system 2.1 represents a set of four simultaneous, nonlinear, differential equations involving thresholds and the discontinuous recruitment of nauplii and there is little point in looking for non-trivial solutions in closed form. A series of simplifications and approximations is employed here to obtain some understanding of the behaviour of the model over corresponding regions in parameter space. These approximate results are then checked and extended by computer simulation. The basic step in this qualitative analysis is the recognition of

Table I.

Parameters used in Steele's model (2.1).

R...nutrient concentration (carbon equivalent) in mixed layer.

RO...nutrient concentration (carbon equivalent) below mixed layer.

V...mixing rate through thermocline.

U...fraction of excreted nutrient recycled.

P...phytoplankton carbon concentration in mixed layer.

A...maximum phytoplankton growth rate (day^{-1}).

B...half-saturation constant (carbon equivalent) for nutrient-dependent growth.

Z...zooplankton density (#/l).

W...zooplankton weight (ug C/ind).

C...fixes maximum zooplankton ingestion rate.

P1..threshold for zooplankton grazing on phytoplankton carbon.

D...fixes zooplankton grazing rate above P1.

E...fixes component of metabolic rate proportional to ingestion.

F...fixes basal metabolic rate.

GW..maximum of weight and density-dependent mortality rate.

W1..weight threshold for mortality.

Z1..number threshold for mortality.

H...'half-saturation' constant for mortality.

GX..constant mortality rate.

ZO..initial number of nauplii in cohort.

WO..initial naupliar weight.

W2..adult weight.

S...reproductive store.

J...period over which reproductive store accumulates.

two aspects of the seasonal behaviour studied by Steele and Landry; namely, the transient response to high initial nutrient concentrations (the spring bloom), and the approach to a stable cyclic pattern in the nutrient-limited period which follows. The latter is more likely to be amenable to qualitative analysis and is treated here first.

The analysis proceeds through the recognition of three distinct time scales in the model under nutrient limitation. (For an instructive example of the use of multiple time scales in the analysis of a complicated ecological model, see Ludwig,Jones and Holling(1978).) A time scale for nutrient turnover can be obtained by dividing the source term, V.RO, by the half-saturation constant for nutrient uptake, B. For Steele's values of V (0.01 day^{-1}) and RO (760 $\mu g\ C(eq).l^{-1}$), V.RO equals 7.6. Steele used a rather high value of B (96 $\mu g\ C(eq).l^{-1}$ according to Landry). Recent chemostat results, combined with observations of very low nutrient concentrations in the oceans, suggest that half-saturation constants for growth should be smaller than this, of order 0.1 μg at $N.l^{-1}$ or approximately 10 $\mu g\ C(eq).l^{-1}$ (McCarthy and Goldman,1978). This results in a time scale for nutrient turnover of order 1 day, much shorter than that of phytoplankton (maximum growth rate 0.2 day^{-1}, yielding a time scale of 5 days) or zooplankton. We proceed therefore by treating R as a fast variable; that is, by assuming that nutrient concentration adjusts rapidly to changes in other state variables so that $R \approx \bar{R}(P,Z,W)$, where $\bar{R}$ makes the right-hand side of equation 2.1a zero. Substituting $R = \bar{R}$ in equation 2.1b gives

$$\dot{P} = V.R0 - V.P - Z.W^{0.7}.((C-U.E).f(P) - U.F) \quad , \qquad 2.2a$$

where f(P) stands for (P-Pl)/(D+P), and the term V.R has been neglected since R is assumed to be of order B or approximately one-hundredth RO. When combined with equations 2.1 c,d,e, equation 2.2a forms a system (2.2), from which nutrients have been eliminated.

The second and third time scales can be distinguished provided the copepod mortality rate is low enough that Z changes slowly compared with potential growth rates of P and W. Then Z can be treated as a slow variable and the behaviour of P and W considered with Z fixed. The system

$$\dot{P} = V.RO - V.P - Z.W^{0.7}.((C-U.E).f(P) - U.F) \qquad 2.3a$$

$$\dot{W} = ((0.7.C-E).f(P) - F).W^{0.7} \qquad 2.3b$$

has the phase plane portrait shown in Fig 8. The non-trivial equilibrium solution $(\bar{P},\bar{W}(Z))$ of 2.3 is stable provided $f'(\bar{P})$ is positive, a condition which is always satisfied regardless of the value of Pl. Then, according to the slow-variable approximation, as Z(t) decreases through mortality, P(t) and W(t) should track the quasi-equilibrium solution $(\bar{P},\bar{W}(Z(t)))$. According to 2.3, $\bar{P}$ and $Z(t).\bar{W}^{0.7}$ are both constant. It follows that a cohort will reach adult weight, W2, from an initial weight, WO, when the density has dropped by a factor $(WO/W2)^{0.7}$. For example, if the per capita mortality is constant (GW = 0, GX $\neq$ 0), Z(t) = ZO.exp(-GX.t) and, allowing for the incubation period J, the generation time is given by

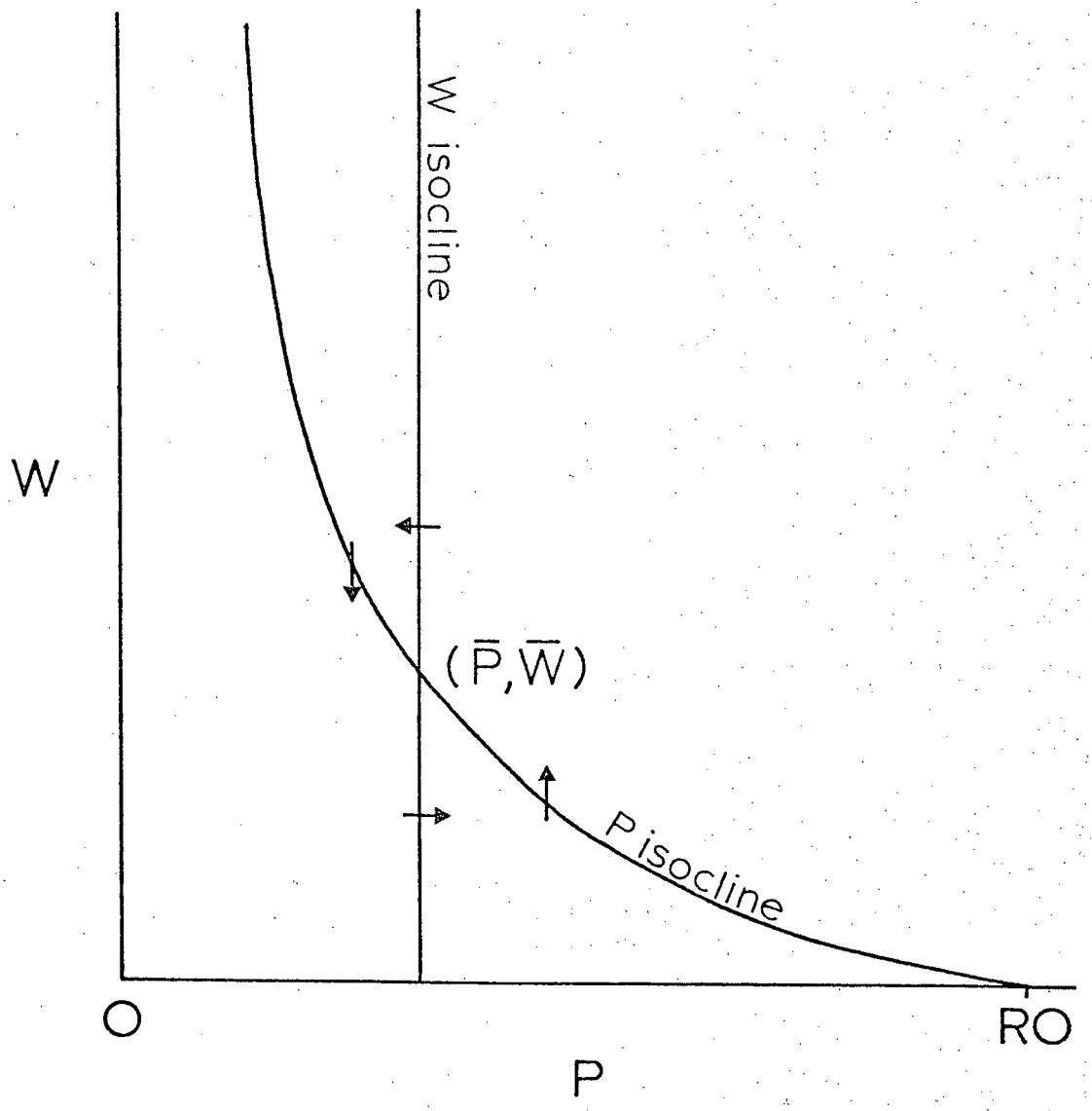

Figure 8. Phase plane portrait for the system 2.3.

$$\tau = J + 0.7.\ln(W2/W0)/GX. \qquad 2.4$$

So far, only the growth of a single cohort has been dealt with but an approximate treatment of reproduction is also possible. During the period of J days over which reproductive stores are accumulated, W is fixed at adult weight W2, so that equation 2.3b and the equilibrium value P are not relevant. It is consistent with the slow-variable approximation to assume that P is approximately equal to $\tilde{P}(Z)$, where $\tilde{P}$ makes $\dot{P} = 0$ in 2.3a for W = W2. Substituting $P = \tilde{P}(Z)$ in the equation for S and integrating gives, after J days:

$$S = S0 - Z.W^{0.7}.S1$$

where $Z.W^{0.7}$ is evaluated at the beginning of the reproductive period and

$$S0 = V.R0.J.(0.7.C-E)/(C-E.U) ,$$
$$S1 = F.C.(1.-0.7.U) . (1.-\exp(-GX.J)) / ((C-E.U).GX) .$$

But according to the approximate treatment of growth, $Z.W^{0.7} = ZO^{g}.WO^{0.7}$ where ZO^{g} is the initial size of the gth cohort. Using equation 2.1e, it follows that

$$ZO^{g+1} = S0.X/W0 - ZO^{g}.S1.X/W0^{0.3} . \qquad 2.5$$

This constitutes a difference equation for ZO^{g}. If the coefficient of ZO^{g} in equation 2.5 is less than 1 in magnitude, the equation has a stable constant solution ZO^{*} and, according to

this approximate theory, there is a corresponding stable cyclic solution of the phytoplankton-zooplankton system 2.2. If the coefficient is greater than 1 in magnitude, ZO^* is unstable and a stable cyclic solution to 2.2 having constant amplitude cannot be expected. This coefficient is proportional to the basal metabolic rate, F.

2.3 Simulation Results.

The approximate theory predicts a stable cyclic solution to Steele's model under conditions of nutrient-limitation without any need for thresholds or quadratic predation terms. This is in keeping with the results of Chapter 1 but somewhat surprising in view of Steele's simulation results. The prediction has been tested by computer simulation of both the simplified phytoplankton-zooplankton model 2.2 and the full model 2.1 for the simplest case of no thresholds, constant mortality rate and fixed metabolic rate (Pl=E=GW=O).

The first set of simulations were obtained by fixing the metabolic rate F and varying the mortality rate GX in the simplified model 2.2. For F = 0.4 and GX ranging from 0.02 to 0.06 day^{-1}, stable cyclic solutions were approached with generation time decreasing as GX increased, in qualitative agreement with the slow-variable theory. However, quantitative agreement between simulated generation times and those predicted according to 2.4 is not particularly good (Fig 9). Part of the explanation for the poor agreement can be seen in Fig 10a, where a simulated cycle is portrayed. The phytoplankton density is far from being constant over the period of copepod growth, due partly

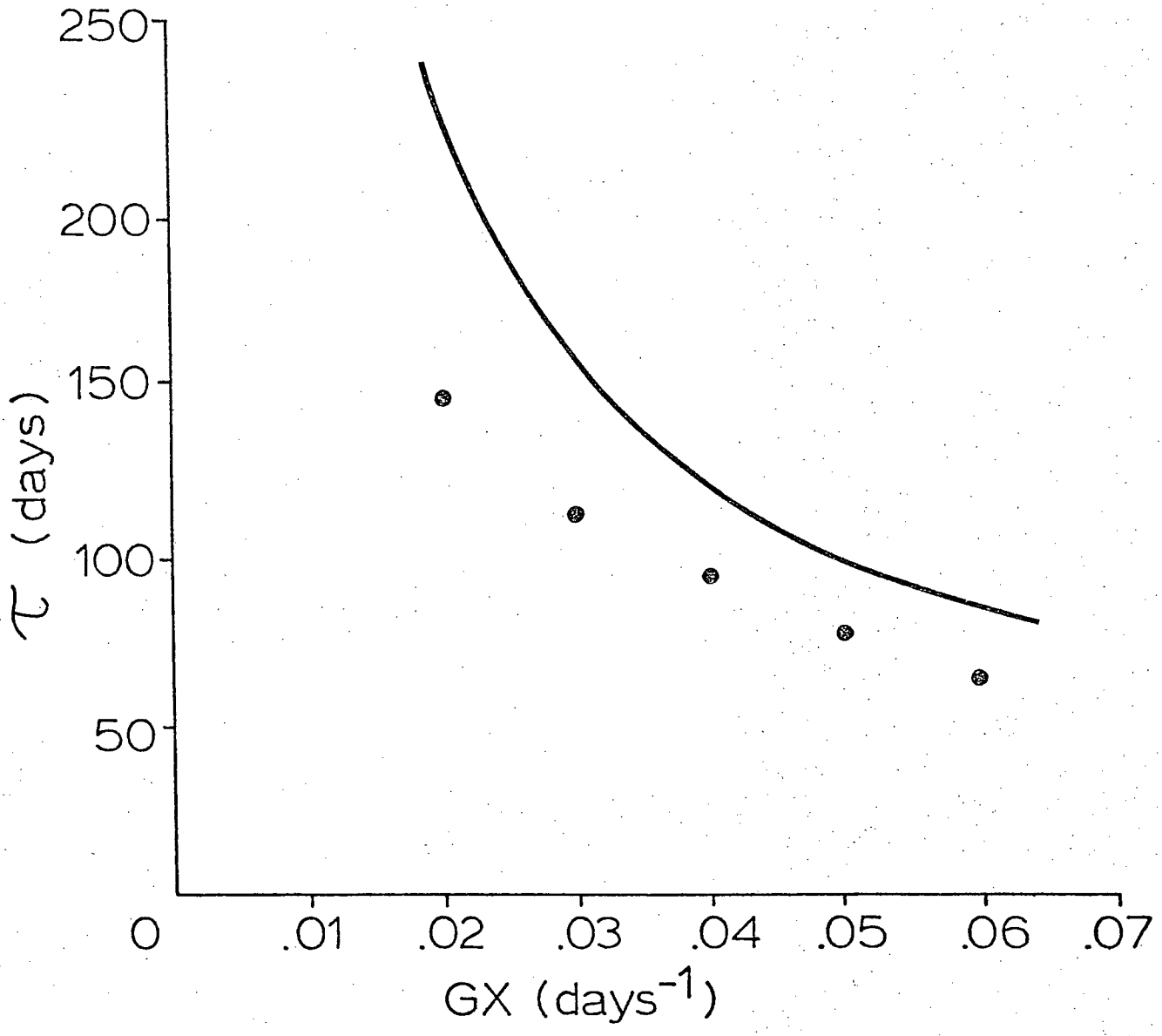

Figure 9. Comparison of generation times predicted by equation 2.4 (solid line) and those obtained in numerical solutions of the system 2.2 (dots).

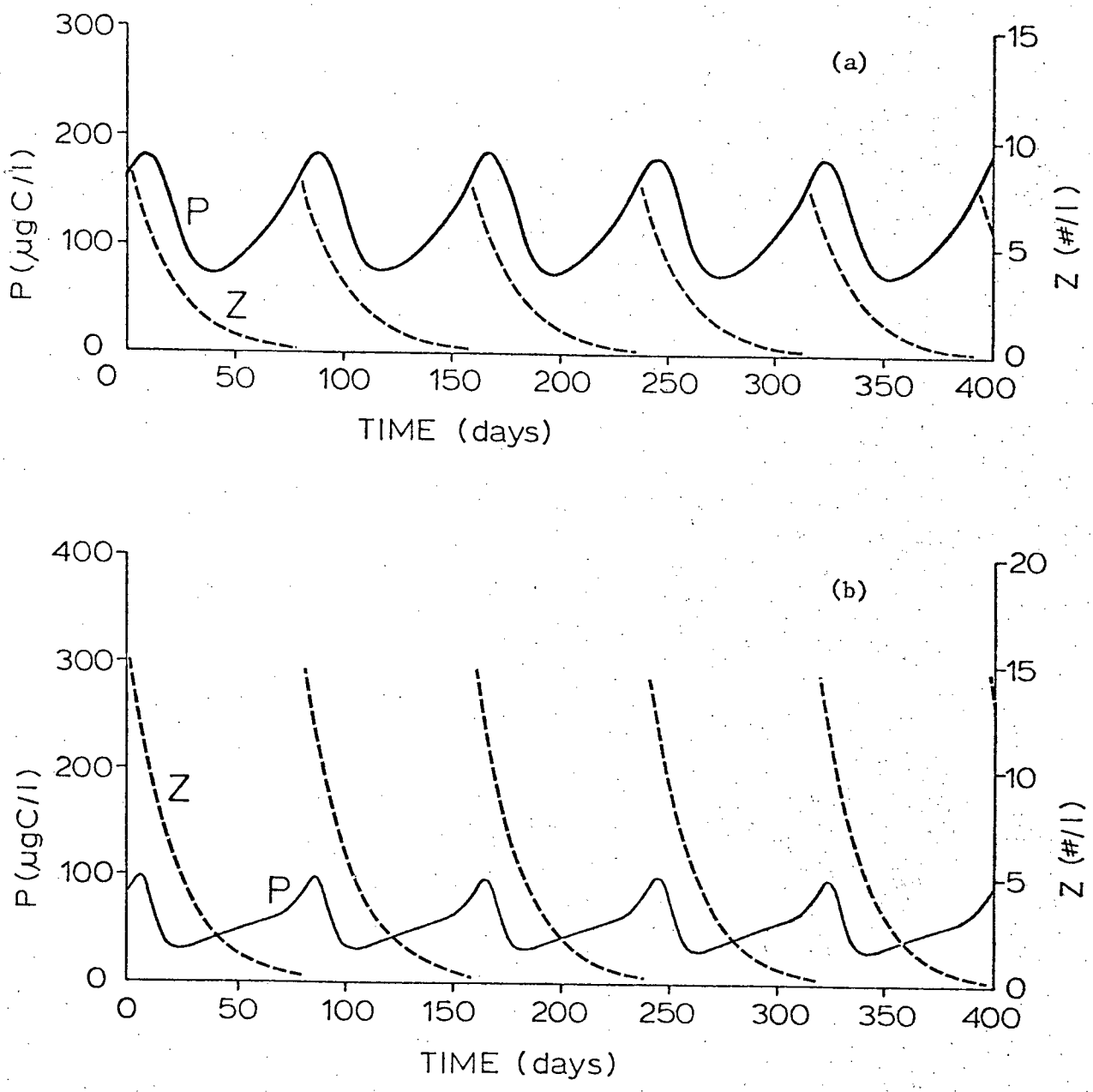

Figure 10. Stable cyclic solutions of the system 2.2 for:

(a) F=0.4, GX=0.05; (b) F=0.2, GX=0.05.

to the limitations of the slow-variable approximation and partly to the perturbation imposed by the release of nauplii at the end of each reproductive period.

In spite of this, further qualitative agreement between the approximate theory and simulation was found. When F is decreased to 0.2, the cycle period is not affected, but, as shown in Fig 10b, the simulated cycle involves lower P and higher ZO, as predicted by the slow-variable theory. Also, increasing F to 0.6 in the simulation results in an approach to a rather curious cycle involving alternately high and low naupliar recruitments (Fig 10c). This behaviour corresponds in the approximate theory to a stable solution of period 2 in the difference equation 2.5, ZO^* having been destabilized by increasing F. The phenomenon of periodic and aperiodic solutions to difference equations in simple ecological models has aroused considerable interest (eg May,1975).

The validity of using the fast-variable assumption to eliminate nutrients has been tested by computer simulation of Steele's full model 2.1. For F = 0.4, GX = 0.05 day^{-1} and low B (10 μg C(eq).l^{-1}), numerical solutions of the full model approach a stable cyclic solution (Fig 11a), which is almost identical to that obtained from system 2.2 (Fig 10a). Throughout the cycle, R remains low (of order B) and the fast-variable approximation is quite accurate. However, it can be violated in a number of ways. For example, if F is reduced to 0.2, with other parameters unchanged, large, diverging oscillations in R, P and Z appear (Fig 11b). The explanation for this can be found in the nutrient equation 2.1a and the fact that, for F=0.2, the cyclic solution

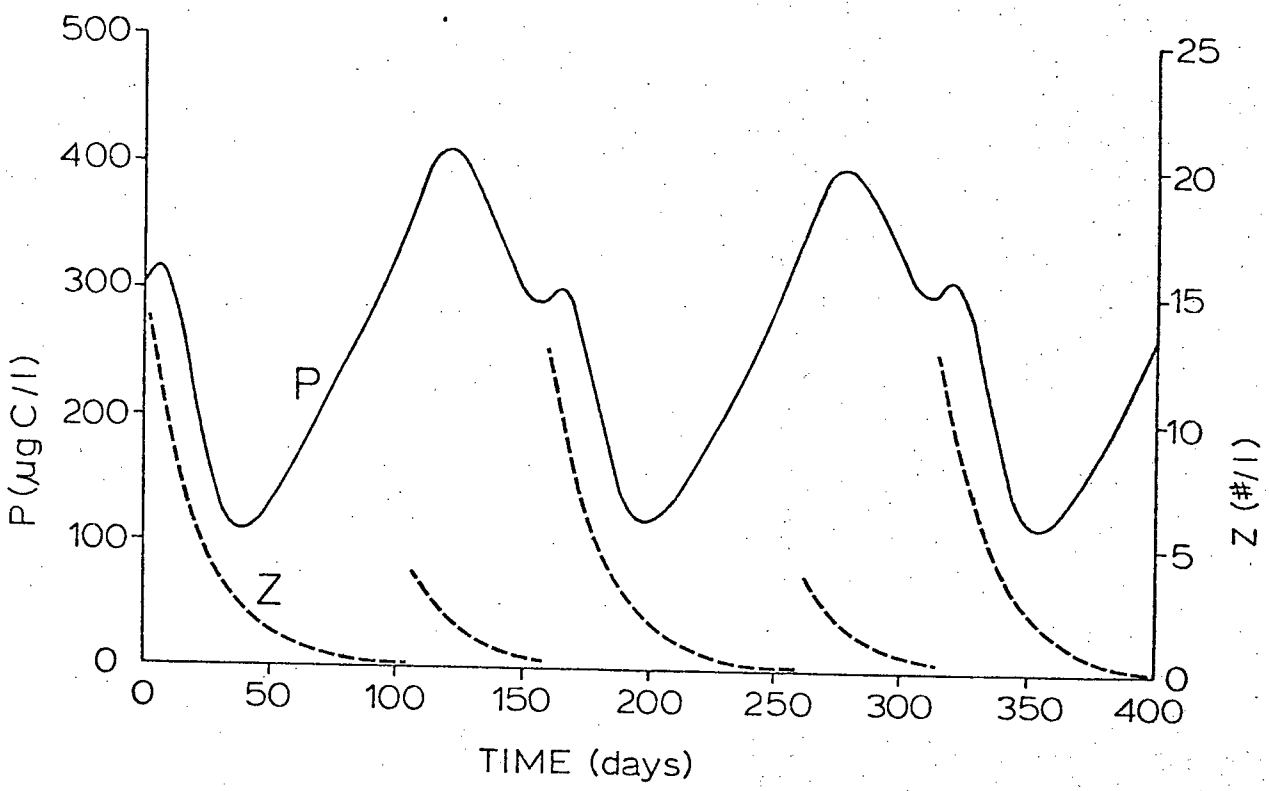

Figure 10c. Stable cyclic solution of the system 2.2 for F=0.6, GX=0.05.

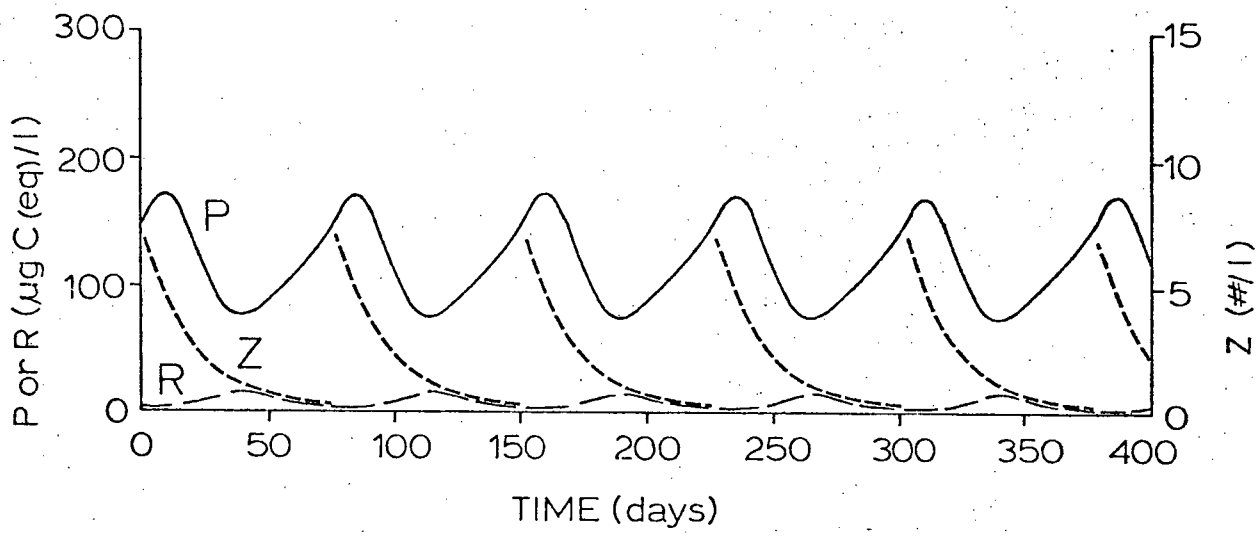

Figure 11a. Stable cyclic solution of the system 2.1 for F=0.4, GX=0.05 and B=10.

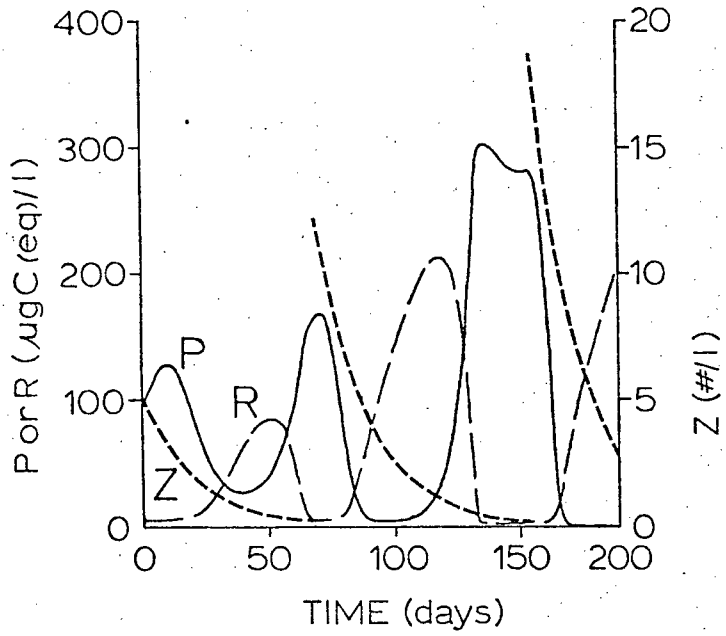

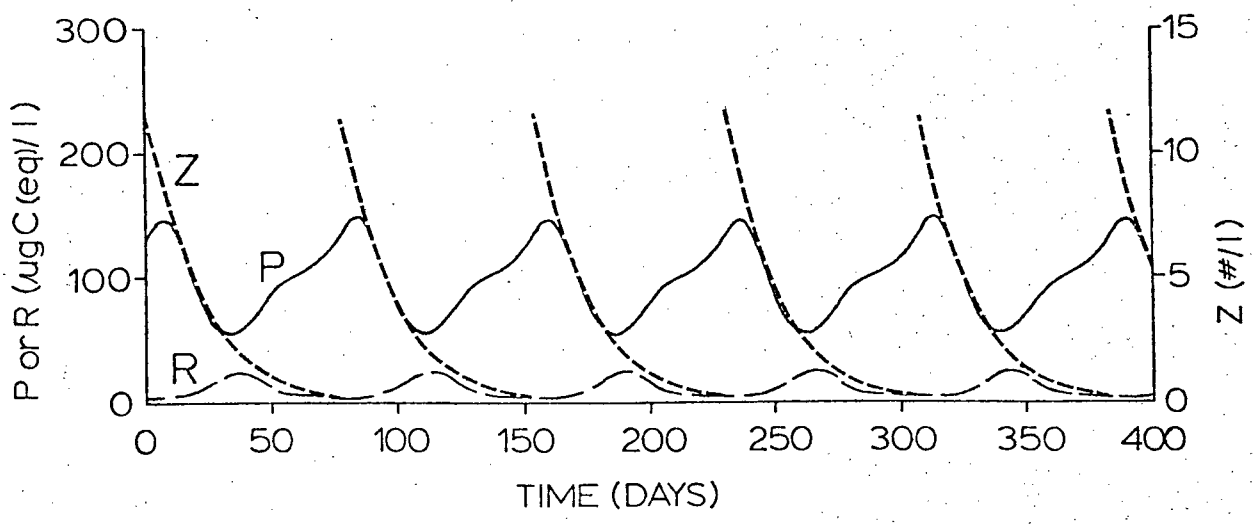

Figure 11b,c. Behaviour of the system 2.1 for F=0.2, GX=0.05 and B=10 with: (b) D=100. (unstable oscillations) and (c) D=175. (stable cycle).

predicted under the fast-variable approximation (Fig 10b) involves low phytoplankton concentrations. Nutrient uptake by the phytoplankton is non-linear in R with a maximum value of A.P. Thus, if P is too small, phytoplankton uptake cannot match the mixing input V.RO and the equilibrium solution R(P,Z) switches from a low value (of order B) determined by phytoplankton uptake, to a high value (of order RO) determined by mixing losses. The fast-variable assumption for nutrients is of course no longer valid and, in the computer simulation, the instability associated with the phytoplankton-zooplankton interaction appears to dominate.

This explanation suggests a number of ways to recover stable cycles for low F. A sufficient decrease in the rate of nutrient input, V.RO, or increase in maximum growth rate, A, will prevent nutrient build-up. Changes can also be made in other parameters which increase P, compensating for the decrease in F. For example, $\bar{P}$ is scaled by the grazing half-saturation constant, D. When D is increased from 100 to 175 $\mu g\ C.l^{-1}$, (the value used by Landry), the solution of the full model for F=0.2 (Fig 11c) approaches the stable cyclic solution predicted by the fast-variable model 2.2 (Fig 10b).

An obvious way to violate the fast-variable assumption is to increase B. If Steele's value for B of 96 $\mu g\ C(eq).l^{-1}$ is adopted, the time scale for changes in nutrient becomes comparable to that of changes in phytoplankton and the preceding approximate treatment cannot be applied. In fact, for F=0.4,GX = 0.05 and D = 100 $\mu g\ C.l^{-1}$, rapidly diverging oscillations in P and R are obtained in numerical solutions on increasing B to 96.

A stable cyclic solution can be recovered by increasing D to 175 $\mu g\ C.l^{-1}$, this solution being characterised by consistently high P and low R/B.

Another approach which appears to be useful in interpreting these numerical results is to compare them with analytic results from a more mathematically tractable model obtained by dropping the copepod age structure:

$$\dot{R} = V.RO - A.R.P/(B+R) + U.F.G \qquad 2.6a$$

$$\dot{P} = A.R.P/(B+R) - G.C.f(P) \qquad 2.6b$$

$$\dot{G} = 0.7.G.C.f(P) - m.G \qquad 2.6c$$

where G is copepod biomass.

This system possesses a non-trivial equilibrium solution $(\hat{R},\hat{P},\hat{G})$ determined by

$$f(\hat{P}) = m/(0.7.C)$$

$$\hat{G} = 0.7.V.R0/(m-0.7.U.F)$$

$$A.\hat{R}.\hat{P}/(B+\hat{R}) = V.R0.m/(m-0.7.U.F).$$

A Taylor-series expansion about this equilibrium yields the linear system

$$\begin{pmatrix} \dot{\delta R} \\ \delta P \\ \delta G \end{pmatrix} = \mathcal{G}. \begin{pmatrix} \delta R \\ \delta P \\ \delta G \end{pmatrix}$$

where the constant matrix $\mathcal{G}$ has trace

$$\sum c_{ii} = -A.B.\hat{P}/(B+\hat{R}) + \hat{G}.C.(f(\hat{P})/\hat{P} - f'(\hat{P})) . \qquad 2.7$$

It is well-known that a necessary condition for the local stability of $(\hat{R},\hat{P},\hat{G})$ is that $\sum c_{ii}$ be negative. In the absence of thresholds (Pl = 0), the second term in 2.7 is positive; this is the destabilizing effect of the type II functional response (Holling,1965). The first term is negative and represents the stabilizing effect of nutrient limitation. If B is increased with the other parameters in 2.6 held constant, the first term decreases like 1/B while the second term remains constant; thus increasing B tends to destabilize the system. If D is increased and the other parameters held constant, it can also be shown that the second term decreases like 1/D while the first term increases in magnitude, so that increasing D tends to stabilize the system. This is consistent with the simulation results reported above for Steele's model.

This concludes the analysis of the nutrient limited period. Before proceeding, it seems advisable to summarise the results obtained so far. By use of a series of approximations based on the recognition of fast and slow time scales, stable cyclic solutions to Steele's model have been predicted in the absence of thresholds and for constant per capita mortality rate and fixed metabolic rate. Computer simulation has shown that these solutions do exist but are restricted to a region in parameter space for which the stabilizing effects of nutrient limitation outweigh the destabilizing effects of the saturating type II functional response of the copepods.

Of course, Steele demanded of his model that it reproduce

the qualitative features characteristic of the observed seasonal cycle in the North Sea, starting from a prescribed set of initial conditions corresponding to the initiation of the spring bloom. The existence of a stable cyclic solution for a particular set of parameters in no way guarantees that the transient approach to this cycle from the prescribed initial conditions will satisfy Steele's criteria. In fact, if the values B = 10 μg C(eq).l^{-1}, F = 0.4, D = 100 μg C.l^{-1} and GX = 0.05 day^{-1}, corresponding to the stable cycle of Fig 11a, are used together with Steele's initial conditions, the resulting simulation is most unrealistic (Fig 12a). During the spring bloom, a large cohort of copepods is produced. Individual copepods initially see high phytoplankton concentrations and grow rapidly, quickly producing a very high grazing pressure on the phytoplankton. The phytoplankton concentration declines quickly and during the prolonged period of low P which follows, the copepods starve in an impressive but rather unrealistic manner, the constant metabolic rate reducing their weight to zero by day 54.

To prevent this from happening, it is obviously necessary to reduce this burst of intense grazing pressure. One way to do this is to introduce a predation term which results in high copepod mortality rates when copepod numbers are high, thereby rapidly reducing the size of this large second cohort. This appears to be the primary role of Landry's quadratic predation term; any stabilizing effect of this term in the later nutrient-limited regime is of secondary importance. Another alternative is to set a maximum limit on cohort size in the manner of Steele and Mullin (1977), who made ZO a hyperbolic function of

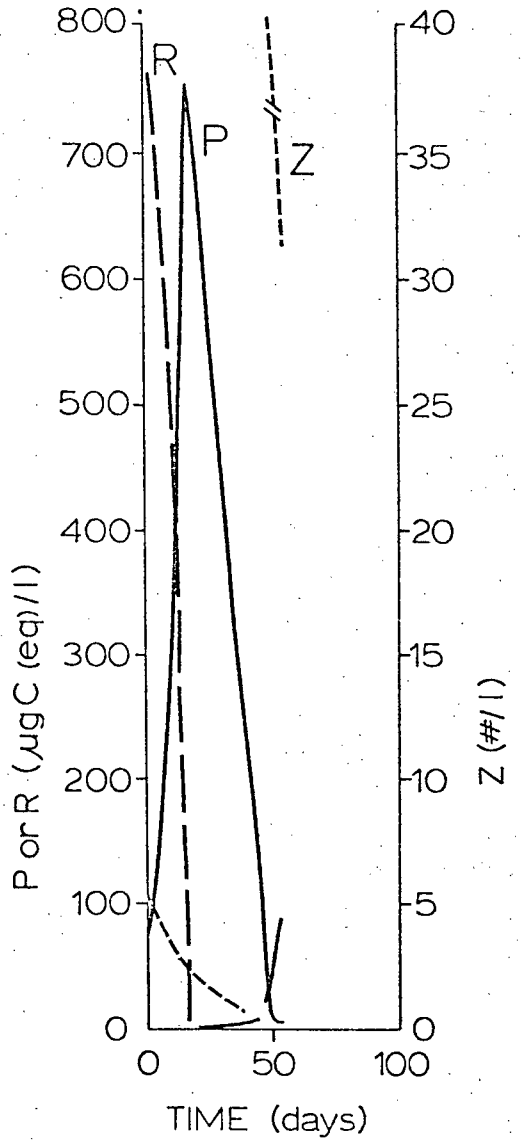

Figure 12a. Attempted simulation of spring bloom using the system 2.1 with B=10, F=0.4, D=100 and GX=0.05.

reproductive store, S.

A third alternative is to increase the half-saturation constant for grazing, thereby reducing grazing pressure at low phytoplankton densities. This has already been done by Landry, who increased D from 100 to 175 $\mu g\ C.l^{-1}$. If the same change is made to the simulation described above, the result is much improved (Fig 12b). Phytoplankton depletion is less pronounced and of shorter duration and a rapid approach to the stable cyclic solution occurs. Unfortunately, weight loss following the spring bloom is still unrealistically high, individuals being reduced from more than 3 μg C to less than 0.35 μg C by starvation. It is possible to do much better than this without adopting thresholds or Landry's predation term. In Fig 12c, the results of a simulation using F=0.5,GX=0.04, B=10 and D=175 are presented. The period of phytoplankton depletion is reduced to the extent that copepod weight loss following the spring bloom is only about 50%. The final simulation (Fig 12d) uses an even larger value of D (250 $\mu g\ C.l^{-1}$) and Landry's combination ingestion-dependent and constant metabolic rate (E=0.3, F=0.2). The resulting copepod weight loss following the spring bloom is limited to less than 25%.

2.4 Conclusions.

Perhaps the most striking result of this review of Steele's simulation model is that 'realistic' imitations of the seasonal plankton cycle in the North Sea can be obtained from the model without invoking thresholds in herbivore grazing or quadratic predation terms. This of course does not establish that

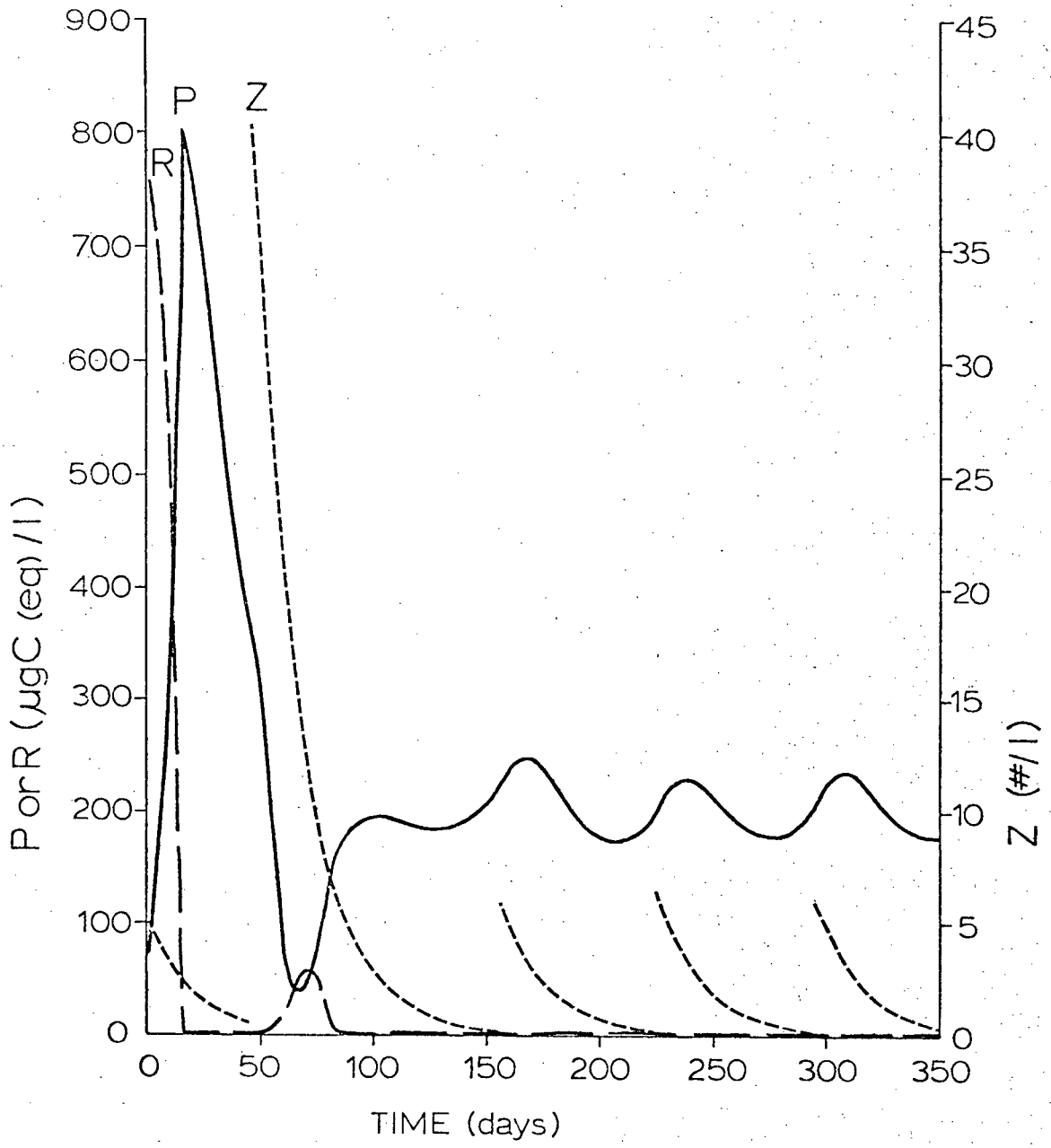

Figure 12b. Simulation of spring and summer with parameters used for Fig 12a except D=175.

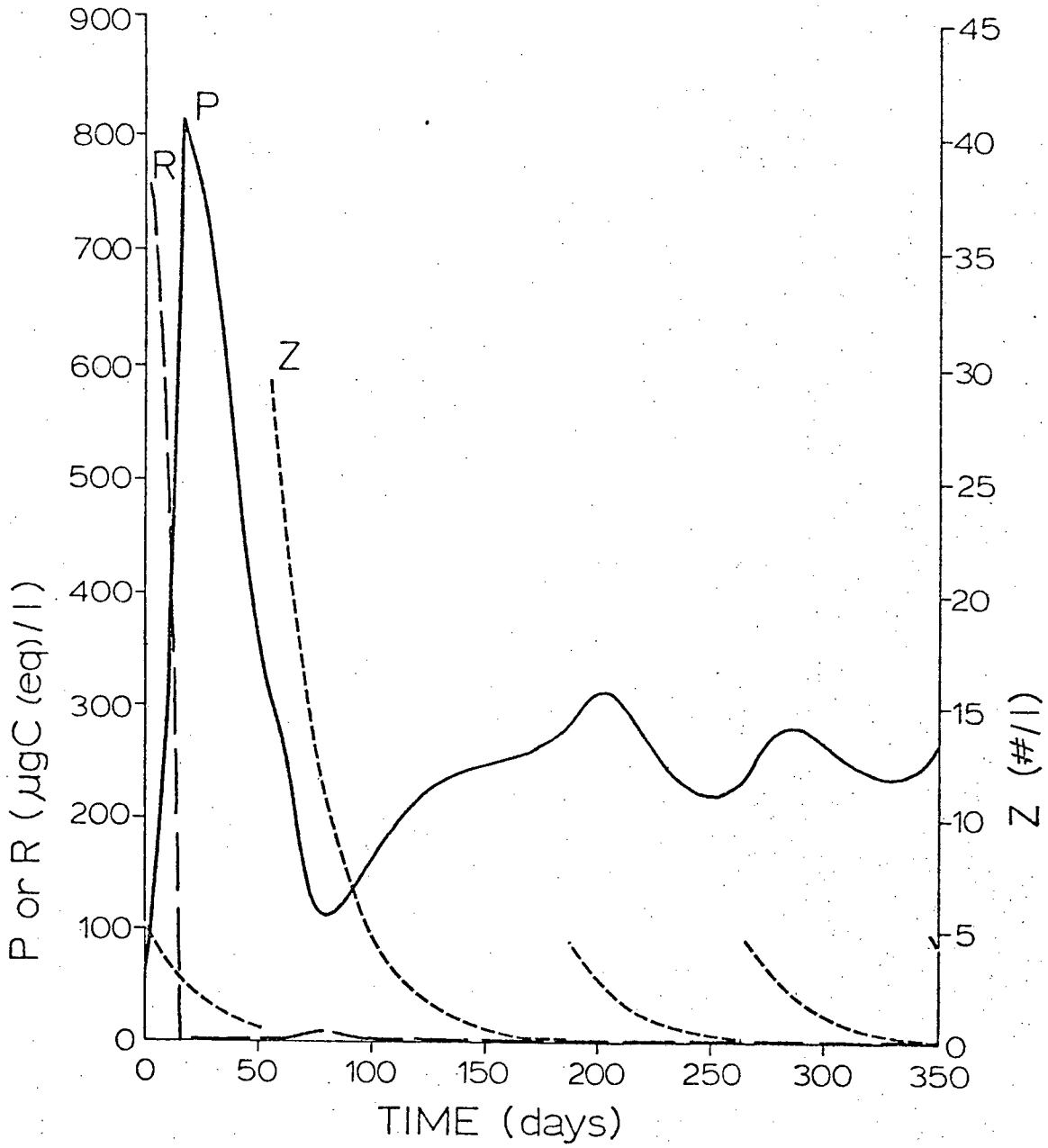

Figure 12c. As for Fig 12b except GX=0.04.

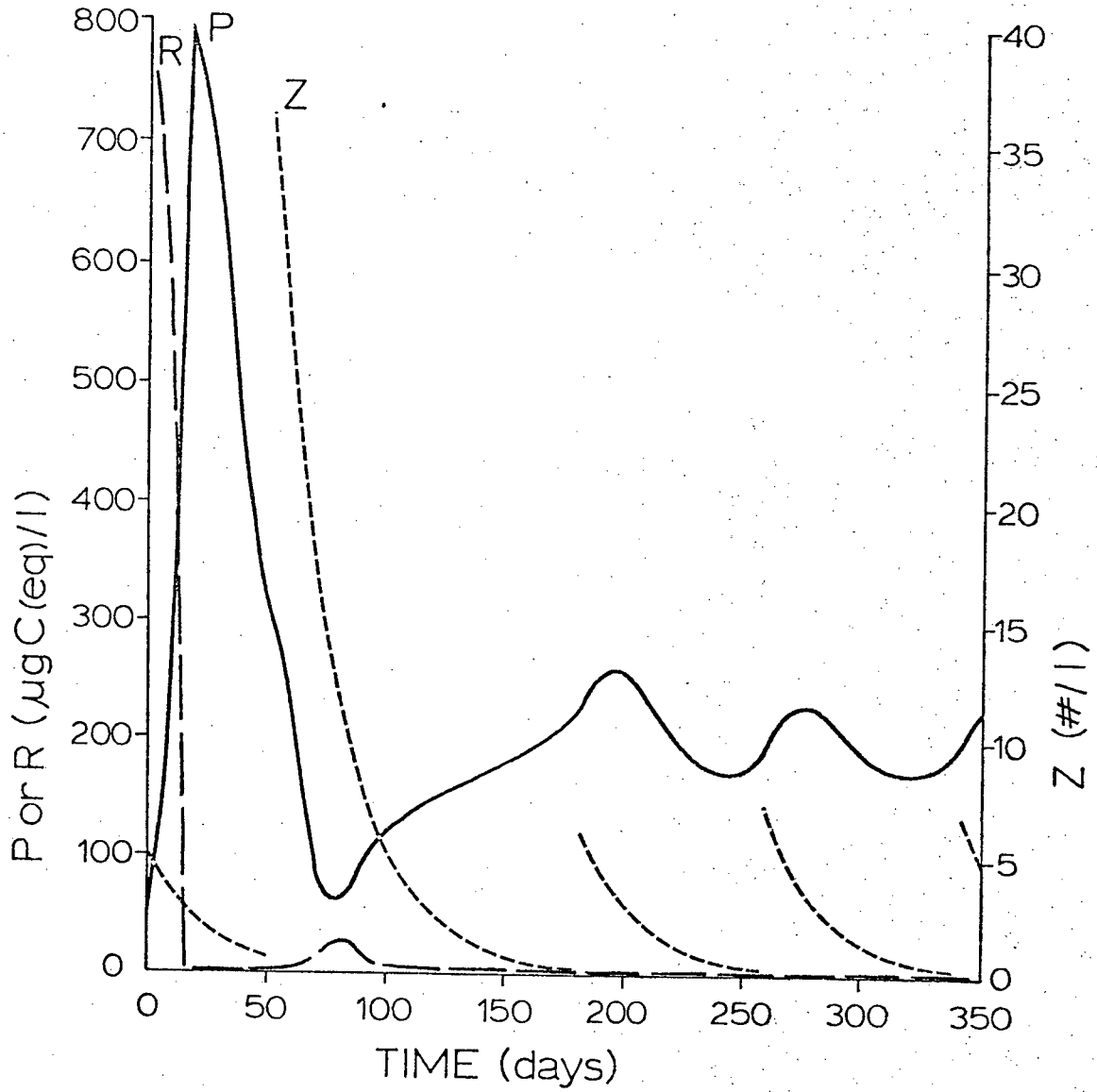

Figure 12d. Simulation of spring and summer with F=0.2, E=0.3, GX=0.05 and D=250.

thresholds or quadratic predation are not present and important in the North Sea ecosystem, although it weakens any argument for their existence based on their necessity in Steele's model. In fact, there appears to be better experimental evidence now for the existence of threshold-type phenomena, at least in some species of copepods (Frost,1975), and the assumption of a constant per capita mortality rate for copepods is certainly no more satisfactory a way of truncating the food chain than using Landry's predation term.

The preceding results do illustrate the advantages of the qualitative analysis of complex ecological models, wherever this is possible. The analysis conducted here, although approximate and incomplete, led to the discovery of stable cyclic solutions in the nutrient-limited regime in the absence of thresholds and quadratic mortality. These exist over a limited region of parameter space and might not have been found at all by simply trying various parameter combinations in computer simulations. The interactions between parameters which were revealed by the qualitative analysis testify to the inadequacy of standard sensitivity analyses in which parameters are varied one at a time. For example, if the half-saturation constant for grazing is large enough, stable cyclic solutions exist over a wide range of values of B, at least $0 < B < 100$ $\mu g\ C(eq).l^{-1}$. However, if D is lower, stable solutions only exist for B small and it could be concluded that the value of B in nature is critical. Steele's simulation results were insensitive to changes in B, but thresholds in grazing and predation were already in force. He did not obtain reasonable results when the thresholds were

omitted due partly to the values assumed for B and D.

The insight into Steele's model obtained here suggests a broader approach to the biological question of herbivore response to low food concentrations, including the matter of thresholds. The major problem encountered here in obtaining a realistic seasonal pattern from Steele's model involves the transient response rather than stability; of the region of parameter space allowing stable cyclic solutions, only a small sub-region allows a realistic approach to this cycle from initial conditions of high nutrient. As was explained earlier, the difficulty lies in the unrealistic weight losses which can occur in the post-bloom period of phytoplankton depletion due to the assumption of a high basal metabolic rate.

Steele avoided this difficulty in his standard simulation by assuming a threshold in grazing (thereby preventing extreme depletion of phytoplankton) and a metabolic rate entirely proportional to ingestion (zero basal metabolism), so that copepod weight loss was impossible. (When a non-zero basal metabolic rate was adopted in one of Steele's trial simulations, copepod weight loss did occur and the result was consequently dismissed as unrealistic). In a later, more detailed analysis of the energy budget and optimal feeding response of copepods, Steele and Frost (1977) concluded that there is an important component of metabolism proportional to filtering rate, not ingestion rate. However, the optimal feeding response they obtained is roughly consistent with Steele's (1974) assumption as both involve reduced filtering rate at low food densities and non-negative growth at all food densities.

Steele and Frost's argument does imply that an organism which does not behave optimally, and instead maintains a high filtering rate at low food densities, will be subject there to a high metabolic cost and rapid loss of body weight. This is equivalent to an assumption of no threshold and a high basal metabolism in Steele's (1974) model. Obviously, this weight loss, which will be especially severe for small individuals according to the $W^{0.7}$ metabolic law, cannot continue indefinitely. There appear to be two extreme outcomes possible.

One possibility is that, as its body condition deteriorates, the organism's filtering rate and consequently its metabolic rate will decrease. Provided this occurs on a short-enough time scale (most likely for small organisms), this physiological response will have the same effect in the simulation model as an 'optimal' behavioural response or a threshold. This possibility may have been envisaged by Steele (1974), when he mentioned that responses to food concentrations might occur on several time scales. An important point is that the physiological response would not be observed in short-term grazing experiments of the type commonly conducted over 24 hours or less using large, late-stage copepods collected in the field (Marshall,1973). Effects of food concentration and duration (up to 5 days) of pre-conditioning on functional response parameters have been reported for fresh-water crustaceans (Buckingham,1978).

The second possibility is that the individual continues to filter and lose weight at maximum rates until weight loss exceeds some maximum permissable amount, when the organism dies. In the highly simplified single cohort version of Steele's model, the

entire cohort will die simultaneously. In a more realistic multi-cohort version, as presented by Landry (1976), or one involving differences in growth rate between individuals, as reported even in laboratory cultures under homogeneous conditions (Paffenhoffer and Harris,1976), starvation mortality will lead to a decrease in grazing pressure on the phytoplankton and, at least for small zooplankton, may have a similar qualitative effect to a grazing threshold.

Thus all three types of response to low food densities (the short-term behavioural response, the longer-term physiological response and starvation mortality) could ensure reasonable transient behaviour in Steele's model. The actual response, which probably lies somewhere between these extremes, may be important in other circumstances,such as the Subarctic Pacific, and its experimental definition appears to be a challenging and valuable goal. Most of the current experimental approaches address only one aspect. The short-term grazing experiments referred to above can consider only the behavioural response. There have been a number of laboratory studies of respiration rates and weight loss in starved individuals (Reeve et al ,1970; Ikeda,1977). Again, most of the studies have been conducted on late-stage individuals, and any physiological effect of weight loss on filtering rate cannot be measured in starved individuals, while measurements of respiration rates are open to the problems of interpretation discussed by Steele(1974). It is interesting to note that Checkley (1980) has reported mean survival times for Paracalanus parvus females without food to be 4-5 days so that starvation mortality could be a significant factor, at least for

small copepods without fat stores. It is obviously not an important consideration for the late stages of larger species such as Calanus plumchrus which build up extensive fat stores (Fulton,1973).

The experimental procedures most likely to resolve this question appear to be those reported by Paffenhoffer (1970), and reviewed by Paffenhoffer and Harris(1979), for studying growth, mortality and clearance rates over the entire copepod life cycle in laboratory cultures. Increased mortality has been reported for Calanus pacificus and Temora longicornus at low food densities (about 20 μg $C.l^{-1}$), although these food densities were still sufficient to allow growth at close to maximum rates (Paffenhoffer,1970; Paffenhoffer and Harris,1976). It would certainly be interesting to see these experiments repeated at even lower food densities.

CHAPTER 3

PHYTOPLANKTON AT O.S.P.: DATA ANALYSIS AND MODELLING

3.1 Introduction

The aim in this chapter is to develop a realistic model of phytoplankton growth at O.S.P. The model is based primarily on an analysis of data collected from the weatherships at O.S.P. and the level of detail considered has been chosen to match these observations. The underlying structure of the model is adapted from the literature, as are certain parameter values which cannot be inferred from the data. The model is used only to predict net primary production from a fixed standing stock in this chapter, but is constructed in such a way that it can easily be extended to include grazers in Chapter 4, where the qualitative hypotheses raised in Chapter 1 will be addressed quantitatively.

3.2 Data Analysis

3.2.1 Description of the Data Set.

Weathership observations related to phytoplankton for the years 1964 to 1976 have been published in manuscript form (Stephens,1966; Stephens,1968; Stephens,1970; Stephens,1977). Variables measured include Secchi depth, chlorophyll a, ^{14}C uptake rates and nitrate concentration. Chlorophylls b and c were measured starting in 1969. The data record consists of approximately 200 depth profiles and an additional 600 surface observations, although not all variables were necessarily measured on all days or at all depths.

There are certain peculiarities to the sampling regime which

can be seen in the scatter plot of surface chlorophyll concentrations given in Fig 13. From 1964 to 1968, observations were made from only one of the two weatherships, resulting in a series of 6 week gaps in the time series. While on station, surface samples were collected every second day, more or less regularly. After 1968, observations were made from both weatherships, but the sampling frequency dropped to one to six observations per 6 week cruise. Usually one or two profiles were taken on each cruise.

3.2.2 Chlorophyll Data.

The concentration of chlorophyll a has been routinely measured from the weathership at O.S.P. and is the principal indicator of phytoplankton standing stock. The surface values plotted in Fig 13 are generally representative of the mixed layer described in Chapter 1. It is clear from Fig 13 that chlorophyll a at O.S.P. tends to be uniformly low: less than 1 μg Chl $a.l^{-1}$ in all but a few observations. This feature of the Subarctic Pacific has been remarked upon by many researchers (Semina,1958; Heinrich,1962; Parsons,1965) and is in sharp contrast to the classic spring bloom seen in other temperate planktonic ecosystems such as the Strait of Georgia (Parsons,1965), the North Sea (Steele,1974) and the North Atlantic (Cushing,1959).

Exceptions to the rule of constancy can be seen in Fig 13: scattered high values, from 1 to 4 μg Chl $a.l^{-1}$ were observed in 1964,1965,1969,1972 and 1975. In 1964,1965 and 1969, these high values occur in small groups, a pattern consistent with a short-lived bloom (of low intensity compared with coastal blooms (eg Parsons,1965)), or with the advection of a 'patch' past the

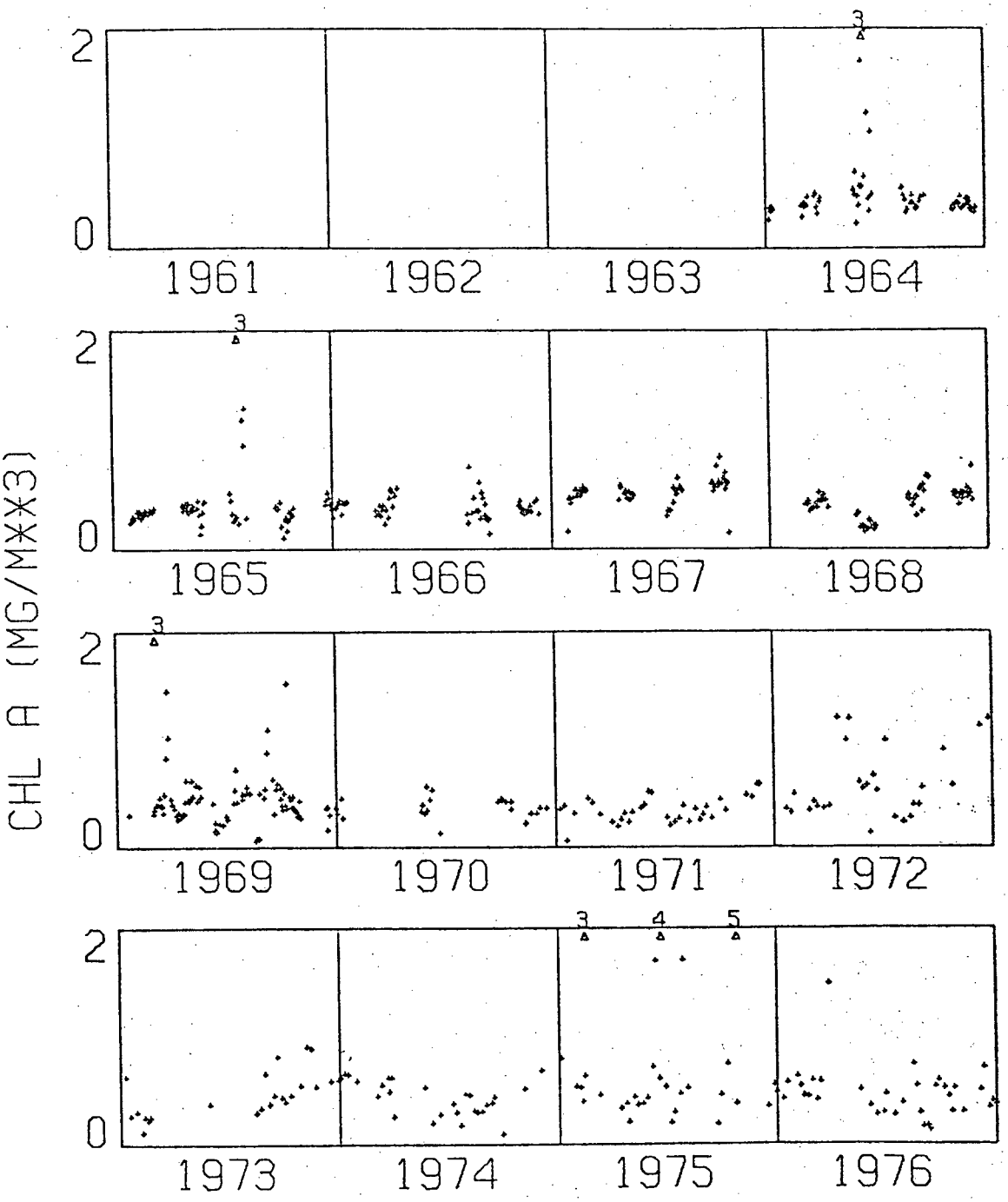

Figure 13. Surface observations of chlorophyll a from the weatherships at O.S.P. (Triangles denote high values, given to nearest integer by digit above.)

station. The high observations in 1975 are isolated but the sampling frequency is low there, so that only one observation might be expected to coincide with a short-lived bloom.

The implications of these high observations for theories of phytoplankton regulation in the Subarctic Pacific will be discussed later. Any seasonal or annual pattern in their occurrence would be of interest, but it is clear from Fig 13 that the sampling intensity is not sufficient to reveal such a pattern. High values occur in June,1964, July and August,1965, March and September,1969, April and December,1972 and January, June, July and October,1975, revealing no consistent seasonal pattern. Gaps in the time series are such that high values could have easily been missed in other months or years.

Any consistent low-amplitude seasonal pattern in the background Chl a values could also be of interest. Annual and seasonal contributions to variability in a time series can be distinguished by performing a running annual average and looking for seasonal variation in the residuals (Kendall,1973). (The word 'annual' is used here, following Kendall (1973), to denote year to year variations. These may be referred to as inter-annual variations by some authors. The seasonal patterns discussed here are shorter term fluctuations of 12 month period.) Two problems prevent such a straight-forward approach to these data. One is that the occasional high values contribute overwhelmingly to the variance and will dominate any resulting pattern. This has been overcome here by looking for a seasonal pattern in the six week cruise medians, plotted in Fig 14a,c. The second problem is that the presence of irregular gaps in the

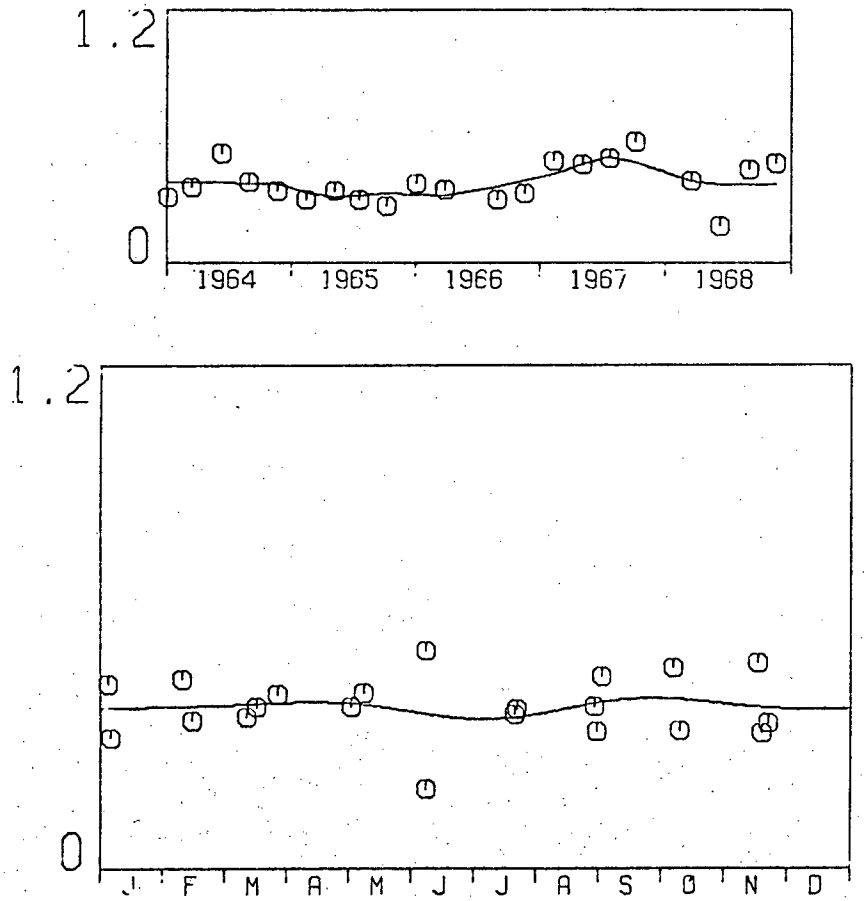

Figure 14. Surface chlorophyll a ($mg.m^{-3}$): (a) Cruise medians and annual smooth for 1964-68. (b) Seasonal fit plus residuals for 1964-68.

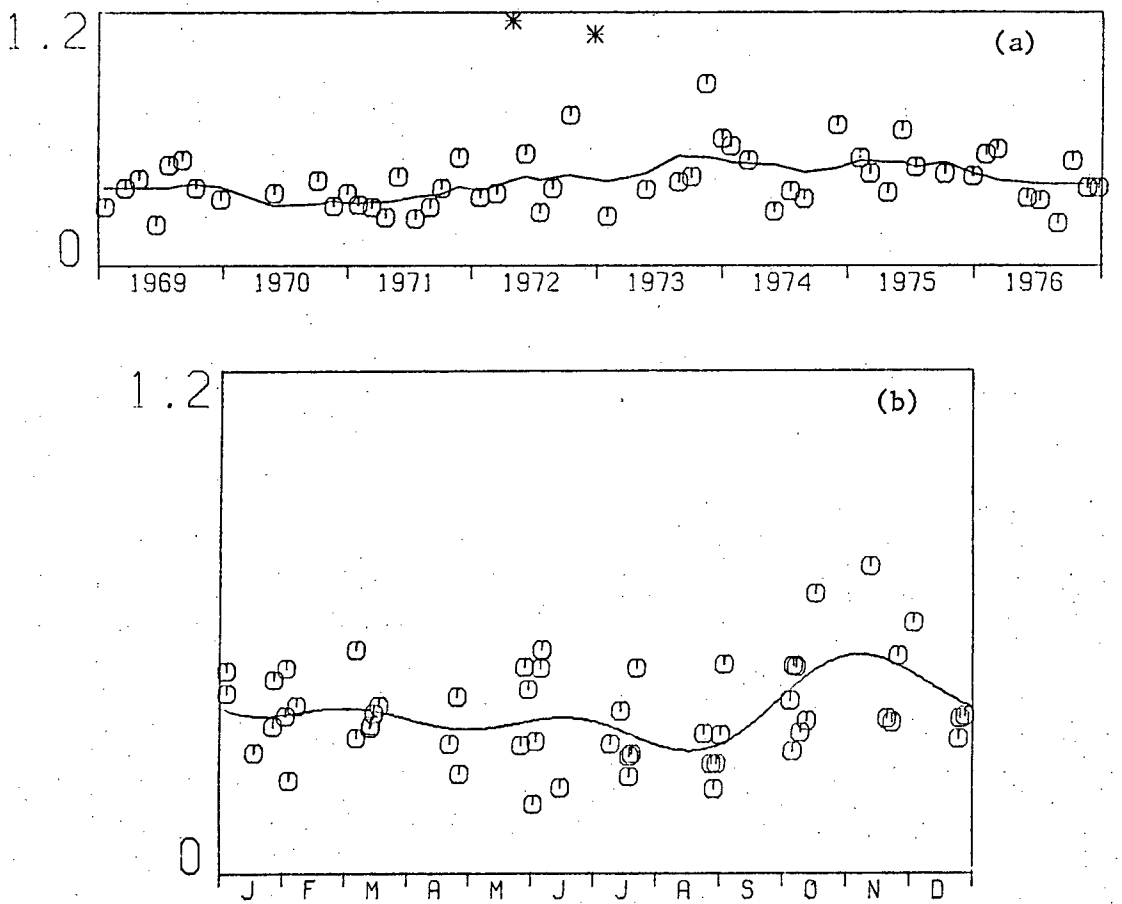

Figure 14. Surface chlorophyll a ($mg.m^{-3}$): (c) Cruise medians and annual smooth for 1969-76. (d) Seasonal fit plus residuals for 1969-76.

time series will lead to confusion of annual and seasonal contributions to variation. This is a similar problem to the two-way analysis of variance with empty blocks. A solution to the latter problem, suggested by Mosteller and Tukey(1977), is to iterate.

The procedure they describe has been adapted to the time series problem as follows. An annual smoothing (moving window of width one year) is applied to the time series and the first three seasonal harmonics (period one year, one-half year and one-third year) are least-squares fitted to the residuals. The residuals from the seasonal fit are then added back to the annual smooth and re-smoothed; the resulting residuals are added back to the seasonal fit and the seasonal harmonics are refitted. This procedure is repeated until no further change occurs in annual smooth or seasonal harmonics. (The same final results are of course obtained if the seasonal fit is applied first). The procedure is equivalent to assuming a model for observations of the form:

$$Y(t) = Y_A(t) + Y_S(t) + e(t)$$

where $Y_A(t)$ represents an annual effect, $Y_S(t)$ a seasonal effect (repeated each year) and e(t) a residual effect, and choosing annual and seasonal components so as to minimize the sum of squares of unexplained residuals.

In the case of Chl a, the final annual and seasonal components accounted for 19% and 12% respectively of the original SSQ about the mean. Because of the gaps in the time series, no

attempt has been made to test for significance of these components. The estimated standard deviation of residuals is 0.12 μg Chl $a.l^{-1}$ compared with a seasonal cycle amplitude of 0.2 μg Chl $a.l^{-1}$. This cycle arises almost entirely from the second half of the time series. When the procedure is applied to the periods 1964-1968 and 1969-1976 separately, the seasonal cycle for the first period has much lower amplitude (0.04 μg Chl $a.l^{-1}$) and explains only 1.5% of the SSQ about the mean (Fig 14).

Concentrations of Chl b and Chl c, measured after 1968, potentially contain information about the taxonomic composition of the phytoplankton. Scatter plots of the ratios Chl b/Chl a and Chl c/Chl a are given in Fig 15. Seasonal and annual patterns were sought among cruise medians of these ratios using the procedure already described for Chl a. The seasonal 'cycle' found for the Chl b/Chl a ratio is of very small amplitude, explaining only 4% of the SSQ about the mean. The annual smooth explained 44% of the SSQ and varied from a low of 0.28 in 1969 to a high of 0.83 in 1975 (Fig 16).

The seasonal cycle obtained for Chl c/Chl a (Fig 17) explained 11% of the SSQ about the mean, while the annual smooth explained 30%. The average value of Chl c/Chl a was 1.6, compared with 0.6 for Chl b/Chl a, both ratios showing an increasing trend throughout the period of observations.

3.2.3 ^{14}C Data.

Primary productivity has been routinely measured at O.S.P. since 1964. Incubations were usually conducted from noon to 1800 h (local time) and average uptake rates reported as μg $C.l^{-1}.hr^{-1}$). Uptake rates per unit Chl a have been calculated

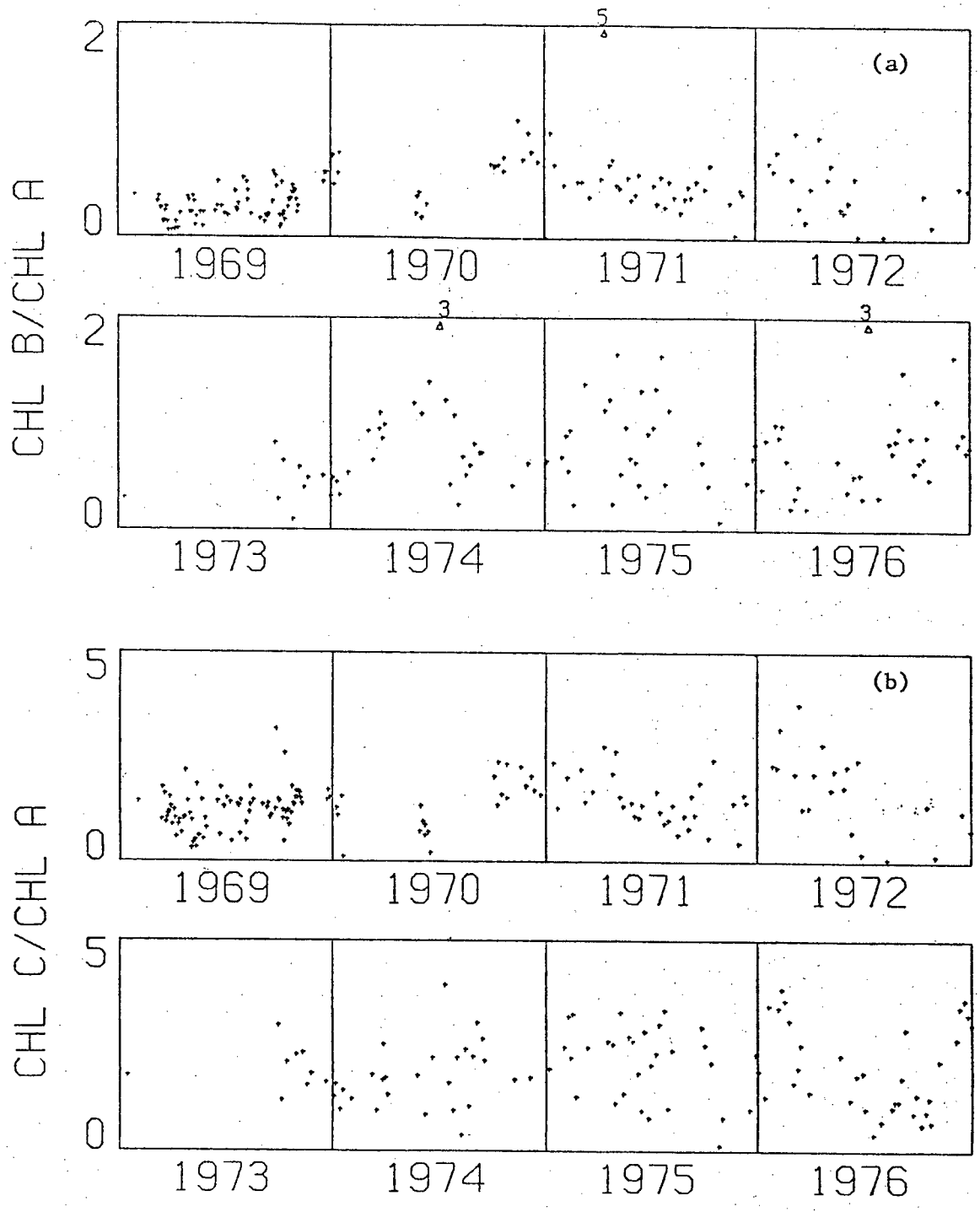

Figure 15. Observations of (a) Chl b/Chl a and (b) Chl c/Chl a from the weatherships at O.S.P. (Triangles as in Fig 13.)

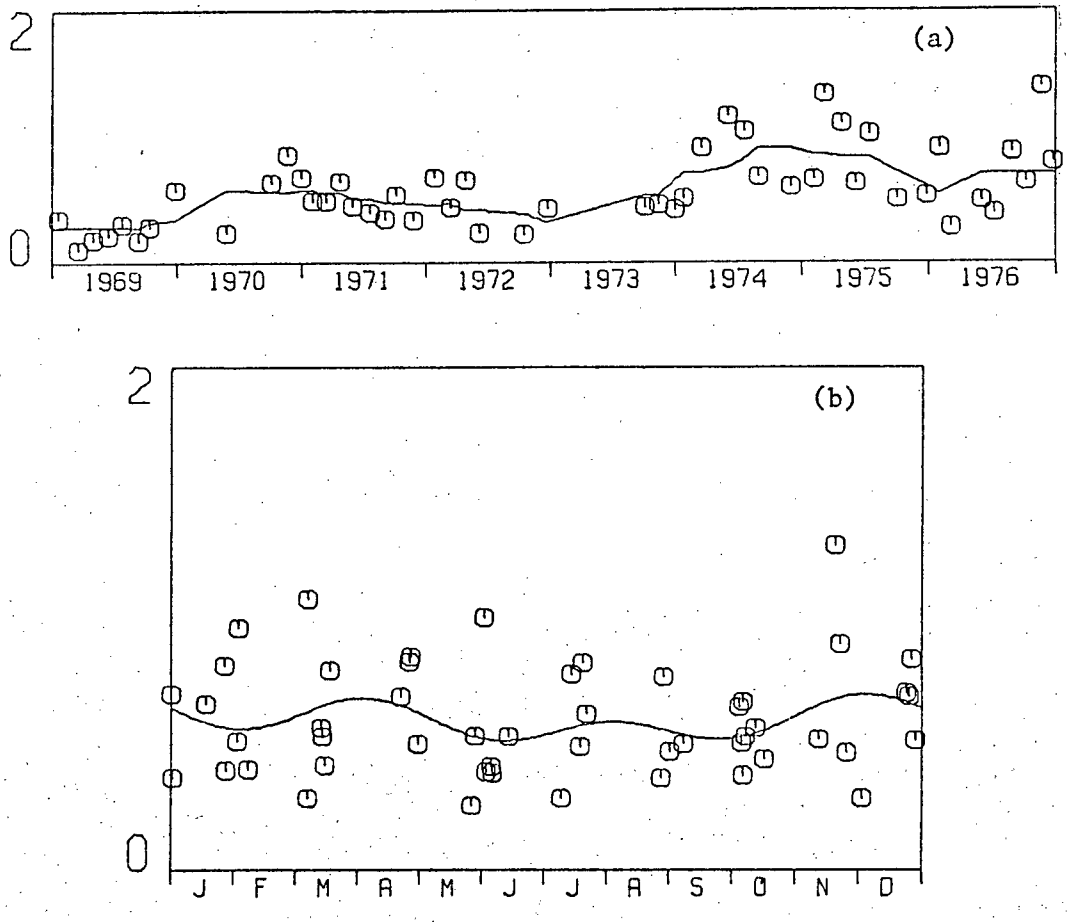

Figure 16. Surface Chl b/Chl a: (a) Cruise medians and annual smooth for 1969-76. (b) Seasonal fit plus residuals for 1969-76.

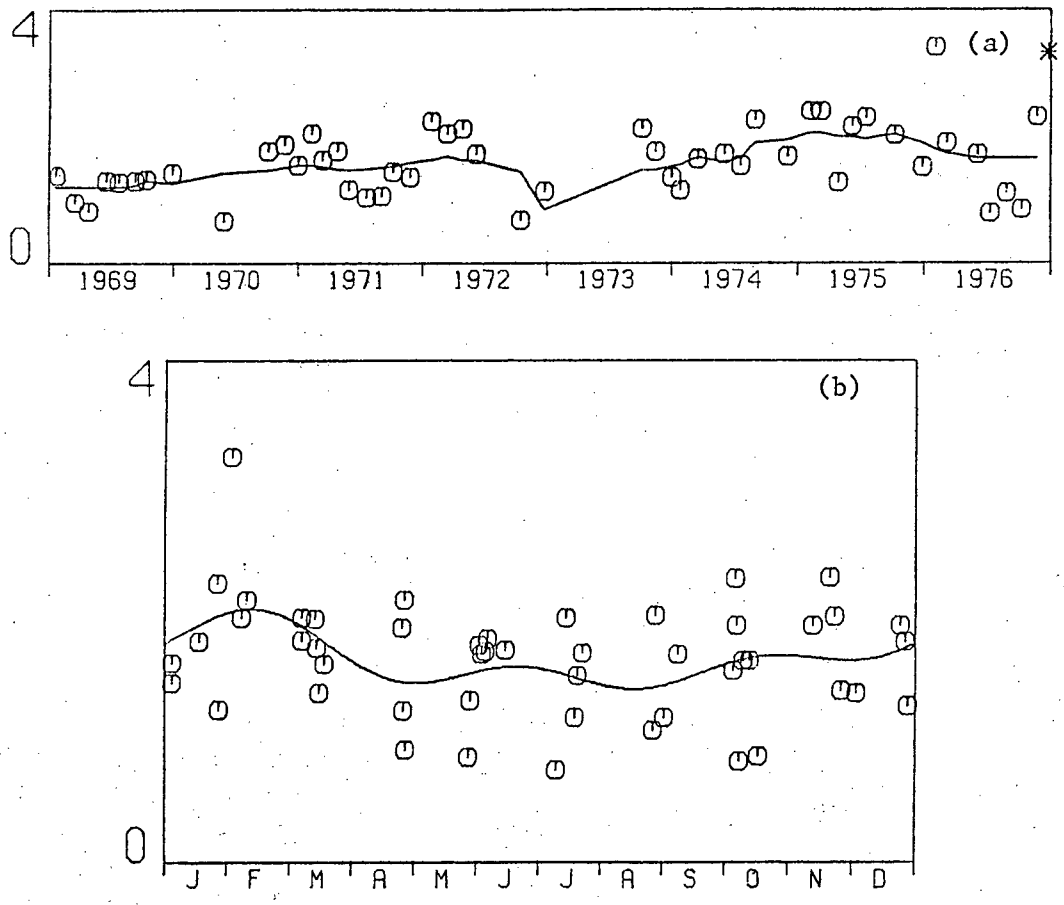

Figure 17. Surface Chl c/Chl a: (a) Cruise medians and annual smooth for 1969-76. (b) Seasonal fit plus residuals for 1969-76.

using the coincident measurements of Chl a and will be referred to here by the symbol P. Values of this ratio for all surface samples, denoted by P(0) (μg C.μg Chl $a^{-1}.hr^{-1}$), are plotted in Fig 18. It can be seen there that the scatter in P(0) increases markedly after 1968. A number of anomalous values (for example, 21 μg C.μg Chl $a^{-1}.hr^{-1}$ on 13th December,1970, which saw a daily total of 20 ly solar radiation) also appear in the second half of the time series. Histograms of the frequency distribution of P(0), square-root scaled to reduce skewness, for the periods 1964-1968 and 1969-1976 are plotted in Fig 19. While the high values are most impressive in the second half of Fig 18, the histogram reveals a large number of very low values from 1969 on, and a tendency for the gaussian-shaped distribution for 1964-1968 to become almost uniform in 1969-1976.

Seasonal and annual patterns based on cruise medians of P(0) were extracted using the procedure described above for chlorophyll. The seasonal pattern for 1964-1968 is as expected with low values from December to March and a broad peak from June to August (Fig 20a,b). This cycle explains 47% of the SSQ about the mean, with the annual smooth explaining an additional 24%. The seasonal cycle obtained for 1969-1976 (Fig 20c,d) explains only 20% of the SSQ about the mean, and the high standard deviation of residuals (0.71) is not surprising in view of the increased scatter noted above. The mid-winter peak in the seasonal cycle obtained for this period may well be an artifact. The surface observations of ^{14}C uptake rates from 1969 to 1976 are not included in the remaining analysis because of the discrepancies already noted, and others discussed later.

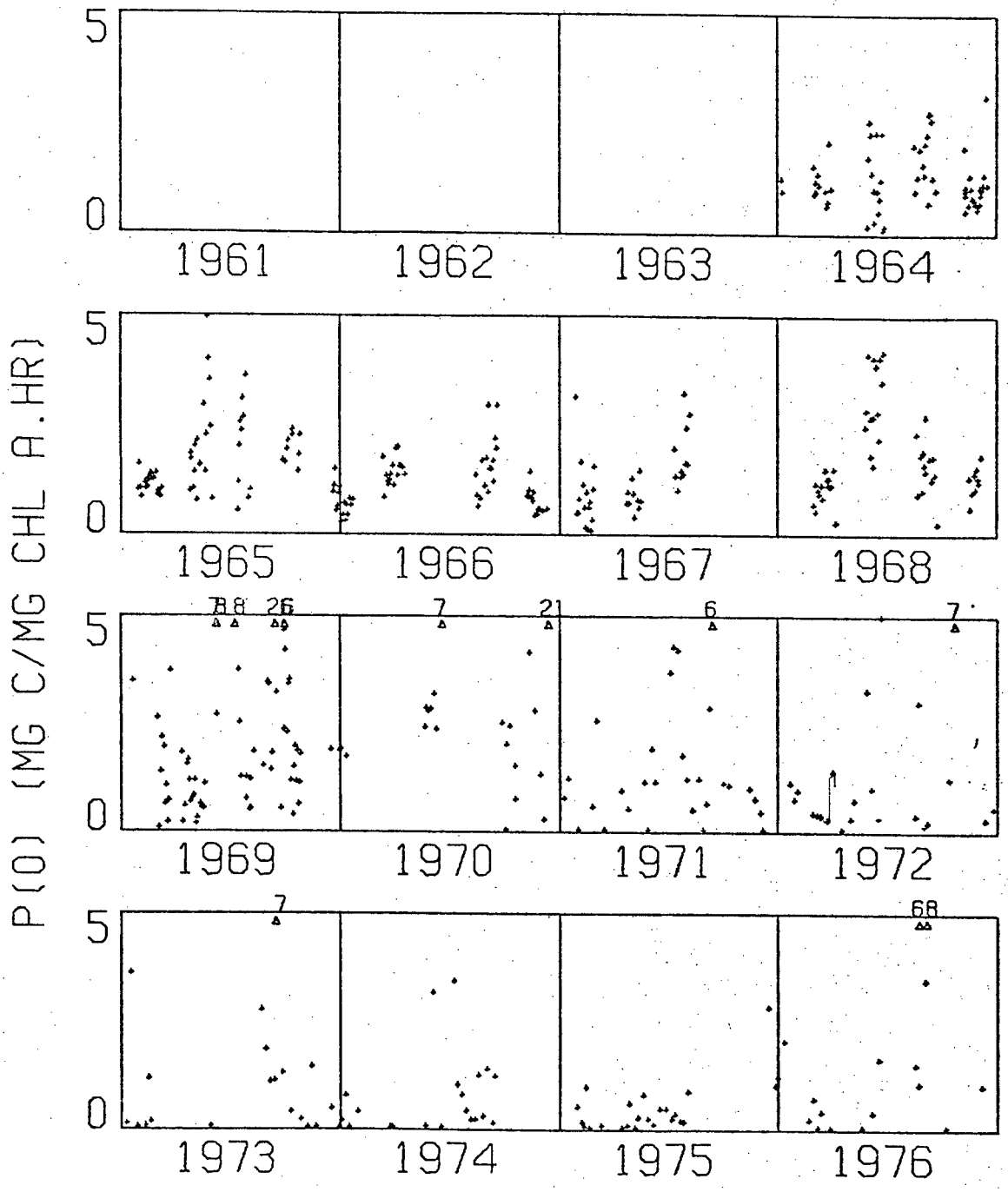

Figure 18. Surface observations of productivity per unit Chl a from the weatherships at O.S.P. (Triangles as in Fig 13.)

Figure 19. Frequency histograms for P(0)
(square-root scaled) :
(a) 1964-68,
(b) 1969-76.

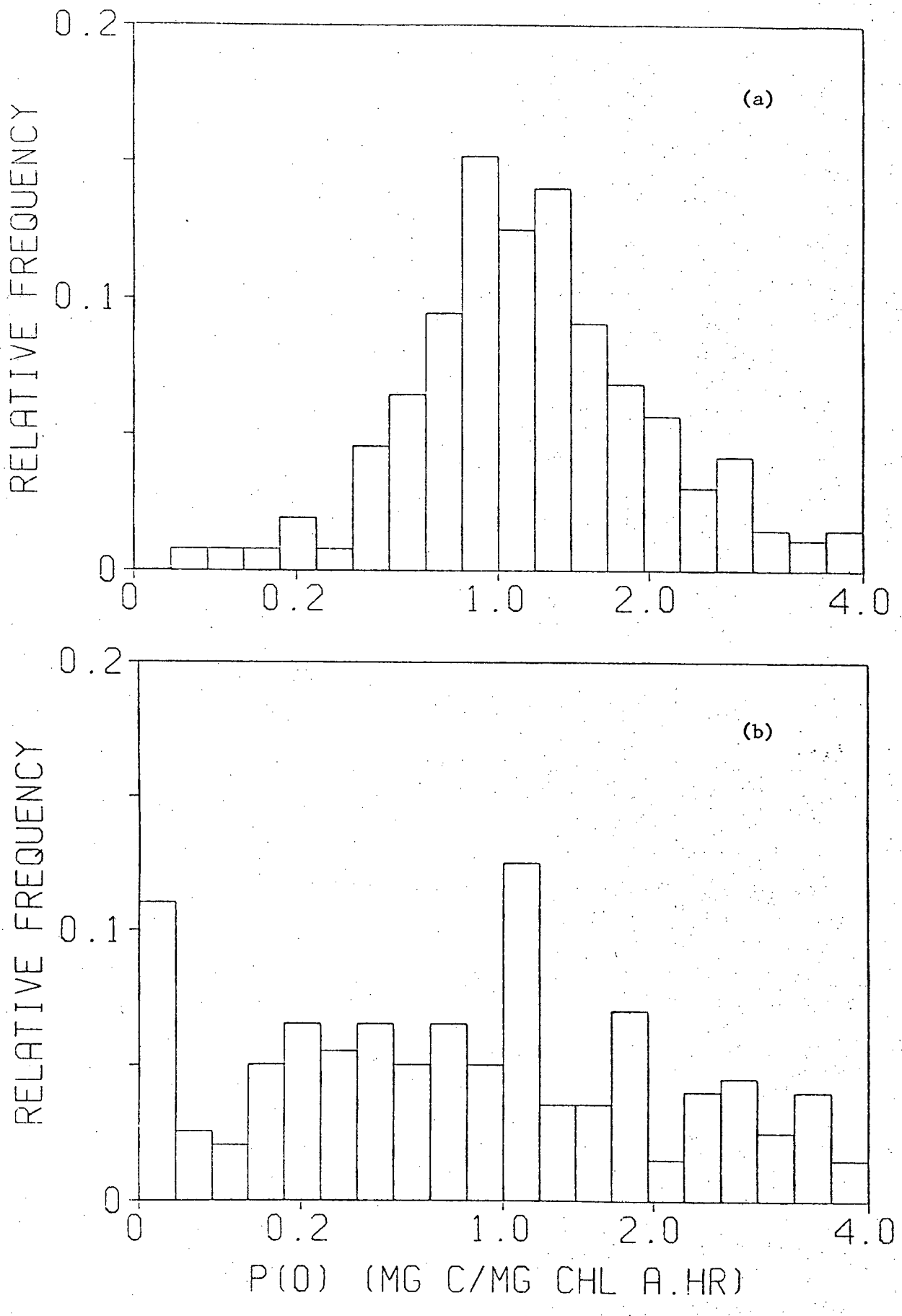
(a)
RELATIVE FREQUENCY
0.2
0.1
0
0
0.2
1.0
2.0
4.0
(b)
RELATIVE FREQUENCY
0.2
0.1
0
0
0.2
1.0
2.0
4.0
P(O) (MG C/MG CHL A.HR)

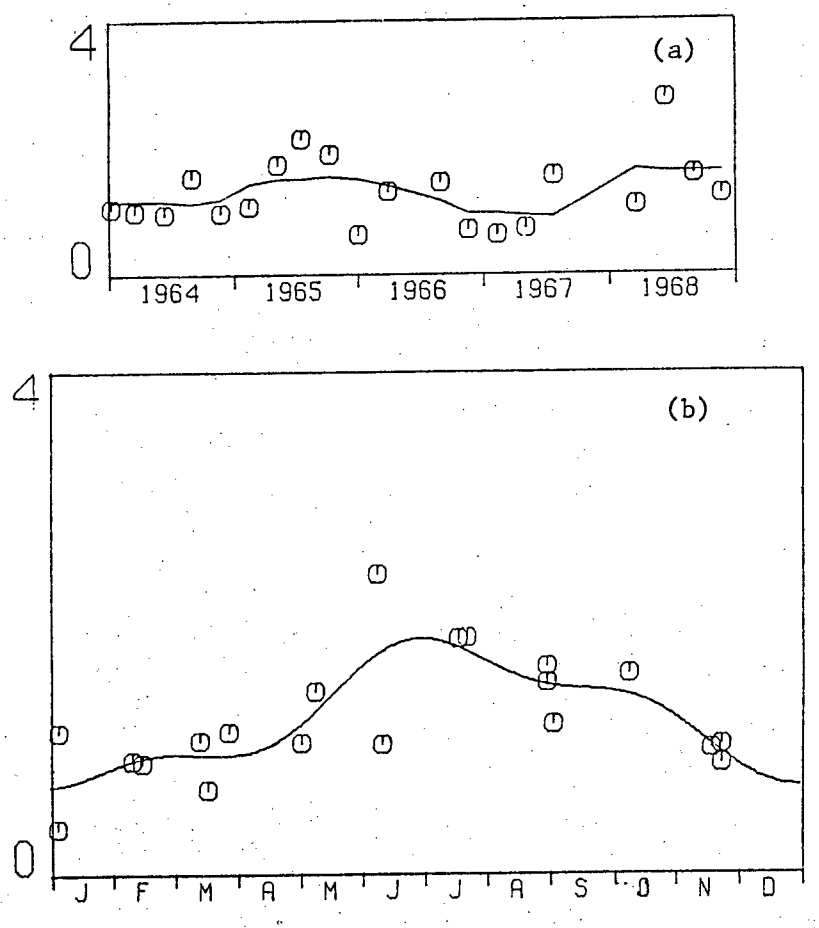

Figure 20. P(0) (mg C.mg Chl $a^{-1}.hr^{-1}$) (a) Cruise medians and annual smooth for 1964-68. (b) Seasonal fit plus residuals for 1964-68.

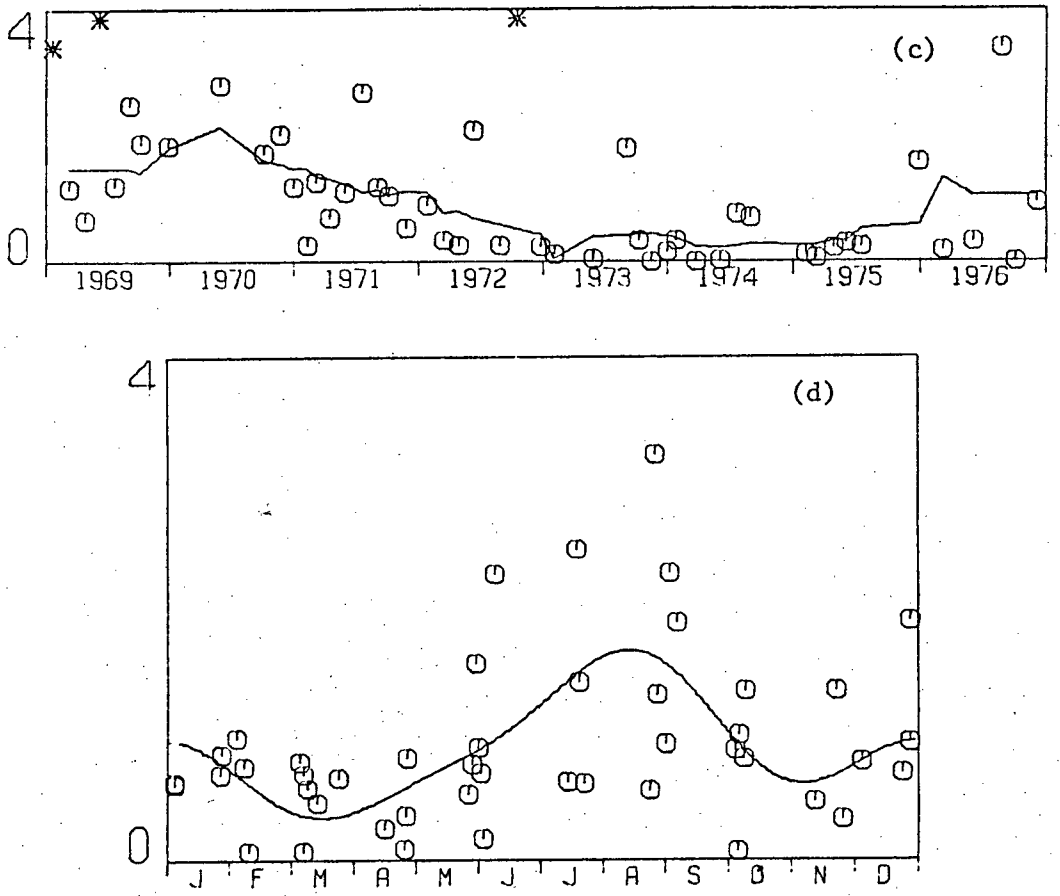

Figure 20. P(0) (mg C.mg Chl $a^{-1}.hr^{-1}$) (c) Cruise medians and annual smooth for 1969-76. (d) Seasonal fit plus residuals for 1969-76.

As noted in Chapter 1, macro-nutrients are abundant at O.S.P. and primary production is apparently light-limited. Total daily solar radiation is measured on the weatherships and reported in the Monthly Radiation Summary. Photosynthetically active radiation at the surface has been calculated following Parsons and Anderson (1970) as the minimum of observed total radiation and one-half the theoretical clear sky radiation for the same day, and is denoted here by I_o. A plot of P(0) against I_o (Fig 21) suggests some relationship between P(0) and I_o despite the large scatter. A linear regression of P(0) on I_o gives

$$P(0) = 0.81 + 0.003.I_o \ ,$$

the slope being significantly different from zero at the 5% level, although the regression explains only 14.6% of the total SSQ about the mean. Both P(0) and I_o tend to be high in winter and low in summer so that it is not clear how this statistical relationship should be interpreted. Attempts to find a consistent relationship between P(0) and I_o on time scales distinct from this seasonal co-variation were not successful. Regressions of P(0) on I_o within cruises yielded only two out of 18 slopes significantly different from zero at the 10% level, with 12 out of 18 slopes being negative. Similar results were obtained for regressions of P(0) on I_o by month.

This failure to find a consistent short-term effect of I_o on P(0) may be partly due to the large scatter in observations, but it can also be expected on theoretical grounds in the absence of

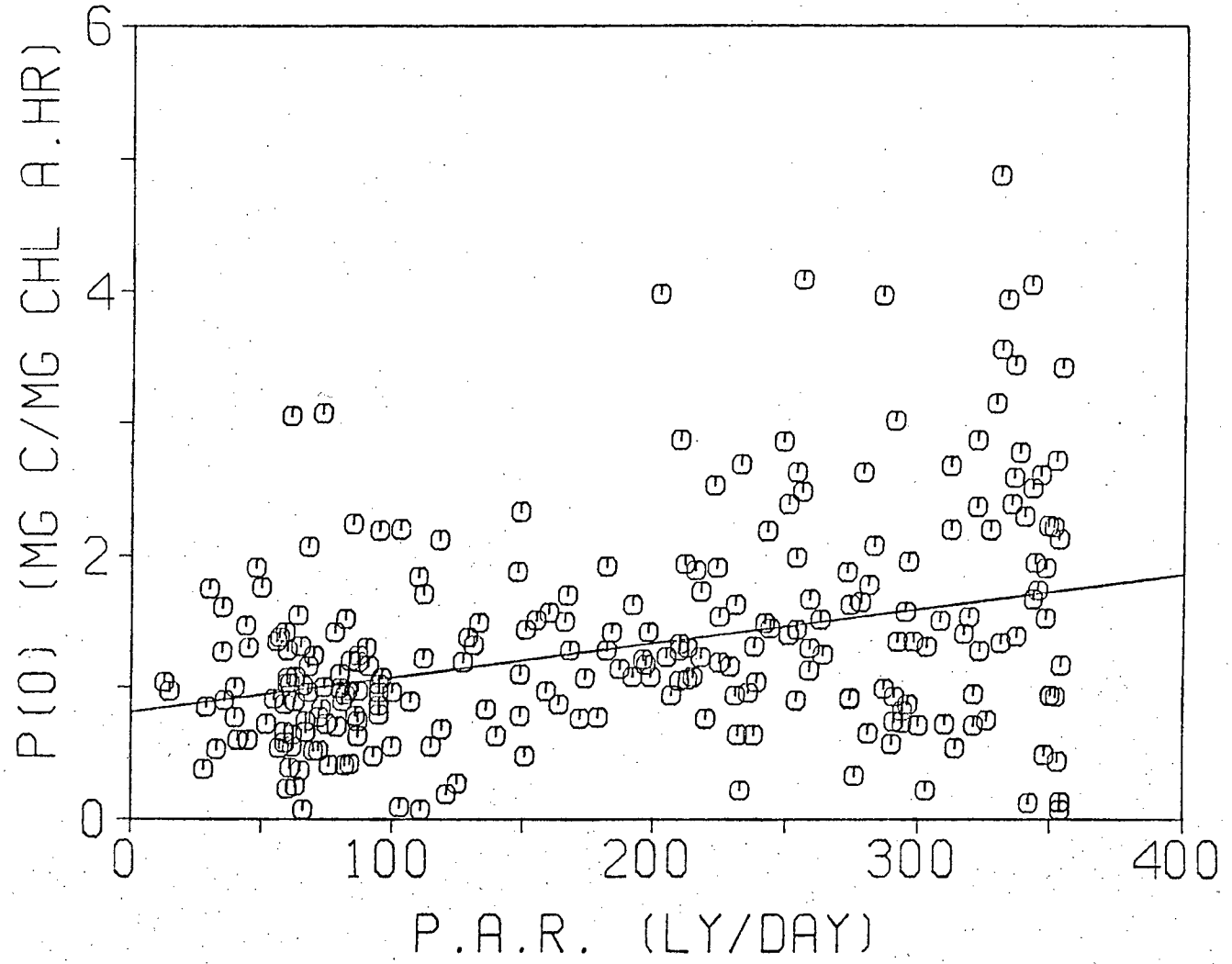

Figure 21. Scatter plot of P(0) vs I_0 for the period 1964-68.

any scatter. While phytoplankton growth over the mixed layer as a whole may be light-limited, photo-saturation or even photo-inhibition can be expected at the surface. The information available in depth profiles from O.S.P. can potentially contribute much more to an understanding of the light-dependence of phytoplankton production there.

The profiles taken at O.S.P. consist of samples at between six and twelve depths. The ^{14}C uptake measurements were made at the upper six depths, which, with a few exceptions, belonged to one of 3 standard sets: (0,2,5,12,25,50m), (0,3,7,15,25,60m) and (0,6,10,25,33,75m). Uptake rates were measured using simulated in-situ incubations on deck under a standard set of mesh light screens. The Secchi depth (and presumably the extinction coefficent) at O.S.P. varies as much as two-fold or more from summer to winter (Parsons,1965). Consequently, the light intensity at the incubated sample (under a standard light screen) need not coincide with the light intensity at the (standard) depth from which the sample was taken. In fact, their ratio can vary widely depending on the extinction coefficient at the time. This means that direct depth-integration of profiles to obtain total production under 1 m^2 is not valid.

The profiles can still be used to examine the relationship between photosynthesis and light intensity as follows. The transmission coefficients for the standard light screens, and the surface light intensity, are known. The profile can then be regarded as a single P vs I experiment, disregarding the stated depths except as an index to the corresponding screen. This requires the strong assumption that the phytoplankton population

is homogeneous with depth, or at least that the relationship between production per unit Chl a and light intensity is independent of depth. This seems plausible in late fall, winter and spring when the mixed layer extends below the deepest ^{14}C sample. However, in the late summer and early fall, when the seasonal thermocline is shallowest, a distinct shade-adapted population can be expected below the thermocline, and results obtained under the assumption of vertical homogeneity must be regarded with suspicion.

Each profile from O.S.P. has been used here to estimate parameters in a formula for the light-dependence of photosynthesis. There are a number of formulae of this type in the literature (for a review, see Jassby and Platt,1976), ranging from the simple to the complex (eg Bannister,1979). A simple version of that proposed by Steele (1962):

$$P = \alpha.I.\exp(-I/I_{MAX}^{\circ}) \qquad 3.1$$

has been used here. This equation has been satisfactorily fitted to other sets of field observations involving photo-inhibition (Hameedi,1977; Chan,pers comm). Other formulae have been found to give a superior description at sub-optimal light intensities (Jassby and Platt,1976), but these require three parameters to account for photo-inhibition, and fitting more than two parameters to the six observations in each profile seems unwise, to say the least. The theory proposed by Steele(1962) for the seasonal variation of parameters in equation 3.1 and their interpretation in terms of light adaptation and changing

carbon:chlorophyll ratios will also prove useful.

Equation 3.1 is used here to predict daily uptake rates on the basis of daily radiation totals. The equation was first proposed for instantaneous rates, but it was shown to be applicable to daily totals on the basis of an idealised diurnal variation in light intensity (Steele,1962). As noted earlier, incubations at O.S.P. were usually made from 1200 to 1800 hr local time and average ^{14}C uptake rates per hour over the incubation period were reported. These have been multiplied by 12 to give a crude estimate of daily uptake. Where the incubation period includes dusk, this procedure is most reasonable. Where it does not, daily uptake is underestimated by a small undetermined amount. Other sources of error, such as diurnal variation in photosynthetic activity and particularly afternoon depression (Yentsch and Ryther,1957;McAllister,1963) may be more important.

To fit equation 3.1 to the profiles, it was rewritten as

$$P_i = \alpha . I_o . tr_i . \exp(-I_o . tr_i / I_{MAX})$$

where P_i is the uptake rate per unit Chl a at depth i, I_o the surface light intensity and tr_i the transmission coefficient of the filter used for depth i. The quantities $A = \alpha . I_o$ and $B = I_o / I_{MAX}$ were estimated for each profile and their dependence on I_o considered later. If errors in P_i were log-normally distributed, the statistical model could be written as :

$$\ln(P_i) = \ln(A) + \ln(tr_i) - B.tr_i + e_i \quad (e_i \text{ i.i.d. } N(0,\sigma^2))$$

resulting in a convenient linear regression for ln(A) and B. This was tried but it was found that deep (low light intensity) observations then contributed disproportionately to the SSQ of residuals. Inspection of curves fitted through individual profiles revealed a tendency to ignore shallow observations entirely. The observation error does not decrease quickly enough with the mean to be log-normal.

When a non-linear least-squares fit to the raw data was tried, it was found that shallow (high light intensity) observations made a disproportionately large contribution to the SSQ of residuals, and, especially where surface inhibition was exaggerated, deep observations were ignored. A third attempt was made, again using the non-linear least-squares approach, but first square-root scaling the original P_i. This scaling is used to normalize observations from a Poisson distribution (Barnes,1952), but was used here as an empirical measure which resulted in equal weight being attached to shallow and deep observations (cf Fig 19a).

As a check on parameter estimates obtained using Steele's equation (1), an ad-hoc procedure was also used. A straight line was fitted through the three deepest observations and the origin to estimate A. Observations at successively shallower depths were then included, but unless this resulted in a higher estimate of A, the original estimate was retained. The highest observed P_i, denoted by P_{MAX}, was also noted for each profile.

The parameter α represents a photosynthetic efficiency, having units of mg C.mg Chl $a^{-1}.ly^{-1}$, and has been measured on many occasions. Early values are given in terms of lux-hr rather

than 1y and conversion can be problematical. Steele(1962) proposed a universal value of 4.10^{-4} mg C.mg Chl a^{-1}.lux-hr^{-1} or .48 mg C.mg Chl $a^{-1}.ly^{-1}$. Steeman Nielsen(1978) suggests that a value of 0.5 mg C.mg $Chla^{-1}.ly^{-1}$ may be assumed for most phytoplankton. On the other hand, a theoretical maximum of 2 mg C.mg Chl $a^{-1}.ly^{-1}$ is proposed by Bannister(1974), and high values, greater than 1mg C.mg Chl $a^{-1}.ly^{-1}$, have been reported for laboratory populations (Chan,1978), and in the field (Hameedi,1977).

A plot of $\hat{A}$ (estimated using the ad hoc procedure) versus I for the period 1964-1968 is given in Fig 22. The line drawn is the best fit to a straight line through the origin; it has a slope corresponding to α = 0.25 mg C.mg Chl $a^{-1}.ly^{-1}$. The estimates of A obtained using equation 3.1 yielded a similar plot, with α =0.34 mg C.mg Chl $a^{-1}.ly^{-1}$. Because of the considerable scatter, the 95% confidence limits for each value includes the other.

An equivalent plot for the period 1969-1976 showed no relationship at all between $\hat{A}$ and I_o. The reason for this quickly became apparent on inspection of individual profiles. In Fig 23, 10 randomly selected profiles of P_i versus depth are given for the periods 1964-1968 and 1969-1976. Stephens(1977) has expressed reservations concerning some of the ^{14}C observations after 1969. In view of the increased scatter and altered frequency distribution of surface values reported earlier, and the incoherent pattern of P with depth as shown in Fig 23, all ^{14}C observations after 1969 have been ignored and the remaining discussion applies only to the period 1964-68. This

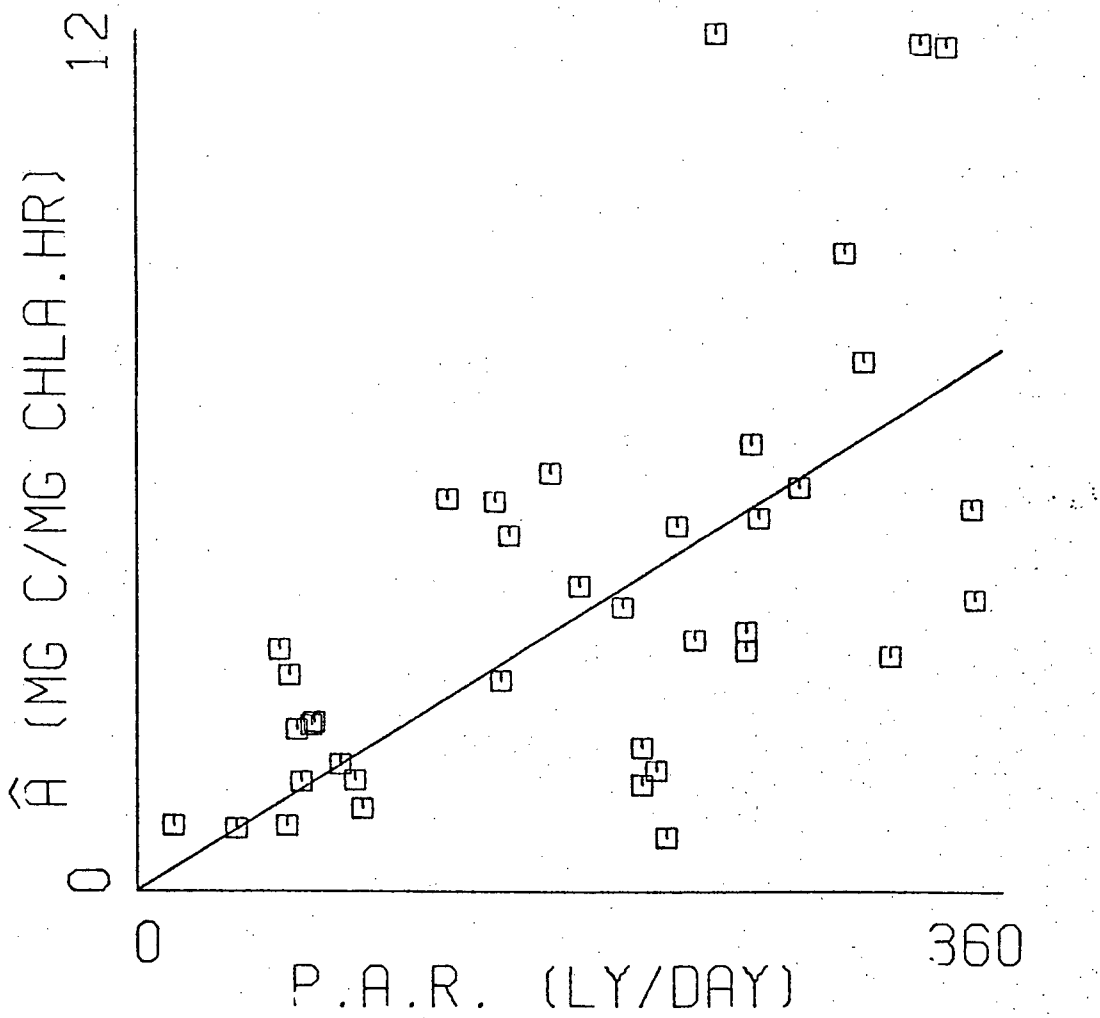

Figure 22. Scatter plot of $\hat{A}$ vs I_0 for 1964-68. (Line drawn is least-squares fit through origin.)

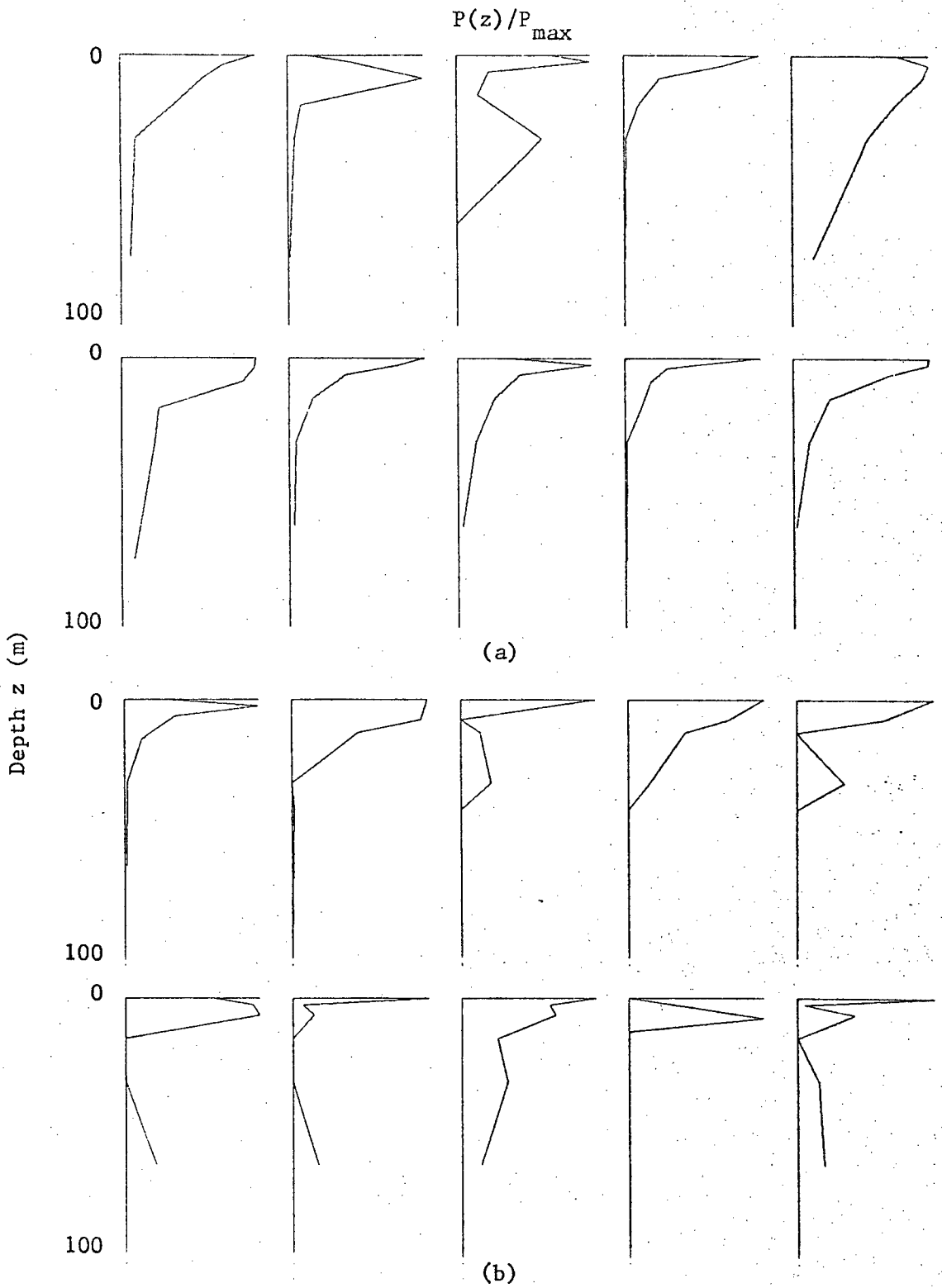

Figure 23. Depth profiles of P for (a) 1964-68 and (b) 1969-76. (Straight-line segments connect observations.)

reduces the number of profiles from 200 to 45 and severely restricts the usefulness of the data set, particularly for examining seasonal patterns and annual anomalies.

Rather than plot $\hat{A}$ vs I_o and estimate a single mean value of α, an estimate $\hat{\alpha} = \hat{A}/I_o$ can be calculated for each profile. A plot of monthly means of $\hat{\alpha}$ (Fig 24) suggests a strong seasonal pattern in α with a maximum in winter and minimum in summer. In laboratory experiments, α has been found to vary with phytoplankton composition and with environmental conditions such as temperature, nutrients and light quality (Parsons et al, 1977). The low values in August and September must be viewed with some suspicion as the thermocline is shallow at this time and the assumption of vertical homogeneity of the phytoplankton may be violated. Even discounting these very low values, the remaining monthly means are less than or equal to Steeman Nielsen's value of 0.5 mg C.mg Chl $a^{-1}.ly^{-1}$ which is in turn low compared with other recent observations mentioned above.

The interpretation of estimates of B is not as straightforward. If I_{MAX} was constant, a plot of $\hat{B}$ vs I should show a linear relation. However, Steele(1962) quotes a number of studies in which I_{MAX} was found to co-vary with I_o so that I_o/I_{MAX} lay between 2 and 3. Steele and Baird(1961) found lower values of this ratio, between 1 and 2, in the North Sea in summer. In a theoretical discussion, Steele(1962) attributed this co-variation to light adaptation by phytoplankton to seasonal light intensity through changes in the carbon:chlorophyll ratio, and used a fixed value for I_o/I_{MAX} of 2.

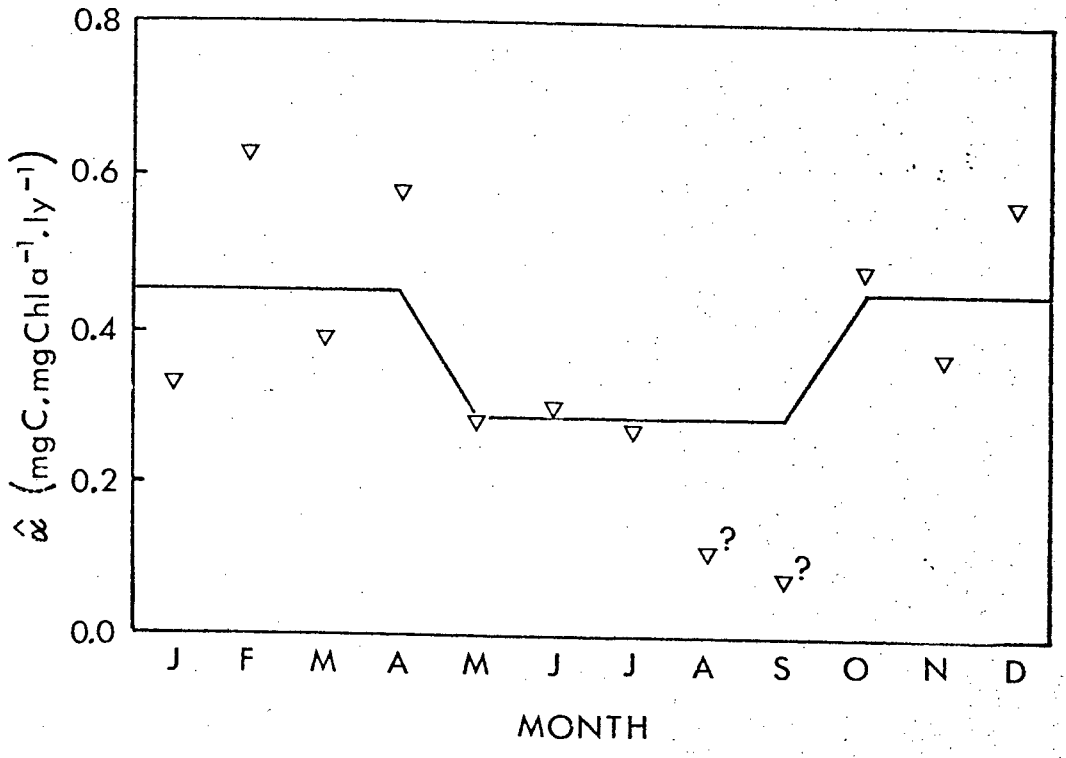

Figure 24. Monthly averages of $\hat{\alpha}$. (Line fitted by eye.)

Estimates of B are plotted against I_o in Fig 25. While there is no suggestion of a linear relation between B and I_o, as would be expected if I_{MAX} was constant, the scatter is rather large to describe B as constant. The average value of B, 1.2, lies in the range suggested by Steele and Baird(1961) and is lower than values reported in other references quoted in Steele(1962).

Theory suggests that the scatter in Fig 25 might be explained by a more careful consideration of the time-course of light adaptation. It is unlikely that phytoplankton can maintain a constant ratio of I_o/I_{MAX}, since this requires instantaneous adaptation to changing light intensity. Cells could adapt to seasonal light intensities (Steele,1962) through some long-term averaging response. A seasonal average light intensity, $I_s(t)$, was calculated using a running average with a window of width 20 days. Estimates of the seasonal adaptation parameter, B_s, given by $\hat{B}_s = I_s/I_{MAX} = \hat{B}.I_s/I_o$, showed no less scatter than estimates of B itself. Light adaptation through changes in C:Chl a ratios has been reported to occur on time scales of a few days (Steeman Nielsen and Park,1964). A simple model for light-adaptation on these time scales would allow the parameter I_{MAX} to vary as a linear combination of radiation on the preceding days. Such a model was fitted to the profile results as a linear regression in the form:

$$1/B(t) = I_{MAX}/I_o(t) = b_o + b_1.I_o(t-1)/I_o(t) + b_2.I_o(t-2)/I_o(t) + b_3.I_o(t-3)/I_o(t) \ ,$$

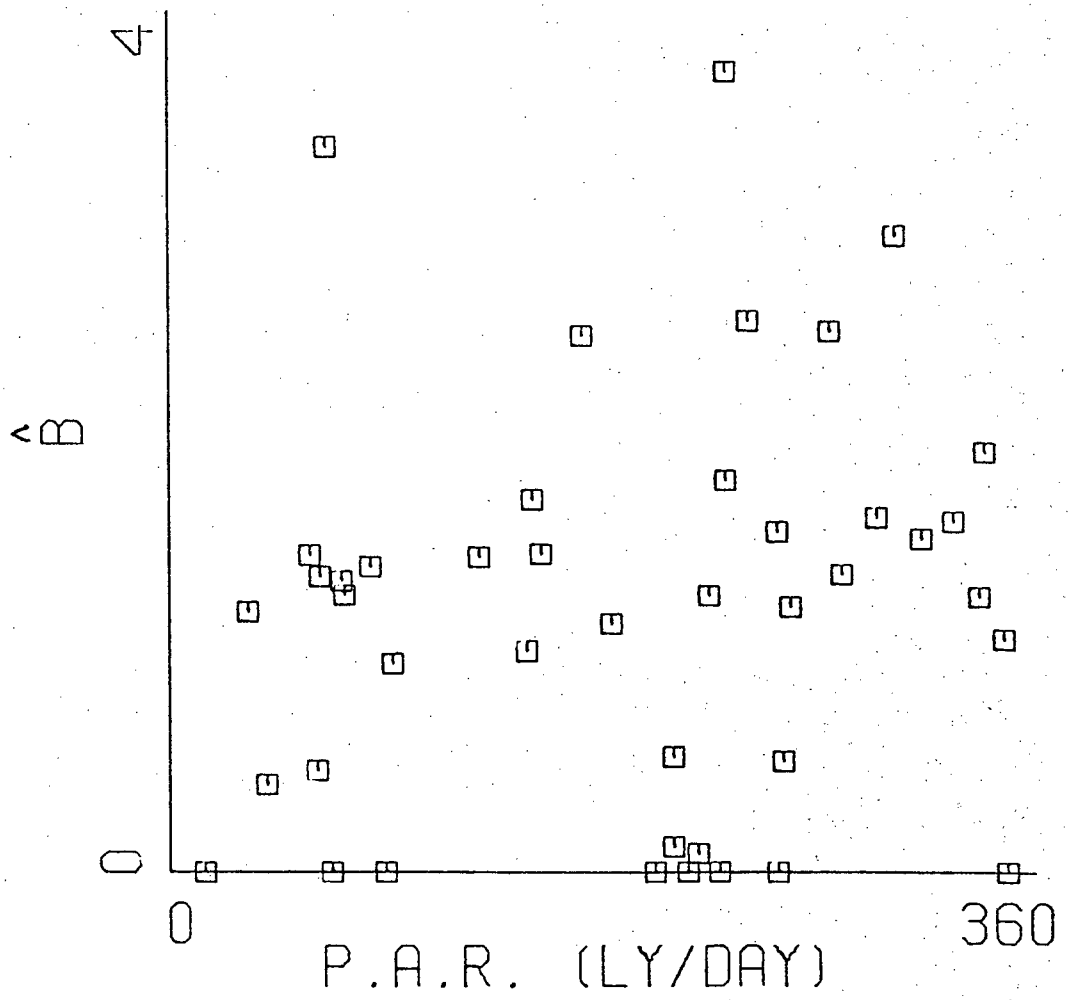

Figure 25. Scatter plot of $\hat{B}$ vs I_0 for 1964-68.

but this did not produce a significant reduction in the variance of $1/\hat{B}$.

In Fig 26, a plot of P_{MAX} versus I_o is given. Under instantaneous adaptation (I_o/I_{MAX} constant), P_{MAX} should increase linearly with I_o. The line in Fig 26 represents the best fit to a straight line through the origin and has a slope of 0.01 ± 0.001, corresponding to an average value for I_o/I_{MAX} between 0.9 and 1.2, consistent with the average value obtained by fitting equation 3.1 to profiles. It is interesting that the points in Fig 26 at low light intensities (less than 120 ly/day) tend to lie above this line through the origin. This is consistent with the existence of a lower limit to light adaptation; that is, a minimum value of I_{MAX}, and according to Steele(1962) a minimum C:Chl a ratio, which is encountered at these light intensities.

The results obtained from analysis of ^{14}C profiles at O.S.P. can therefore be summarised as follows. Photosynthetic efficiency α is low at O.S.P., with a seasonal cycle ranging from about 0.45 mg C.mg Chl $a^{-1}.ly^{-1}$ from October to April to 0.3 mg C.mg Chl $a^{-1}.ly^{-1}$ or less from May to September. There is reasonable evidence of adaptation to light intensity with an increase in I_{MAX} and P_{MAX} with increasing I_o, although the data are not sufficient to distinguish amongst 'instantaneous', short-term or long-term adaptation to changes in solar irradiance.

Some of the scatter in Fig 25 can be explained by allowing the ratio I_{MAX}/I_o to vary seasonally. Monthly averages of $\hat{B}$ and $\hat{B}_s$ are plotted in Fig 27. Both show the same seasonal trend. The high values in February to May agree roughly with Steele's figure of 2.0. This is a period of deep mixed layers and

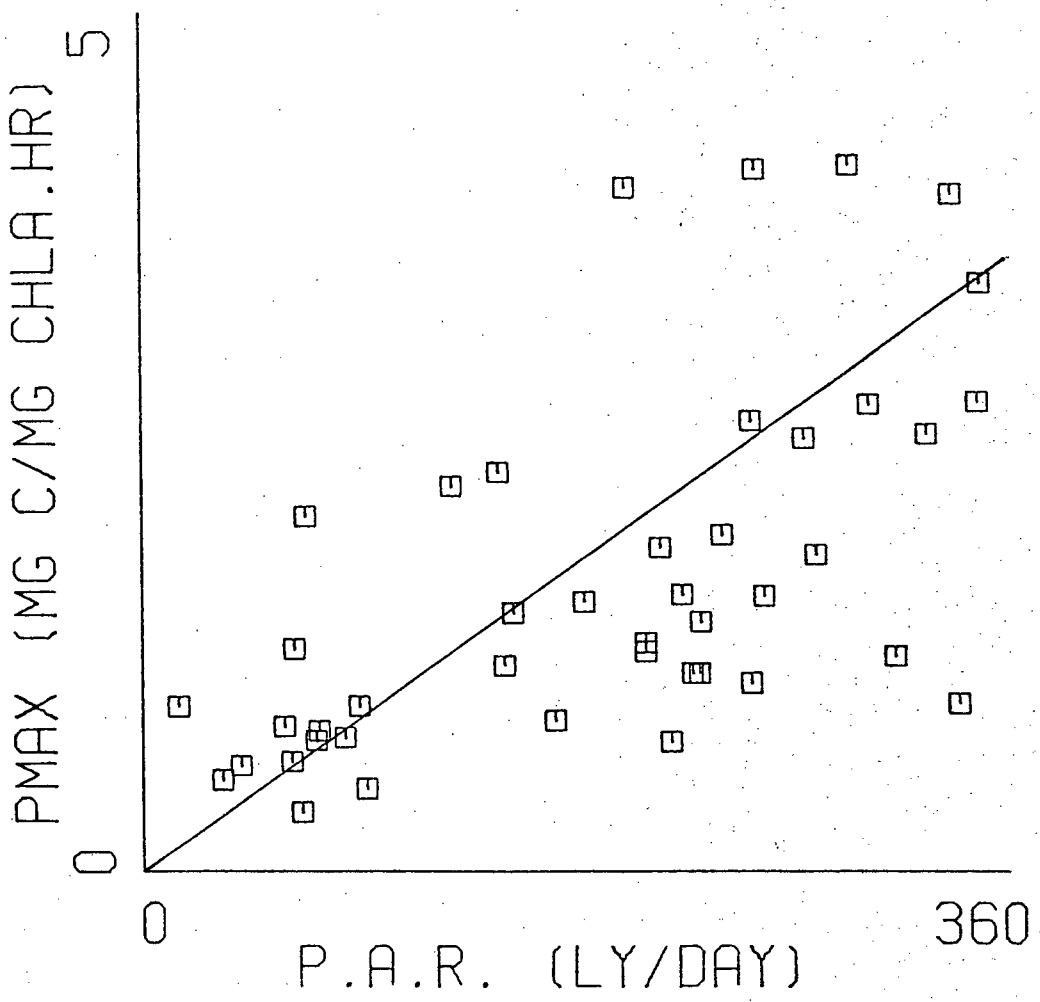

Figure 26. Scatter plot of P_{max} vs I_0 for 1964-68. (Line is least-squares fit through origin.)

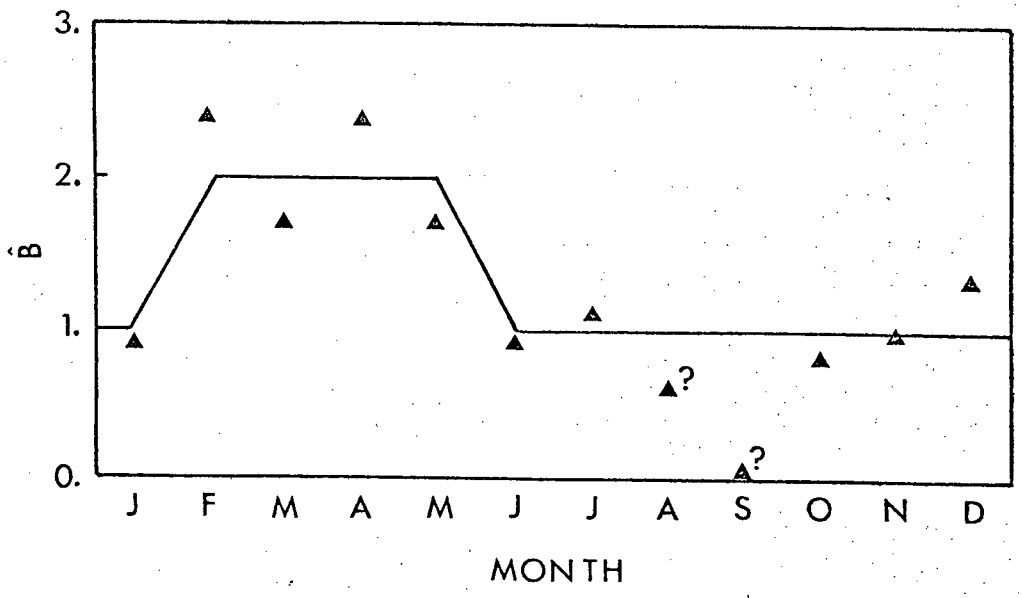

Figure 27a. Monthly averages of estimates of light adaptation parameter B. (Line fitted by eye.)

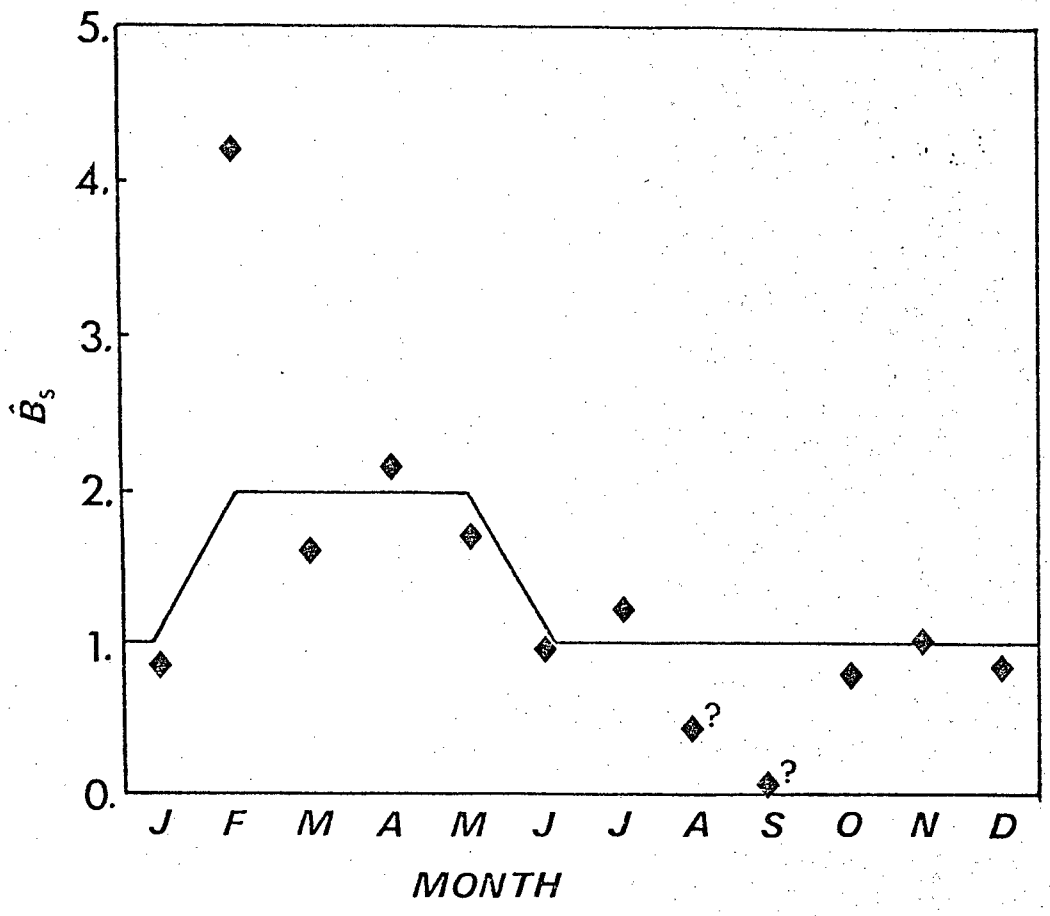

Figure 27b. Monthly averages of estimates of light adaptation parameter B_s. (Line fitted by eye.)

increasing light intensity. Throughout the remainder of the year, monthly averages of $\hat{B}$ are low and correspond to maximum growth at or near the surface. The very low values in August and September may again be due to the breakdown of the assumption of vertical homogeneity.

In view of the low number of profiles considered and the unexplained scatter in estimates of α and B, these seasonal cycles in α and B must be regarded as being suggested rather than confirmed by the data. The high scatter, together with the six week gaps in the sampling regime during 1964 to 1968, has also prevented a search for annual variation in these parameters. The loss of the ^{14}C data from 1969-1976 has been a considerable handicap in these respects.

3.2.4 Nitrate Data.

Nitrate concentrations in both surface and deep samples were recorded after 1966. The frequency of observations is low during 1966-1968 and increases substantially thereafter (Fig 28). Seasonal and annual summaries were calculated as for other variables and are given in Fig 29. The annual smooth and seasonal cycle remove 42% and 37% respectively of the total SSQ about the mean. The standard deviation of residuals is 2.1 μg $at.l^{-1}$ compared with a seasonal cycle ranging from 7 to 15 μg $at.l^{-1}$.

In addition, average nitrate values in the depth ranges 0-20,20-40,40-80, 80-130 and 130-200 m were calculated for each profile and the annual smooth and average seasonal cycle extracted (using individual profiles rather than cruise medians) for each depth range. The resulting seasonal cycles and the

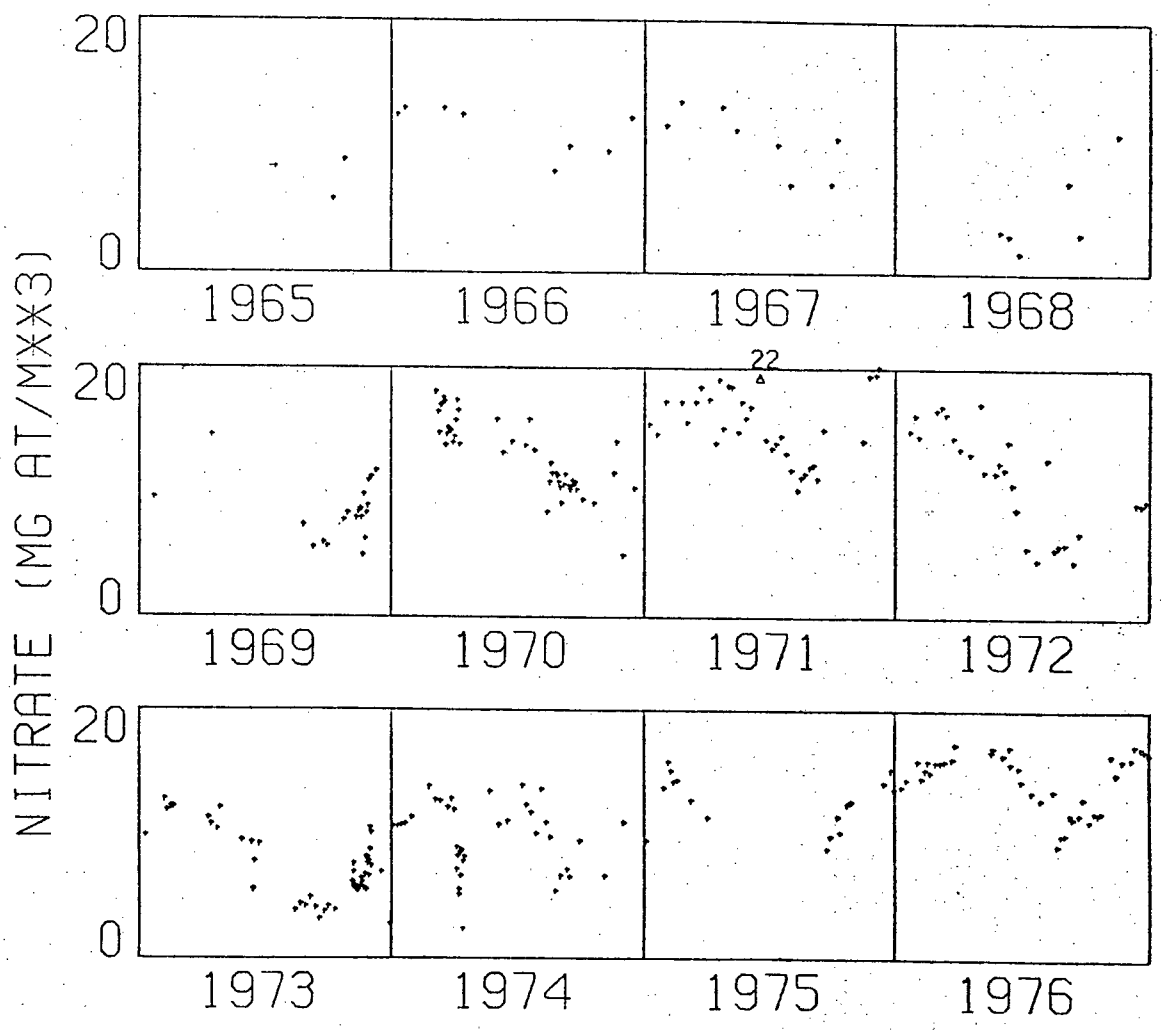

Figure 28. Surface observations of nitrate concentration from the weatherships at O.S.P.

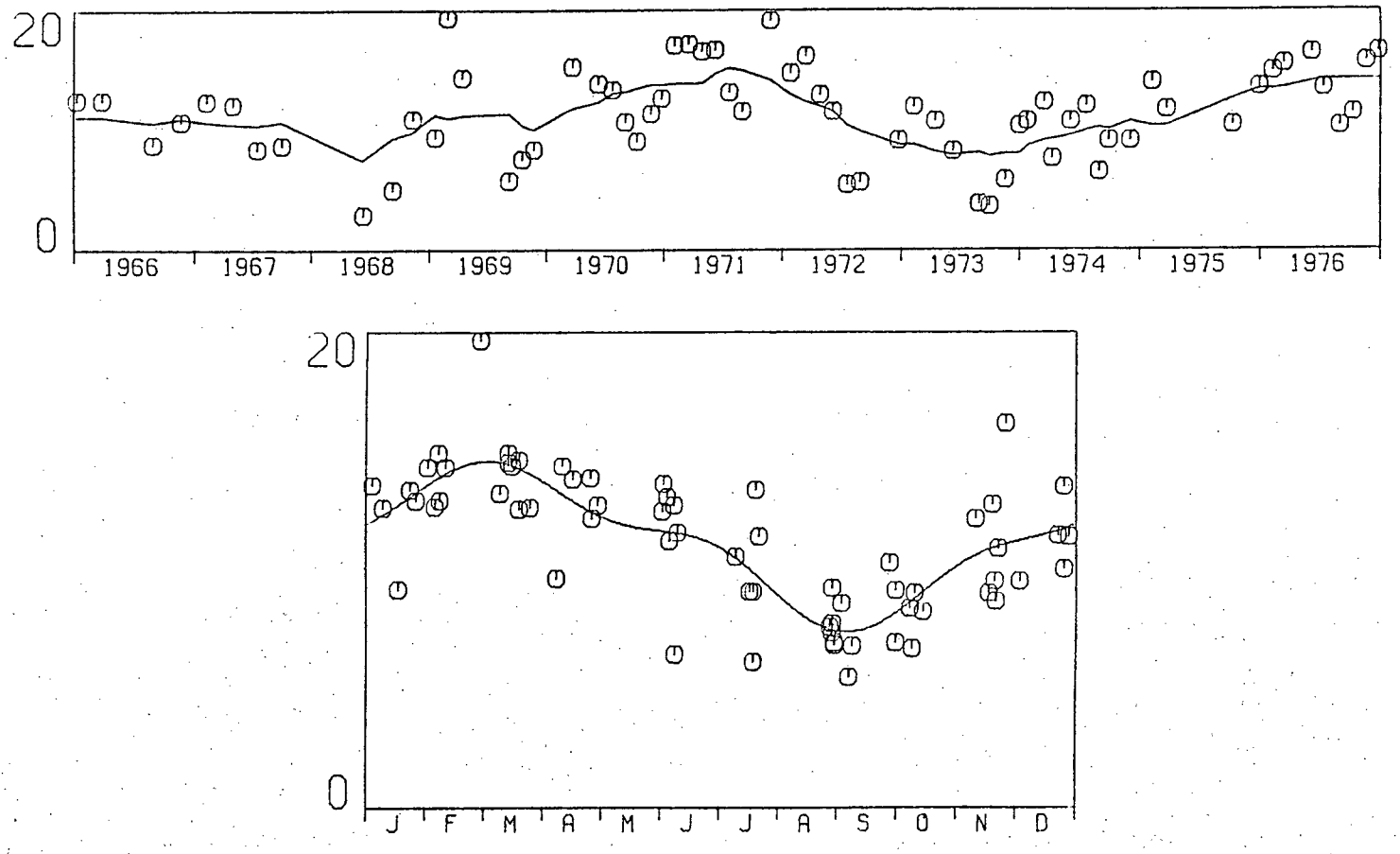

Figure 29. Surface nitrate concentrations (mg at.m^{-3}): (a) Cruise medians and annual smooth. (b) Seasonal fit plus residuals.

annual smooths are plotted in Fig 30. The seasonal cycles for 0-20m and 20-40m are both similar to that obtained for surface samples and all can be explained as a result of uptake by phytoplankton during spring and summer, with a minimum occurring about the time of maximum stabilisation of the water column. The first change in seasonal cycle with depth comes at 40-80m and is quite interesting. A small decline in nitrate concentration occurs in spring and early summer, but as the thermocline shallows to above 40m, an increase in nitrate concentration occurs. This is presumably due to a combination of reduced nitrate uptake (phytoplankton at these depths are no longer mixed upward into regions of high light intensity), vertical mixing from below and possibly recycling.

The seasonal cycles for the three upper depth ranges explain 41%, 33% and 8% respectively of the total SSQ about the means. The seasonal cycle at 80-130m explains only 6% of the SSQ; the principal interpretable feature in the cycle is the minimum in February and March, the time of maximum mixed layer depth, when nutrient depleted water from the previous summer is mixed to these depths. The seasonal cycle at 130-200m explains only 3% of the total SSQ while the annual smooth explains 49%. The considerable variation in nitrate concentration at these depths is not of a seasonal nature and presumably reflects the passage of large water masses with different nutrient histories past the station.

3.2.5 Nitrate Concentration and Production.

The average seasonal cycle in nitrate concentration at the surface has a minimum of 7 $\mu g\ at.l^{-1}$ but lower values of 2.7, 1.9

Figure 30. Nitrate concentrations (mg at.m^{-3}) from depth profiles. Layer averages and annual smooths, seasonal fits plus residuals.

(a) 0 - 20m.

(b) 20 - 40m.

(c) 40 - 80m.

(d) 80 - 130m.

(e) 130 - 200m.

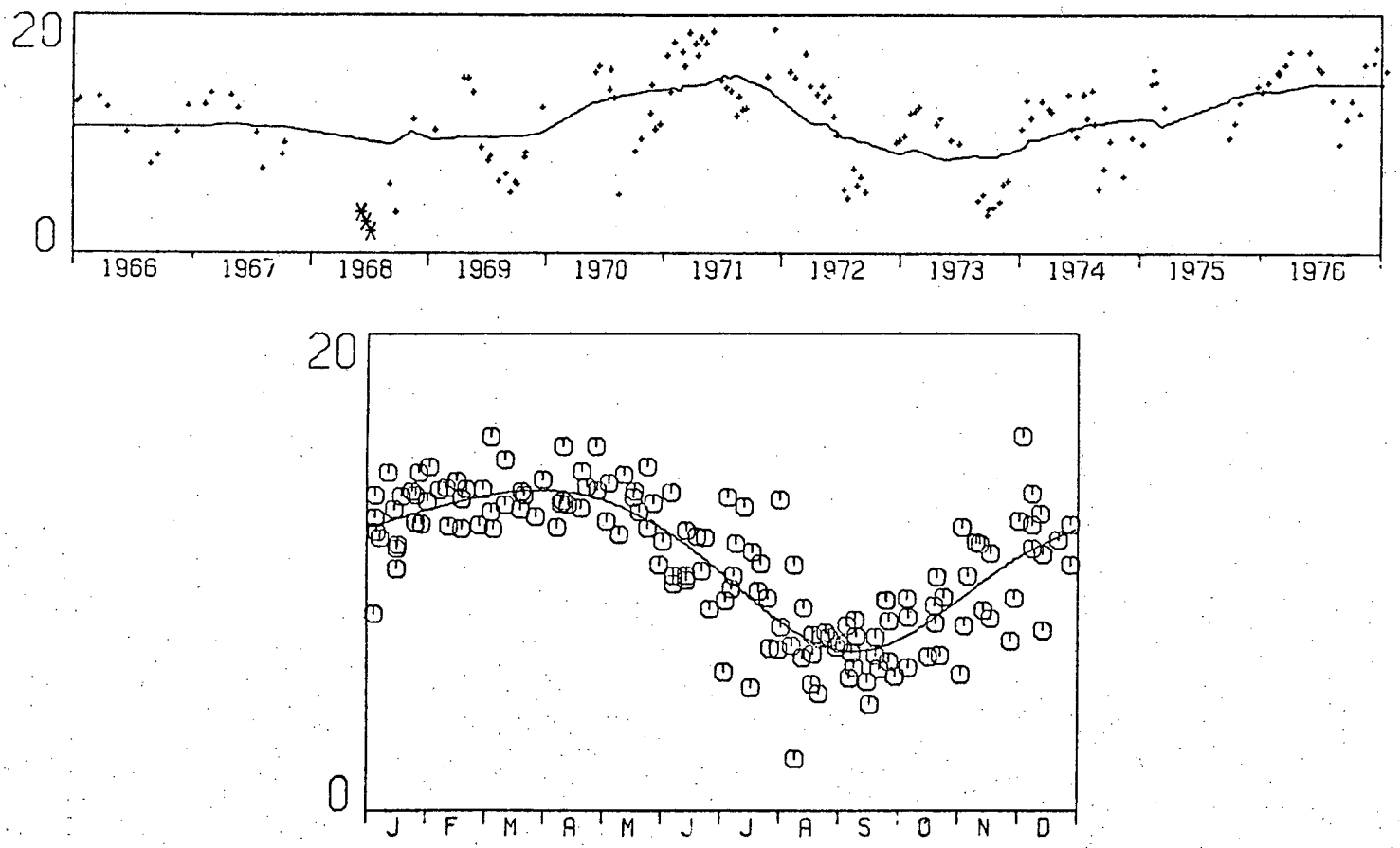
20
0
1966
1967
1968
1969
1970
1971
1972
1973
1974
1975
1976
20
0
J
F
M
A
M
J
J
A
S
O
N
D

Figure 30a.

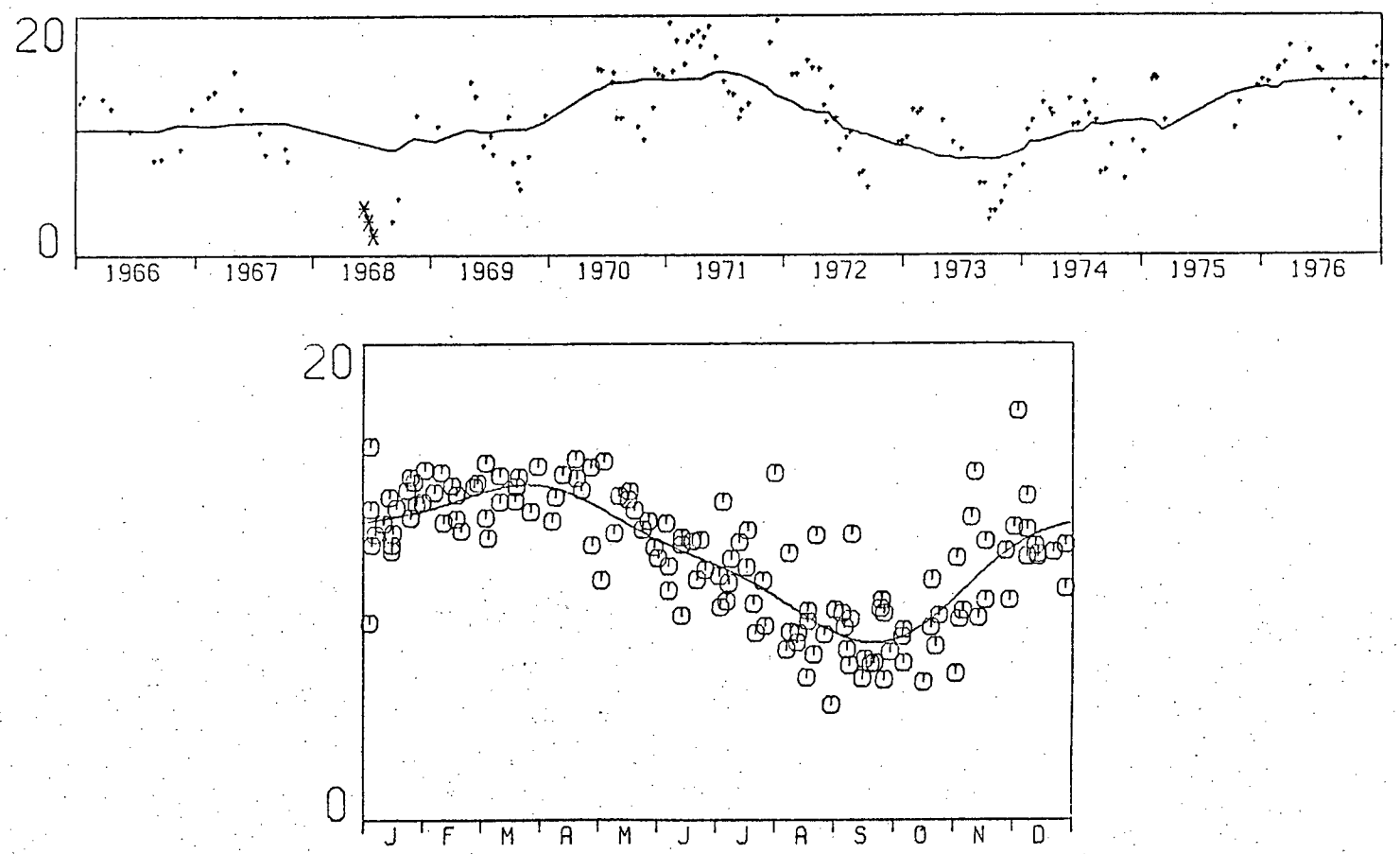
20
0
1966
1967
1968
1969
1970
1971
1972
1973
1974
1975
1976
20
0
J
F
M
A
M
J
J
A
S
O
N
D

Figure 30b.

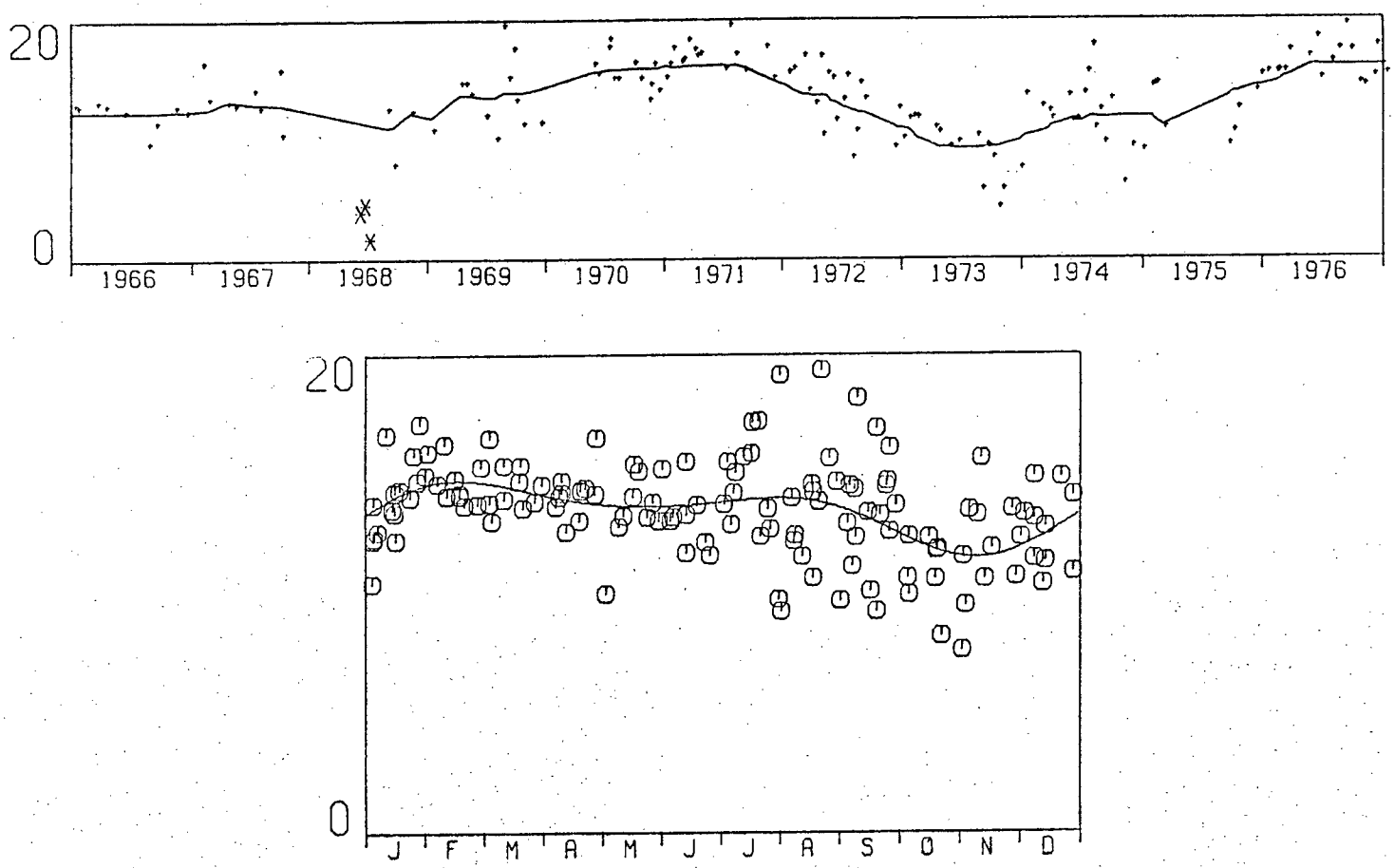
20
0
1966
1967
1968
1969
1970
1971
1972
1973
1974
1975
1976
20
0
J
F
M
A
M
J
J
A
S
O
N
D

Figure 30c.

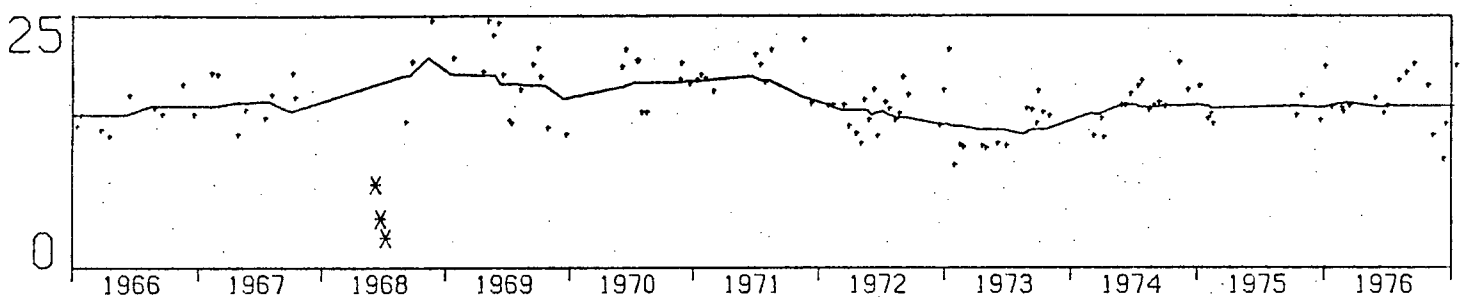
25
0
1966
1967
1968
1969
1970
1971
1972
1973
1974
1975
1976

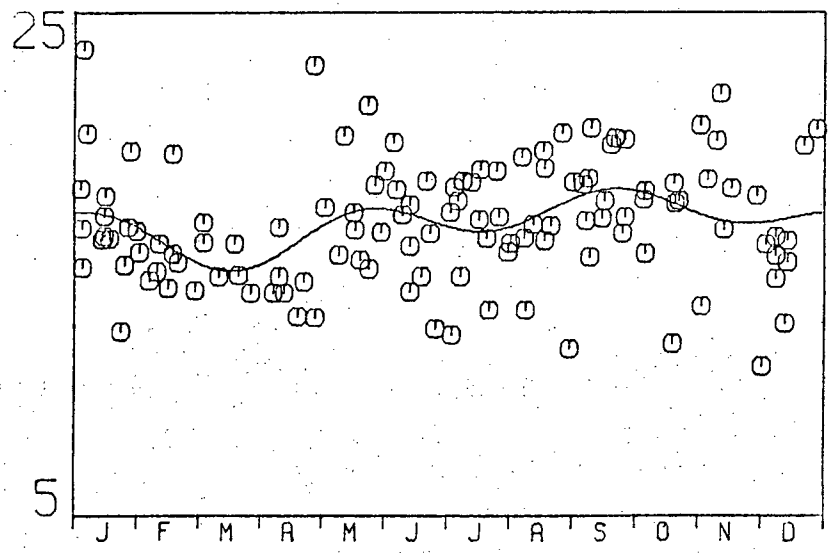
25
5
J
F
M
A
M
J
J
A
S
O
N
D

Figure 30d.

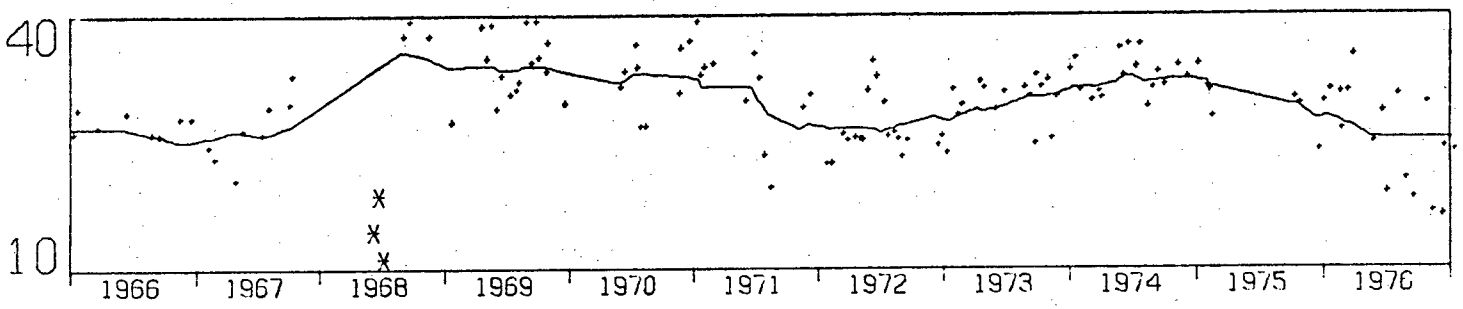
40
10
1966
1967
1968
1969
1970
1971
1972
1973
1974
1975
1976

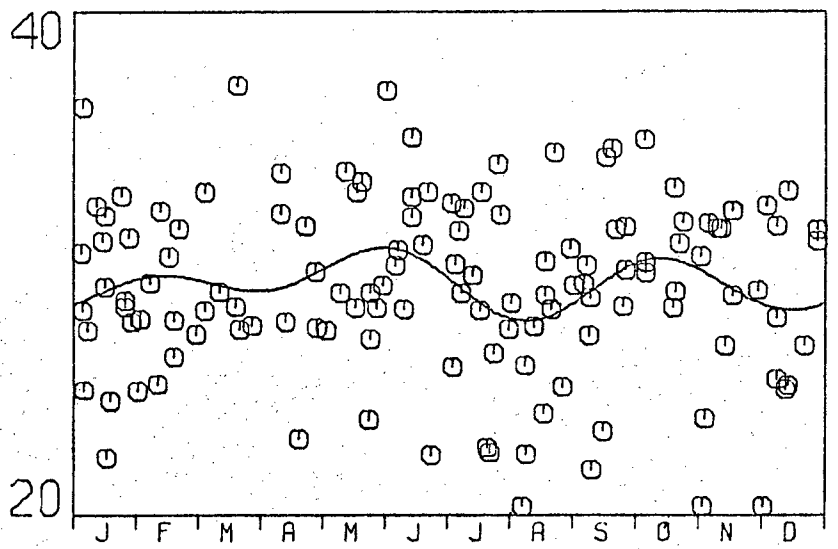
40
20
J
F
M
A
M
J
J
A
S
O
N
D

Figure 30e.

and 1.1 μg at.l^{-1} were observed to depths of 50 to 75 m. Values reported from nutrient-depleted waters are usually less than 1 μgat.l^{-1} (McCarthy and Goldman,1978) and even the lower values from O.S.P. would not normally be considered to limit phytoplankton growth. The possibility remains that phytoplankton at O.S.P. have unusually high half-saturation constants for growth and this would affect greatly the treatment of phytoplankton-zooplankton interactions.

The time series available here are not suited to testing for nutrient dependence of photosynthesis. However, in the absence of experimental evidence concerning nutrient uptake kinetics at O.S.P. , a check was made for unusually low values of P(0) at these times of low nutrient concentration. To avoid confusion with effect of light intensity, values of P(0) over the period May to October were plotted against nitrate concentration. There is no evidence of any decrease in P(0) at low nitrate concentrations (Fig 31). Again, these results must be taken as suggestive only. The scatter in Fig 31 is large enough to mask any slight downward trend at low nitrate concentrations so that values of a half-saturation constant between 0.1 and 2 μg at.l^{-1} would probably not be distinguished. A second reservation is that, if cells responded to nutrient limitation by increasing their C:Chl a ratio (Steele,1962; Antia et al ,1963), a decrease in growth rate might not be reflected in decreased P(0).

3.3 A Phytoplankton Growth Model.

3.3.1 Introduction.

The preceding data analysis, together with information from

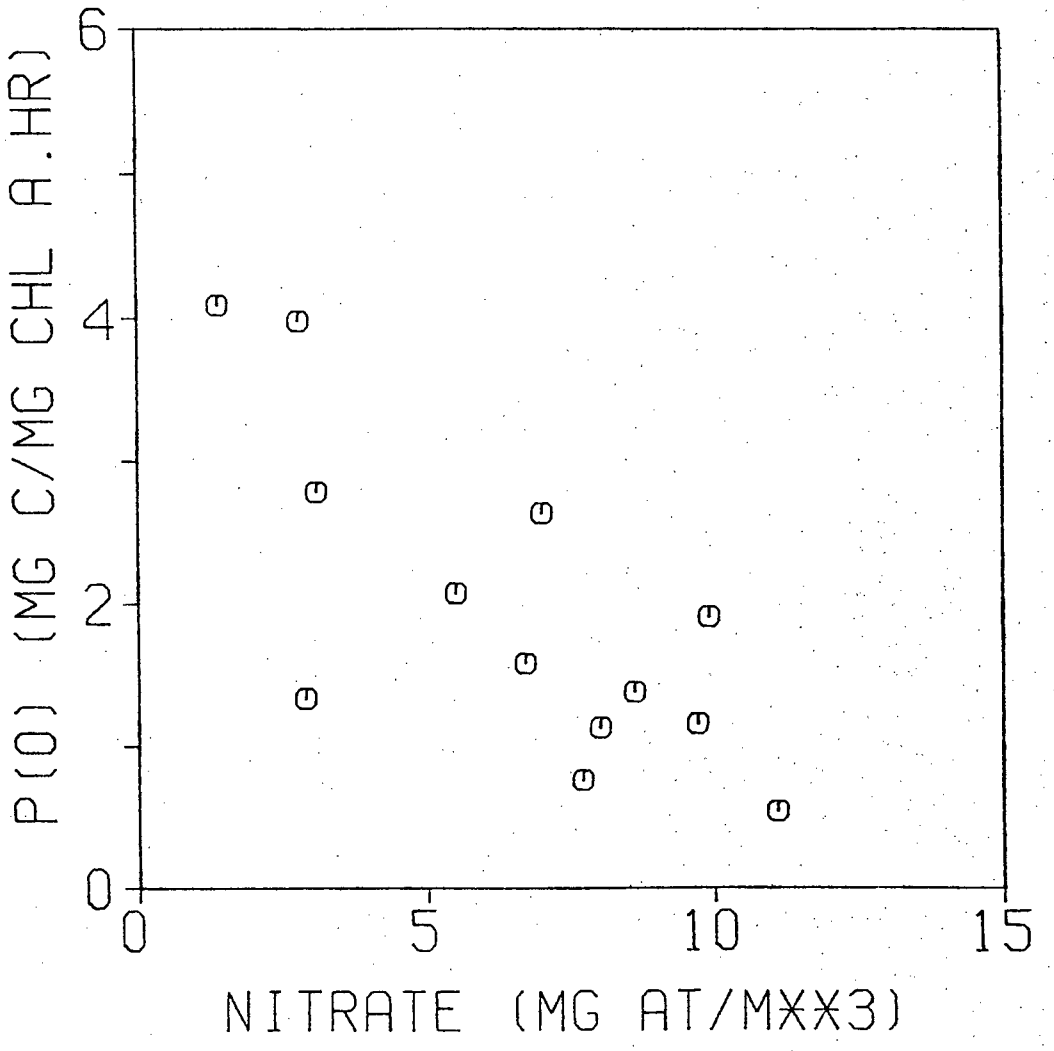

Figure 31. P(0) vs low surface nitrate values, May to October, 1964-68.

the literature where necessary, will now be used to construct a model of phytoplankton growth at O.S.P. which can be driven by time series of observations of physical variables. A simple study of the seasonal cycle of net primary production at O.S.P. has appeared previously (McAllister,1969), but a more sophisticated approach, following the example of Steele(1974) and Jamart et al(1977), is intended here.

3.3.2 Physical Structure and Driving Variables.

Based on the arguments presented in Chapter 1, phytoplankton state variables will be treated as functions of time t and depth z but not horizontal position; that is, a water column 1 metre square will be modelled. The vertical distribution of phytoplankton will be determined by the depth-dependent processes of growth and grazing as well as vertical mixing. The seasonal changes in the physical structure of the water column are reviewed here as background to the modelling of vertical mixing of phytoplankton.

The mixed layer is deepest (greater than 100m) in March, at the end of the period of net heat loss. The formation and maintenance of the seasonal thermocline in subsequent months occurs through the alternation of periods of calm, sunny weather which produce shallow, transient thermoclines, with periods of high wind action during which these transient structures are mixed downward to strengthen the seasonal thermocline (Denman,1972). The latter shallows through the period of net heat gain to reach a minimum of about 30m in August to September. It is then eroded during the period of net heat loss, both by convectional overturn and by wind mixing.

There are two conventional ways to represent vertical mixing in a phytoplankton model. It can be represented as a diffusion process, as in Jamart et al (1977), with diffusion rates dependent on depth and time, high rates being assumed above the thermocline and lower rates within and below it. The resulting partial differential equation for phytoplankton concentration as a function of depth and time can be solved numerically. A simpler approach is to regard the mixed layer above the thermocline as a uniform or well-mixed region, in which physical mixing overwhelms depth-varying biological processes (eg Steele,1974).

It is clear from the above review that neither approach is entirely realistic. The alternation of calm and rough periods and the formation and breakdown of transient thermoclines mean that both a seasonally-varying diffusion rate and a uniform mixed layer can only be regarded as approximations, which may be satisfactory on longer time scales, but are certainly inaccurate on a day to day basis. It also seems unlikely that the process of convective overturn in fall or winter will be accurately represented by a simple diffusion process. As there is little reason to believe that the diffusion representation is more accurate, the simpler uniform mixed-layer model is used here. (The fact that almost all Chl a profiles from O.S.P. show no significant vertical variation within the mixed layer can be taken as empirical support for the simpler approach).

The top 150m of the water column is represented in the model. This includes a mixed layer of depth $z_M(t)$ within which phytoplankton concentration will be assumed to be independent of

depth. Since z_M varies over time, the concentration below the mixed layer as a function of depth must be modelled. In the model, phytoplankton concentration C(z,t) is represented by the values $C(z_i,t)$, i=1...30, in 5m thick layers. (The nominal depths z_i are arbitrarily taken at the midpoints of their respective layers.) The mixed layer depth is given to the nearest 5m and concentrations $C(z_i,t)$ for z_i less than $z_M(t)$ are set equal at each daily step. When z_M increases from one day to the next, the layers above the new mixed layer depth are averaged. In view of the slow changes in salinity and nutrient concentrations below the seasonal thermocline, it can be assumed that mixing rates there are very low. For simplicity, it is assumed here that local depth-dependent processes of growth and grazing dominate the effects of mixing below the thermocline; the 5m layers there are left unconnected.

The physical driving variables are mixed layer depth, temperature as a function of depth, daily solar radiation and secchi depth. These are available as time series (at varying levels of completeness) from weathership observations. The mixed layer depth has been determined from STD profiles, provided by Environment Canada on magnetic data tape, in the following manner. The potential energy required to mix the water column down to depth z, PE(z), was calculated as:

$$PE(z) = g.\int_0^z (\rho(z') - \bar{\rho}).z'.dz'$$

A value of PE(z) of 0.02 $j.cm^{-2}$ was chosen to define the mixed layer depth z_M. This is comparable to the mixing energy provided

by a typical wind storm (Denman,1973) or the decrease in PE which would result from several calm sunny days. By using this criterion, transient shallow thermoclines created during short periods of calm were ignored and a smoother time series for mixed layer depth resulted. If profiles had been available for each day, these transient thermoclines could have been treated as shallow mixed layers but it was necessary to interpolate over gaps of several days and occasionally several weeks. Under these circumstances, the use of the above criterion was judged less likely to result in erroneous interpolation. It is consistent with the use of the uniformly-mixed layer approach as an approximation valid on time scales of several days or longer.

The temperature in the mixed layer was taken as the surface temperature in STD profiles. To avoid storing and reading large quantities of temperature profile data on each simulation run, the temperature below the mixed layer was assumed to drop off exponentially towards 5 C with a decay constant of 20m, chosen after inspection of temperature profiles in one year. This rather crude representation was considered sufficient as almost all phytoplankton production at O.S.P. occurs within the mixed layer and the effects of small errors in temperature-dependent growth rates below the mixed layer are insignificant.

Daily solar radiation was taken from the Monthly Radiation Summaries and photosynthetically active radiation, I_o, was calculated as described in the analysis of ^{14}C profiles. Gaps in the time series were filled by the 1964 to 1976 means for that day of the year.

The driving variable with the least complete time series is

secchi depth, SD, which was used to determine the background extinction coefficient for light according to the formula : k_g = 1.7/SD (Parsons et al ,1977). The observations suggest a seasonal cycle with a minimum in summer and maximum in winter, as well as considerable year to year variation. As observations are not available for all years, an average seasonal cycle was extracted and used for all years :

$$SD = 14.4 + 2.8\ SIN(2.\pi.(t+41)/365) \qquad 3.2$$

3.3.3 Biological Basis for the Model.

The phytoplankton biomass in the model is defined as plant carbon (μg $C.l^{-1}$). Standing stock is observed as Chl a and comparison of predictions with observations will require a knowledge of the carbon:chlorophyll ratio. This is necessary in any case as our analysis of ^{14}C uptake rates allows us to predict carbon produced per unit Chl a, whereas a dynamic model requires a growth rate in $days^{-1}$. The significance of this problem was emphasized by Eppley(1972), but it remains unsolved due to the lack of a reliable method for measuring living plant carbon in the field.

In the absence of direct observations of C:Chl a ratios, a theoretical framework which will allow their prediction is necessary. The theory used here was presented by Steele(1962) and depends on three assumptions :

(1) At low light intensities, photosynthesis is proportional to Chl a, with some constant photosynthetic efficiency α which is not subject to change through light adaptation.

(2) The maximum rate of carbon fixation per cell is governed by the dark reaction and, more specifically, by the enzyme content which is assumed proportional to plant carbon. This implies the existence of a maximum growth rate, μ_H (hr^{-1}) which is temperature-dependent but does not change through light adaptation. The dark respiration rate is assumed to be a fixed percentage of μ_H. (Nutrients will be assumed to be non-limiting at O.S.P.).

(3) Light adaptation occurs through changes in the C:Chl a ratio.

The theory was recognized to be a simplification by Steele(1962) at the time of its proposal. More is now known of the structure and function of the photosynthetic apparatus in relation to light adaptation. Examples include the special role of the P-700 molecule in the light collecting apparatus (Steeman Nielsen,1974) and the significance of dark-reaction enzymes such as RuDP carboxylase (Beardall and Morris,1976). However, these molecular studies have yet to give rise to a coherent theory of light adaptation at the cellular or population level. Recent support for aspects of Steele's theory (Myers and Graham,1971; Bannister,1974; Steeman Nielsen,1974) has encouraged its use here.

The light-dependence of growth is based on the relationship

$$P = \alpha.I.\exp(-I/I_{MAX}) \qquad 3.1$$

used in the analysis of ^{14}C profiles. The daily net growth rate of phytoplankton exposed to daily radiation I is then given by

$$\mu = \alpha.I.\exp(-I/I_{MAX})/V - d \qquad 3.3$$

where V is the C:Chl a ratio and d is the respiration rate (day^{-1}). The maximum daily growth rate is given by

$$\mu_{MAX} = \alpha.I_{MAX}/(V.e) - d$$

According to assumption (2), a maximum (temperature-dependent) hourly growth rate $\mu_H(T)$ can be defined, so that

$$\alpha.I_{MAX}/(V.e) = \mu_H(T).DL + d \qquad 3.4$$

where DL is daylength in hours.
Respiration is assumed to be a fixed proportion, ν, of $\mu_H(T)$; that is,

$$d = \nu.\mu_H(T).24 \qquad 3.5$$

Equations 3.4 and 3.5 can be regarded as defining I_{MAX}, given $\mu_H(T)$ and V, or as defining V, given I_{MAX} and $\mu_H(T)$.

Light intensity is assumed to fall off exponentially with depth, so that $I(z) = I_o \exp(-\int_o^z k(z').dz')$, the extinction coefficient k(z) being defined by $k(z) = k_s + 0.02.C(z)/V(z)$ (Lorenzen,1980, Megard et al ,1980). The conventional method for calculating the average growth rate over a mixed layer of depth z_M (in which k is constant) is to integrate 3.3 vertically to obtain :

$$\bar{\mu} = \alpha.I_{MAX}.(\exp(-I_M/I_{MAX}) - \exp(-I_o/I_{MAX}))/(k.z_M.V) - d \qquad 3.6$$

where $I_M = I_o \exp(-k.z_M)$ is the light intensity at the bottom of the mixed layer. Using equations 3.4 and 3.5, this can be rewritten as:

$$\bar{\mu} = \mu_H(T).DL.e.(1+24.\nu/DL).(\exp(-I_M/I_{MAX})-\exp(-I_o/I_{MAX})) / (k,z_M) - d \qquad 3.7$$

Some recent laboratory and field evidence presented by Marra(1978 a,b) suggests that this approach may not be correct. Marra found that light-saturation and photo-inhibition occur over time scales of tens of minutes to hours and that photosynthetic rates over short exposure periods may increase linearly with light intensity up to very high levels. It follows that, provided circulation times in the mixed layer are short enough, phytoplankton in the ocean may not experience photo-inhibition or even photo-saturation, although in-situ incubations at fixed depths will show these effects.

An accurate assessment of the Marra effect at O.S.P. would require much more information about circulation in the mixed layer on short time scales, and about phytoplankton physiology, than is currently available. Ultimately, the assessment of true in-situ phytoplankton production in the ocean may require that the same attention be paid to short-term fluctuations in ambient light intensity as is currently being paid to fluctuations in nutrient availability (Turpin,1980; Turpin, Harrison and Parslow,1980). As a crude appraisal of the importance of the Marra effect, the average growth rate in the mixed layer can be determined as a function of the average light intensity there :

$$\bar{\mu} = \alpha.\bar{I}.\exp(-\bar{I}/I_{MAX})/V - d \qquad 3.8$$

where $\bar{I} = I_o.(1 - \exp(-k.z_M))/(k.z_M)$. This almost certainly exaggerates the importance of the Marra effect as, for all but very shallow mixed layers, $\bar{I}/I_{MAX}$ is much less than 1 and equation 3.8 represents a linear response to light intensity, as might be expected for continuous very rapid mixing of cells through the mixed layer.

Below the mixed layer, where daily vertical movements of phytoplankton cells are assumed to be very small, the local growth rate at depth z is given by

$$\mu(z) = \alpha.I(z).\exp(-I(z)/I_{MAX})/V - d \qquad 3.9$$

In the numerical model, this expression has been integrated over each 5m layer to give

$$\mu(z_i) = \alpha.(\exp(-I(z_i+2.5)/I_{MAX}) - \exp(-I(z_i-2.5)/I_{MAX})) / (5.k.V) - d \qquad 3.10$$

Using the above expressions, phytoplankton growth rates throughout the water column can now be predicted, given daylength, I_o, mixed layer depth and temperature, and secchi depth. In addition, the parameters α, $\mu_H(T)$, and either I_{MAX} or V must be specified.

The temperature dependence of μ_H was reviewed by Eppley(1972) who gave as an upper bound

$$\log_{10}(\mu_{MAX}) = 0.0275.T - 0.070 \qquad 3.11$$

corresponding to an increase in growth rate per 10°C (Q_{10}) of 1.88X. Growth rates for particular species generally lie below this curve and fall sharply away from it at sufficiently high temperatures. Taxanomic differences in μ_H were clearly shown by Chan(1978), who found that maximum growth rates of diatoms were approximately twice as large as those of dinoflagellates at 20 C. These differences can be allowed for by retaining the coefficient of temperature in equation 3.11 and varying the intercept.

The seasonal pattern of phytoplankton species composition at O.S.P. is not well-known. An extensive set of observations of larger diatoms and dinoflagellates has been accumulated as part of regular microzooplankton sampling from the weatherships (data provided by Kennedy and Fulton). However, preliminary analysis of more carefully collected and preserved phytoplankton samples has suggested that the primary producers are predominately small (less than 10 μ) flagellates throughout the year (R. Waters,pers. Comm.). The growth of marine nanoflagellates as a function of light intensity has not been as well studied as that of diatoms and dinoflagellates. Coccolithophorids have been reported as the dominant phytoplankter at O.S.P. on certain occasions (McAllister,1961; Ishimaru and Nemoto,1977). A maximum growth rate of 2 divisions/day was reported by Paasche(1967) for Coccolithus huxleyi under a 16H:8H light:dark cycle at 20°C. This corresponds to

$$\log_{10}(\mu_H) = 0.0275.T - 1.65 \qquad 3.12$$

The phytoplankton respiration rate in the model is a constant fraction ν of $\mu_H(T)$. The value of ν will be shown to be critical in determining net phytoplankton growth rates, particularly for deep mixed layers. An oft-quoted value of 0.1 was suggested by Ryther(1956), although he noted the large range in reported values, and observed that a lower value seemed to be needed to explain phytoplankton persistence in deep mixed layers in the ocean. There have been many measurements of ν since, but little more consensus has resulted. It has recently been reported as between 0.03 and 0.07 by Harris and Piccinin(1977) and as consistently greater than 0.1 by Burris(1977).

In standard simulations, the seasonal pattern of α represented by the solid line in Fig 24 will be used. The seasonal pattern for B given by the solid line in Fig 27 will be used to determine I_{MAX} for the mixed layer, subject to the constraint that the corresponding value of V according to equations 3.4 and 3.5 must be greater than 20. Below the mixed layer, V is set equal to 20 to represent a shade-adapted population. The use of these estimates in equation 3.3 hinges on an interpretation of the ^{14}C data which deserves some discussion. The parameters α and I_{MAX} in equation 3.3 determine gross photosynthesis, and equation 3.1 has been fitted to weathership observations as if the ^{14}C technique measured gross photosynthesis. The interpretation of ^{14}C uptake rates has seen much controversy: it is generally accepted to measure something between net and gross photosynthesis (Parsons et al ,1977). At low light intensities, especially near or below the compensation depth, the ^{14}C uptake rate must be close to gross photosynthesis,

as negative ^{14}C uptake rates are not technically possible. Much of the sampled depth range at O.S.P. corresponds to such low light intensities, especially in winter. The interpretation of ^{14}C uptake rates as gross rather than net photosynthesis is then less likely to involve major error. If an interpretation as net carbon uptake is preferred, the estimates of α and I_{MAX} used in equation 3.3 can be regarded as predicting net daylight production,with a reduced value of ν corresponding to nocturnal respiration only (cf McAllister,1969).

3.3.4 Simulation Results.

The development so far allows the prediction of phytoplankton growth rates over time. The prediction of phytoplankton standing stock over time requires that zooplankton grazing be modelled, and this will be done in the following chapter. In this chapter, phytoplankton production will be predicted on the basis of the observed phytoplankton standing stock. It will be assumed that grazing is sufficient to keep standing stock in the mixed layer at 0.4 μg Chl $a.l^{-1}$, the mean observed concentration. Standing stock below the mixed layer will not be allowed to exceed this concentration and will be allowed to fall below it where respiration exceeds photosynthesis.

In Fig 32, the time series of physical driving variables for the years 1964 to 1976 are plotted. These were used to predict primary production on the fixed standing stock basis, using the seasonal patterns for α and B (Fig 24,27) discussed above, equation 3.12 for $\mu_H(T)$ and a value for ν of 0.05. One of the noteworthy results of this and subsequent simulations is the lack

Figure 32. Time series of total solar radiation, surface temperature and mixed layer depth used to drive simulation model.

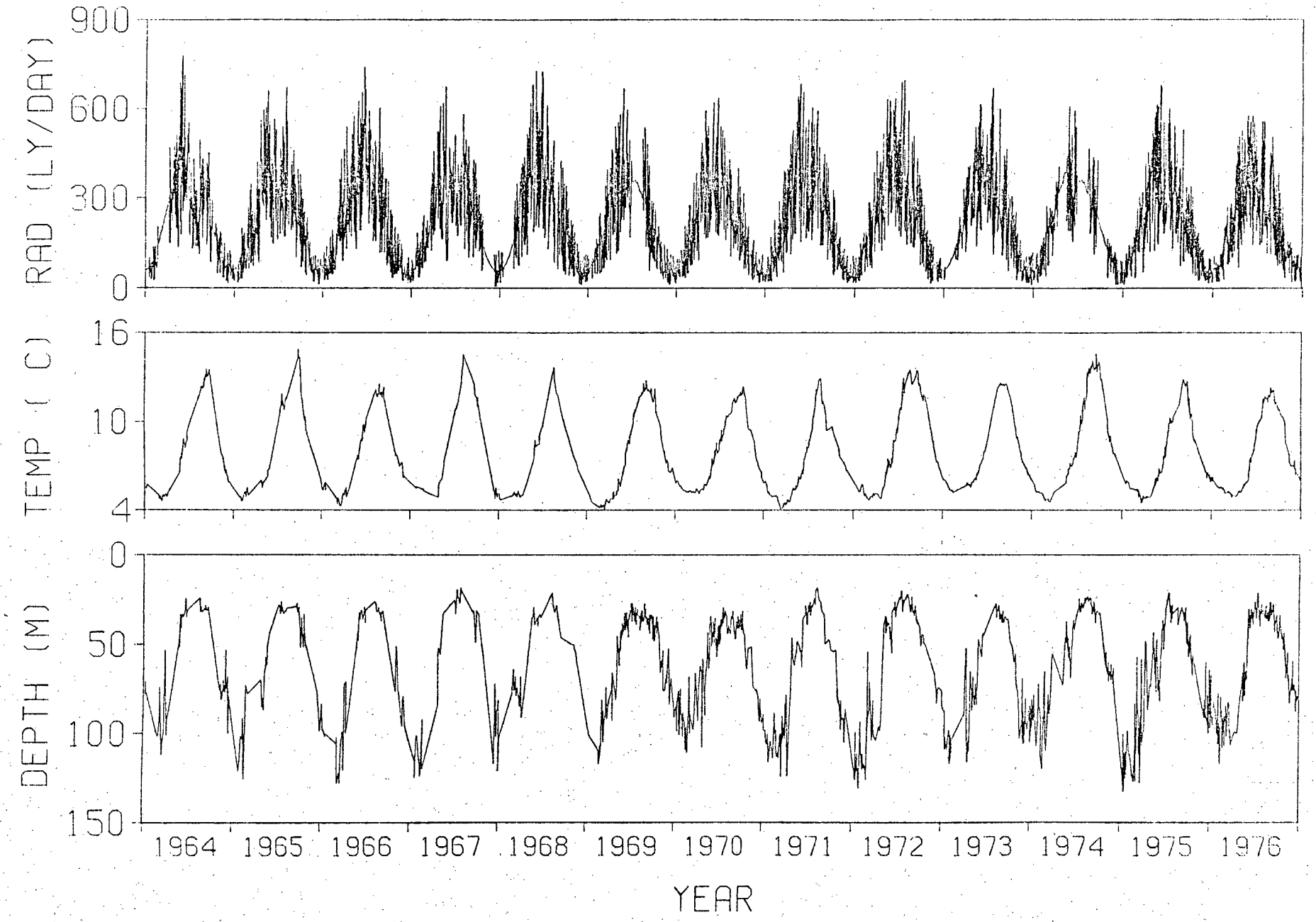
RAD (LY/DAY)
900
600
300
0
TEMP (C)
16
10
4
DEPTH (M)
0
50
100
150
1964
1965
1966
1967
1968
1969
1970
1971
1972
1973
1974
1975
1976
YEAR

of year to year variation in predicted phytoplankton production (Fig 33 and Table II). This feature will be of interest in Chapter 4; for the remainder of this chapter, attention will be focused on seasonal patterns and results presented for one year, 1976, to avoid repetition.

In the analysis of ^{14}C profiles, it was found that the time scale of adaptation to changing light intensities could not be inferred from the data. The effects of different adaptation time scales on predicted primary production can now be considered using the model. Three cases will be considered:

(1) $I_{MAX}(t) = I_o(t)/B$ (instantaneous adaptation),

(2) $I_{MAX}(t) = (I_o(t-1)+I_o(t-2)+I_o(t-3))/(3.B)$ (short time scale)

(3) $I_{MAX}(t) = I_s(t)/B$ (seasonal time scale).

Before considering the first two cases, the concept of fixing phytoplankton standing stock must be considered more carefully.

In the first simulation, light adaptation on a seasonal time scale was assumed and it follows from equations 3.4 and 3.5 that

$$V(t) = \alpha . I_s / (\mu_H(T).DL.(1+24.\nu/DL).e.B) \qquad 3.13$$

so that both V and phytoplankton carbon concentration in the mixed layer, (C = V.0.4), vary smoothly over time. If instantaneous light adaptation is assumed (case 1), V(t), given by replacing I_s in equation 3.13 by I_o, will undergo very large fluctuations from day to day, as I_o does. Fixing the Chl a concentration at 0.4 μg Chl $a.l^{-1}$ will cause the carbon

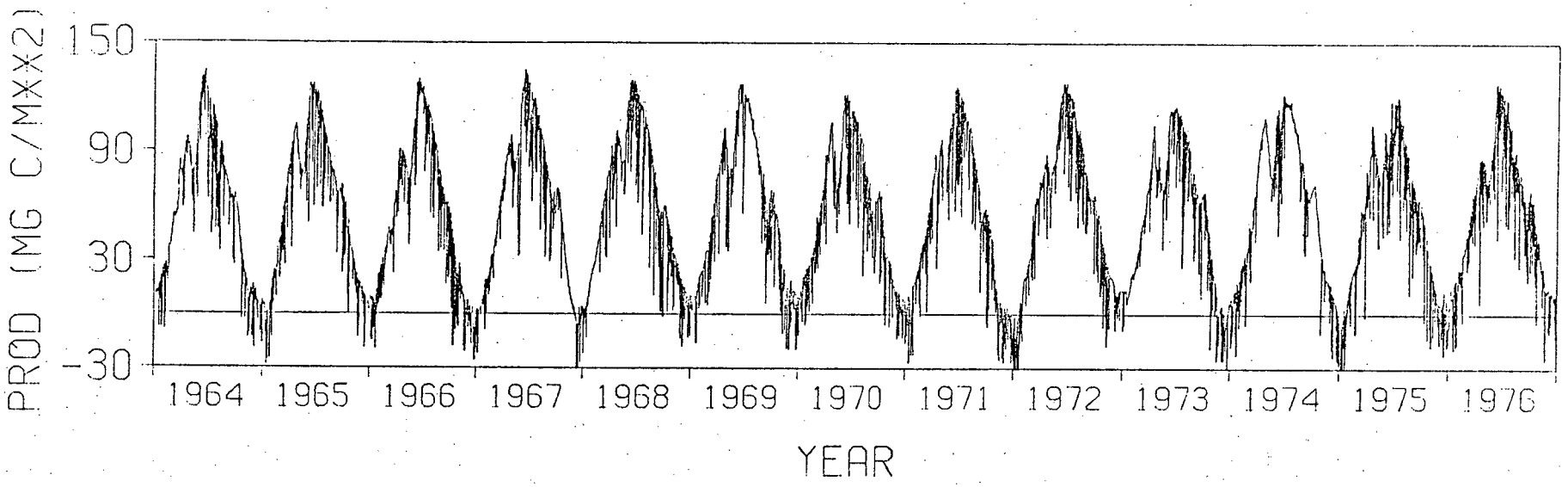

Figure 33. Predicted daily net production using standard parameter set (see text).

Table II

Predicted annual primary production ($g\ C.m^{-2}$) at O.S.P. for 1964 to 1976. (Details of simulation provided in text.)

Year	Gross (Daylight)	Net
1964	35.2	20.6
1965	35.5	21.2
1966	35.2	19.1
1967	35.6	20.5
1968	35.4	21.5
1969	35.6	20.7
1970	35.2	19.8
1971	35.1	18.7
1972	35.3	20.0
1973	35.6	19.2
1974	36.2	21.6
1975	34.6	17.9
1976	34.9	19.6

concentration to fluctuate in the same manner. Although these simulations are not explicitly concerned with conservation of carbon, such rapid fluctuations in plant carbon are not realistic, especially in view of the generally low carbon growth rates predicted. If V is to vary rapidly, it seems more reasonable that this should occur through changes in Chl a concentration. This can be accomplished while keeping average Chl a concentrations near 0.4 μg Chl $a.l^{-1}$ as follows:
(a) Fix a seasonally varying carbon concentration, $C_s(t)$, in the mixed layer by

$$C_s(t) = V_s(t).0.4 \qquad 3.14$$

where $V_s(t)$ is given by equation 3.13.
(b) Fix the actual C:Chl a ratio, V, using one of the short time scale models; the Chl a concentration is then given by Chl $a(t) = C_s(t)/V(t)$.

In Fig 34, the net daily primary production predicted for 1976 in the first simulation is plotted again on an expanded time scale. The daily values of V and Chl a concentration in the mixed layer are also plotted. Light adaptation in this simulation occurred on a seasonal time scale, so that V ($= V_s(t)$) varies smoothly while Chl a is constant at 0.4 μg $.l^{-1}$. The corresponding output for instantaneous adaptation is plotted in Fig 35. Here, V fluctuates markedly with daily changes in I_o and so does Chl a concentration. On the other hand, short-term fluctuations in net primary production are much reduced. There is a simple explanation for this. The dominant contribution to

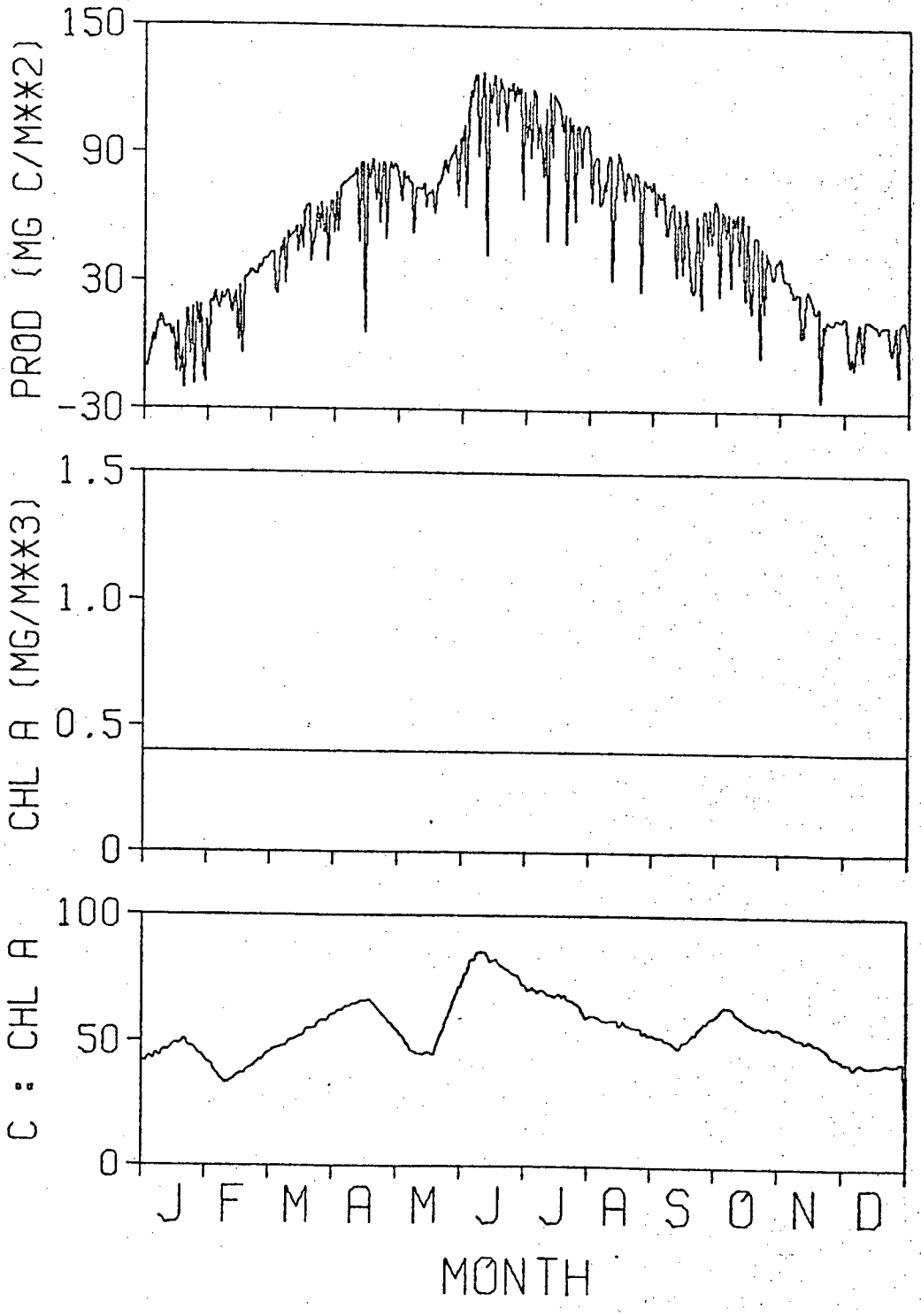

Figure 34. Predicted net production, mixed layer Chl a and mixed layer C:Chl a ratio for 1976 using standard parameter set and seasonal light adaptation.

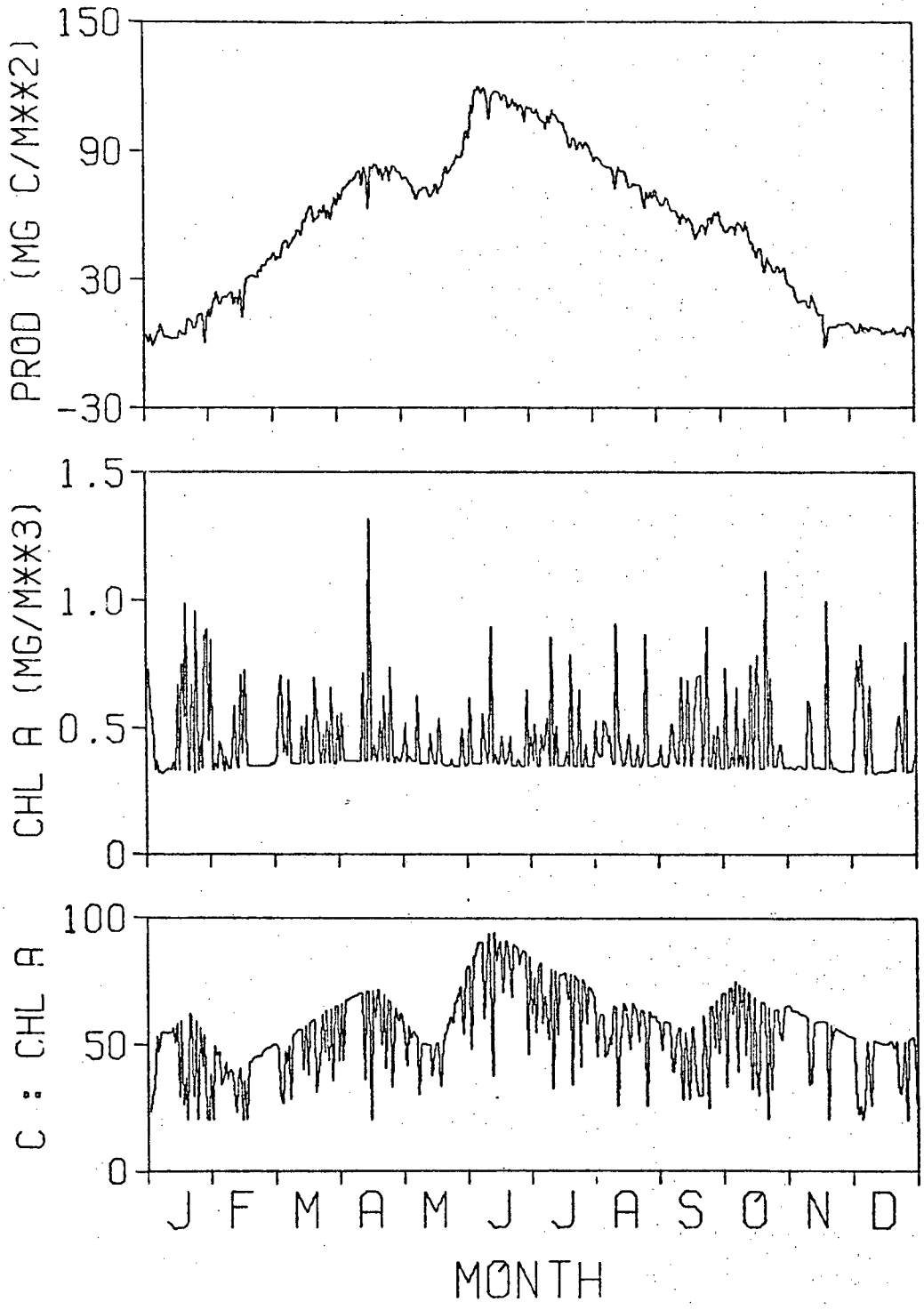

Figure 35. As for Fig 34, but with 'instantaneous' light adaptation.

net primary production in the water column comes from the mixed layer. Using equation 3.7, daily primary production in the mixed layer is given by

$$\bar{\mu}.C_S.z_M = C_S.\mu_H(T).DL.e.(1+24.\nu/DL).(\exp(-I_M/I_{MAX}) - \exp(-I_o/I_{MAX}))/k - 24.\mu_H(T).\nu.C_S.z_M \qquad 3.15$$

As T and z_M vary smoothly over time, the major contributor to daily fluctuations in production is the exponent I_o/I_{MAX}. For seasonal adaptation, I_{MAX} varies with I_S and this exponent fluctuates from day to day with I_o. For instantaneous adaptation, I_{MAX} varies with I_o and the exponent does not fluctuate from day to day. For the intermediate case (2), V and Chl a show reduced short-term fluctuation as expected (Fig 36).

The choice of the adaptation time scale therefore determines the size of short-term fluctuations in V, Chl a and daily primary production. It has very little effect on average primary production levels, as shown in Table III. Comparison of the predicted time series for Chl a in Fig 35 with observations in Fig 13 shows that instantaneous adaptation results in much larger day to day fluctuations in Chl a than were observed during the intensive sampling periods from 1964 to 1968.

The seasonal variation in V is small compared with the five-fold variation in I_S from winter to summer. This variation in I_S is partly compensated for by the seasonal variation in $\mu_H(T)$ and DL. The predicted values of V are reasonable for flagellates although they would be considered large for diatoms, where C:Chl a ratios of 20 or less can be expected under low light

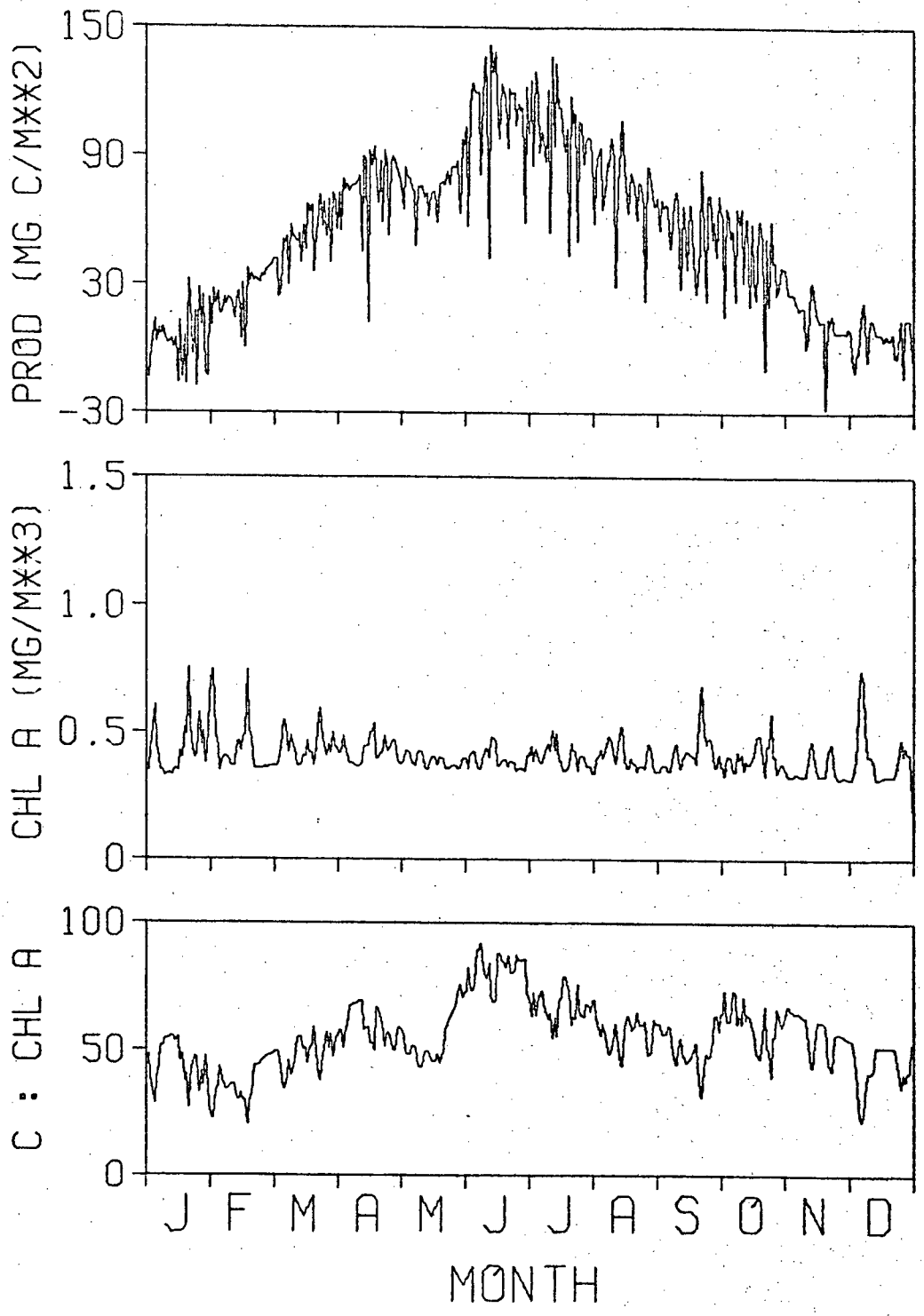

Figure 36. As for Fig 34, but with 3-day adaptation.

Table III

Monthly means of predicted daily net primary production ($mgC.m^{-2}$) at O.S.P. using three light adaptation time scales.

Month	Seasonal	3-day	Instantaneous
January	3.	5.	6.
February	26.	26.	26.
March	51.	53.	54.
April	73.	75.	77.
May	77.	75.	76.
June	112.	111.	111.
July	99.	100.	102.
August	77.	78.	80.
September	57.	58.	61.
October	47.	47.	49.
November	22.	18.	19.
December	7.	6.	7.

conditions. It is interesting that the seasonal variation in and B, based on analysis of the ^{14}C profiles, also reduces the seasonal variation in V. The predicted C:Chl a ratio for 1976 under the assumption of constant α (0.5 mg C.mg Chl $a^{-1}.ly^{-1}$) and constant B (2.0) (Fig 37) shows a much greater percentage increase from winter to summer. This suggests that the seasonal pattern in α and B may be partly a result of constraints on attainable C:Chl a ratios in O.S.P. phytoplankton.

The net annual production totals in Table II are rather low compared with previous estimates for this region (Sanger,1972; McAllister,1969). McAllister (1969) gave upper and lower bounds of 47 g $C.m^{-2}$ and 31 g $C.m^{-2}$ for net primary production, and 61 g $C.m^{-2}$ and 48 g $C.m^{-2}$ respectively for daylight production. The upper bounds were obtained by using a correction factor of 1.25 to allow for effects of enclosure of samples over 10 to 20 hr periods. His annual cycle of daily production (Fig 4) has a peak exceeding 300 mg $C.m^{-2}.day^{-1}$, whereas the peak in Fig 34 does not reach half this total. The possible sources of this discrepancy become clearer when equation 3.14 for net daily production in the mixed layer is rewritten as:

$$Prod = 0.4.\alpha.I_S.(1-\exp(-B)-24.\nu.z_M.k/(e.(DL+24.\nu))/(B.k) \quad 3.16$$

(This is for the case of instantaneous adaptation. The approximation $\exp(-I_M/I_{MAX}) \approx 1$ has been made). Note that gross (or daylight, McAllister) production depends only on the parameters α and B which were estimated from ^{14}C profiles, and the extinction coefficient. Of the parameters taken from the

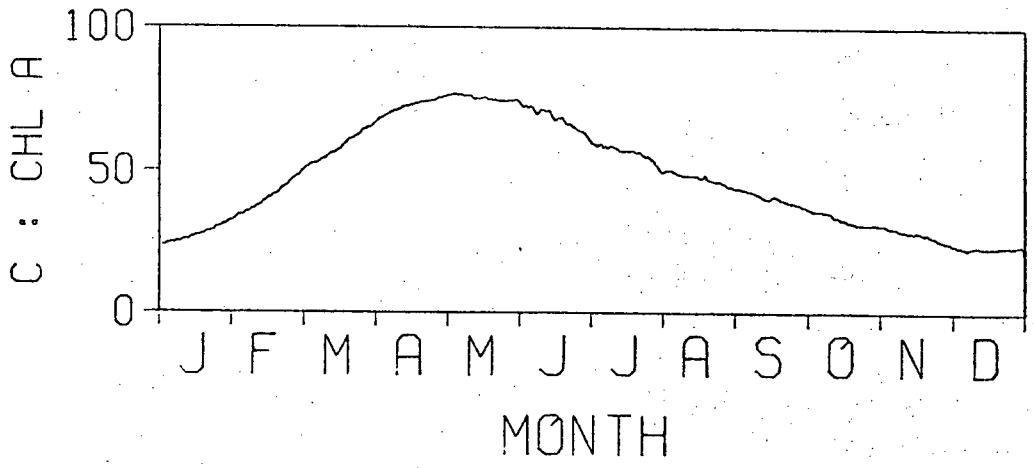

Figure 37. Predicted C:Chl a ratio in the mixed layer for 1976 using α =0.5 and B_s = 2.0.

literature, ν determines respiration but $\mu_H(T)$ does not appear at all. This is not surprising, since under the constant standing stock assumption, the model is predicting production per unit Chl a, precisely what is measured in the field.

It follows that the difference between McAllister's estimate for annual daylight production of 48 g $C.m^{-2}$ and the estimate produced here of about 35 g $C.m^{-2}$ cannot be attributed to the assumption of different parameter values from the literature, but must be due to the use of different weathership data, or different techniques of data analysis. The direct depth integration of ^{14}C profiles from the weathership to obtain daily production for the water column, used by McAllister, was criticised earlier. However, this was now done for the 1964-1968 data to see if it resulted in higher production estimates than the parameter estimation and simulation approach. The resulting annual daylight production estimate was 32 g $C.m^{-2}$, a little lower than that obtained through parameter estimation, and about 2/3 of McAllister's lower value. There are other possible causes of the disagreement. McAllister used an empirically obtained relationship between depth-integrated production and the product of surface production and surface light intensity to allow the inclusion of surface observations in the annual production estimate. He also used observations from an earlier time period, which were based on different incubation techniques.

Given the low estimate of gross or daylight production, the respiration term is responsible for the very low net annual production in Table II, reducing gross production almost by half. The choice of ν is clearly critical in the prediction of net

primary production. For example, increasing γ to 0.10 (the value chosen by Ryther (1956)), reduces net annual production almost to zero and results in negative daily production over half of the year (Fig 38). It is clear that for oceanic environments with deep mixed layers, such as O.S.P., a better understanding of phytoplankton respiration is essential to the accurate estimation of net primary production. Laboratory reports of partial cell shutdown and/or low positive net production at very low light intensities (Smayda and Mitchell-Innes,1974) are interesting in this regard. Again the time scales of fluctuations in ambient light intensity and of the physiological response of cells in the mixed layer may be of critical importance. The inclusion of long time scale adaptation such as the formation of resting spores involved in the life cycles of some phytoplankters could also reduce predicted loss rates in winter.

Inspection of equation 3.16 shows that a simple way to increase annual production to McAllister's levels is to increase α. The seasonal patterns of net daily primary production and C:Chl a ratios predicted by the model for α = 1.0 and B = 2.0, with the additional constraint that V be less than 100, are plotted in Fig 39. Annual gross production is 67 g $C.m^{-2}$ and net production is 45 g $C.m^{-2}$. A value of α as large as 1.0 is not supported by the O.S.P. data but is certainly within the range of values reported from other field or laboratory studies, as discussed above.

Another way to increase production is to introduce the Marra effect by using equation 3.8. With the seasonal cycles of α and B obtained from profile analysis and used earlier, predicted

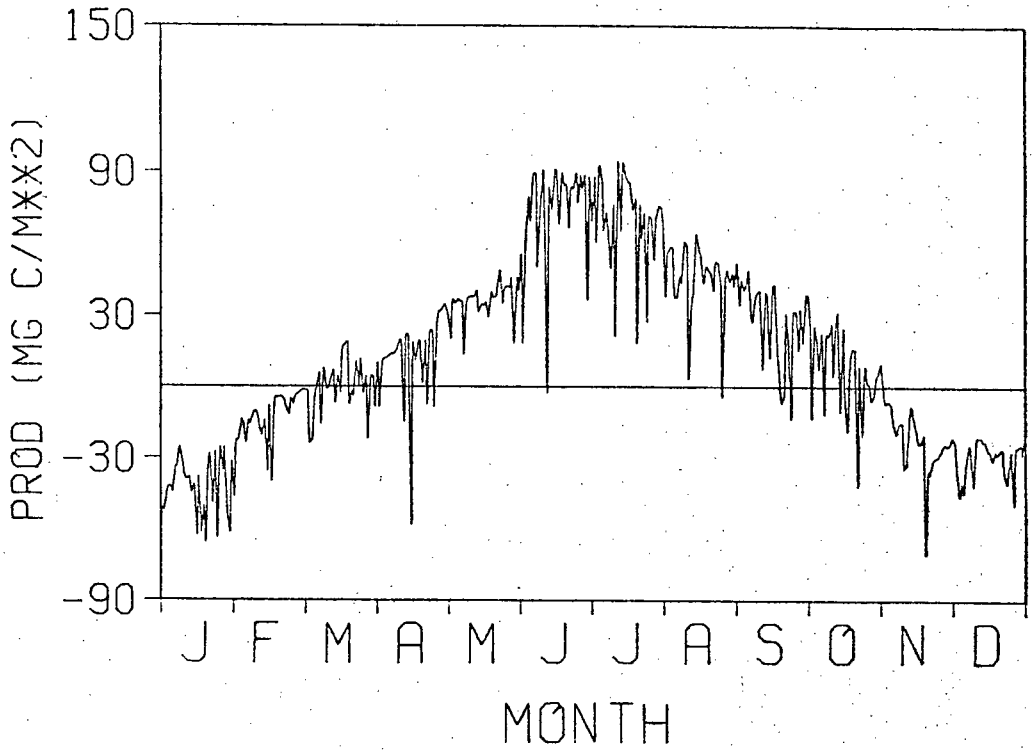

Figure 38. Predicted daily net production on increasing V to 0.1.

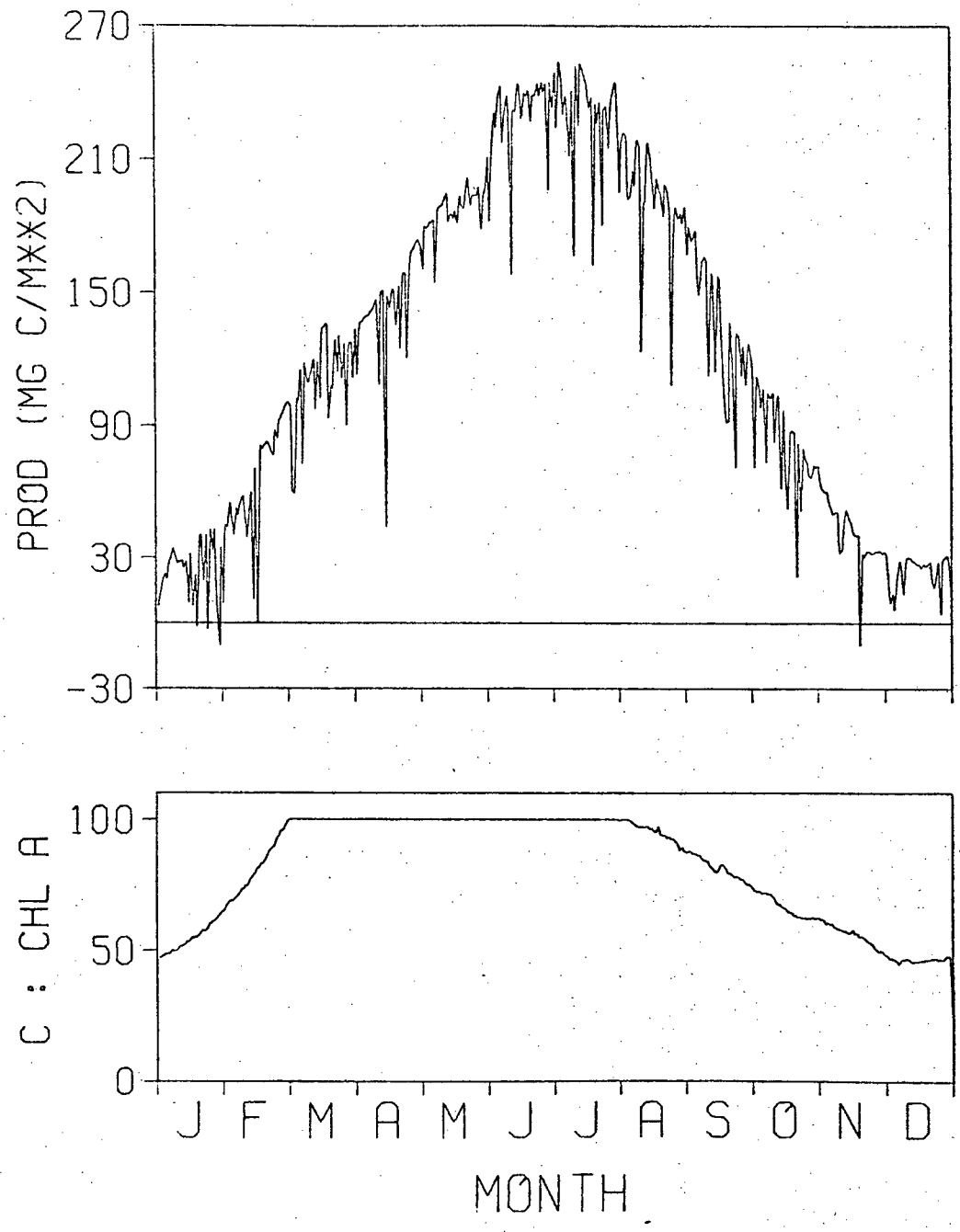

Figure 39. Predicted daily net production and mixed layer C:Chl a ratio for α =1.0, B_s=2.0 with constraint V $\leq$ 100.

gross and net annual production increases to 54 and 39 g $C.m^{-2}$ respectively. The doubling in net primary production is striking (Fig 40) and is due to the subtraction of a constant respiration loss from an increased gross production level. As discussed earlier, equation 3.8 almost certainly exaggerates the importance of the Marra effect, but on the basis of these results further theoretical and experimental investigation appears warranted.

The extinction coefficient, k, also directly affects production estimates (equation 3.15). The values of k in the above simulations are based on the average seasonal cycle of Secchi depth (equation 3.2). (The effect of observed low Chl a levels on the extinction coefficient is negligible.) The secchi depth is the one physical driving variable which was not observed in sufficient density to provide an interpolated time series for each year and consequently represents a source of annual variability not included in Fig 33 or Table II. Upper and lower envelopes to a plot of Secchi depth against time of year (Fig 41) were used to generate seasonal cycles of predicted net daily production, corresponding to extreme seasonal cycles of extinction coefficients (Fig 42). Estimates of gross and net annual primary production were 61 g $C.m^{-2}$ and 35 g $C.m^{-2}$ respectively for maximum Secchi depths (minimum extinction coefficients) and 25 g $C.m^{-2}$ and 10 g $C.m^{-2}$ respectively for minimum Secchi depths. This more than three-fold variation in annual net production is impressive, although annual cycles in Secchi depth need not match the extremes obtained by using envelopes for all years.

The causes of observed seasonal and annual variations in

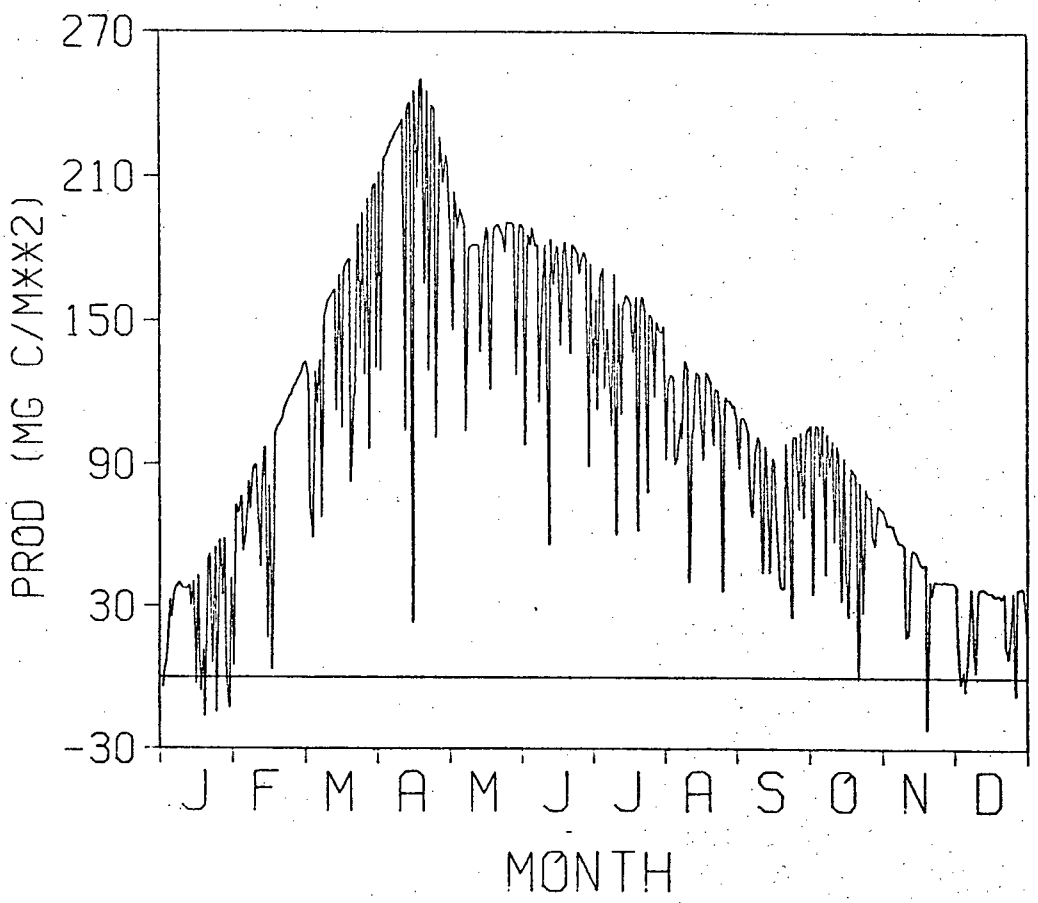

Figure 40. Predicted daily net production for standard parameter set with Marra effect introduced.

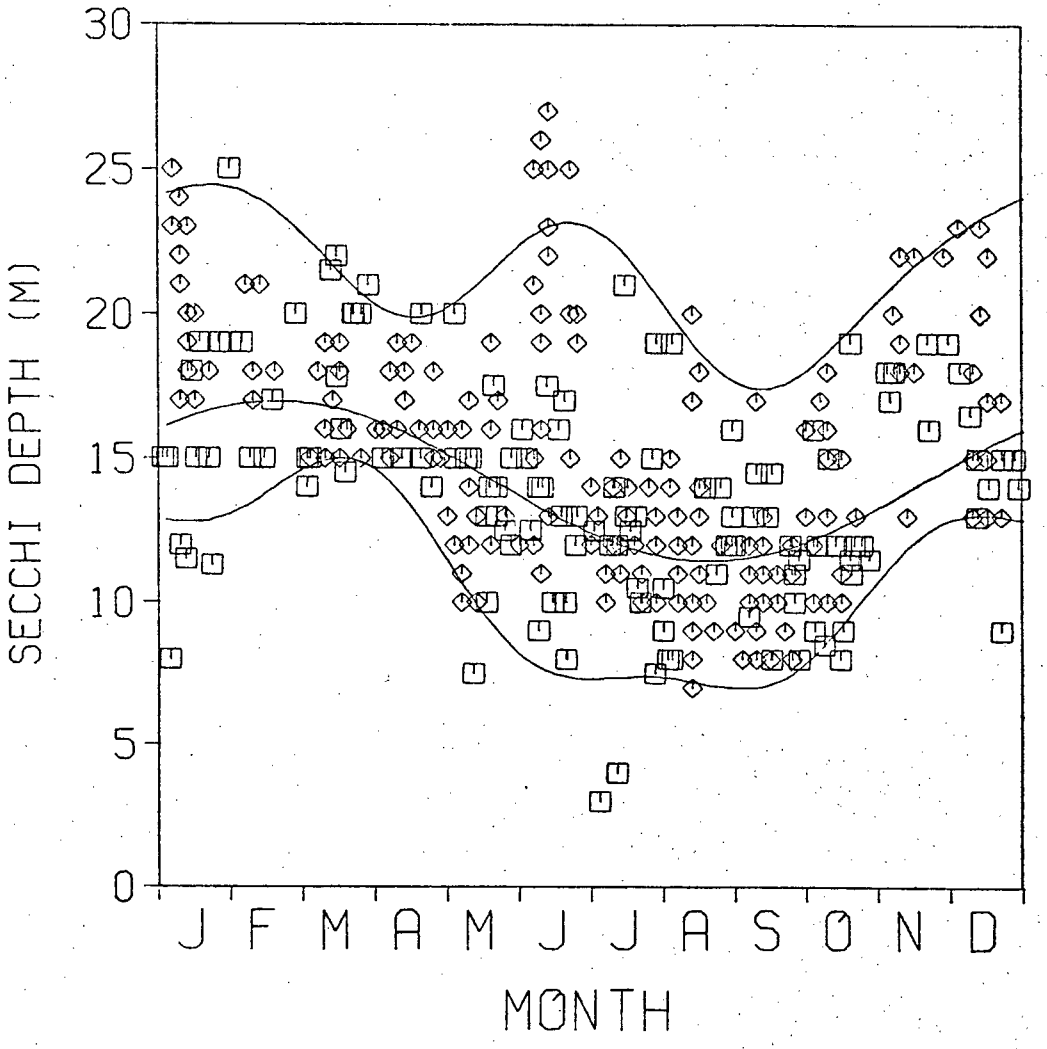

Figure 41. Observed Secchi depths at O.S.P. vs time of year. ◇ before 1964, □ 1964 to 1976. Solid lines represent upper and lower evelopes and seasonal fit to observations after 1964.

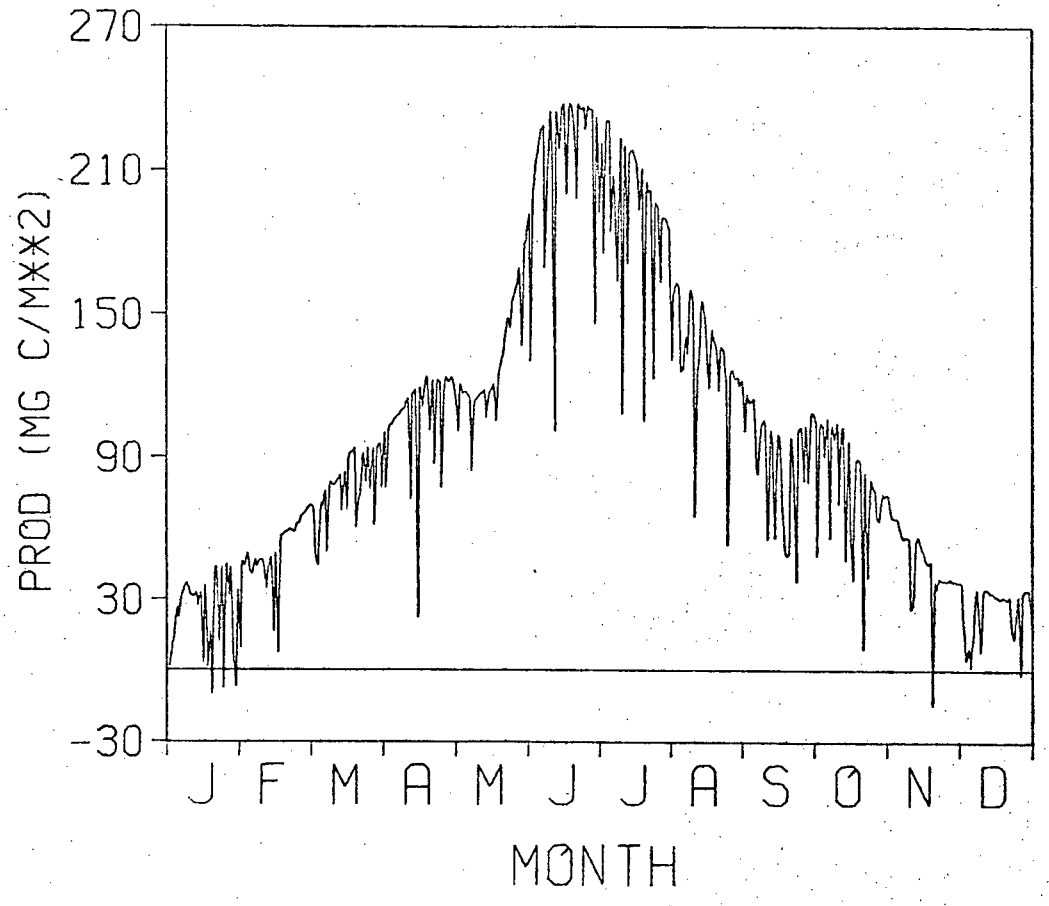

Figure 42a. Predicted daily net production using standard parameter set and upper envelope to Secchi depths.

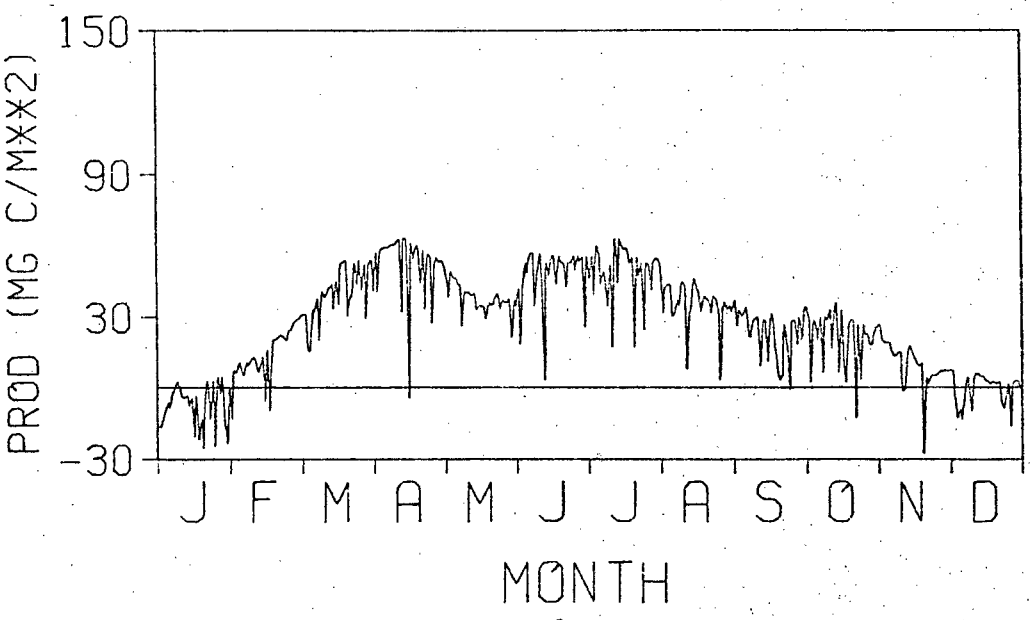

Figure 42b. Predicted daily net production using standard parameter set and lower envelope to Secchi depths.

Secchi depth is not clear. The concentration of Chl a is generally insufficient to account for observed Secchi depths and in any case does not show corresponding seasonal or annual variations. McAllister et al(1961) reported 100-200 mg $C.m^{-3}$ of detrital material in the surface waters at O.S.P. in July-August, some four to eight times the estimated living plant carbon. Recent observations indicate a seasonal cycle in detrital carbon with a minimum in winter and maximum in summer, (K.Iseki and C.S.Wong,pers. comm.), consistent with the notion that changes in the extinction coefficient may be due to changes in detritus levels.

Rather than fixing V or I_{MAX} empirically in equation 3.4, it is interesting to consider using an optimality principle for phytoplankton by demanding that light adaptation of phytoplankton should proceed so as to maximise the average growth rate in the mixed layer. Taking α and $\mu_H(T)$ as given, it is easy to show that in both equation 3.6 and equation 3.8, $\bar{\mu}$ is maximised when

$$V = \alpha.\bar{I}/(e.\mu_H.DL.(1.+24.\nu/DL)).$$

When V was calculated in this way, using the observed seasonal cycle for α, it did not exceed the minimum value of 20 allowed in the model (Fig 43a). Even for α=1.0, the resulting seasonal cycle of V was much lower than that obtained using the values for α and B estimated from profiles (Fig 43b). Apparently, phytoplankton at O.S.P. are not adapted so as to maximise growth rates in the mixed layer. As some marine phytoplankton are known to achieve C:Chl a ratios of 20 or lower (eg Chan,1978), other

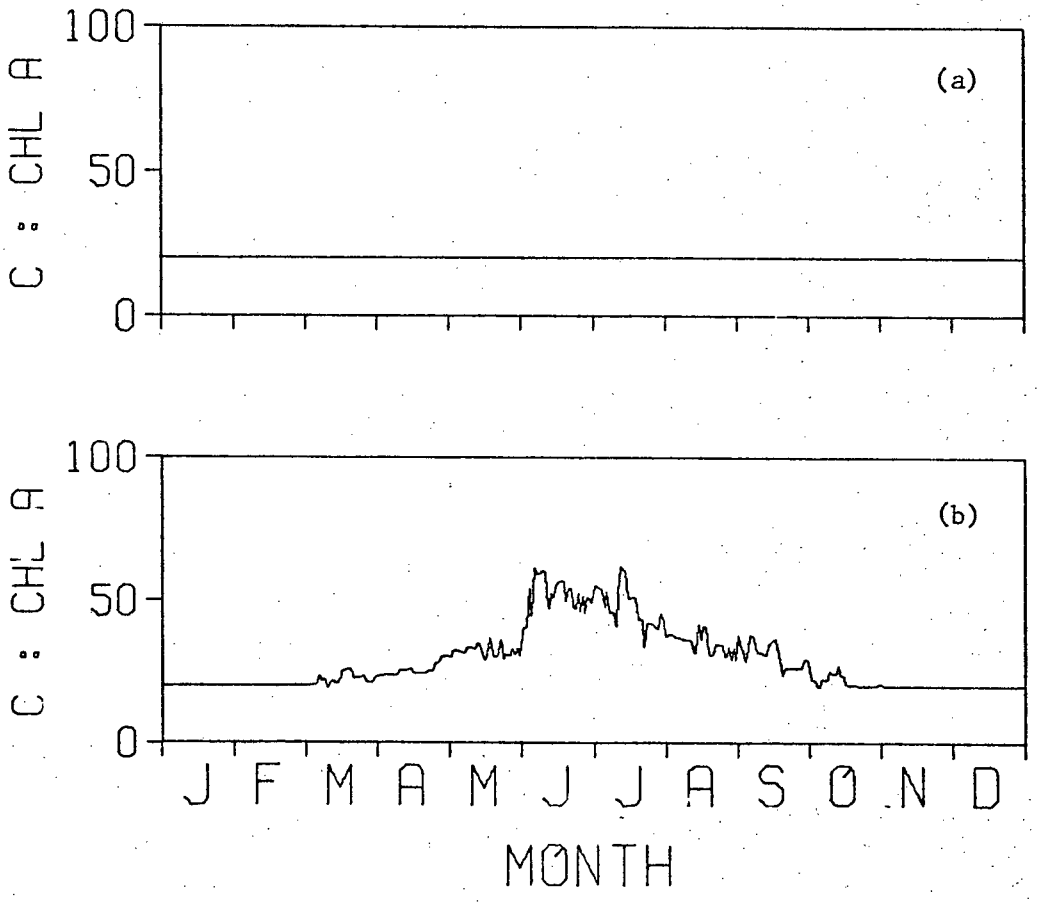

Figure 43. Predicted seasonal cycle in mixed layer C:Chl a ratio using optimality criterion and constraint $V \geq 20$ for

(a) estimated α .

(b) $\alpha = 1.0$.

selective pressures not considered in the growth model, such as grazing, must prevent their dominance at O.S.P.

3.3.5 Primary Production and Nitrate Depletion.

The amount of confidence placed on the initial simulation of primary production at O.S.P. (Fig 33) depends on a number of factors. If the ^{14}C profiles for 1964-1968 are accepted as accurate measures of production, and this period is characteristic of the simulation period, 1964-1976, then the estimated gross production may be taken as accurate to within the standard error in α : approximately +30%. As noted above, estimates of net primary production depend critically on ν, and values between 0 and 26 g $C.m^{-2}$ can be obtained using the estimated α and B without departing from literature ranges for ν. If the ^{14}C observations are discounted, gross production can easily be doubled without assuming values for α and B outside literature ranges.

The nitrate profiles offer the possibility for an independent check on primary production, although other problems of interpretation are involved. A lower limit to gross annual production can be obtained by taking the average annual decrease of 6.4 μg at NO $.m^{-3}$ in the top 40m (Fig 30) and assuming a C:N ratio of 7 $mg.mg^{-1}$ to give 25 g $C.m^{-2}$. This estimate does not allow for growth below 40m, vertical mixing of nitrate from below 40m or nitrate recycling. A slightly higher estimate can be obtained by summing all decreases in the average seasonal cycle for 40 to 80 m (Fig 30). The resulting figure of 28 g $C.m^{-2}$ includes production down to 80m and at least some effect of vertical mixing and/or nitrate recycling as discussed earlier.

The C:N ratio can potentially vary from 3 to 15 (Banse,1974) although higher values are most likely to occur under nitrogen limitation. The nitrate time series has not been used to look at annual variations in primary production, as the large-scale fluctuations in deep-water nitrate concentrations (Fig 30), presumably corresponding to advection of different water masses past the station , prevent an interpretation of nitrate decreases in any particular year as phytoplankton uptake. (These long-term effects have been removed in the average seasonal cycles). The estimates of average annual production based on nitrate decreases are underestimates by an unknown amount which depends on mixing and recycling rates. As they are lower than the predicted annual production (Table II), they allow only the weak conclusion that there is no evidence in the nitrate observations for higher production than predicted in the standard simulation (Fig 33).

CHAPTER 4

HERBIVOROUS ZOOPLANKTON AT O.S.P.: DATA ANALYSIS AND MODELLING.

4.1 Parameter Estimation.

4.1.1 Description of Data.

The time series of observations of zooplankton from the O.S.P. weatherships extends from 1956 to the present and constitutes one of the most extensive open ocean data sets of its type. Following an early report on variation with season and depth of zooplankton composition and abundance (McAllister,1961), two summaries of the time series have appeared in manuscript form (LeBrasseur,1965; Fulton,1978). The data have also been used as a basis for trophodynamic studies (LeBrasseur,1969; McAllister,1969,1972).

The abundance data analysed here come from 150 m vertical hauls using a 350 μm net. Qualitative data from surface tows will not be considered. Changes in the design of the 350 μm net over the sampling period are discussed by Fulton(1978) : earlier abundance estimates based on the NORPAC net have been adjusted here to match the currently-used SCOR net using Fulton's correction factor.

Wet weights of 150m vertical haul samples were recorded throughout the sampling period. These sample wet weights, together with estimated wet weights of four major taxanomic groups : copepods, chaetognaths, euphausiids and amphipods, were reported as time series by LeBrasseur(1965) for the period 1956 to 1964. Average seasonal cycles and abundance for 28 important species during this period were presented and discussed by

LeBrasseur(1965,1969).

Sample analysis changed after 1965 and the summary statistics presented by Fulton(1978) consist of sample wet weight and #ind/m^3 in each of 5 taxanomic groups which include LeBrasseur's 4 groups and the trachymedusae, Aglantha. Starting in 1969, samples were analysed in detail with most organisms being identified to species level and assigned to size classes. These data are stored on magnetic tape and a preliminary analysis has been made in co-operation with J. Fulton. The data are sufficiently comprehensive to allow LeBrasseur's average seasonal cycles to be refined, and annual variations in these cycles to be considered. This analysis will be reported elsewhere. The data are used in this thesis in two rather specialised roles. In this section, a parameter estimation technique developed for analysing copepod cohorts is adapted and applied to the size-structured abundance data for the dominant herbivorous copepods at O.S.P. In the remainder of the chapter, the data will be used in the construction and study of a model of the phytoplankton-zooplankton interaction at O.S.P.

4.1.2 Review of Parameter Estimation Techniques.

As background to the parameter estimation for O.S.P., the results of Parslow et al (1979) and Sonntag and Parslow(1980) are reviewed. In these papers, methods for obtaining population parameters from time series of densities in life history stages using a technique of systems identification were explored. The underlying technique has the following general structure. Given a set of observations $Y(t_i)$, $i = 1,\ldots,N$, and a model which allows predictions $\hat{Y}(t_i,\underset{\sim}{p})$ as a function of time and parameters

$\underset{\sim}{p}$, that set of parameters $\hat{\underset{\sim}{p}}$ is sought which minimizes the sum of squared errors ($SSQ = \sum_i (\hat{Y}(t_i)-Y(t_i))^2$).

In Parslow et al (1979), the observations consisted of densities $S_j(t)$, $j = 1,\ldots,M$ in M stages (or groups of stages) and the parameters consisted of the residence times τ_j and mortality rates θ_j in these stages (or groups of stages). A model is then required which predicts $S_j(t_i)$ given a set of parameters, $\underset{\sim}{\tau}$ and $\underset{\sim}{\theta}$. Underlying the stage-structure of the population is the age-structure model which has the form

$$\frac{\partial Z}{\partial t}(a,t) + \frac{\partial Z}{\partial a}(a,t) = -\theta(a).Z(a,t),$$

where $Z(a,t)$ is the population density of age a at time t and $\theta(a)$ is the per capita mortality rate for individuals of age a. This must be coupled with a formula for mapping $Z(a,t)$ into $S_j(t)$. If all individuals spend the same time τ_j in stage j,

$$S_j(t) = \int_{\sum_{k=1}^{j-1}\tau_k}^{\sum_{k=1}^{j}\tau_k} Z(a,t).da \ .$$

More complicated formulae are required if individual residence times are allowed to vary about a mean value, τ_j. The problem in fitting such an age-structure model to observations is that the initial conditions $Z(a,0)$ and the boundary conditions $Z(0,t)$ are required, but are not directly available. Various simplifying assumptions can be made to overcome this difficulty and these result in a number of simpler models which predict $S_j(t)$. Four such models were considered by Parslow et al (1979), and their performances in the parameter estimation procedure compared.

Any model which predicts $S_j(t)$ can be thought of as a compartment model, with $S_j(t)$ being the compartment contents. There is a flux in, $R_j(t)$, which represents recruitment from the previous stage (or from reproduction) and two fluxes out, one being recruitment to the next stage, $R_{j+1}(t)$, and the other being mortality. Thus

$$\dot{S}_j = R_j(t) - R_{j+1}(t) - \theta_j . S_j(t)$$

The simpler models differ in the way the R_j's are calculated.

The lag model is essentially an age-structure model with fixed residence times. Recruitment rates into and out of stage j are then connected by the relationship

$$R_{j+1}(t) = R_j(t-\tau_j).\exp(-\theta_j.\tau_j)$$

The boundary condition problem appears when we try to calculate recruitment into the first stage, $R_1(t)$. This cannot be done exactly but an approximate recruitment rate into the second stage can be calculated if the residence time in the first stage is short compared with the time scales of changes in $S_1(t)$. Then the linear transfer rate approximation $R_2(t) = p.S_1(t)$ can be used, where the observed densities $S_1^o(t)$ are used to construct a driving variable. Clearly, if observations start at t=0, $R_j(t)$ is only calculable after $t = \sum_{k=1}^{j-1} \tau_k$, so that some observations in later stages have to be discarded.

If the residence times in all stages are assumed to be short compared with time scales of changes in densities, the linear

transfer rate assumption :

$$R_{j+1}(t) = p_j . S_j(t)$$

can be made for all stages, with $S_1(t)$ again being used as a driving variable. The resulting 'linear transfer' model is simple (and linear) and all observations can be used.

A rather different solution to the boundary condition problem was proposed by Manly(1974) for time series representing distinct cohorts. Manly assumed that recruitment into each stage follows a gaussian distribution over time. Rather than predict $S_j(t)$, this model predicts $\sum_{k=j}^{M} S_k(t)$ by assuming a common mortality rate for these stages. Estimates of the size, mean time and spread of recruitment are obtained for each stage. Although stage-dependent mortality rates can be obtained, the model is not internally consistent if mortality rates vary over stages.

The lag-Manly model uses Manly's assumption of gaussian recruitment into the first stage and the lag-model's relationship between recruitment into and out of each stage. It allows the consistent estimation of stage-dependent mortality rates, under the assumption that individual residence times in each stage do not vary.

The performance of the parameter estimation technique using each of these models in turn was considered for data produced by a more complex simulation model designed to probe the weaknesses of each of the models. It was found that the linear transfer model was markedly inferior to the others under almost all

conditions. The other three models provided good estimates of residence times for a range of sampling intervals and degrees of stage aggregation. The lag-Manly model performed best, with estimation errors of a few percent at most. Estimation of residence times by the lag and lag-Manly models was relatively insensitive to log-normal observation error in the data, with average errors less than 25% for coefficients of variation up to 0.4 in the observation errors.

The estimation of mortality rates was much less satisfactory. Reliable estimates of mortality rate in each stage were not obtained for any model. The lag-Manly model did produce reliable estimates of average mortality rates in aggregated stages for small sampling intervals under zero or low observation error.

When applied to a set of CEPEX data representing Pseudocalanus minutus, unsatisfactory results were obtained for all models. It was not clear whether this was due to unexpectedly high observation errors in the data, or to a violation of the models' assumption that population parameters are constant over time.

Estimates of secondary production, including mortality, can be obtained as a by-product of the parameter estimation procedure, once average individual weights in each stage are specified. Estimates generated in this way have been compared with these obtained using a classical technique (Winberg,1968) for both simulated data and a different set of CEPEX data representing a Paracalanus parvus population. Estimates of secondary production for simulated data were found to be much

more reliable than mortality rate estimates. The latter are calculated essentially as differences between estimates of total recruitment into successive stages, while secondary production represents a weighted average of these recruitments.

4.1.3 Application to O.S.P. Data.

Although these techniques were developed for time series of densities in life history stages, they are equally applicable to time series of densities in size classes. However, their application to the data from O.S.P. has presented a number of problems due to the life history strategies of the dominant copepods, the sample methods employed, and the details of sample analysis.

The life-history strategies of Calanus plumchrus and Calanus cristatus were described in Chapter 1. Both species are recruited as nauplii in the surface waters in late winter or early spring. Individuals feed and grow in the surface waters until they reach stage V and have accumulated a lipid reserve. These copepods then leave the surface waters and over-winter below 200m. Reproduction takes place at depth in the case of Calanus plumchrus (Fulton,1973) and nauplii are recruited to surface waters the following spring. There is some suggestion in the O.S.P. data that C. cristatus adults may appear briefly in the surface waters in spring.

These cycles are quite compatible with the estimation techniques discussed above, as they result in a distinct annual cohort. However, the vertical hauls at O.S.P. sample the top 150m only so that the departure of over-wintering copepodids from surface waters appears in the time series as a decline which can

potentially be confused with mortality. This will badly distort estimates of mortality rate using the Manly model, unless all observations taken after the departure commences are discarded. Even assuming there was some a priori way to choose this time, this would result in an unacceptable loss of information for broad cohorts of the type observed at O.S.P. Over-wintering can be simply represented in the lag-Manly model as recruitment out of the largest observed size-class into another which is not observed. This does not eliminate the potential confusion between over-wintering and mortality however, which will appear later as uncertainty in recruitment and mortality rate estimates.

There is also a problem in the interpretation of recruitment in the spring. The smallest size classes identified as C. plumchus or C. cristatus have a nominal length of 1mm. (Naupliar stages are not identified and are probably poorly retained by the 350 μm net). It is assumed here that a size threshold exists, due either to net aperture size or sample analysis techniques, below which all individuals are ignored, and above which all are sampled with constant efficiency. Estimates of recruitment produced here therefore apply to recruitment across this size threshold. It is possible that size classes above this threshold are sampled with variable efficiency, or that some individuals are recruited into the top 150m at sizes above the threshold. To the extent that either occurs, the estimates produced here may be distorted. Estimates of secondary production produced here do not include mortality of small individuals but this usually makes a negligible contribution to total secondary production (Sonntag and Parslow,1980).

The above problems can be handled by simple adjustments of the lag or lag-Manly models. A third problem has required the creation of a new estimation model. The analysis of O.S.P. zooplankton samples has involved a large number of technicians over several years. While care has been taken to ensure consistency of counting and species identification (Fulton,1978), the size classes used have varied amongst technicians and over time. As a result, several different sets of size classes, involving from one to five different divisions, can be found even within one year's data for one species. Any attempt to force these data into a standard set of size-classes in order to apply the lag or lag-Manly models will involve much loss of information, through the blurring of some size classes and the discarding of poorly resolved samples.

An alternate approach has been developed which avoids any loss of information in using the available data. Rather than assume a set of fixed residence times τ_j for a unique set of size classes, a continuous relationship between age and length, $a = A(l)$, is assumed and parametrised. The assumption of gaussian recruitment, together with the age-structure model, allow the prediction of an age-distribution $Z(a,t)$ over time, which can then be translated into a size-distribution $Z'(l,t)$. For each sample, integration of the predicted size-distribution between appropriate limits provides predictions of densities in size classes which exactly match the size classes used in the analysis of that sample.

A power law is chosen for $A(l)$:

$$a = a_1.(l^\gamma - l_R^\gamma)$$

where l_R is the threshold size below which individuals are not sampled. The parameters a_1 and γ are estimated. Note that if weight is proportional to l^3 and growth (dW/dt) proportional to l^2, $\gamma = 1$. If growth is a smaller power of length (eg Steele and Frost(1977) suggest ingestion may be proportional to length), γ is larger than 1. As exponential growth is approached, γ approaches zero. The mortality rate law $\theta(a)$, or equivalently $\theta'(l)$, must also be parametrized. While some dependence of mortality rate on size might be expected (eg Cushing,1976), scatter in the data, the lack of size-class resolution and confusion due to over-wintering discouraged any attempt to go beyond a constant mortality rate.

The exact parameter estimation procedure is therefore as follows. Given initial guesses at total recruitment, R^T, spread of recruitment σ, mean time of recruitment μ and mortality rate θ, the age-distribution $Z(a,t)$ is given by

$$Z(a,t) = R^T.\exp(-(t-a-\mu)^2/(2.\sigma^2) - \theta.a) \;/\; (\sqrt{2\pi}.\sigma)$$

Given values for a_1 and γ, the length-distribution can be deduced. The lengths at recruitment, l_R, and at over-wintering, l_F, are fixed for each species based on minimum and maximum observed lengths. On each day, given a set of M size classes with nominal sizes $l_1^\circ, l_2^\circ, \ldots, l_M^\circ$, a corresponding set of size class limits is defined by

$$l_0 = l_R$$
$$\vdots$$

$l_j \triangleq (l_j^\circ + l_{j+1}^\circ)/2 \qquad j=1,\ldots,M-1$

$l_M = l_F$

Predicted densities $\hat{S}_j(t) = \int_{l_{j-1}}^{l_j} Z'(l,t).dl$ can then be compared with observed densities $S_j^\circ(t)$ and the parameters corresponding to minimum SSQ errors obtained using the Marquardt algorithm (Marquardt,1963).

4.1.4 Statistical Considerations.

In view of the lack of comparable estimates of the parameters sought here, an attempt was made to provide at least an indication of statistical uncertainty in estimated parameters. As a preliminary step, the nature of variability in the zooplankton samples from O.S.P. was investigated. Analysis of 10 replicate samples taken within a short time period (3 hours) on 10th June, 1978, indicated that the variance in species counts increased with the mean at low densities (Poisson) and with the mean squared at high densities (log-normal) with an asymptotic coefficient of variation of 0.2. Following Barnes (1952), the normalising transformation

$$Y' = \sinh^{-1}(\beta.\sqrt{Y})/\beta$$

with $\beta = .2$, was employed and the SSQ errors between transformed predictions and observations was minimized. (Estimates initially obtained without transforming the data showed great variability from year to year and inspection of predicted timestreams showed a tendency to fit one or two anomalous high observations closely and ignore the rest.)

The exact statistical distribution of estimates obtained through non-linear, least-squares techniques can not generally be found. However, an approximate distribution can be obtained by approximating the non-linear function of parameters by a linear function in the neighborhood of the parameter estimate. Under this approximation, if the statistical model is $Y_i = f_i(p) + \varepsilon_i$ ... ε_i iid $N(0,\sigma_\varepsilon^2)$, $\underset{\sim}{p}^*$ is the true parameter set and $\hat{\underset{\sim}{p}}$ is the least-squares estimate, $\hat{\underset{\sim}{p}} - \underset{\sim}{p}^*$ has a multivariate normal distribution with covariance matrix

$$\left[\left(\frac{\partial \underset{\sim}{f}}{\partial \underset{\sim}{p}}\right)^T \cdot \left(\frac{\partial \underset{\sim}{f}}{\partial \underset{\sim}{p}}\right)\right]^{-1} \cdot \sigma_\varepsilon^2$$

evaluated at $\hat{\underset{\sim}{p}}$ (Benson,1978). The accuracy of the approximation clearly depends on the relative magnitude of the likely error in $\hat{\underset{\sim}{p}}$ and the scale of non-linearities in $\underset{\sim}{f}$.

4.1.5 Results for Calanus plumchrus.

It was possible to apply the parameter estimation techniques to size-structured data for C. plumchrus in the years 1969,1970,1973,1975,1976 and 1977. In 1971 and 1972, size-structure information was either not present or insufficient to allow parameter estimation. In 1974, transition water appeared in mid-summer and this, combined with a 6-week data gap, made it impossible to fit a cohort model sensibly.

Six parameters were estimated in each year. These were total recruitment R^T, mean recruitment time μ, standard deviation of recruitment σ, individual residence time in samples τ, age-length power γ and mortality rate θ. The total residence time, τ, estimated in place of the constant a_1, is given by

$$\tau = a_1 . (l_F^\gamma - l_R^\gamma)$$

These six parameters could be divided into two groups based on the properties of the approximate covariance matrices. One set consisted of μ, σ and τ. These variables, all related to timing, were not highly correlated with one another or with members of the second set, consisting of R^T, θ and γ. Estimates for this second set were very highly correlated with one another, correlation coefficients of 0.98 being common. There was essentially one degree of freedom involving these parameters which could not be resolved by the estimation technique from these time series.

The parameter estimates are given in Table IV. The 95% confidence intervals given in that table for μ, σ and τ are actually the limits of a 95% confidence region for all 6 parameters determined by $F_{6,n-6}$ statistics. Because of the high correlation amongst R^T, θ and γ, individual confidence intervals are uninformative and instead projections of the 95% confidence regions on the (R^T,θ) and (θ, γ) planes have been presented in Fig 44.

Note that, because of the confusion of θ, R^T and γ, it became necessary to constrain θ to be non-negative in some years. In fact, as zero mortality rates are unlikely in nature, the constraint $\theta \geq 0.005$ day^{-1} was imposed and confidence regions for (R^T,θ) and (θ, γ) are truncated accordingly.

The mean recruitment time occurs in April and early May with apparently earlier recruitment in 1975 and 1976. The standard deviation of recruitment into the smallest size class is fairly constant at about 30 days, with a larger spread in 1975. Residence times above 150m are remarkably consistent from year-

Table IV.

Parameter estimates for Calanus plumchrus.

Year	μ (days)	σ(days)	τ(days)	R^T(ind.m^{-3})	θ(day^{-1})	
1969	121.±27.	27.± 9.	56.±34.	50.	0.005*	1.4
1970	126.±21.	31.± 5.	58.±23.	238.	0.005*	1.0
1973	112.±18.	24.± 7.	66.±31.	318.	0.040	2.2
1975	93.±30.	48.±12.	65.±65.	72.	0.005*	0.45
1976	96.±29.	34.± 8.	64.±37.	141.	0.005*	1.0
1977	105.±10.	31.± 4.	66.±20.	498.	0.027	1.6

* These values were frozen to allow convergence.

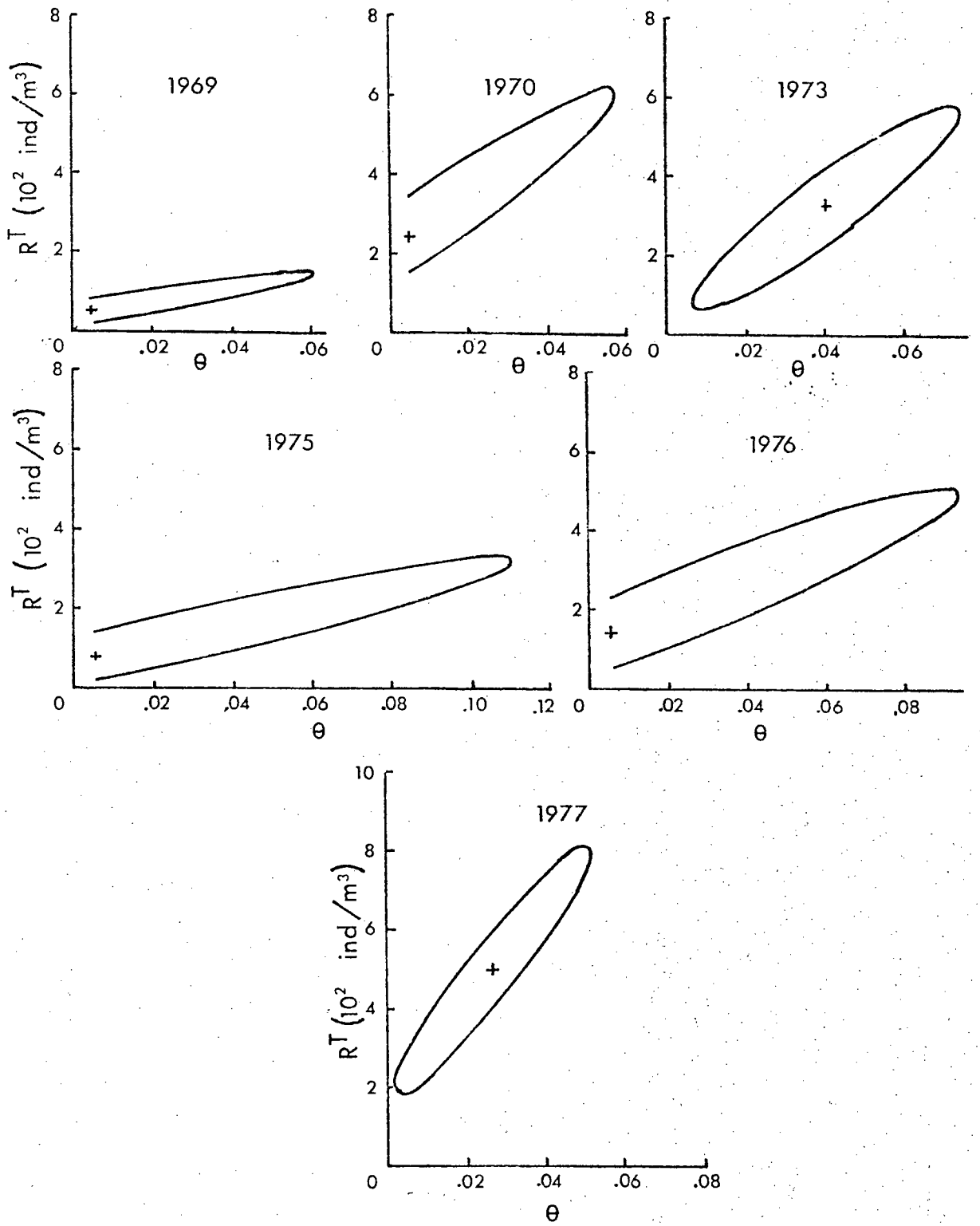

Figure 44a. Projection of approximate 95% confidence regions for Calanus plumchrus parameter estimates on (θ, R^T) plane.

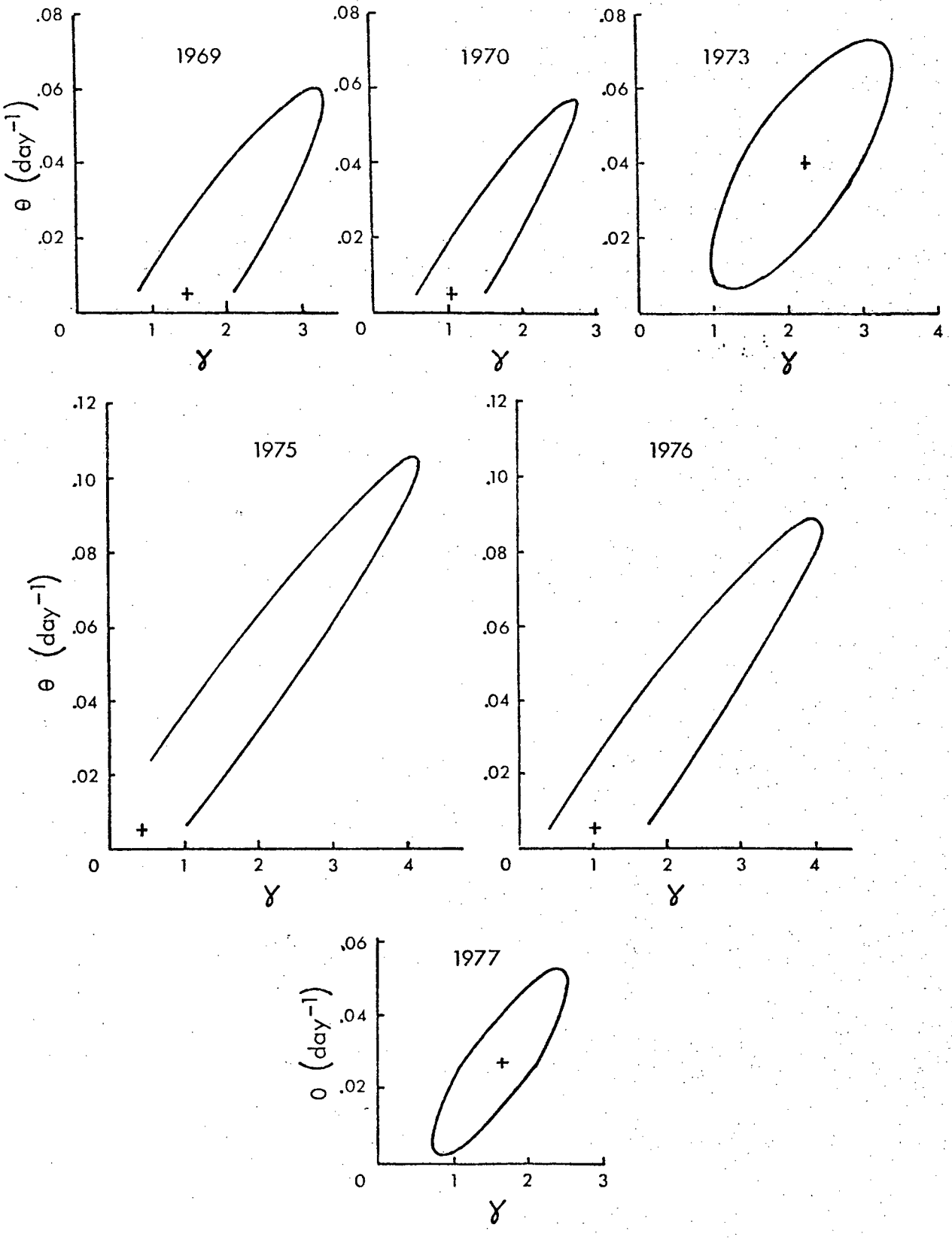

Figure 44b. Projection of approximate 95% confidence regions for Calanus plumchrus parameter estimates on (γ,θ) plane.

to-year considering the large confidence intervals. The sampled population of C. plumchrus above 150m at O.S.P. can therefore be characterized as a broad cohort, recruited over 2 months or more from March to May, of individuals which spend about 60 days in the surface layer and leave during June and July.

A detailed account of the life history of C. plumchrus in the Strait of Georgia was given by Fulton(1973). In that study, deep vertical hauls allowed the full life cycle, including maturation and reproduction, to be followed. Fulton reported that maximum egg production occurred on March 5th and maximum abundance of nauplii in surface waters on March 17th. The peak abundance of copepodite stage V occurred 62 days later, on May 18th. His schematic diagram suggests that a broad cohort, exceeding 2 months in width, is recruited into the top 150m during February, March and April and departs as stage V copepodids in May, June and July.

Comparison of his results with the estimates produced here is difficult as nauplii are not sampled at O.S.P. and our recruitment estimates refer to early copepodids. Also, depending on the importance of mortality, his peak to peak times may not be comparable to the mean recruitment and residence times estimated here using a dynamic model. Ignoring the second problem, it is clear that recruitment of nauplii in the Strait of Georgia precedes recruitment of early copepodids at O.S.P. which is not surprising. In fact, it might be expected that recruitment of nauplii would occur later at O.S.P. as well, as the spring increase in primary production occurs earlier in the Strait of Georgia (Parsons,1965). The period of 62 days between peak

naupliar and peak CV abundance in the Strait of Georgia is the same as the estimated residence times from early copepodite to stage V at O.S.P. If these are technically comparable, growth is slower at O.S.P. which would hardly be surprising, in view of the much lower phytoplankton standing stock there.

The large uncertainty in R^T, Θ and γ is unfortunate, as a knowledge of mortality rates would be of great interest. The uncertainty arises from a combination of the confusion of mortality and over-wintering departure, observation errors, a relatively small number of coarse size classes and the broad cohort width. For example, increasing the mortality rate in the model would normally have the effect of decreasing the number of individuals in larger size classes. However, because of the broad cohort width, this effect can be counteracted by increasing total recruitment and increasing γ, which increases the relative duration and consequently the relative abundance, of larger size classes.

Note that in 1973 and 1977, the optimum parameter set occurs for positive Θ while in the other years, Θ must be constrained to be positive. However, the confidence regions in the (Θ, γ) plane show similar orientation and position, so that some overlap occurs amongst all years. A range for Θ of 0.0 to 0.1 day^{-1} is implied by the confidence regions. Much smaller confidence regions can be obtained for R^T and Θ by fixing the growth law parameter γ. For $\gamma = 1$, low values of R^T, ranging from between 200 and 450 ind/m^3 in 1977 to between 25 and 60 ind/m^3 in 1969, are estimated. Higher values of R^T and Θ are obtained for $\gamma = 2$.

4.1.5 Results for C. cristatus.

Parameter estimates could be obtained for the years 1969,1970,1974,1975,1976 and 1977. The years 1971 and 1972 were again omitted for lack of size-structure information. As C. cristatus is present later in the year than C. plumchrus, a fall intrusion of transition water in 1973 interrupted the time series for this species. The technique was applied to 1974 but the early presence of transition water clearly distorts parameter estimates.

In general, the C. cristatus time series were not as 'well-behaved' as those for C. plumchrus and estimates show greater uncertainty. Estimates of μ, σ and τ are given in Table V. There is clearly much less consistency from year to year in mean recruitment time for this species, with μ ranging from day 67 in 1977 to day 142 in 1970. (The very late recruitment in 1974 is due to transition water intrusion.) Discounting 1974, the spread of recruitment is similar to that for C. plumchrus, ranging from 20 days in 1977 to 42 days in 1970. Great variability is shown in residence times, with τ ranging from 83 and 89 days in 1976 and 1969, to 213 days in 1977.

No really consistent picture of the life history of C. cristatus emerges from this analysis. Excluding 1974, it can be said that a broad cohort is recruited over approximately a 2 month period at some time between February and June and leaves at some time between June and October. In view of the large approximate confidence intervals, this apparent annual variability may be a statistical artifact. Especially with regard to the variation in residence time, it is interesting that

Table V.

Parameter estimates for Calanus cristatus.

Year	μ(days)	σ(days)	τ(days)	R^T(ind.m^{-3})	θ(day^{-1})	
1969	89.±45.	24.±17.	89.± 61.	9.5	0.008	0.5*
1970	142.±25.	42.±13.	119.±100.	97.	0.034	1.4
1974	188.±29.	18.± 9.	53.± 39.	16.	0.005*	3.0
1975	100.±35.	34.±19.	134.±171.	34.	0.005*	0.9
1976	99.±22.	34.± 8.	83.± 41.	118.	0.020	0.5*
1977	67.±27.	20.±15.	213.± 84.	12.	0.027	1.7

* These values were frozen to allow convergence.

observations of C. cristatus in late summer and fall are often very low except for rare, high observations. This may be due to spatial aggregation, as late stages of C. cristatus are large (7-8mm) and may show active swarming behaviour (Nemoto,1957). Diurnal vertical migration by these late stages has also been reported (Marlowe and Miller,1975) and it is quite possible that they are poorly sampled by the 150m daylight vertical hauls.

Projections of the 95% confidence regions on the (Θ, γ) and (R^T, Θ) planes are given in Fig 45. As for C. plumchrus, high correlations were found between R^T and Θ in all years. However, γ was not highly correlated with R^T or Θ in 1970,1975 and 1977. In these years, numbers of large (ca 8mm) individuals appeared before day 100, coincident with or earlier than small individuals. These were regarded as part of a separate cohort, and a cohort starting with small size classes was distinguished by eye. The resulting time series showed a clearer lag in the appearance of larger size classes and this would be expected to reduce confusion between γ and Θ.

To obtain convergence, it was necessary to freeze γ (at 0.5) in 1969 and 1976, and to freeze Θ (at 0.005 day^{-1}) in 1974. The simultaneous appearance of small and intermediate sized individuals following a transition water intrusion in 1974 resulted in an anomalously high estimate of γ. Otherwise, low estimates of γ, in the range 0.5 to 2.0, were obtained. Again, the confidence regions encompass a wide range of Θ, from 0.005 day^{-1} to 0.07 day^{-1}, excluding 1974. Fixing the value of γ results in smaller ranges in 1969 and 1976, but has little effect in those years where (Θ, γ) correlations are low. The estimates

Figure 45. Projection of approximate 95% confidence regions for Calanus cristatus parameter estimates on (a) (θ, R^T) plane and (b) (γ, θ) plane.

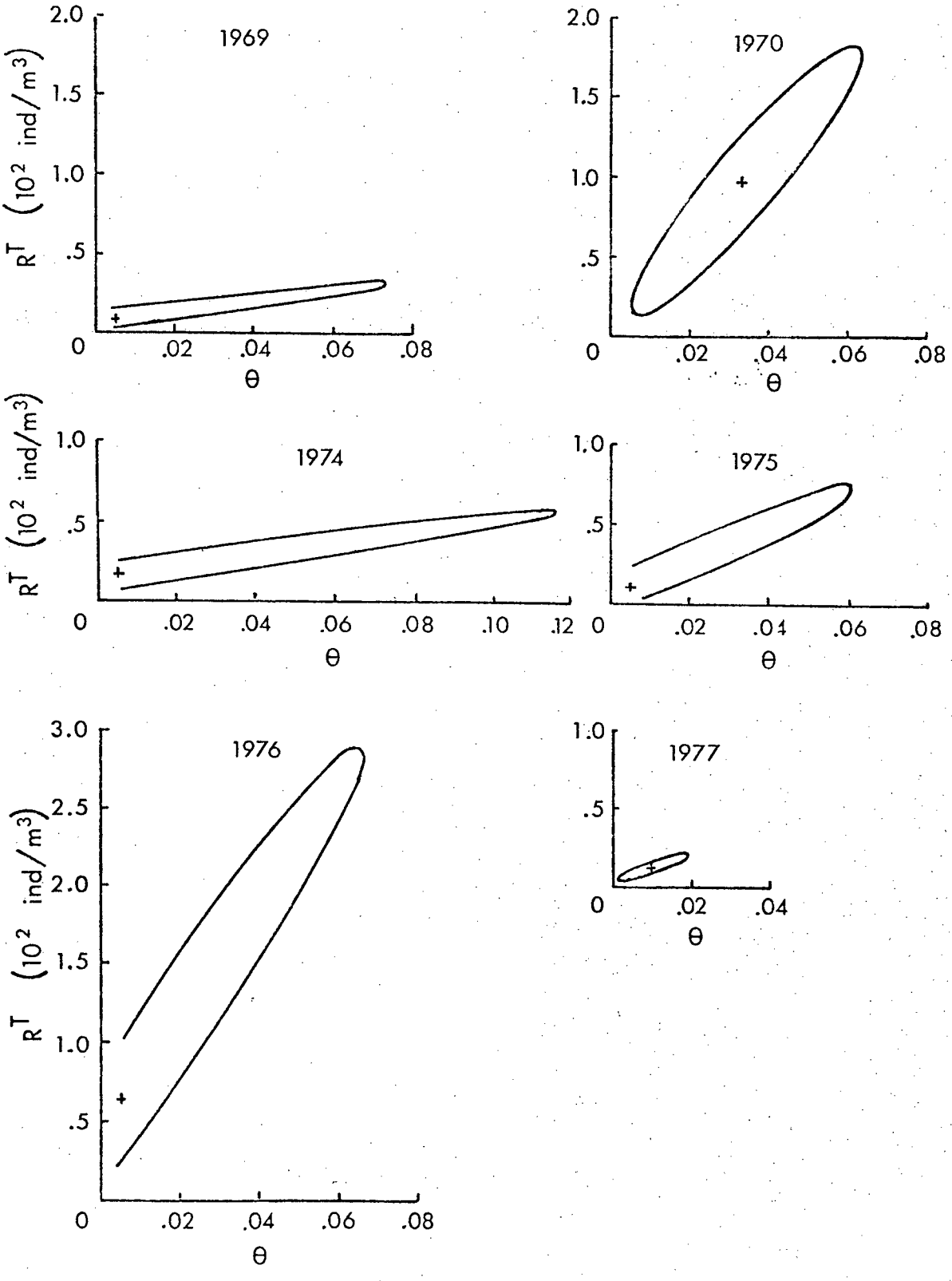

Figure 45a.

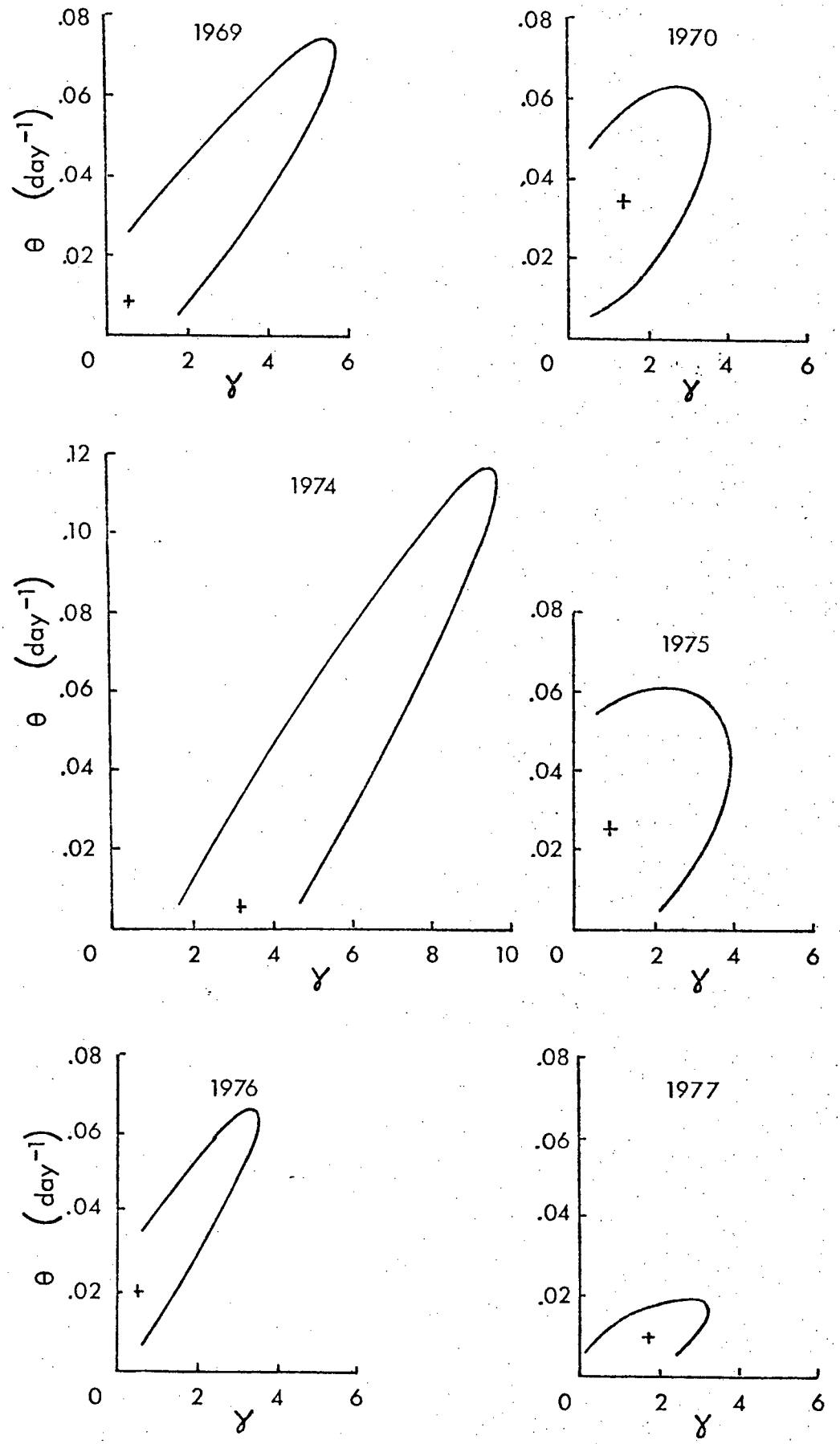

Figure 45b.

of recruitment in 1970 and 1976 are approximately 10 times those for 1969 and 1977. Estimates of recruitment for C. cristatus are low compared with those for C. plumchrus, except in 1976.

4.1.7 Other species.

The next major contributor to herbivore biomass at O.S.P. is also a large copepod, Eucalanus bungi. The life history of this species is not as clear from observations. Individuals typically appear in the 150m vertical hauls in intermediate (2.5 to 5 mm) size classes in March. There is a fairly clear progression through to the largest (6.5 to 7 mm) size classes by June or July. In July or August, large numbers of small (1.5 to 2.5mm) individuals appear, and the large individuals disappear. Growth occurs through to intermediate size classes (3 to 5 mm) but these individuals disappear by the end of October.

These observations are mostly consistent with a life history for Eucalanus which involves over-wintering below 150m as early copepodite stages, rather slow growth in the euphotic zone to mature by June or July and production of a new generation which grows to over-wintering size by late fall. This picture is complicated by the appearance of small numbers of small (1.5 to 2.5 mm) individuals in spring. Whether some individuals over-winter at this size, or whether some reproduction takes place below 150m in the spring, is not clear. A spring breeding period has been reported for Eucalanus in coastal waters (Krause and Lewis, 1979).

In any case, it was not possible to apply the parameter estimation techniques to Eucalanus data. The growth of Eucalanus from early to late copepodite stages is interrupted by the over-

wintering period. Both halves of the growth period usually involve only 2 size classes, so there is a lack of size class information. Another problem is that individuals may over-winter at a range of lengths, so that over-wintering departure and spring recruitment may affect a number of size classes. Numbers of Eucalanus are typically low (5 - 15 ind/m^3) and its contribution to standing stock and secondary production is probably small compared with that of C. cristatus and C. plumchrus. Other herbivorous copepods at O.S.P. are of small (Oithona, Pseudocalanus) or intermediate (Calanus pacificus, Metridia pacifica) size and rarely contribute significantly to standing stock by weight. Their population parameters would still be of interest, of course, but data for these species were not adequate for parameter estimation. Part of the problem is that their generation time is shorter compared with sampling intervals but the main reason is that the size classes used are too coarse, so that individuals are often assigned only to one of two size classes. In the case of Oithona and Pseudocalanus, , only the largest individuals are retained by the 350 μm mesh net.

4.1.8 Secondary production estimates.

Estimates of secondary production can be obtained using the above technique, once a weight-length relationship is prescribed. The weight or carbon content of individual copepods from O.S.P. has not been measured directly and literature values were initially used to define a weight-length relationship. An average wet weight of 4 mg was reported by Fulton(1973) for 4.5 mm C. plumchrus stage V. If it is assumed that W is proportional to l^3, this observation corresponds to $W = .044.l^3$. Fulton

(undated) gives a general weight-length relationship for copepod populations in the Strait of Georgia : $W = .068.l^{2.45}$ which yields a wet weight of 2.7 mg for a 4.5 mm C. plumchrus. Taguchi and Ishii (1970) report wet weights ranging from 2.21 to 4.55 mg/ind and lengths of 5 and 4.5 mm respectively for C. plumchrus stage V, resulting in coefficients of .02 to 0.05 $mg.mm^{-3}$.

Use of any of these formulae with O.S.P. size-structured data resulted in severe over-estimation of sample wet weights. An attempt was made to derive a length-weight relationship appropriate to O.S.P. from the size-structure data as follows. For each sample, all the copepod data was reviewed, and the number of individuals counted in each size class added to one of 9 1mm 'super' size classes according to its nominal size. A multiple linear regression of sample wet weights W^t on numbers N_i^t in each of these super-size classes was then performed : that is, the coefficients W_i in

$$W^t = \sum_{i=1}^{q} N_i^t . W_i$$

were estimated. An obvious criticism is that W^t includes wet weights of organisms other than copepods : while samples having intermediate to high wet weights are predominantly (90%) copepods, the coefficients W_i may tend to be slightly high. These coefficients are interpreted as average weights for each 1mm size class and are plotted against length on a log-log scale in Fig 46. Apart from anomalous results from two, almost empty, size classes, the coefficients fall close to a line having the slope 2.45 suggested by Fulton (undated) and an intercept

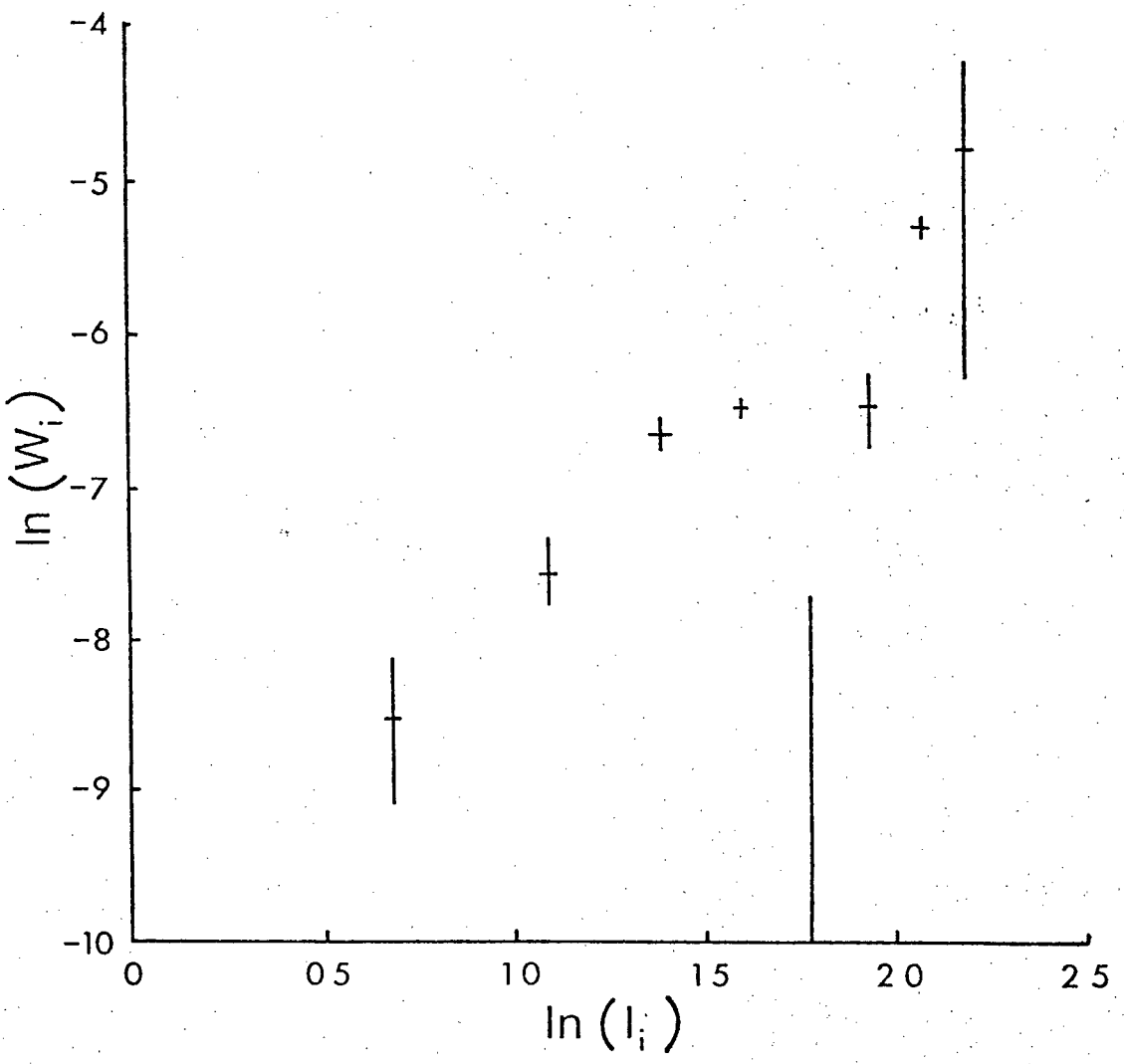

Figure 46. Regression coefficients W_i (±1 standard error) vs corresponding lengths l_i on log-log scale. Line corresponds to $W = 0.033.l^{2.45}$, ignores 6 mm and 7 mm size classes.

corresponding to $W = .033.l^{2.45}$. The coefficient 0.033 is half the value found by Fulton for the Strait of Georgia. Given the coarse nature of the size classes used for the O.S.P. data and the sensitivity of this coefficient to any bias in assigning lengths, it may be rash to conclude that O.S.P. copepods are thinner than their coastal cousins on the basis of this result. While the lower food concentrations and temperatures at O.S.P. might reasonably be expected to result in lower growth rates (Parsons et al ,1977), it is not clear that lower body weights for a given body length should result. In any case, the statistical relationship is used here in the estimation of secondary production based on O.S.P. data.

Estimates of secondary production and 95% C.I. for these estimates are given in Table VI. The uncertainty in these estimates is clearly much less than uncertainty in mortality and recruitment parameters, as found for simulated data by Sonntag and Parslow(1980). Large confidence limits are obtained for 1975 and 1976 for C. plumchrus, but the limits are small enough in other years to clearly distinguish a year of low production such as 1969 from years of high production such as 1970 or 1977. Note that, while highest recruitment estimates for C. plumchrus were obtained for 1973 and 1977, higher mortality rates in these years reduced estimated secondary production to 4th and 2nd rank respectively.

Estimates of secondary production for C. cristatus showed a similar range to those for C. plumchrus. There is no discernible pattern in the absolute or relative contributions of the two species to total secondary production. Both are unusally low in

Table VI.

Secondary production estimates (g wet wt.m^{-2})

Year	C. plumchrus	C. cristatus	Total.
1969	26±10	21±9	47±13
1970	119±45	56±25	165±51
1973	57±17	--	--
1974	--	51±18	--
1975	35±35	20±11	55±37
1976	69±54	146±61	215±81
1977	114±22	15±3	129±22

1969 and 1975 and both are high in 1970 and 1976. In 1977, C. plumchrus is very high and C. cristatus very low.

While smaller species are not included, these large copepods are generally assumed to dominate secondary production and it is interesting to treat their combined totals as a conservative estimate of total secondary production. There is considerable (>4 fold) variation over the 5 years for which totals are available. If these estimates are converted to carbon using a value of .05 for the carbon:wet weight ratio, (Parsons et al ,1977), estimates ranging from 2.4 to 10.7 g $C.m^{-2}.yr^{-1}$ are obtained. For comparison, trophodynamic considerations led McAllister(1969) to a 'most likely' estimate of 13 g $C.m^{-2}.yr^{-1}$, with a minimum value of 2 g $C.m^{-2}.yr^{-1}$, depending on assumed respiration rates.

4.2 Biomass Model for Zooplankton.

4.2.1 Introduction.

In Chapter 1, simple biomass models of the phytoplankton-zooplankton interaction at O.S.P. were considered. A model involving grazing thresholds appeared to be capable of mimicking the seasonal cycle at O.S.P. in a qualitative sense. Using the results of the data analysis of Chapters 3 and 4, an attempt will be made to assign values to the parameters in a model of this kind, and compare predictions and observations quantitatively. The quantitative models considered here are numerical models, based on the phytoplankton production model of Chapter 3, so as to allow a realistic treatment of phytoplankton composition and vertical distribution. The limitations of computer simulation

and sensitivity analysis when parameters are uncertain were discussed in Chapter 2. To overcome these limitations as far as possible, the approximate analytical results of Chapter 1 and Chapter 2 have been used to direct and interpret simulation of the models wherever possible.

4.2.2 Formulation of a Biomass Grazing Model.

In the first model considered, herbivorous zooplankton are represented by a single biomass variable, G (mg $C.m^{-2}$), as in Chapter 1. Phytoplankton carbon ingested per day, F_T, is converted to zooplankton biomass with efficiency e. A constant loss rate, m(day^{-1}) can be regarded as a combination of basal metabolism and mortality in unspecified proportion. Then

$$\dot{G} = e.F_T - m.G \qquad 4.1$$

The phytoplankton carbon in each 5m layer changes according to a growth rate calculated as in Chapter 3 and the calculated grazing loss.

The grazing loss in the model is based upon the functional response of Chapter 1 but the variation of phytoplankton concentration with depth must now be taken into account. Not only must the distribution of zooplankton grazing activity with depth be considered, but, as the non-linear functional response itself represents a fast-variable approximation (Holling,1959), the relative time scales of zooplankton movement and satiation of feeding must be considered.

If the distribution of zooplankton is denoted by q(z), two extreme assumptions which could be used in this model are:

(i) zooplankton are on average uniformly distributed throughout the top 150m so $q(z) = 1/150$.

(ii) zooplankton are on average distributed in proportion to phytoplankton carbon so $q(z) = C(z)/\int_0^{150} C(z')dz'$.

The average distribution q(z) gives no information about the vertical movement of individual zooplankters. For any given q(z), two extreme assumptions concerning the relative time scales of vertical movement and satiation are possible :

(a) Zooplankton vertical movements occur on time scales much faster than those of satiation. Each zooplankter then sees the average phytoplankton concentration (weighted by q(z)), so far as the functional response is concerned. If the functional response at constant food levels is given by f(C), the amount ingested in the water column is given by $f(\bar{C})$, where $\bar{C} = \int_0^{150} C(z).q(z)dz$.

(b) Zooplankton vertical movement occurs on time scales much slower than those of satiation. The amount ingested in the water column is then given by $\overline{f(C)} = \int_0^{150} f(C(z)).q(z)dz$.

The dominant grazers at O.S.P. are large copepods, presumably capable of extended vertical movement. As the phytoplankton concentration is always low, it seems unlikely that they would feed at the very low concentrations below the mixed layer. In fact, as a grazing threshold value C0 will be considered in the model, it seems unlikely that copepods would spend time at depths where $C(z) < C0$. Therefore, q(z) has been set proportional to $(C(z)-C0)^+$.

While the dominant herbivorous copepods are presumably capable of vertical movement, only the late stage Calanus cristatus copepodids were observed to undergo extensive daily

vertical migration (Marlowe and Miller,1975). For individuals undergoing diurnal vertical migration, the extreme assumption (a) would be appropriate if saturation occurred on a long time scale (eg gut-emptying time). For organisms which do not undergo diurnal migration, or become saturated on shorter time scales, assumption (b) is more likely to be appropriate and it has been adopted here, so that the grazing loss rate at depth z is given by $f(C(z)).q(z).G$

4.2.3 Choice of Zooplankton Parameters.

The parameters which must be specified in this simple biomass model of zooplankton are the functional response parameters i_M, D and C0, the growth efficiency e and the combined respiration and mortality rate parameter, m. It would be unrealistic to expect to specify these parameters precisely for a number of reasons. The representation of herbivores by a single biomass variable is itself a crude approximation : the grazers at O.S.P. are composed of individuals covering a range of species and sizes, and these parameters can be expected to vary accordingly (Steele and Frost,1977; Frost,1979). The parameter values inserted in the model must in some sense be regarded as approximate averages.

These parameters have yet to be measured at O.S.P. for a range of size classes of the dominant herbivores. Some have been measured for the same species in coastal locations (Parsons et al ,1969; Taguchi and Ishii,1972; Ikeda,1972; Frost,1979) but the extrapolation of these results to the very different food conditions at O.S.P. is not straightforward (Buckingham,1978). Values obtained for other species of grazers under low food

conditions may prove more appropriate. In addition, as discussed by other authors (Steele,1974; Buckingham,1978) there is still controversy attached to the techniques for measuring these parameters and the interpretation of results. The discussion given here is not an exhaustive review by any means, but is intended to give an indication of the range of parameter values reported in the literature.

The ratio of growth to food ingested is known as the gross growth efficiency, K_1. A range of 10 - 40% for this parameter in marine zooplankton is given by Parsons et al (1977). Maximum values of abut 30% were reported by Paffenhoffer (1976) for C. pacificus in laboratory cultures, while similar experiments yielded values of about 18% for Pseudocalanus elongatus (Paffenhoffer and Harris,1976).

The gross growth efficiency implied by 4.1 varies with ingestion and depends on the proportion of m which is regarded as basal metabolism. Steele (1974) found that the problems in interpretation of respiration experiments make it difficult to assess the relative importance of a basal metabolic rate and one which is proportional to ingestion in copepods. In a series of careful experiments, Ikeda (1977) found respiration rates of 1-2%/day for starved C. plumchrus (stage V) with rates up to 3 times higher for actively feeding individuals. Respiration rates for starved Paracalanus (with approximately 1/100 the body weight of C. plumchrus) were much higher, about 9-18%/day. (The size dependence of respiration rate in copepods is generally accepted (Parsons et al ,1977; Steele,1974).) Taguchi and Ishii (1972) reported respiration rates of 5%/day for C. cristatus and 9%/day

for C. plumchrus under conditions of active feeding. Given the large size of the dominant herbivores at O.S.P., a low basal metabolic rate in the range 1-5%/day seems reasonable. The effective gross growth efficiency will be lower than e by an amount dependent on the ratio of ration to body weight. Given the low basal metabolism suggested above, a value for e of .5 will result in gross growth efficiences of .4 or less at the low food conditions found at O.S.P.

The parameter i_M represents maximum ration as a fraction of body weight. Ranges of 40-60%/day for smaller copepods and 10-20%/day for larger copepods were found by Parsons et al (1967). Values of 20-60%/day were found by Parsons et al (1969) for C. plumchrus feeding on natural phytoplankton assemblages in the Strait of Georgia. Paffenhoffer and Harris (1976) found very high rates for Pseudocalanus in culture (ca 150% body weight/day) and Paffenhoffer (1970) reported values for C. pacificus of ca 100%/day for stage V copepodids and 300%/day for stage V nauplii. Apparent maximum ingestion rates for stage V C. cristatus reported by Taguchi and Ishii (1972) were very low, ca 5%/day. Again the value chosen must represent an average across size classes. A value for i_M of .5 or less may be reasonable for late copepodite stages of the large copepods, but a value of 1.0 may be needed if ingestion by nauplii and early copepodids is included.

Thresholds in zooplankton feeding on natural assemblages from the Strait of Georgia were found by Parsons et al (1967) to range from 50-190 $\mu g\ C.l^{-1}$ with values of D (half-saturation constant) in a similar range. Frost (1972) fitted his

observations on C. pacificus with a type I functional response and half-maximum ration was obtained at food concentrations ranging from 50 to 150 μg C.l^{-1}, depending on food particle size. In a later study, Frost (1975) found that the clearance rate was reduced at food concentrations yielding less than 15% of maximum ration, corresponding to 15-45 μg C.l^{-1}. All these results were based on relatively short-term incubations of indivuals captured from the field.

In a series of long-term culturing experiments, no hint of thresholds down to about 25 μg C.l^{-1} was found for C. pacificus (Paffenhoffer,1970) or Pseudocalanus elongatus (Paffenhoffer and Harris,1976). Their results suggested a half-saturation constant for Pseudocalanus ingestion of 25 to 50 μg C.l^{-1}. The conclusions of Buckingham (1978) and Mayzaud and Poulet(1978) concerning long-term adaptation to food concentration may explain the differences between these results and the short-term incubations reported above. Adaptation to low food concentrations may also explain the high clearance rates (for example, over 200 ml/day for a 10 μg dry weight Pseudocalanus) reported by Paffenhoffer (1970) and Paffenhoffer and Harris (1976). Clearance rates, or equivalently the half-saturation constant D and threshold CO, are well-known to depend on the size and value of food particles (Parsons et al ,1967; Frost,1975; Steele and Frost,1977). Given the small size of the phytoplankton cells and the large size of the dominant herbivores at O.S.P., low clearance rates or high values of CO and D might be expected there. However, Frost (1978) has reported that C. plumchrus feeds efficiently on small cells, due to an unusally

small inter-setule spacing for a copepod of its size. The fact that these zooplankton do grow and reproduce at the low food levels observed at O.S.P. suggests that the half-saturation constant, and certainly grazing thresholds, must be relatively low.

Estimates of mortality rate at O.S.P. were obtained by analysis of time-series of size-class abundances in Section 4.1. Various problems resulted in a high uncertainty in these estimates, but relatively low estimates, in the range 0.0 to 0.05 day^{-1}, were obtained.

4.2.4 Simulation Results and Discussion.

The first simulation is based on the phytoplankton growth parameters used in Fig 33 and the following zooplankton parameter values : i_M = 1.0 day^{-1}, D = 40 $\mu g\ C.l^{-1}$, CO = 20 $\mu g\ C.l^{-1}$, e = .5, m = .05 day^{-1}. This simulation was run over the period 1964 to 1976, but attention will be focused first on the form of the seasonal cycle. The cyle of Chl a in the mixed layer and herbivore standing stock in the top 150m in 1976 is given in Fig 47; while the amplitude of peaks varied somewhat from year to year, as discussed later, this is typical of the qualitative variation in all years. It is immediately clear that the simulation results are not qualitatively consistent either with the observations or the approximate analysis of a similar model in Chapter 1. Instead of phytoplankton remaining constant, a small bloom of about 20 days duration occurs in April and a sharp zooplankton peak follows in May. After June, the chlorophyll concentration settles down at ca .5 mg Chl a/m^3 and zooplankton standing stock then varies approximately with primary production.

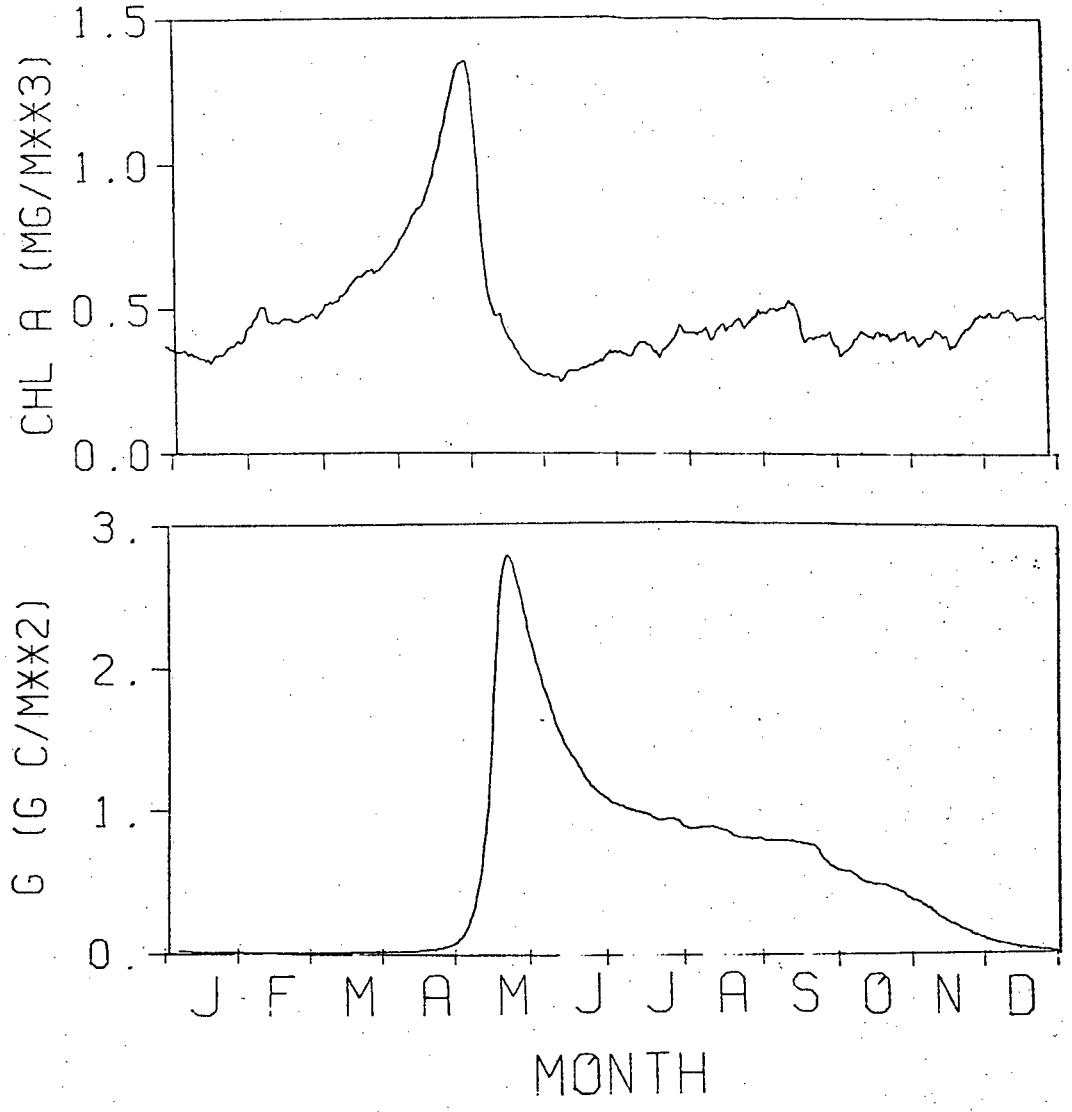

Figure 47. Predicted mixed layer Chl a and herbivore biomass for 1976 using standard parameter set (see text).

It may seem possible that the added complexity of the phytoplankton production model, which takes depth-distribution and varying carbon : Chl a composition into account, has rendered the approximate analysis of Chapter 1 irrelevant. This is not the case and, in fact, the simulation model can be closely approximated by a model as simple as that considered in Chapter 1. This is possible because, as noted in Chapter 3, phytoplankton production below the mixed layer is always very low and phytoplankton carbon falls off quickly below the mixed layer, so that almost all zooplankton feeding takes place in the mixed layer, where phytoplankton can be represented by a single carbon concentration, C(t). If $z_M(t)$ is the mixed layer depth, the concentration of zooplankton in the mixed layer is given by $G_M(t) = G(t)/z_M(t)$. If r(t) is the phytoplankton growth rate in the mixed layer calculated as in Chapter 3, then, on ignoring events below the mixed layer, the simulation model can be replaced by

$$\dot{C} = r(t).C - G_M.f(C) \qquad 4.2a$$

$$G_M = (e.f(C)-m).G_M \qquad 4.2b$$

(Terms resulting from changes in mixed layer depth have been neglected as small on the grounds that changes in mixed layer depth occur relatively slowly).

The approximate stability analysis of Chapter 1 applies to this model : provided seasonal changes in r(t) and $z_M(t)$ occur slowly, the system state should track the quasi-equilibrium cycle given by

$f(\bar{C}) = m/e = \text{constant}$

$\bar{G} = r(t).\bar{C}.z_M(t).e/m$

The phytoplankton concentration should be constant, while zooplankton standing stock should vary with primary production in the water column.

This 'prediction' depends on the slow-variable approximation for $r(t)$ and $z_M(t)$ and the simplest conclusion from Fig 47 is that this approximation has broken down during the spring. The spring increase in production appears to have occurred too quickly for zooplankton to respond, resulting in a transient departure from the quasi-equilibrium cycle, which is returned to in the second half of the year. The rate of approach of the system to equilibrium can be increased by decreasing D and this might be expected to result in a reduction in the spring bloom. The parameter combination CO = 22, D = 20 corresponds to the same value of $\bar{C}$ as C0=20, D=40 and does result in a much smaller spring bloom in 1976 (Fig 48). However, the resulting Chl a peak in March-April is still not consistent with the average observed cycle (Fig 14) and the zooplankton biomass still has a very sharp and unrealistic early peak.

In fact, the basic problem here lies not with the ability of the system to track the quasi-equilibrium cycle after the spring production has begun, but with the very low and often slightly negative net primary production in the preceding winter. During this period, the quasi-equilibrium disappears, phytoplankton standing stock falls below the threshold level and zooplankton standing stock declines exponentially to very low values by

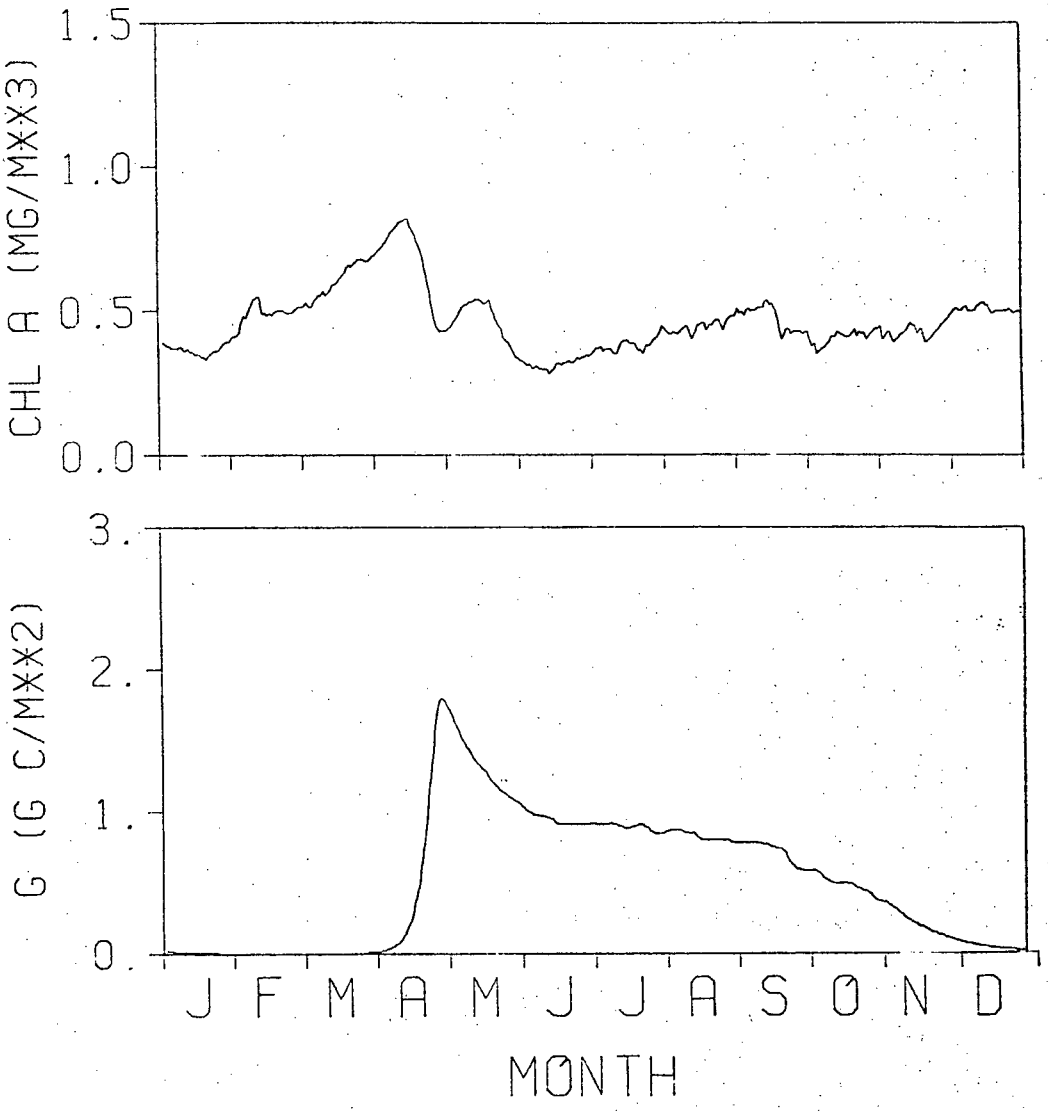

Figure 48. Effect of decreasing D on Fig 47.

March. When positive primary production is resumed, the system lies far from the quasi-equilibrium cycle and a transient phytoplankton bloom is inevitable. Note that while the initial conditions in each year are critical to the model's behaviour in the spring, the close approach of the system to the quasi-equilibrium cycle in the second half of each year means that initial conditions in the following year are determined entirely by the model's parameters and physical driving variables. In particular, in long-term simulations, only the first year is affected by the choice of initial conditions. Similarly, to consider the seasonal cycle in 1976, it is sufficient to simulate only 1975 and 1976.

The problem arising from the decline in zooplankton standing stock in winter immediately brings to mind the life history strategy of the dominant copepods at O.S.P., discussed in Chapter 1. All three of the major species overwinter below 150m and either they, or their offspring, return to the mixed layer in the spring. The obvious advantage of this behaviour to the copepods is that winter losses through mortality and respiration are reduced. It is precisely these losses which are responsible for the spring bloom in this simple model and the recruitment of zooplankton biomass to the surface layer in the spring should prevent this bloom.

Recruitment has been introduced into the model as a daily biomass input, normally distributed over time with mean μ, standard deviation σ and total integrated recruitment, G_R. The parameter estimation results of section 4.1 correspond to σ between 20 and 40 days, μ between 70 and 110 days and G_R between

40 and 400 mg $C.m^{-2}$. The departure of individuals for over-wintering is represented by an additional loss rate, m_w. If all three dominant species are considered, the departure period extends from June to October.

The parameter values of Fig 47, together with σ=30, μ=90, G_R =200 mg $C.m^{-2}$ and m_w = .05 day^{-1} for day 170 to 300, resulted in the predicted time series of Chl a and herbivore biomass given in Fig 49. The spring bloom has essentially disappeared, although small fluctuations in Chl a due to small changes in phytoplankton carbon and variations in carbon:Chl a ratio are present. The pronounced peak in zooplankton biomass in May has disappeared, but the increase in zooplankton biomass is early compared with observations at O.S.P. Biomass declines markedly as over-wintering commences in June and stabilizes at about half the level in Fig 47 over the departure period. The quasi-equilibrium biomass during this period is given by

$$\bar{G}(t) = r(t).\bar{C}.z_M(t).e/(m+m_w)$$

or just half of the value predicted without over-wintering.

The seasonal cyle was found to be insensitive to changes in the timing and spread of recruitment within the ranges given above. As G_R is decreased, the spring bloom starts to reappear gradually, although even a low recruitment level, G_R = 25 mg $C.m^{-2}$, results in a marked reduction (Fig 50) in the chlorophyll and zooplankton peaks of Fig 47.

The predicted phytoplankton standing stock varies between 0.3 and 0.6 mg Chl $a.m^{-3}$ in the mixed layer. The quasi-equilibrium phytoplankton concentration is determined by zooplankton parameters :

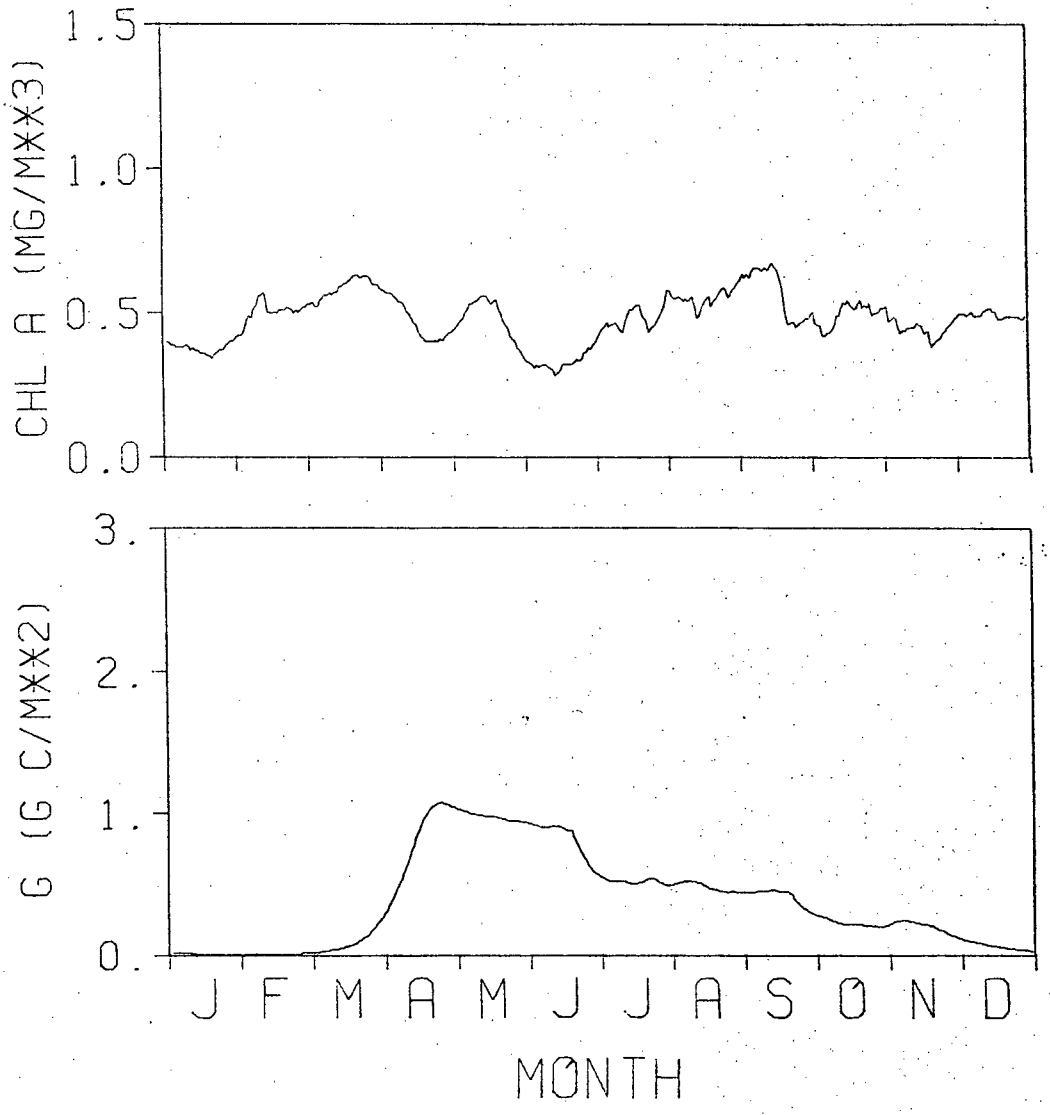

Figure 49. Effect of introducing over-wintering strategy in Fig 47.

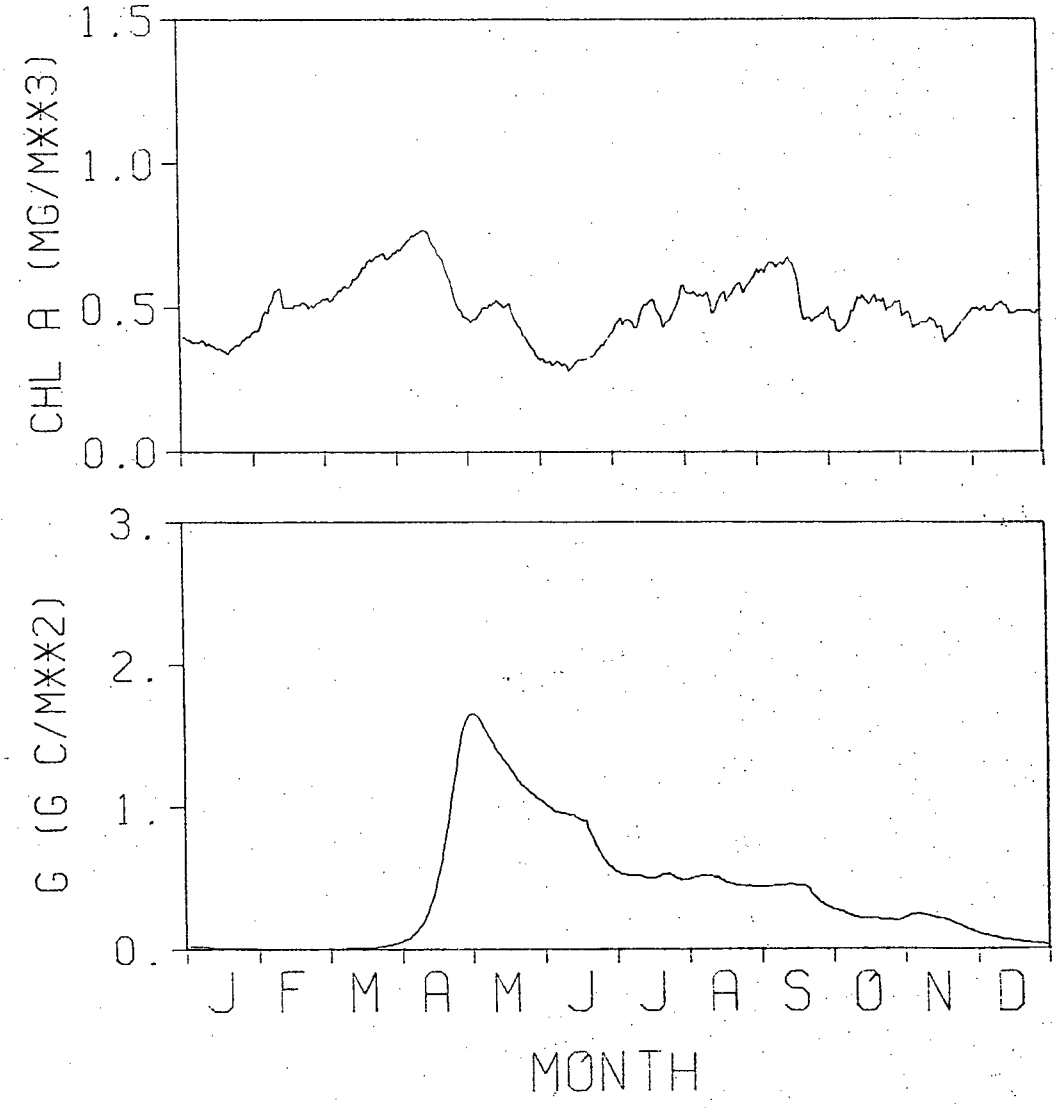

Figure 50. Effect of reducing spring recruitment to 25 mg $C.m^{-3}$ on Fig 49.

$\bar{C} = C0 + m.D/(e.i_M - m)$

The peak zooplankton biomass is about 1100 mg $C.m^{-2}$. Assuming a carbon : wet weight ratio of 20:1, this represents 20 g wet $weight.m^{-2}$, or approximately 150 mg wet $wt.m^{-3}$, corresponding to an intermediate year at O.S.P. Zooplankton standing stock is given approximately by e/m times primary production. The uncertainty in parameter values discussed above is such that it would be meaningless to claim more than that the magnitudes of observed standing stocks are consistent with the very broad range of possible parameter values.

At this point, the discussion of phytoplankton regulation at O.S.P. may appear to have gone almost full circle. It started in Chapter 1 with Heinrich's contention that the life histories of the dominant grazers at O.S.P. were responsible. Consideration of simple, qualitative models suggested that the life histories were not a sufficient explanation and a simple biomass model incorporating thresholds and neglecting life histories appeared at a qualitative level to be capable of explaining the observations. In the simulation model introduced here, both life history strategies and thresholds appear to be necessary.

So far, the spring recruitment of zooplankton biomass has been discussed as if it were a step change in the system state which brings the system closer to quasi-equilibrium before primary production increases. In the simulation model, recruitment of herbivores takes place over an extended period and may allow a phenomenon, reported by Brauer and Soudack (1979) as a predator-stocking effect, to occur. For simplicity, consider a simple neutrally stable Lotka-Volterra type model with a constant

recruitment rate for herbivores added :

$$\dot{C} = r.C - a.C.G$$
$$\dot{G} = e.a.C.G - m.G + R$$

The non-trivial equilibrium, given by

$$\bar{C} = (m-R.a/r)/(e.a)$$
$$\bar{G} = r/a$$

can easily be shown to be asymptotically stable (provided of course $\bar{C}$ is non-negative). That is, during the period of zooplankton recruitment in the spring, the recruitment itself contributes to the stability of the phytoplankton-zooplankton interaction. It is possible that a feeding threshold is not necessary to ensure that the system tracks the quasi-equilibrium cycle during this period of increasing primary production. If the feeding threshold should turn out to be unnecessary with recruitment included, the discussion would indeed have come full circle.

This was tested under the most favourable conditions in the simulation model by replacing the threshold functional response with a type I functional response with an identical maximum clearance rate. The resulting spring bloom is relatively small and somewhat delayed, but a second larger peak in Chl a develops as over-wintering departure commences(Fig 51). The Chl a and herbivore biomass time series show little resemblance to the observations. Both life histories, and a continuing stabilising

effect as provided by a grazing threshold, appear to be necessary to reproduce the observed constancy of phytoplankton standing stock.

4.3 A Cohort Model for Zooplankton.

4.3.1 Introduction.

There are a number of reasons to consider a more realistic model of herbivore dynamics at O.S.P., involving some species and size structure. One good reason is that the zooplankton data collected have been analysed to size and species level, so that such a model need not be constructed or tested in a biological vacuum. While the more detailed model will require the specification of a much greater number of parameters, it will at least avoid the painful task of choosing an 'average' parameter value out of an order-of-magnitude range over size and species. The representation of recruitment and over-wintering departure in the simple biomass model is necessarily crude, and a more realistic representation, based on the results of section 4.1 and the observations of Fulton (1973), can be introduced in a more detailed model. Finally, there is some reason to believe that a size-structured model may reproduce observations, even at the biomass level, more faithfully than the simple biomass model. For example, even in the 'best case' (Fig 49), the biomass model predicts peak zooplankton biomass in April, much earlier than is observed. At this time, the zooplankton are dominated by recently recruited early stages of the dominant copepods. These small copepods should have a higher metabolic rate per unit body weight and a reduction in zooplankton biomass can be expected if

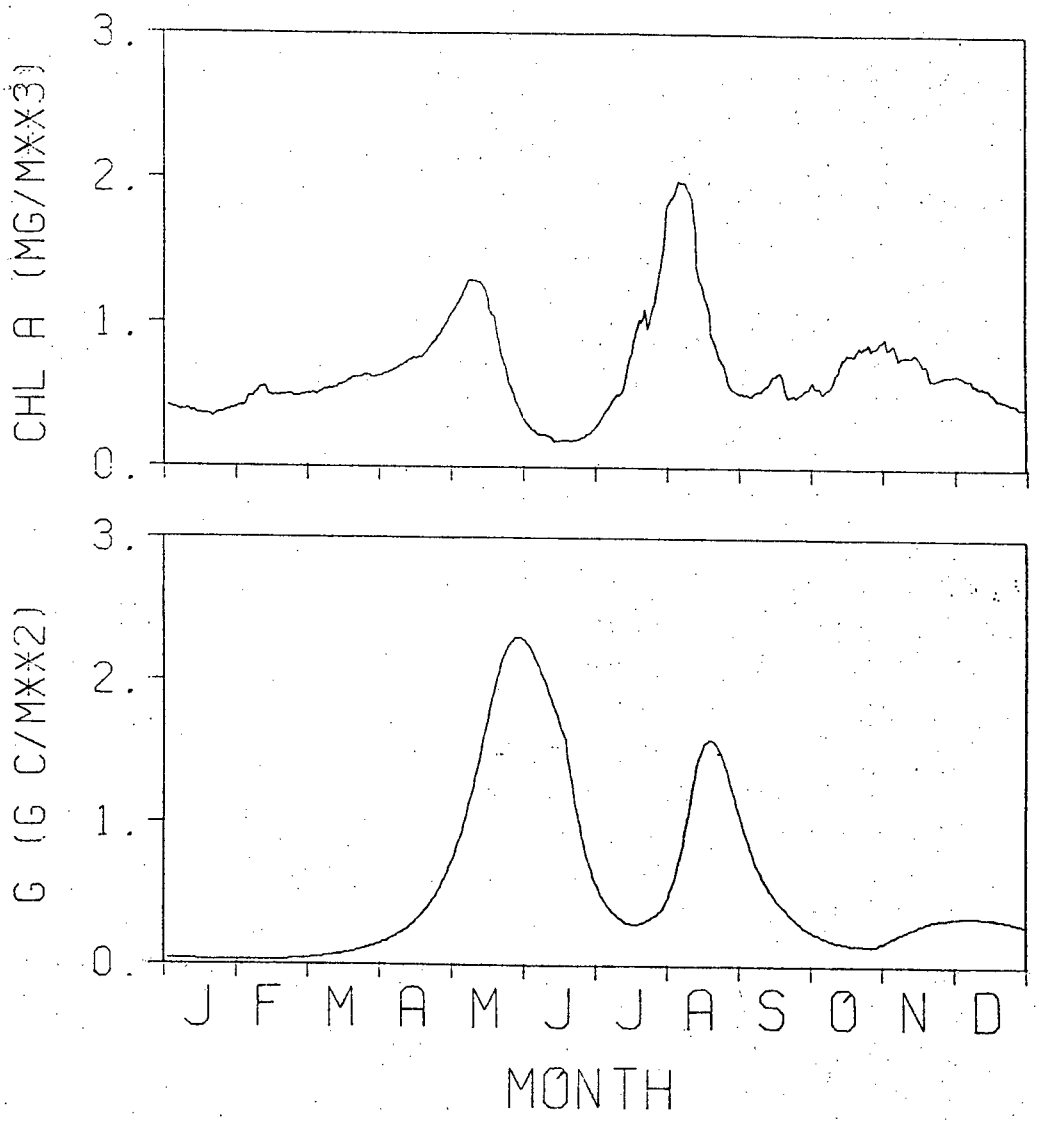

Figure 51. Predicted Chl a and grazer standing stock for biomass model with Type I functional response and standard spring recruitment.

this is taken into account.

4.3.2 Model Formulation.

The size-class model constructed here is based on the models of Landry (1976) and Steele (1974). For each species, a cohort is recruited as a series of day classes, with initial numbers normally distributed over time. Each day class has an associated abundance and weight, so that $Z_i(t,s)$ is the number of individuals of species i left on day t in the day class recruited on day s, and $W_i(t,s)$ is the weight of each individual. The initial conditions corresponding to recruitment are

$$Z_i(s,s) = R_i^T.\exp(-(s-\mu_i)^2/(2.\sigma_i^2)) \;/\; (\sqrt{2.\pi}.\sigma_i)$$
$$W_i(s,s) = W_i^\circ,$$

where W_i° is the weight of the earliest, actively-feeding naupliar stage.

Again, following Landry (1976) and Steele (1974), ingestion and basal metabolism are assumed to be proportional to $W^{0.7}$, so that, at phytoplankton concentration C,

$$\dot{W}_i(t,s) = (e_i.f_i(C)-b_i).W_i^{0.7}(t,s)$$

Integration of feeding over the phytoplankton profile is done in the same manner as in the biomass model. A species-specific mortality rate θ_i is assumed, so that

$$\dot{Z}_i(t,s) = -\theta_i.Z_i(t,s) \;.$$

The two dominant large copepod species, C. plumchrus and

C. cristatus, are represented in the model as cohorts. During the fall and winter, when these copepods are absent, a group of smaller copepods (C. pacificus, Metridia pacifica, Pseudocalanus minutus, Oithona) becomes important. This group is represented in the model simply as a biomass, G, in the manner of section 4.2.

4.3.3 Parameters.

The C. plumchrus and C. cristatus nauplii are recruited in the spring at an initial weight of .3 μg C (Fulton,1973). The recruitment parameter estimates obtained in Section 4.1 represent recruitment into the sampled size classes, not recruitment of nauplii. Typical estimates of 300 and 75/m^3 were increased by a factor of 2 to account for naupliar mortality to give 1.10^5 and $2.5.10^4$ ind/m^2 for C. plumchrus and C. cristatus respectively. The mean recruitment time was set back to 70 days to account for naupliar growth.

The functional response parameters C0 and D were initially given the same values (20 and 40 μg $C.l^{-1}$ respectively) for both dominant species and for small copepod biomass, G. Ingestion is of course weight-dependent and the value $i_M = 2.0$ assigned to C. plumchrus and C. cristatus corresponds to a maximum rate as a fraction of body weight ranging from 2.9 day^{-1} for the smallest weight to 0.3 day^{-1} for a large (400 μg C) C. cristatus. The value $i_M = 1.0$ day^{-1} assigned to the biomass fraction corresponds to an 'average' weight of 10 μg C/ind on the C. plumchrus, C. cristatus scale. The parameter b was fixed at 0.075, yielding a basal metabolic rate as a fraction of body weight ranging from 0.10 day^{-1} for smallest nauplii to 0.01 day^{-1} for large

C. cristatus. The combined basal metabolic rate and mortality rate for the biomass fraction, m, was fixed at 0.075 day^{-1}. Based on the average size of the biomass fraction calculated above, this can be regarded as half mortality and half basal metabolism. The mortality rates for C. plumchrus and C. cristatus were initially set equal at .025 day^{-1}.

In the simple biomass model, the over-wintering departure of the dominant copepods was represented as a constant loss rate over an extended period. According to Fulton (1973), C. plumchrus individuals in the Strait of Georgia leave the surface waters as stage V copepodids, once they have built up sufficient lipid stores. A simple and apparently realistic way to represent over-wintering departure in the model is to have day classes leave at a specified over-wintering weight. This weight was fixed at 100 µg C for C. plumchrus and 400 µg C for C. cristatus. The value for C. plumchrus is lower than observed by Fulton (1973) for the Strait of Georgia but consistent with the wet weight vs length relationship derived for O.S.P. copepods in Section 4.1.8.

4.3.4 Simulation Results and Discussion.

The predicted time streams of mixed layer Chl a and standing stock (g $C.m^{-2}$) of C. plumchrus, C. cristatus and small copepods (plotted cumulatively) are drawn in Fig 52. Note that the control of phytoplankton in the spring is as good as in Fig 49, despite the much lower recruited biomass (37 mg $C.m^{-2}$ compared with 200 mg $C.m^{-2}$). The larger figure used in the biomass model corresponded to recruitment into sampled size classes (individuals greater than 1 mm), not naupliar recruitment. A

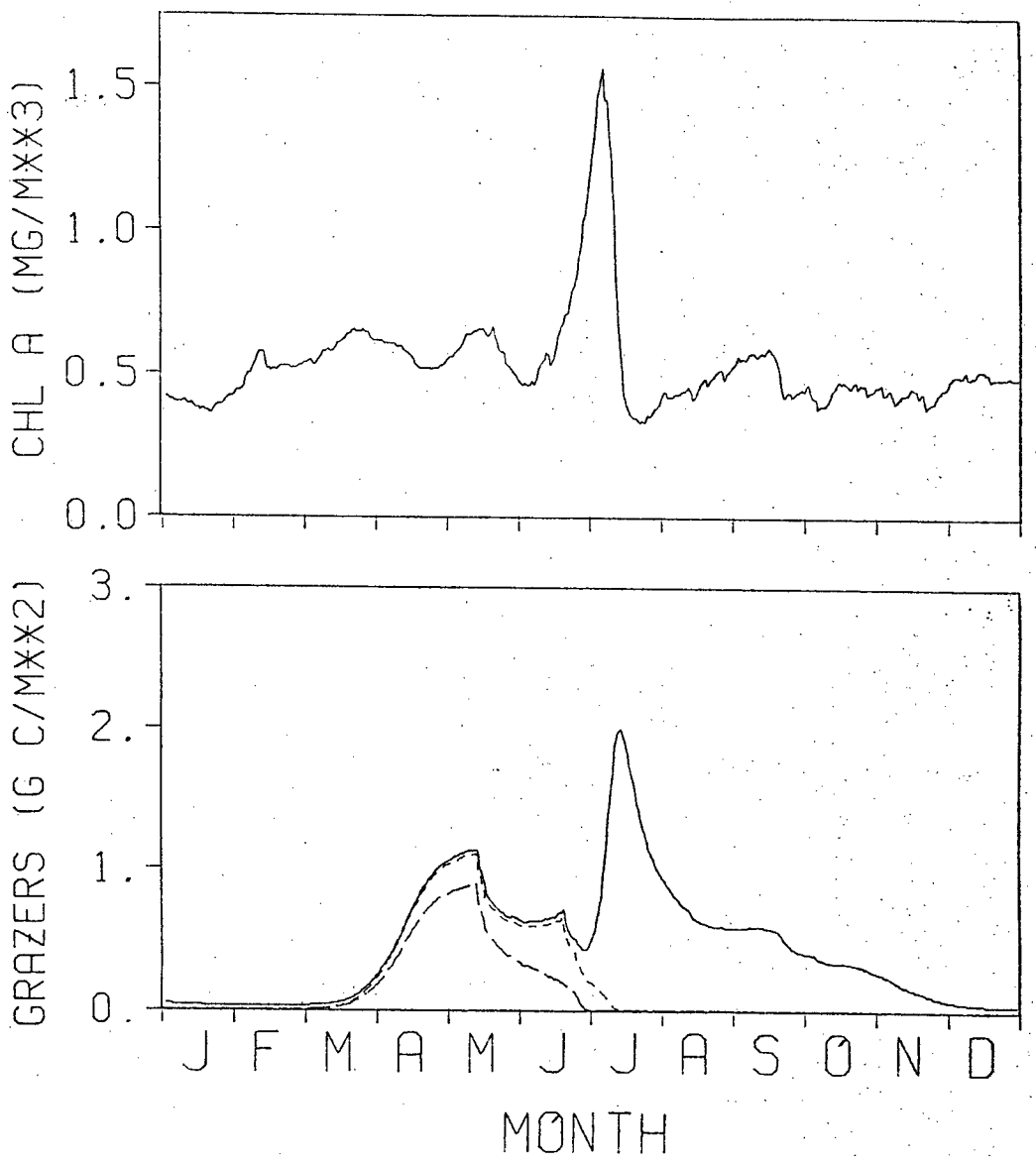

Figure 52. Predicted Chl a and zooplankton biomass (long dashes = C. plumchrus, short dashes = C. cristatus + C. plumchrus, solid line = total biomass) for 1976, using weight thresholds for departure in cohort model.

recruitment of 37 mg $C.m^{-2}$ in the simple biomass model would result in some deterioration in phytoplankton control in the spring. This does not occur in the size-structure model because of the high growth rates achieved by small nauplii.

The behaviour in summer and fall is, however, not realistic. The departure of C. plumchrus starts rather early, in May, and proceeds very quickly. The decrease in biomass stops for a while in June as C. cristatus biomass increases, but then this species also reaches over-wintering weight and leaves. A phytoplankton bloom occurs in June and July as a result of this rapid disappearance of both major grazers and this triggers a peak in the small biomass fraction in July. The phytoplankton are controlled and the system approaches the quasi-equilibrium cycle of the biomass model for the remainder of the year.

There is a simple instability associated with the threshold over-wintering departure strategy which is responsible for this behaviour. While all day-classes are below over-wintering weight, the system is near a quasi-equilibrium state, with relatively constant phytoplankton. As the oldest day classes reach over-wintering weight and leave, there is a small increase in phytoplankton abundance due to the relaxation in grazing pressure. As a result, the remaining day classes grow faster, reach over-wintering weight and depart more quickly. This causes a greater relaxation in grazing pressure, a larger increase in phytoplankton abundance and higher growth rates for remaining day classes. The end result can be seen in Fig 52, where C. cristatus day classes, recruited at fixed initial weight over a period exceeding 60 days, all leave within a 20 day period.

It is clear that if the predicted phytoplankton concentration is to remain constant through this period of over-wintering departure, a smooth replacement of C. plumchrus by C. cristatus and then by small copepods is required and it seems as though a different departure strategy is needed to achieve this. Two different departure strategies were tried in simulations using the same parameters as in Fig 52.

In the first, the departure of C. plumchrus and C. cristatus was slowed down by the simple device of having individuals leave a day class at a constant rate (.05 day^{-1}) once they pass a minimum departure weight, until they reach a maximum departure weight, when the remainder leave. In a simulation using this departure strategy, with minimum and maximum weights of 100 and 200 μg C respectively for C. plumchrus, and 200 and 800 μg C respectively for C. cristatus, the departure period was prolonged slightly, but the basic instability, with a resulting phytoplankton bloom in July followed closely by a small copepod bloom, persisted.

In the parameter estimation of section 4.1, it was assumed that individuals spent a fixed time in the surface waters. This departure strategy ensures that the departure period is as prolonged as the recruitment period. However, in a simulation using a fixed residence time of 100 days for C. plumchrus and 180 days for C. cristatus, a (somewhat reduced) phytoplankton bloom still occurred in July. The decrease in numbers of C. plumchrus and then C. cristatus due to departure is made up by a large increase in weight of remaining day classes, so that the later day classes of C. plumchrus and earlier day classes of

C. cristatus leave at large weights (ca 400 and 1700 μg C/ind respectively). The phytoplankton bloom is in fact controlled by a very rapid increase in small copepod biomass, although not to the peak levels seen in Fig 52.

It seems as though a tight control of phytoplankton during departure is not to be found simply by changing the departure strategy. In the simulations so far, C. cristatus has either left too early, or, in the case of a fixed residence time, reached too high a departure weight. In a hypothetical model where C. cristatus was present by itself as a single day class, the analysis of Steele's (1974) model, presented in Chapter 2, would apply. The approximate governing equations would be

$$\dot{C} = r.C - f(C).Z.W^{0.7}$$

$$\dot{W} = (e.f(C)-b).W^{0.7}$$

$$\dot{Z} = -\theta.Z$$

If the system remains near quasi-equilibrium, with C constant or changing slowly, the level of grazing intensity, proportional to $Z.W^{0.7}$, must change slowly with primary production. As discussed in Chapter 2, the weight W will increase as Z decreases so that $Z.W^{0.7}$ is maintained at an appropriate level. In such a model, the rate of growth of C. cristatus can be reduced by decreasing the mortality rate, θ.

In the simulation model, C. cristatus is present with C. plumchrus which is initially dominant numerically and by biomass. Decreasing the mortality rate for C. cristatus alone will initially result in a replacement of C. plumchrus biomass by

C. cristatus biomass before any departure takes place, which is not desired. There will be little change in C. cristatus growth rate until it becomes the dominant grazer. To reduce the growth rate of C. cristatus in the simulation model, a decrease in its feeding efficiency relative to that of C.plumchrus is also required. Note that this decrease alone would result in a relative decline in C. cristatus biomass while C. plumchrus is present, which is not likely to lead to better phytoplankton control when C. plumchrus departs. However, the two changes together mean that the biomass of C. cristatus as C. plumchrus starts to over-winter need not change, but it will now be composed of a larger number of smaller individuals. As C. plumchrus departs, the decrease in zooplankton grazing pressure must be made up by an increase in weight of remaining C. plumchrus and especially by C. cristatus. According to the $W^{0.7}$ metabolic law used here, the percent increase in weight per day increases like $W^{-0.3}$ as W decreases. Thus, a population of smaller, more numerous C. cristatus should respond much more quickly to small increases in phytoplankton carbon as C. plumchrus departs, leading to tighter phytoplankton regulation.

All three simulations described above were therefore repeated, with the mortality rate for C. cristatus reduced to 0.01 day^{-1} and C. cristatus ingestion reduced to 0.8 times that of C. plumchrus. A smooth transition of control from C. plumchrus to C. cristatus to small copepods was obtained with all three departure strategies, although for the weight-dependent strategies, some C. cristatus never reached over-wintering

weight, owing to the low mortality rate.

The predicted timestreams of Chl a in the mixed layer and biomass of C. plumchrus, C. cristatus and small copepods are shown in Fig 53. It can be seen that the slight increase in phytoplankton caused by the departure of C. plumchrus triggers a rapid increase in C. cristatus biomass in July and August. Total biomass is in fact larger in this peak as it consists of larger individuals and must maintain a grazing pressure proportional to $W^{0.7}$. The maximum departure weights for C. plumchrus and C. cristatus in this simulation are ca 240 μg C/ind and 510 μg C/ind, more reasonable than in the earlier simulation using this departure strategy. The range of departure weights is also much smaller.

While the summer bloom has been avoided by using this parameter combination, the intrinsic instability associated with the departure of copepods has not really been removed and the importance of the size and number of C. cristatus during this period raises questions about the sensitivity of the results to changes in other parameters. For example, the parameter estimation results of section 4.1 suggest a large variation in recruitment of C. cristatus from year to year. The model's sensitivity to small changes in mortality rates and growth parameters must also be suspect.

The effects of changes in recruitment can be qualitatively predicted using the argument for a single day-class given above. Provided phytoplankton abundance remains approximately constant, individual growth occurs so as to maintain a constant grazing pressure in the face of mortality losses. Increasing the

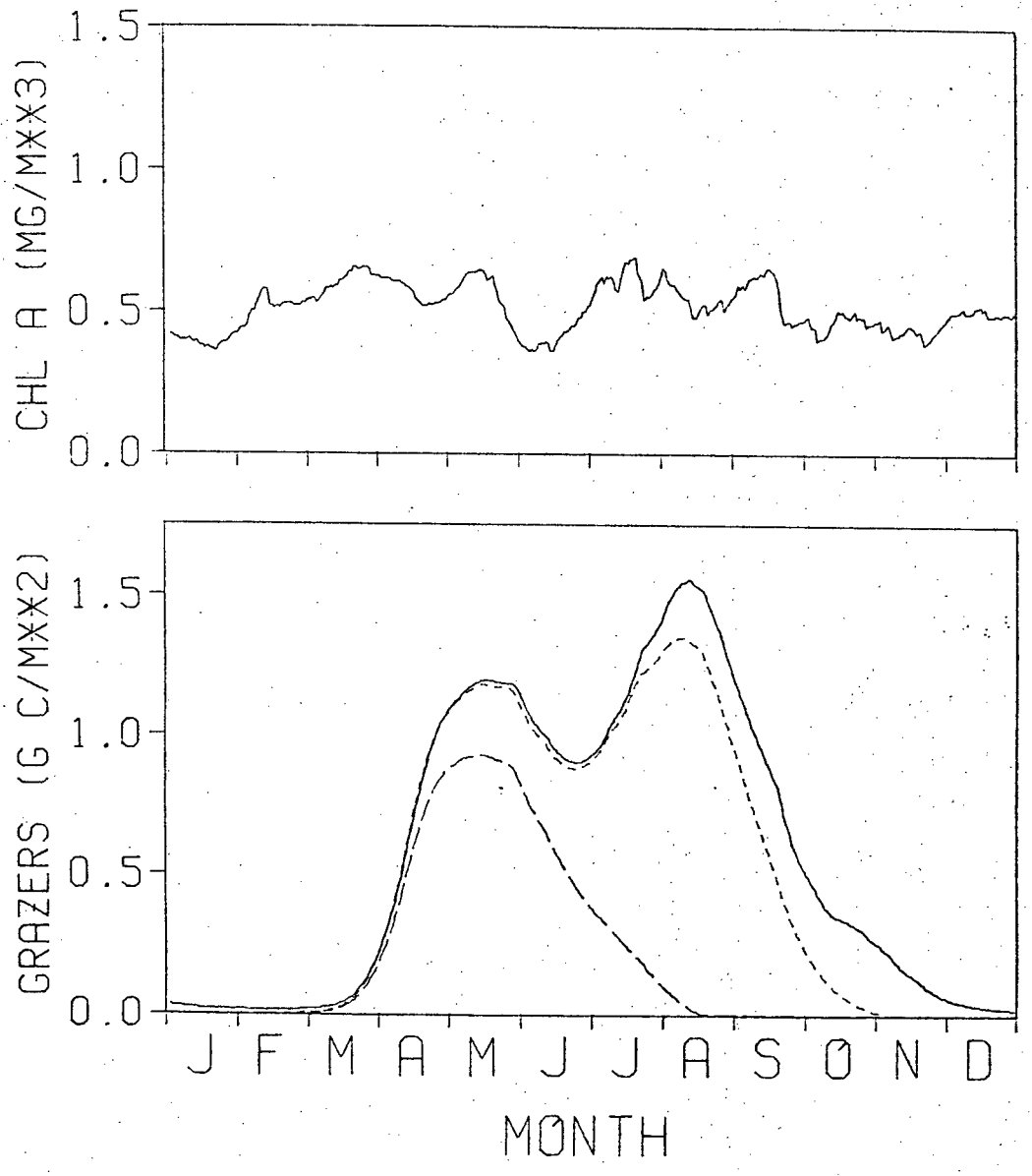

Figure 53. As for Fig 52, with fixed residence times and lower growth and mortality rates for C. cristatus.

recruitment level produces a larger number of individuals which must be smaller at any particular time. For the weight-dependent departure strategy, over-wintering will be delayed, while for the fixed residence time, departure weights will be smaller. Doubling the spring recruitment of both species to 200 and 50 thousand individuals/m^2 has just the expected effect. For the fixed residence time strategy, departure weights average about 100 and 300 μg C/ind. For the single weight threshold departure, no C. cristatus reach over-wintering weight. Doubling the recruitment again to 4.10^5 and 1.10^5 ind/m^2 results in even lower departure weights for C. plumchrus (23 to 100 μg C/ind) and C. cristatus (100 to 370 μg C/ind). There is a marked reduction in biomass for the higher recruitment levels (Fig 54), due again to the $W^{0.7}$ dependence of metabolism and ingestion and the smaller mean size of copepods present. There is also a slight fall phytoplankton bloom due to a delay in the growth of the small copepod biomass, G. The parameters chosen are such that this fraction is outcompeted by the dominant grazers except when the latter are very large. In this simulation, the prolonged presence of relatively small C. plumchrus and C. cristatus delays a significant increase in G until C. cristatus has left.

Halving total recruitment to 5.10^4 and $1.25.10^4$ ind/m^2 respectively results ,as expected, in larger departure weights with the fixed residence time strategy. The small copepod fraction, G, contributes relatively more to total biomass as C. plumchrus departs (Fig 55). The low recruitment results in a generally higher chlorophyll a level in the spring and a larger C. plumchrus biomass peak in May and June, due both to higher

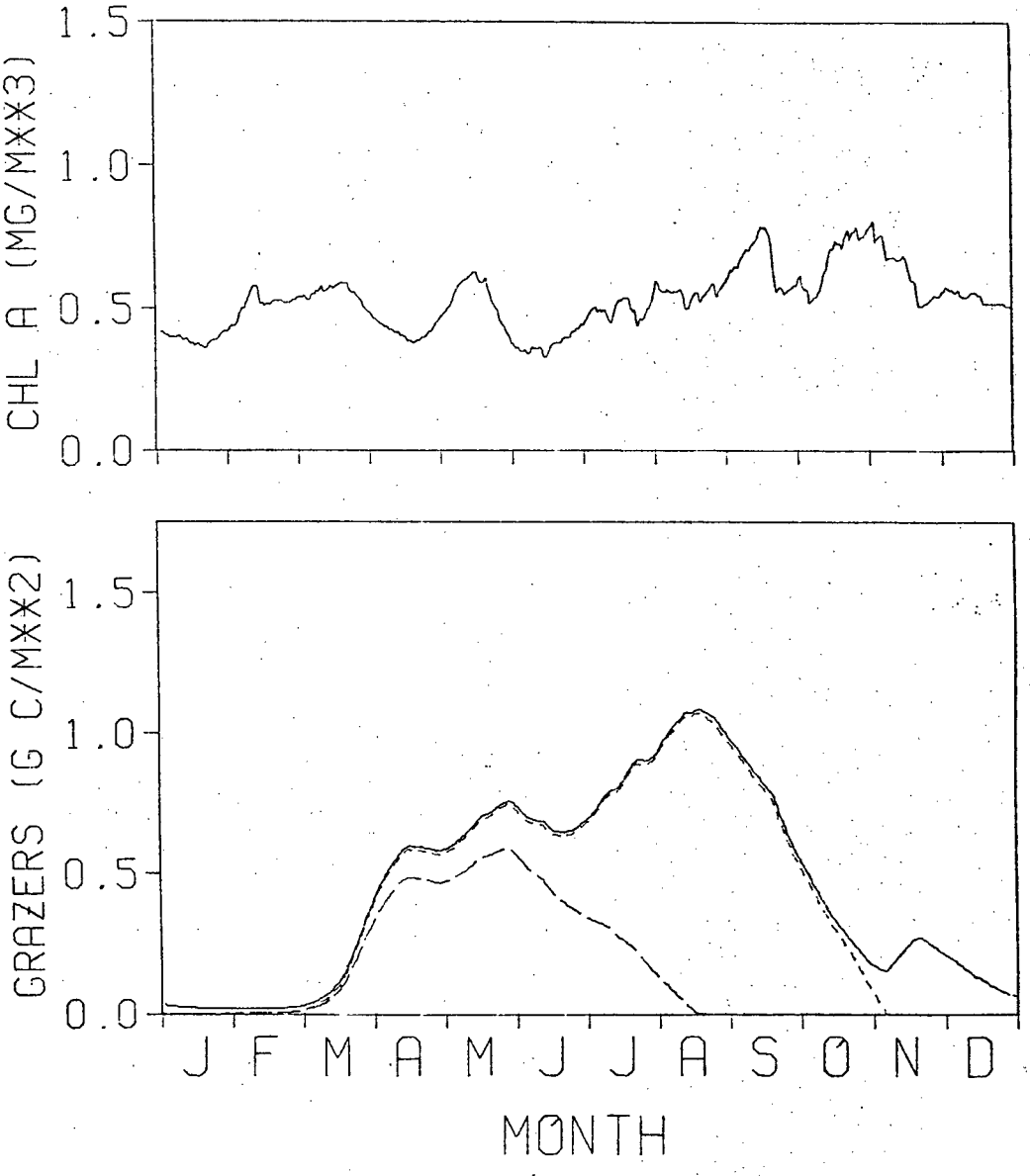

Figure 54. Effect of quadrupling spring recruitment in Fig 53.

primary production and the larger size of individuals present. This inverse effect of recruitment level on zooplankton biomass, while consistent with a simple qualitative understanding of the model, is rather counter-intuitive.

According to the qualitative analysis, increasing the mortality rate should have a similar effect on departure weight, and/or timing, as decreasing total recruitment. This was found to be the case when values of θ were increased to 0.03, 0.015 day^{-1} respectively for C. plumchrus and C. cristatus. The original recruitment levels of 1.10^5 and $2.5.10^4$ ind/m^2 were used and the principal effects were a slight increase in Chl a and an increase in the contribution of small copepods after C. plumchrus leaves (Fig 56). Departure weights for C. plumchrus and C. cristatus were ca 300 µg C/ind and 500 µg C/ind respectively.

According to the qualitative analysis, recruitment and mortality rates should be the principal determinants of departure weight and/or timing. The other zooplankton parameters will determine the quasi-equilibrium levels of phytoplankton and zooplankton standing stock. For example, decreasing the parameters D and C0 should decrease the equilibrium phytoplankton concentration, determined roughly in the single day class model by

$$\bar{C} = C0 + D.(b+\theta.W^{0.3})/(i_M.e-(b+\theta.W^{0.3})) \qquad 4.3a$$

In fact, the values of b and θ chosen in previous simulations produce values of $\bar{C}$ corresponding to .5 mg Chl $a.m^{-3}$ or higher. This can be reduced to the vicinity of the observed average (.4

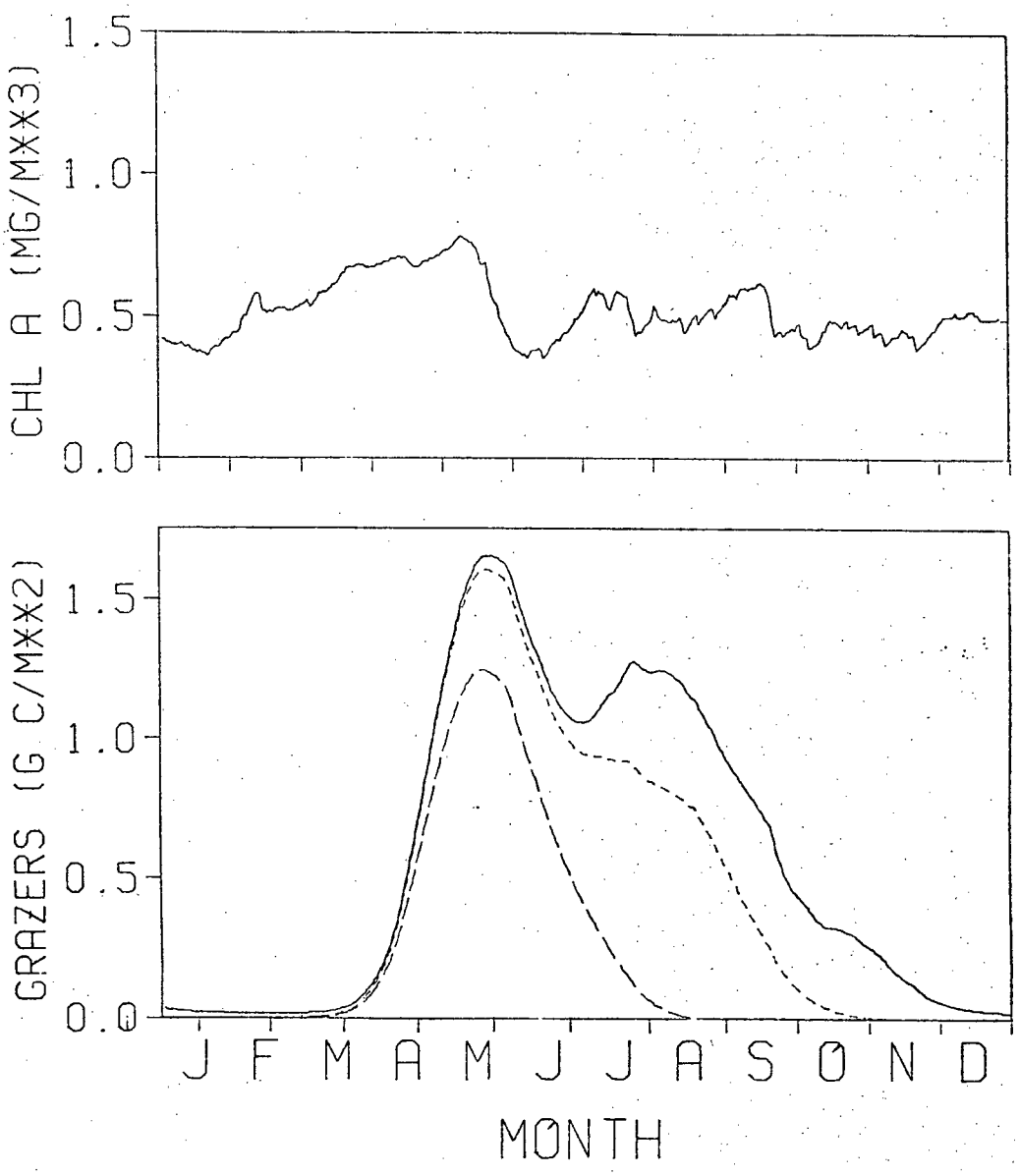

Figure 55. Effect of halving spring recruitment in Fig 53.

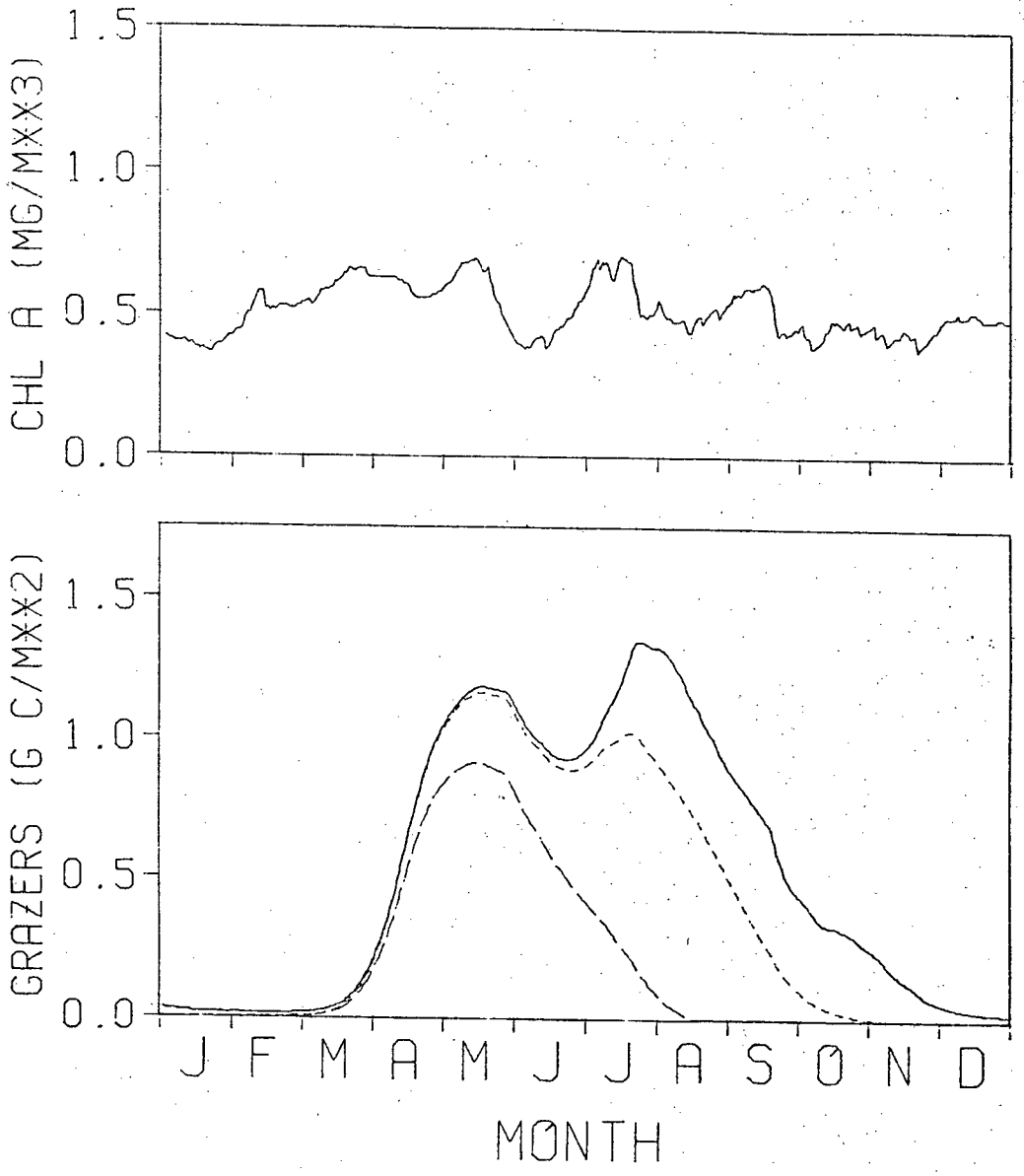

Figure 56. Effect of increasing mortality rates for Calanus in Fig 53.

mg Chl a.m^{-3}), by reducing D and C0 to 30 and 15 μg C.l^{-1} respectively. The resulting Chl a and grazer biomass levels are shown in Fig 57; both phytoplankton and zooplankton standing stock is reduced, but departure weights and phytoplankton control are not affected.

The quasi-equilibrium zooplankton biomass in a single day class model is determined by

$$\overline{Z.W^{0.7}} = r.\overline{C}.e/(b+\theta.W^{0.3}) \qquad 4.3b$$

Increasing b and m from .075 to 0.10, keeping D and C0 at 30 and 15 μg C.l^{-1}, results in an increased phytoplankton level, especially in the fall as C. cristatus leaves (Fig 58). There is a delay in the response of small copepods, G, to the departure of C. cristatus. The small copepods have suffered competitively by an equal increase in b and m, as the mortality rates of the large copepods were not changed. There is little change in total zooplankton biomass (cf Fig 57); the increase in phytoplankton carbon (equation 4.3a) balances the direct effect in equation 4.3b.

In most of these simulations, phytoplankton has stayed relatively constant and the results have been consistent with the qualitative, quasi-equilibrium theory. The parameter changes have all been applied equally to both major copepods. The first three simulations with equal mortality rates showed that the regulation of phytoplankton during over-wintering departure is very sensitive to changes differentially affecting the major copepods. On two occasions parameter changes which slightly

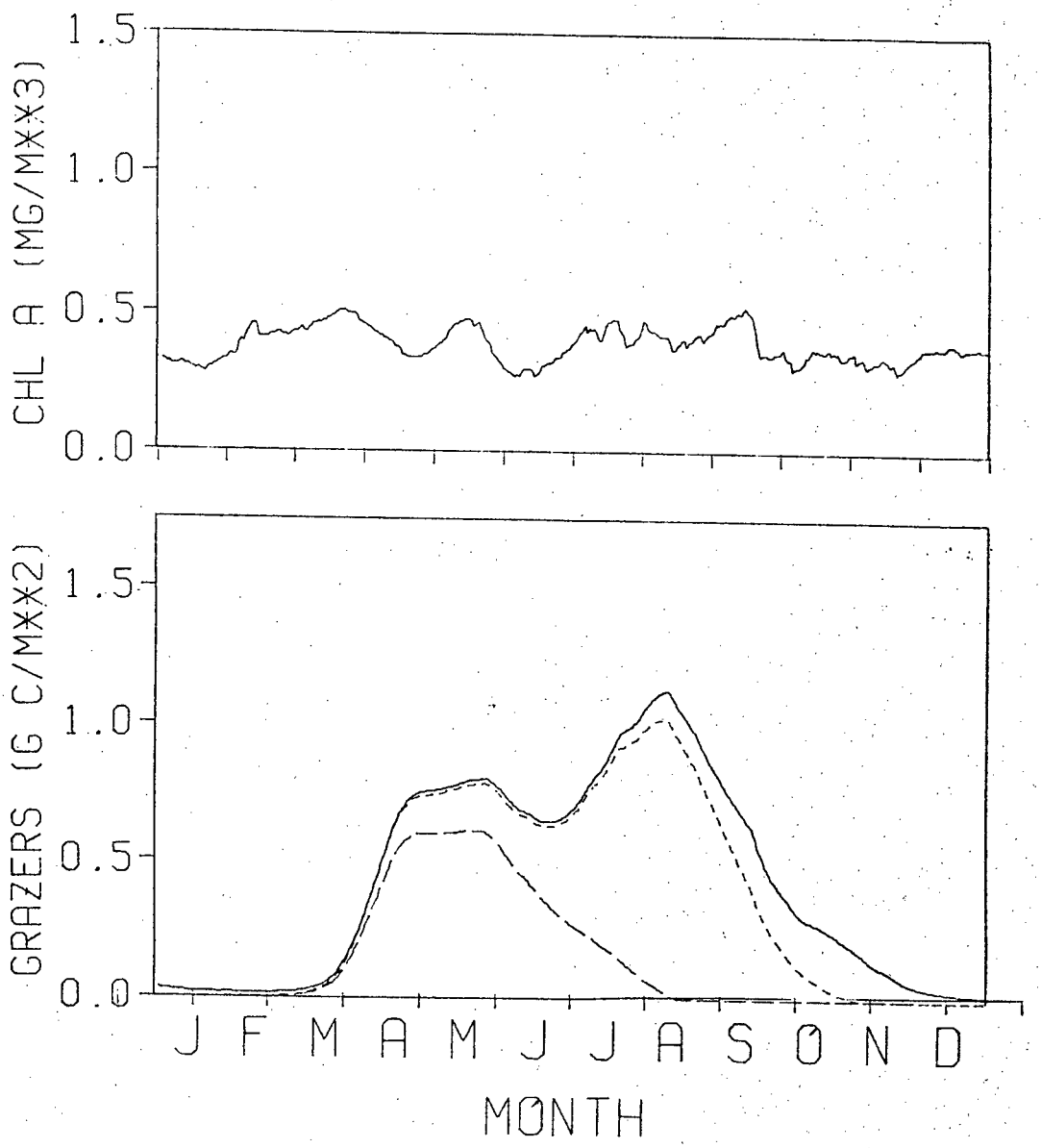

Figure 57. Effect of decreasing grazing parameters CO and D in Fig 53.

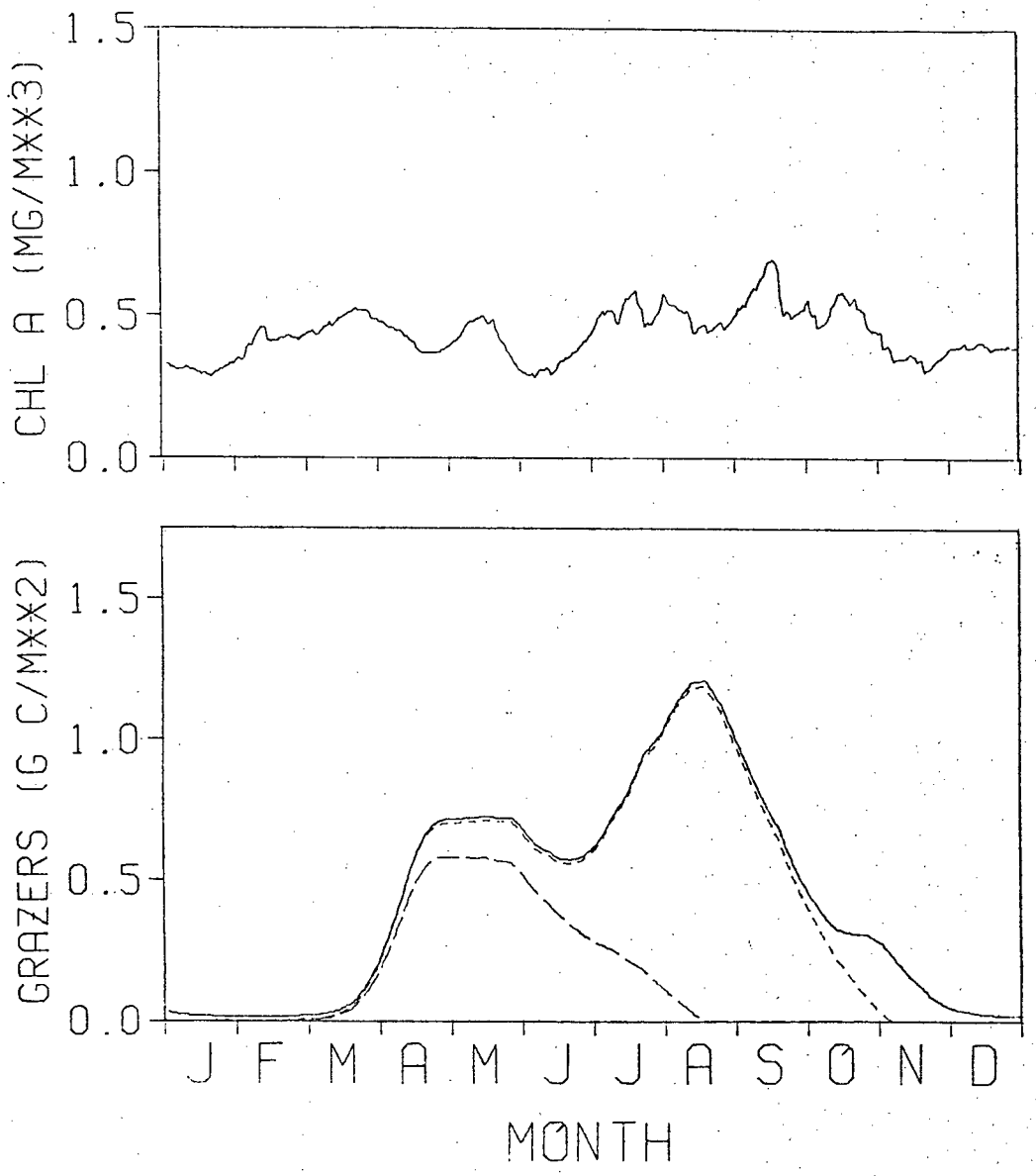

Figure 58. Effect of increasing metabolic rates in Fig 57.

affected the relative success of the small copepod group and the large copepods have led to small phytoplankton excursions in the fall (Fig 54,58).

So far, only the predicted timestreams for one year, 1976, have been shown. Long-term simulations have also been performed for the period 1964 to 1976. These simulations have used the same set of parameters as Fig 53, including the fixed residence time departure strategy. In the first simulation, constant recruitment totals of 1.10^5 and $2.5.10^4$ ind/m^2 were assumed in all years. Phytoplankton biomass and the small copepod biomass, G, were continued from each year to the next. The predicted primary production cycle with chlorophyll fixed (Fig 33) showed remarkably little variation from year to year. Given that spring recruitment is fixed, the qualitative slow-variable analysis and the preceding simulation results suggest that the predicted cycle of zooplankton biomass should also show little year to year variation.

This does not turn out to be the case, as shown in the plot of mixed layer Chl a and total zooplankton carbon (Fig 59). Short-lived phytoplankton blooms and unusally high zooplankton peaks occur in late summer in 1967, 1972, 1974 and, to a lesser extent, 1971. Closer examination of the model output shows that these zooplankton peaks consist of C. cristatus which reach high departure weights (up to 1000 μg C/ind) as a result of the blooms.

The cause of these blooms was somewhat unexpected. Each of the years involving large peaks follows a severe winter, in which the small copepod biomass, G, falls to unusually low levels, an

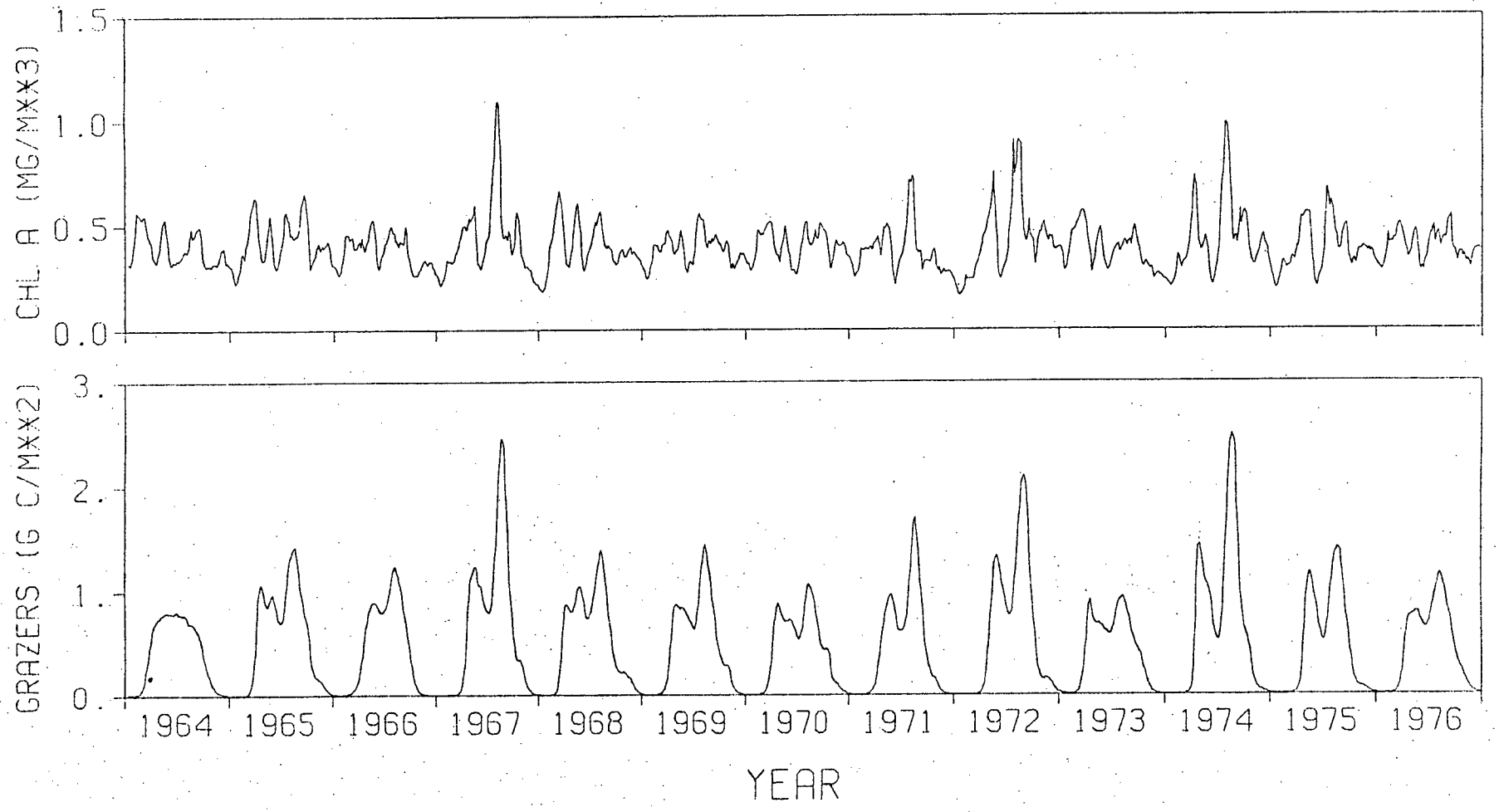

Figure 59. Predicted mixed layer Chl a and total zooplankton carbon for 1964-76, using the parameters and fixed recruitment levels of Fig 53.

order of magnitude lower than the minimum in other years. As a result, there is a lag in the response of small copepods to the departure of the large copepods and phytoplankton escape grazing control. It is interesting to note that, while the predicted minimum annual small copepod biomass varies by 2 orders of magnitude, depending on the severity of the winter, the predicted maximum varies by less than a factor of 4 and there is no tendency for G to decrease or increase over the long-term. The predicted co-existence of small and large copepods is clearly a case of partitioning of the resource by time, through the life history strategies of the major copepods.

The long-term simulation results again emphasize the delicate balance required in this model to achieve a smooth transition of phytoplankton control among the three zooplankton groups. It should at once be pointed out that as an explanation of observed annual variation in zooplankton standing stock at O.S.P. (Fig 60), this simulation is sadly lacking. Of the predicted peak years, 1967 and 1972 are high years at O.S.P. but 1974 is a very low year. The predicted peaks occur in August, whereas the peaks in 1967 and 1972 occur in June. Finally, there is no evidence that high zooplankton peaks at O.S.P. follow phytoplankton blooms.

In the second long-term simulation, an attempt was made to couple the spring recruitment of C. plumchrus and C. cristatus in each year to the predicted over-wintering biomass of each species from the previous year. This exercise has rather more theoretical than practical interest, as the factors affecting over-wintering success are poorly known, and horizontal advection

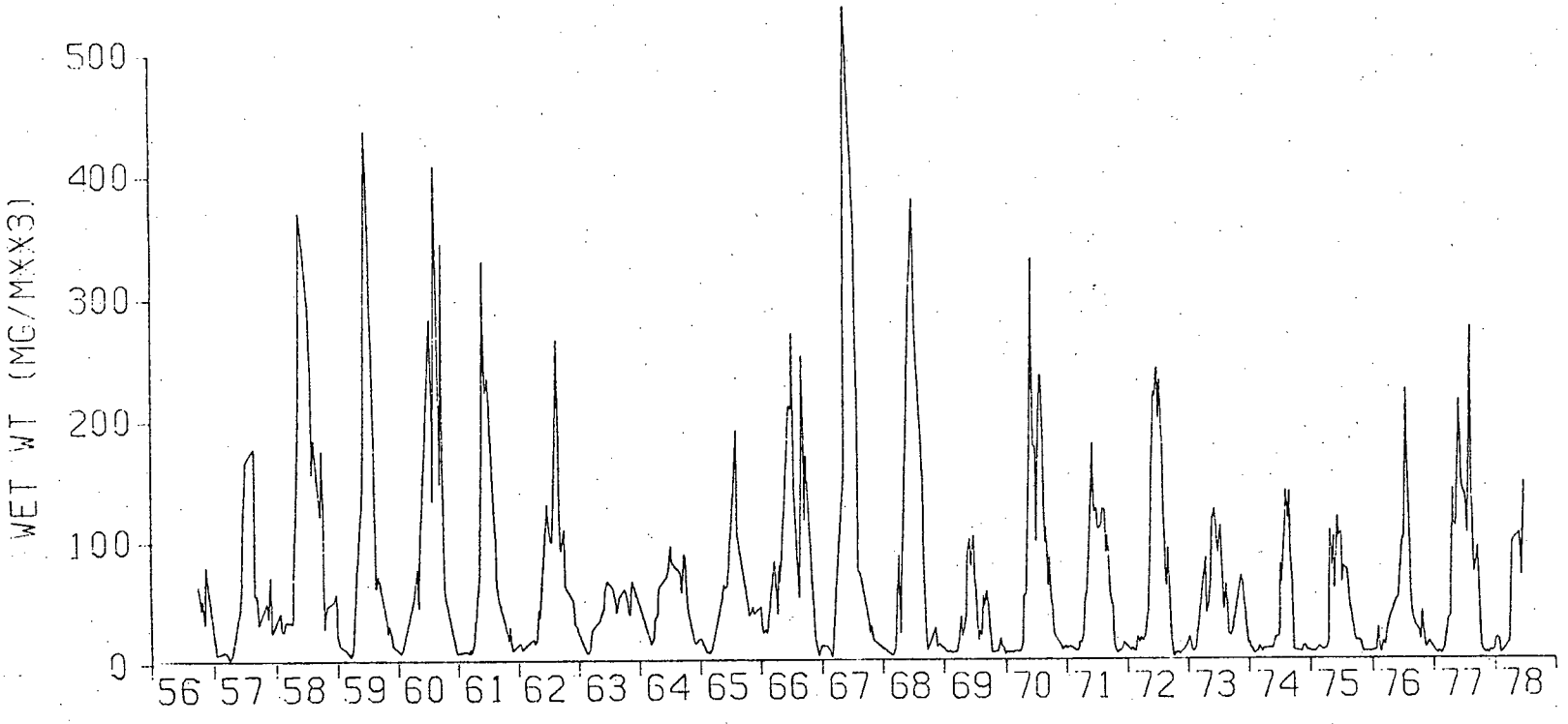

Figure 60. Observed zooplankton wet weights (10 day means) at O.S.P. 1956-1978.

is significant on the time scale of over-wintering, so that relating recruitment at O.S.P. to the predicted over-wintering biomass at the same location is a dubious undertaking. The fraction of over-wintering biomass converted to nauplii was decided in rather arbitrary fashion, by looking at the average over-wintering levels in the previous long-term simulation, and choosing a fraction which would provide the 'fixed' total recruitments used there. The resulting over-wintering efficiencies, which take account of mortality and reproductive efficiency, were low (.04 for C. plumchrus and .005 for C. cristatus).

The corresponding predicted timestreams of Chl a and total zooplankton biomass are shown in Fig 61. (Note the change in scale). The predictions are qualitatively similar to those with constant recruitment, but the phytoplankton and zooplankton peaks in 1967, 1971, 1972 and 1974 are even higher. This is due to slightly higher average recruitment of C. plumchrus (ca $1.5.10^5$ ind/m^2) than expected. There is considerable annual variation in recruitment and in the year of poorest control, 1967, the recruitment of C. plumchrus is very high, $2.1.10^5/m^2$, while that of C. cristatus is unusually low, $1.7.10^4/m^2$, which undoubtedly contributes to the control problem as C. plumchrus departs. In this year, both species reach unreasonable departure weights (900 and 2000 μg C/ind respectively). Again, despite the annual variation in recruitment levels, there is no long-term trend and coexistence of the major copepods is predicted, presumably due to the partitioning of the food resource over time. (C. plumchrus can grow at lower food levels than C. cristatus ,but the latter

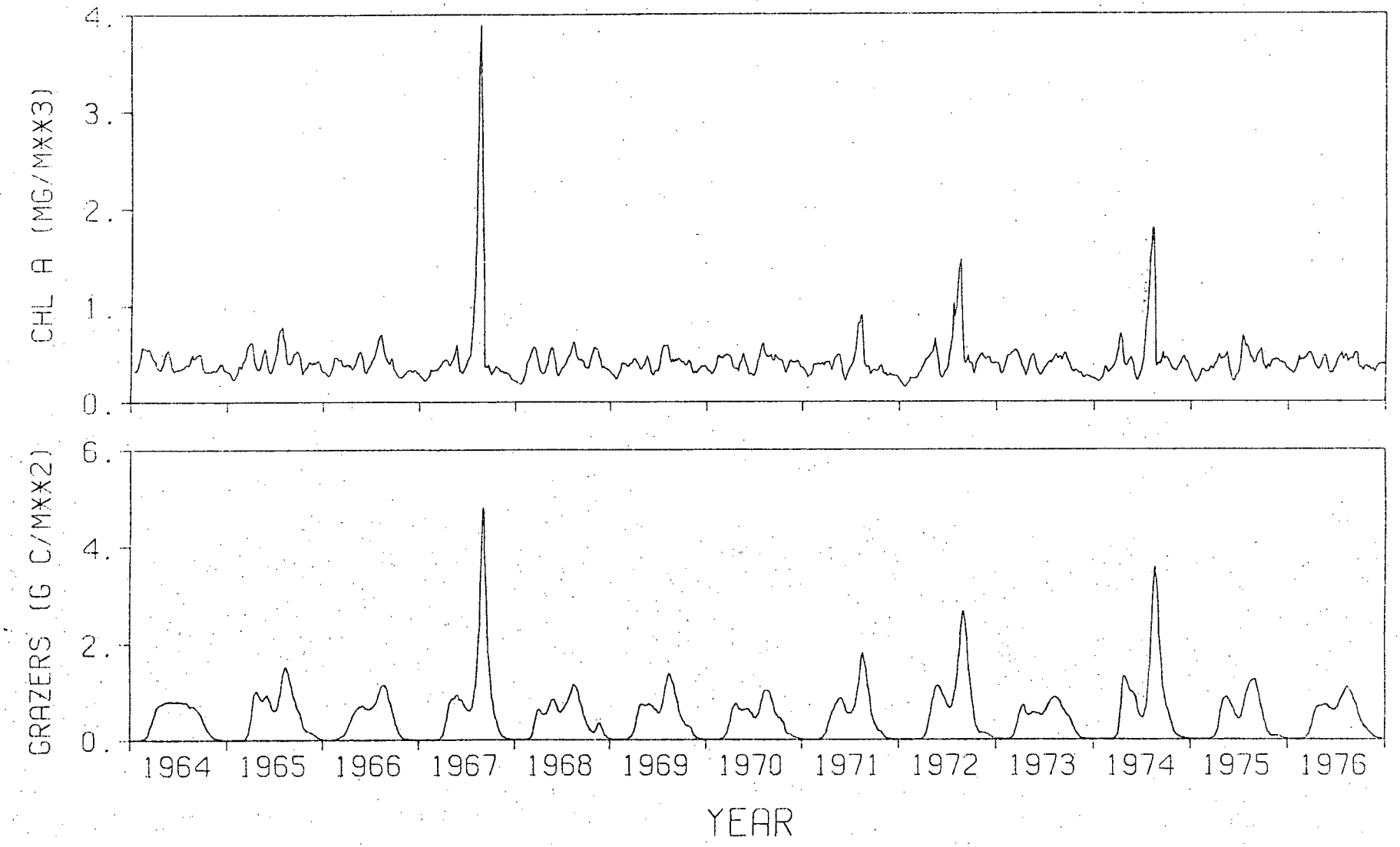

Figure 61. Predicted mixed layer Chl a and zooplankton carbon for 1964-76 using coupled recruitment.

has the resource to itself in the fall).

The long-term equilibrium balance between recruitment of C. plumchrus and C. cristatus is particularly sensitive to changes in the over-wintering efficiencies. For example, if the over-wintering efficiency of C. cristatus is doubled to .01, the ratio of spring recruitment shifts over several years from about 6:1 to about 1.3:1, with annual recruitments fluctuating about $6.7.10^4/m^2$ for C. plumchrus and $5.10^4/m^2$ for C. cristatus. As might be expected, control of phytoplankton during the departure of C. plumchrus is much improved and the peaks in 1967, 1972 and 1974 virtually disappear. The behaviour of the model with this recruitment ratio is more robust, but the ratio is not consistent with the recruitment estimates of Section 4.1.

4.4 Conclusions.

According to one philosophy, a model of the type presented here should be regarded as a complex hypothesis, stated explicitly, which is thereby subject to rigorous testing against observations. It may even be claimed that a model is most useful when it fails to match observations, thereby revealing an error in the hypothesis. There are, however, limitations to this usefulness, due to the complex nature of the hypothesis-model. While simple verbal hypotheses such as 'phytoplankton at O.S.P. are controlled by zooplankton grazing' or 'the life history of the dominant copepods at O.S.P. is the cause of the distinct seasonal cycle' or 'thresholds in zooplankton grazing occur at O.S.P. and are a component in maintaining phytoplankton constancy' sound reasonable alone, they can be addressed via the

model only within a framework of other hypotheses involving phytoplankton growth dynamics, zooplankton mortality, etc. Within the framework constructed here, it is possible to produce a (reasonably) constant chlorophyll concentration and a seasonal cycle in zooplankton biomass which roughly corresponds to observation in form and magnitude, by including thresholds and life history strategy in the model, and this is not possible if either is removed. If the other assumptions of the model are accepted, this can be taken as evidence for the importance of these phenomena at O.S.P.

It is important to consider carefully the areas in which the model's predictions fail to match observations. These may be due to small errors of detail in the model which do not affect the above conclusions, or to fundamental flaws in the model's assumptions or structure which invalidate these conclusions. Such questions cannot be answered without further experimental and field studies. The following examination of the model's failures and speculation as to their causes will hopefully assist in the direction of these studies.

Much of the simulation study of the species, size-structure model has centred around the problem of how to achieve a smooth transfer of phytoplankton control as large copepods cease feeding. The problem here is not so much in matching observations as in the model's sensitivity. A suspiciously delicate balance of growth rate, mortality and recruitment is required among the three zooplankton groups in the model in order to prevent a small phytoplankton bloom. This has been attributed to the unstable feedback associated with the over-wintering

strategies used so far.

Another over-wintering strategy was tried in the model. If it is accepted that at over-wintering depths, C. plumchrus experiences a lower mortality rate (by an amount $\Delta\theta$ day^{-1}) and negligible respiration (Fulton,1973), it follows that an individual's fitness, measured in terms of expected biomass for conversion to eggs in the spring, is increased by staying a day longer in the surface layer whenever its daily weight increase ΔW exceeds $W.\Delta\theta$. Presumably a minimum biomass is required for over-wintering, but above this, an individual which stays or leaves according to the above criteria is following an optimal strategy, at least on a day by day basis. This strategy also appears to be a potential solution to our instability problem. Departure will occur when ΔW, or phytoplankton abundance, is low, decreasing grazing pressure. It will cease when phytoplankton abundance is high, allowing an increase in grazing pressure through growth. An additional attractive feature is that, since $\Delta W/W$ is proportional to $W^{-0.3}$, larger copepods should leave first.

The simulation results using this strategy did not live up to these expectations. If $\Delta\theta$ is less than θ, no departure occurs, as the phytoplankton level required to maintain grazing pressure ($Z.W^{0.7}$) constant is higher than that required for the departure criterion. If $\Delta\theta$ is greater than θ, the biological interpretation becomes strained and the behaviour is still disappointing. Instead of a smooth, orderly departure of copepods, larger individuals first, with phytoplankton abundance hovering around the departure criterion level, departure occurs in a prolonged series of bursts, each followed by phytoplankton

blooms which slowly decline to the departure level. The new departure strategy succeeds only in adding an oscillatory aspect to the instability associated with weight-dependent departure.

Besides the problem of phytoplankton control, all of the departure strategies suggested here can lead to unreasonable departure times or departure weights if recruitment or mortality rates are too high or low. The weight threshold, which seems more reasonable biologically, leads to a complete failure of over-wintering of C. cristatus for high recruitments. A careful study of the depth distribution of copepods, including over-wintering depths, during the departure period would answer questions concerning the variability of over-wintering weights and the timing of departure. Field studies over several years may reveal a pattern to departure timing or weight from which a strategy can be inferred. Laboratory manipulation of stage V copepodids may be a quicker way to uncover a true departure strategy.

Aside from these sensitivity problems, there is a discrepancy between predicted and observed zooplankton biomass in the fall. Departing C. plumchrus are replaced by C. cristatus which reach large individual weights. Predicted phytoplankton production in August is still high (Fig 34) and, due to the $W^{0.7}$ metabolic law, the annual zooplankton biomass peak occurs at this time (Fig 53). However, the observed zooplankton biomass declines sharply in August in all years at O.S.P. (Fig 62a). Three possible explanations for this discrepancy will be discussed.

The first depends on the observation of Marlowe and Miller

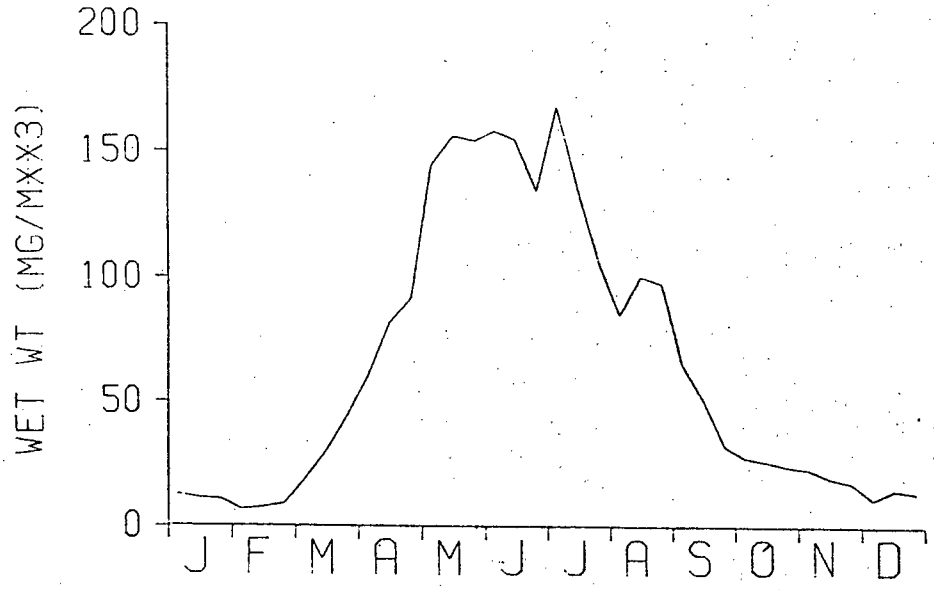

Figure 62a. Average seasonal cycle in observed zooplankton wet weight (10 day means, 1956-1978).

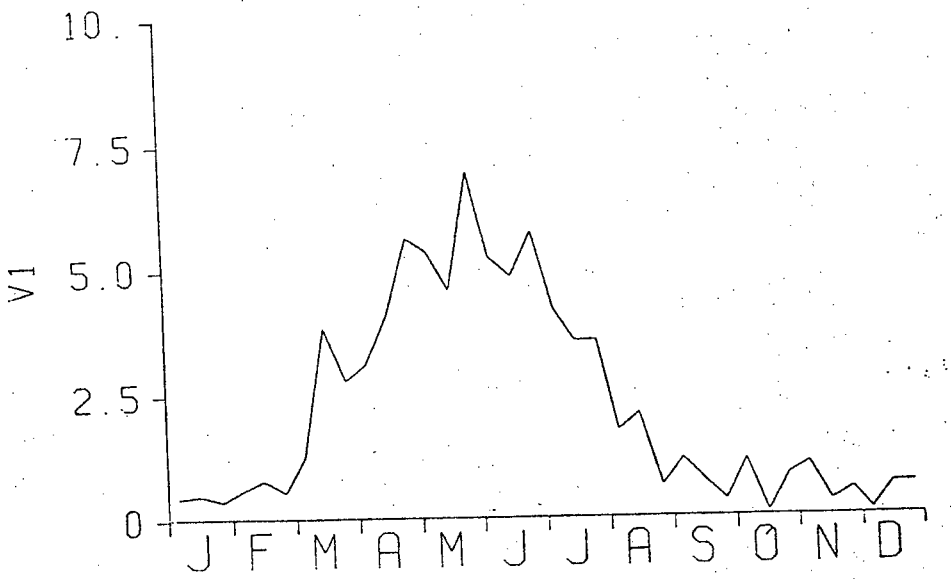

Figure 62b. Average seasonal cycle in ingestion variable V1 (10 day means, 1969-78).

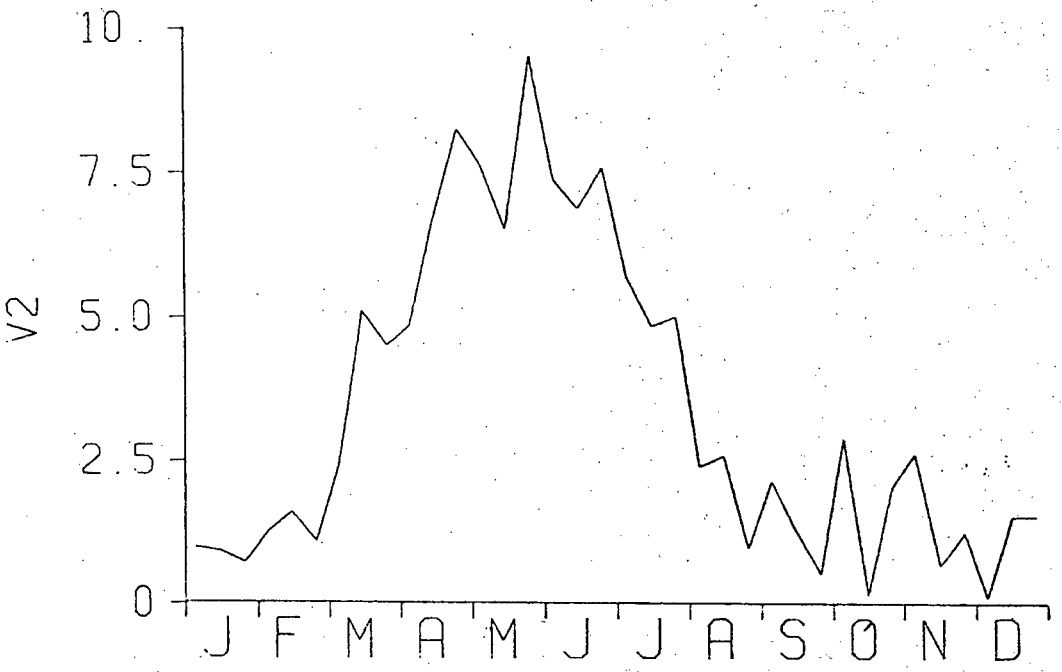

Figure 62c. Average seasonal cycle in ingestion variable V2 (10 day means, 1969-78).

(1975) that late-stage C. cristatus undergo extensive diurnal vertical migration. The 150m daylight hauls at O.S.P. may simply have under-estimated zooplankton biomass badly at this time. (The term zooplankton biomass is being used rather loosely here but as predicted by the model applies to zooplankton feeding on phytoplankton in the surface waters). According to this explanation then, the model may be correct but predictions and observations are not comparable. This can be easily tested by altering the depth and timing of zooplankton samples at O.S.P.

The second possibility is that the model is wrong in its prediction that C. cristatus takes over from C. plumchrus as the dominant grazer. A change in growth and mortality parameters could be arranged so that small copepod biomass will dominate as C. plumchrus leaves. According to the $W^{0.7}$ law, this should result in a lower zooplankton biomass being necessary to maintain phytoplankton control. Incidentally, as small copepods have higher maximum growth rates, their dominance at this time should result in tighter, more robust phytoplankton control. This possibility can be rejected on the basis of the size-structured data collected since 1969. Two derived variables were calculated for each sampling date from the set of densities N_i of copepods of length L_i :

$$V1 = \sum_i N_i . L_i^2$$

$$V2 = \sum_i N_i . L_i$$

If individual weight is proportional to L^3 and ingestion rate to $W^{0.67}$, V1(t) is proportional to ingestion (for fixed phytoplankton

abundance). According to the above proposal, while biomass is observed to decline in August, an increase in small copepods should make V1 constant.

In section 4.1, it was suggested that individual weights vary as $L^{2.45}$. An ingestion rate varying as $W^{0.7}$ would then vary as $L^{1.7}$, placing more relative weight on small copepods than V1. Rather than use this power of L, an even more extreme assumption was made, namely that ingestion is proportional to $L^{1.0}$ (eg Steele and Frost,1977). Under this assumption, V2(t) is proportional to ingestion at fixed phytoplankton density. In fact, both V1 and V2 decline more sharply in August than biomass (Fig 62), reflecting the predominance of large copepods at O.S.P. at this time.

These variables are based on results of 350 μm mesh net samples and it is possible that a bloom of even smaller forms occurs in August. Raw micozooplankton data collected from the weatherships from 1966 to 1977 were used to look for this phenomenon. These data consisted of species counts, primarily from near-surface samples. Protozoans (foraminifera and radiolaria) were numerically dominant and the smaller copepods, especially Oithona, were found at much higher densities than in the 150m vertical hauls. The autecology of many of these taxa is not well-known and individual sizes were not recorded, so that it is difficult to estimate ingestion rates for microzooplankton. However, the average seasonal cycles in abundance for most groups also show a marked decline in August (Table VII).

A third possibility is that the model is wrong in predicting continued high primary production in August-September. These are

Table VII.

Average relative seasonal abundance of microzooplankton.

(Raw data supplied by J. Fulton and O. Kennedy.)

Taxa	J	F	M	A	M	J	J	A	S	O	N	D
Foraminifera	0.6	0.8	1.6	2.1	1.7	0.5	0.8	0.2	0.4	2.8	1.6	2.3
Radiolaria	5.2	1.3	0.5	0.8	1.2	0.8	0.5	0.4	0.6	0.9	2.7	4.4
Tintinnids	1.5	0.8	1.2	2.7	1.7	0.7	2.1	0.3	0.4	---	1.9	5.5
Oithona												
nauplii	0.9	0.6	0.8	1.2	1.7	0.9	2.6	0.7	0.6	1.9	1.5	0.8
copepodids	0.6	0.5	0.7	1.1	1.0	1.6	1.9	2.1	1.2	4.0	0.5	0.5
adults	0.8	0.5	1.1	1.0	1.0	1.4	1.7	1.0	1.2	4.3	1.0	0.5

the months of greatest water column stability and, if nutrients are not limiting, one would expect high phytoplankton production. However, parameters for the P vs I curve corresponding to very low growth rates were found for these months in Chapter 3 (Fig 24,27) but these were ignored, as the underlying assumptions of the estimation procedure were not met, and very few ^{14}C profiles contributed to the estimates. In view of the zooplankton decline in August, a careful field and experimental study of phytoplankton growth parameters at O.S.P. at this time seems warranted.

A disappointing aspect of the model has been its failure to provide any convincing explanation for the year to year variation in zooplankton biomass at O.S.P. The year to year variation which is predicted by the model occurs in the late C. cristatus biomass peak as a result of variation in over-wintering survival of small copepods and is not consistent with the observed variation. Elimination of these peaks, by altering recruitment ratios or changing parameters, will result in a predicted zooplankton biomass which, like the primary production of Fig 33, varies little from year to year.

The simplest explanation of this failure is that advective effects are neglected in the model. There is good evidence for a direct effect of advection on zooplankton biomass at particular times, such as late 1973 and the spring of 1974, when the appearance of 'transition water' at O.S.P. is associated with low zooplankton biomass (Fulton,1978). Such an effect of advection has to be reconciled with the requirement for grazing control of phytoplankton. In the case of transition water, there appear to

be two possible explanations. One is that phytoplankton growth rates are lower in this water mass, for some unknown reason. (Nitrate concentrations appear to be adequate for growth). A second interesting possibility is that the grazer population is quite different in this water mass. The transition water is, in fact, recognised by the appearance of salps and similar gelatinous forms (Fulton,1978). High feeding efficiencies have recently been reported for these taxa (Madin,1974; Harbison and McAlister,1979).

These explanations do not suffice for the large variations in zooplankton biomass which are not associated with the appearance of transition water. One possibility is that annual variations in the spring recruitment of the large copepods which are not predicted by the model are responsible for the biomass variations. These recruitment changes could be due either to advection or to unknown factors affecting over-wintering success. This argument is supported to some extent by the parameter estimation results of Section 4.1 where despite large uncertainties, high recruitment estimates are associated with high biomass years. However, these results are themselves inconsistent with the model's reaction to recruitment changes. An increase in recruitment in the model results in lower biomass due to slower individual growth rates and the weight-dependence of ingestion.

If the estimation results are ignored, and it is accepted that the phytoplankton control requirement must apply, and that primary production does not vary significantly from year to year, then the size-dependence of grazing per unit biomass is left as a

possible explanation. This can be tested for annual variation using the same technique as for the August decline by looking at the 'ingestion' variables V1 and V2. Again, both V1 and V2 vary as much as biomass from year to year (Fig 63) : size-dependence will not explain the annual variations in biomass.

An increase in mortality rate might intuitively be expected to lower zooplankton standing stock. In fact, according to the models used here, increasing the mortality rate has the effect of increasing the equilibrium phytoplankton carbon C (equation 4.3a), thereby increasing primary production. This counteracts the direct effect of mortality (equation 4.3b) and little net change in standing stock results. Further, with the over-wintering strategies used here, relatively small changes in mortality rate severely affect either over-wintering timing or weight of the major copepods. Large changes in mortality rate would result in very unrealistic over-wintering behaviour and probable loss of phytoplankton control. The estimates of secondary production in Section 4.1 provide an additional argument against a mortality rate explanation. According to the model, in years of high mortality, phytoplankton production will increase slightly and zooplankton standing stock (and therefore zooplankton metabolism) will decrease. The result should be a higher trophic efficiency and higher secondary production. However, estimates of secondary production are high in years of high biomass and low in years of low biomass (Table VI)

None of these explanations in terms of variation in zooplankton composition or parameters is really satisfactory. In fact, the simplest explanation which is consistent with the

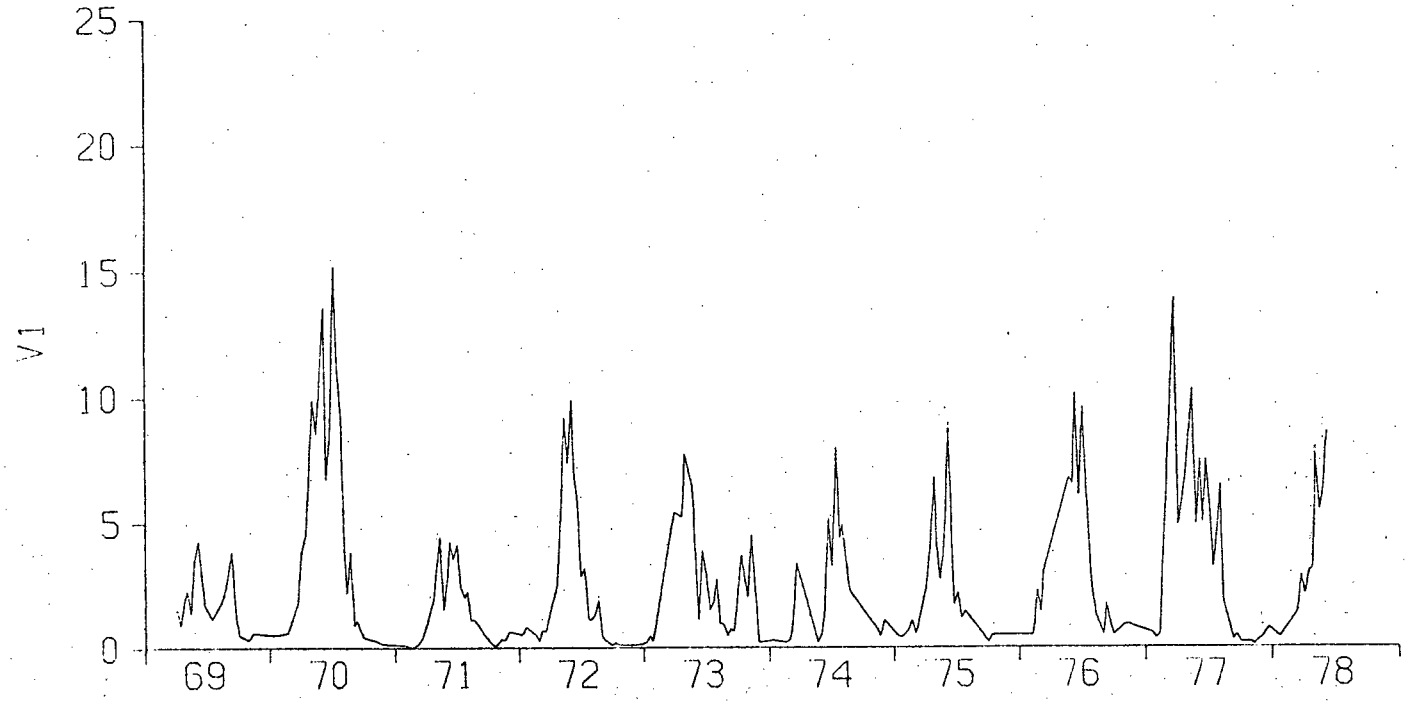

Figure 63a. Annual variation in ingestion variable V1 (10 day means).

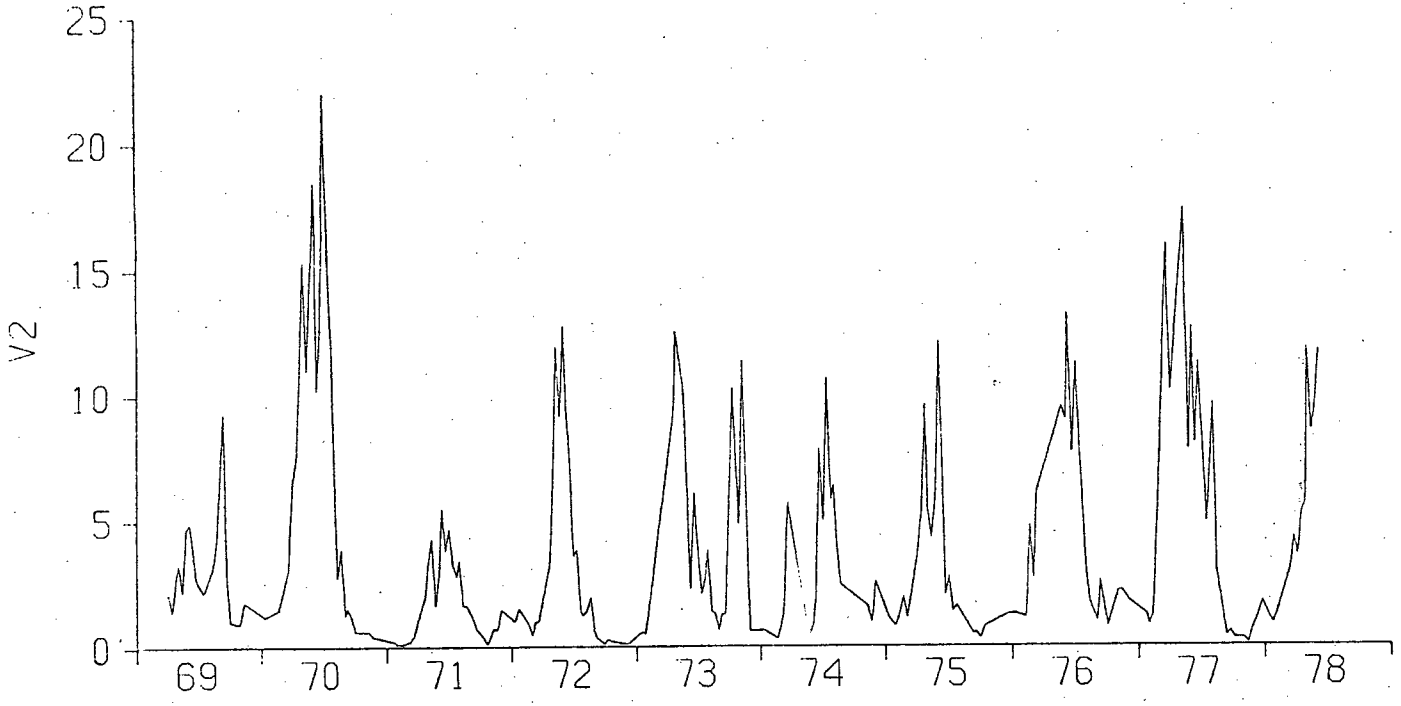

Figure 63b. Annual variation in ingestion variable V2 (10 day means).

grazing control hypothesis, the model and the parameter estimation results is that annual variations in primary production, not predicted by the model of Chapter 3, are responsible. The phytoplankton growth model is driven with observed solar radiation, mixed layer depth and temperature. It is possible that the model is not sufficiently sensitive to these driving variables and that larger annual differences may be predicted for different phytoplankton parameters. For example, increasing the respiration rate will increase sensitivity to mixed layer depth : however, it will also result in a greater loss of phytoplankton in winter, as discussed earlier. It was noted in Chapter 3 that secchi depth could affect primary production but the time series is not adequate to look for a relationship with zooplankton biomass. Changes in species composition and growth parameters could also be responsible for changes in primary production : the lack of species composition data and the problems involving ^{14}C measurements have already been discussed in Chapter 3. The possibility that there is some limiting micro-nutrient whose supply varies from year to year must be considered, although this analysis of the O.S.P. ecosystem rests on the assumption that nutrient limitation does not occur. As discussed in Chapter 1, the macro-nutrients appear to be abundant at all times, but the principal evidence against micro-nutrient limitation is the single culture experiment of McAllister et al (1960). Again, there is a need for phytoplankton growth studies at O.S.P. including the culture of phytoplankton in flasks with grazers excluded under conditions which rule out the inadvertent supply of micro-nutrients.

A correlation between zooplankton abundance at O.S.P. and computed Ekman transport components at 50°N,160°W some months previously was found by Wickett(1967) for the years 1957 to 1964. As in all such statistical correlations, it is not clear whether a causal link is responsible. Wickett suggested that the supply of macro-nutrients through upwelling in the Alaskan Gyre, and their advection to the vicinity of O.S.P. was involved. It is difficult to reconcile such an explanation with the apparent over-abundance of nutrients at O.S.P. in all years.

The discussion so far has centred on the areas of disagreement between prediction and observation and their implications for the model and for future field reserach. Various possible alterations or extensions to the model have been suggested and there are many others which could be discussed. Three topics which have recently received considerable attention in the modelling of marine systems, and have not been included in this model for lack of information, deserve at least a brief mention.

The size structure of phytoplankton was included in a model by Steele and Frost (1977) and found to significantly affect zooplankton dynamics. Although there is no quantitative time series information on phytoplankton size or species composition at O.S.P., various isolated observations suggest that phytoplankton there are predominantly small flagellates. This might normally be attributed to selective grazing on large cells by the dominant large calanoid copepods, but, according to Frost (1978), C. plumchrus has an unusually fine filtering mesh. In fact, Steele and Frost (1977) attributed the dominance of

C. plumchrus over smaller copepods at O.S.P. to its ability to feed efficiently on small cells. The raw data from microzooplankton samples taken from the weathership reveal a diverse assemblage of large diatoms and dinoflagellates at low concentrations (<500 cells.l^{-1}). The conditions at O.S.P. of a deep mixed layer and abundant nutrients might normally be expected to favour faster-growing diatoms. There is clearly an interesting set of problems involving phytoplankton competition at O.S.P. which may be addressed by a size or species-structured model after shipboard experiments on size or species-dependent growth and grazing. It is not clear how the conclusions reached here concerning the phytoplankton-grazer interaction would change for such a model. As a possible example, with a single phytoplankton variable, a delicate competitive balance has been required amongst the three zooplankton groups to ensure a smooth transition of grazing control. Some form of resource partitioning by size amongst these groups could result in more robust model behaviour.

The importance of the size and/or species composition of carnivores in controlling herbivore and phytoplankton dynamics from above has been emphasized recently (Sonntag and Greve,1977; Harris et al ,1980). Representation of predation on herbivores as a constant mortality rate in the model is certainly unrealistic. The information on primary carnivores at O.S.P. is of variable quality. The 150m vertical hauls provide reasonable time series for the planktonic forms, although the larger forms may be under-sampled due to net avoidance (Heath,1977). These planktonic carnivores, dominated by the medusae, Aglantha

digital, the chaetognath Sagitta elegans, the euphausiid Thysanoessa raschii and the amphipod Parathemisto, may feed principally on the smaller copepods or early life history stages of larger copepods. Other nektonic carnivores such as myctophid fish and squid, whose abundance and population dynamics are poorly known, may be more important predators on the larger copepods. Functional response data for all these taxa is lacking, with the partial exception of the chaetognaths (Sullivan,1980).

Introduction of more realistic carnivore dynamics, when possible, will almost certainly affect some of the conclusions reached here. However, the apparent tight coupling of phytoplankton and grazers required by the grazing control hypothesis would seem to require some decoupling between grazers and carnivores. For example, the assumption in Chapter 1 of a herbivore mortality rate which increased with biomass resulted in very unrealistic behaviour of phytoplankton standing stock. Some limited coupling between herbivores and carnivores may be desirable. A correlation between recruitment and mortality rate, arising out of a carnivore response either to numbers of small copepods or to the over-wintering copepod populations in the preceeding winter, would tend to reduce the sensitivity of departure times or weights to recruitment levels which occurs with a constant mortality rate. Switching behaviour or threshold feeding phenomena on the part of carnivores may again decrease the sensitivity of the present model during the departure period by maintaining minimum stocks of small copepods.

The implications of horizontal variation or patchiness in

plankton populations for theories of population interactions has also received much attention in the last decade. Two types of questions have generally been addressed by these studies:
(a) How is patchiness in plankton populations created and maintained?
(b) How does the existence of patchiness affect conclusions about properties of population interactions, such as stability, which have been based on models which ignore horizontal spatial effects?

Plankton populations in the ocean are by definition subject to turbulent mixing processes which are traditionally thought of as smoothing out spatial variation, so the first question is a natural one. It was first addressed theoretically using a simple linear model of phytoplankton growing at a fixed rate in a diffusive environment (Kierstead and Slobodkin, 1953). This analysis gave rise to the idea of a critical patch dimension, L_c, below which diffusive losses from the patch outweigh growth. This length scale has been estimated to be of order a few kilometres up to hundreds of kilometres, depending on growth rates (Steele,1976). There is empirical evidence that spatial variation in phytoplankton at smaller length scales is determined by physical processes (Platt,1972).

If grazing is thought of simply as a reduction in net growth rate in a linear phytoplankton model, it should have the effect of reducing patchiness at small length scales; that is, increasing L_c. If growth and diffusion of zooplankton are considered, a non-linear reaction-diffusion system results. The analysis of such a system is much more difficult. For small

perturbations about a spatially-uniform steady-state, an approximate linear system can be derived and a Fourier analysis applied. For equal diffusion rates for phytoplankton and zooplankton, diffusion again has a smoothing effect. If the steady-state is stable under spatially-uniform perturbations, it is stable under perturbations at all finite wavelengths. If it is unstable under uniform perturbations, there is again a critical length scale below which perturbations are damped out. For unequal diffusion rates and for a certain class of reaction models, the linear theory shows that the steady-state can be stable under uniform perturbations but unstable under perturbations of intermediate wavelength. This diffusion-generated spatial variation, or diffusive instability, has aroused a great deal of interest in a variety of fields (Turing,1952; Segel and Jackson,1972; Kopell and Howard,1973; Okubo,1974). Unequal diffusion rates could arise in the ocean where horizontal mixing is dominated by shear dispersion and zooplankton migrate vertically (Evans,1978).

A truly non-linear analysis of large-amplitude spatial variations is very difficult. There is obviously the possibility of transfer of variability across length scales via the non-linear terms, as in the energy cascade of turbulence. It has been argued (Steele,1974) that highly correlated, large-amplitude variations on small length scales could destabilize a uniform steady state which is stable under uniform perturbations. The nature of horizontal variation in the vicinity of O.S.P. is not well known compared with other regions such as the North Sea (Steele,1976). If a more or less constant flow past O.S.P. of

about 3 km.day^{-1} is accepted (see Chapter 1), some information about spatial variability can be deduced from the weathership time-series. The high-frequency sampling of surface chlorophyll from 1964 to 1968 (Fig 13) represents samples about 6 km apart. The generally low variability in these samples suggests that there is little horizontal variation in Chl a. It was noted in Chapter 3 that the occasional short groups of high values could be interpreted as patches of order 20 to 50 km across. This is a typical length scale at which biological patchiness might be expected (Steele,1976). With the models used here, it is easier to explain these high chlorophyll observations as patches rather than short-lived, wide-spread blooms. Causes of outbreaks such as these are not clear. There is evidence for chemical and physical patches on this length scale (McAllister et al ,1960; Miyake,1979)

According to the linear theories, perturbations on large enough length scales behave as a spatially uniform theory would predict and it has been argued that conclusions concerning stability similar to those reached here, based on models which ignore spatial effects, are still relevant when spatial variation is taken into account (Steele,1974). A possible exception could occur in a spatially restricted region if the critical patch dimension exceeded the size of the region (Steele,1974) but this does not seem likely for a system on the scale of the Subarctic. Properties of unstable systems, such as persistence, can change markedly with the introduction of spatial variation (Hilborn,1975), but such phenomena depend intrinsically on large-amplitude short-term fluctuations in space and time which are not

observed for O.S.P.

Summary.

This study has taken a set of verbal hypothesis regarding phytoplankton-zooplankton interactions at O.S.P. and attempted to explore them more rigorously within the framework of a model based on information taken from the literature and information obtained by the original analysis of raw data from the weathership time series. The results of this study can be summarised by answering two related questions :

(a) What has been learnt about the O.S.P. ecosystem as a result of the study?

(b) What are the open questions about the O.S.P. ecosystem which have been raised during the study?

The analysis of phytoplankton data has yielded information about the seasonal cycle of phytoplankton standing stock and growth rates. The limitations imposed by the types of variables measured and apparent inconsistencies in some data have been discussed at length in Chapter 3. The direct analysis of zooplankton data using the parameter estimation technique of Parslow et al (1979) has provided information about the population dynamics and secondary production of the major copepods, again subject to the limitations imposed by the depth range sampled.

As the data used here are for the most part unpublished, it should perhaps be stressed at this point that the modelling bias of this study and of the author has meant that much of the information in the weathership zooplankton time series has been ignored, either as irrelevant to the questions posed here, or as

unusable until further information on the autecology of the species concerned is available. No claim is made to an exhaustive analysis of this time series. Summaries of the basic information on seasonal and annual abundance of a large number of zooplankton species will be published shortly and the application of other techniques, such as multivariate statistics, to these data may prove illuminating. Nor has the potential of the time series for testing models been exhausted : as further laboratory information is obtained on feeding and growth in various herbivore and carnivore species, more complex models may be built and tested.

The modelling component of this study has allowed questions concerning grazing control of phytoplankton and the importance of thresholds and life history strategies to be addressed. The qualitative analysis and simulation studies have emphasized the potential importance of phytoplankton respiration rates in determining seasonal cycles of primary production, and secchi depths in affecting annual variations in primary production. The stabilizing effects of spring recruitment of herbivores has been discussed. Perhaps more novel has been the destabilising effect of over-wintering departure of the dominant herbivores which has focused attention on the months of August and September where both model and data indicate a number of interesting puzzles.

The questions raised by the model and data analysis should be of interest as a guide to future biological research at O.S.P. Details of the phytoplankton seasonal growth cycle, particularly winter production and growth rates in August and September, have emerged as uncertain and important. Attention needs to be paid

to phytoplankton respiration rates and the possibility of micronutrient limitation. Annual and seasonal variation in light extinction coefficients are also worthy of study. The size and/or species composition of phytoplankton appears likely to be a productive subject for future research problems.

In the case of zooplankton, deeper stratifed samples are needed to resolve problems surrounding seasonal and diurnal vertical migration. These, together with collection and identification of naupliar stages, should help to resolve outstanding questions concerning the population dynamics of the major herbivores. Obviously, the questions concerning grazing thresholds in this study can be addressed directly by grazing studies of the type discussed by Frost (1979), although interpretive problems may remain. The microzooplankton have been virtually ignored in this study, partly because of the relatively poor time series information and partly because of ignorance of these species' feeding and growth characteristics. This group may be important in winter where detrital-based food chains may predominate (LeBrasseur and Kennedy,1972). In view of the high concentrations of non-phytoplankton particulate organic carbon (McAllister et al ,1960) and the seasonal cycle in this material (C.S.Wong and K.Ishi, pers. comm.), the energetic role of detritus deserves more attention. There may also be an interesting feedback between detritus and phytoplankton growth through water transparency, as secchi depth varies seasonally despite a constant chlorophyll level. The microzooplankton will play an important role in any study of the dynamics of the planktonic carnivores,even if their role in phytoplankton

regulation proves marginal.

Although it would be pleasant to provide a definitive answer to the question : 'What is really happening at O.S.P.?', it would be unrealistic to expect one. There are large gaps in our knowledge, and models of the type considered here are necessarily constrained to consider a small subset of the available information and of the possible questions. It is to be hoped that this model study, by yielding fresh insights into the biological problems considered, and raising new questions, both theoretical and empirical, can contribute to a long-term investigation of this interesting ecosystem.

CHAPTER 5

PARAMETER ESTIMATION AND STABILITY FOR A CEPEX ENCLOSURE.

5.1 Introduction.

In Chapter 2, a qualitative analysis of the stability properties of a simulation model of the North Sea (Steele,1974; Landry,1976) was presented. This analysis led to the conclusion that, following nutrient depletion, stable cyclic behaviour could be expected because of the limitation of phytoplankton growth by a nutrient flux due to mixing. However, during the transitory approach to this cycle, the response of zooplankton to low food densities was found to be critical. A behavioural feeding threshold combined with a zero basal metabolic rate was used by Steele(1974) to ensure reasonable behaviour during this period. As indicated in Chapter 2, other types of zooplankton response to low food densities, including a longer-term physiological response or a rapid-enough increase in mortality rate, could achieve the same effect. It was suggested there that these responses might be distinguished in long-term culture experiments (eg Paffenhoffer,1970) if these were carried out at sufficiently low food densities.

The CEPEX experiments (Grice et al ,1977), conducted in Saanich Inlet from 1974 to 1978, involved the capture, perturbation and observation of columns of water in large, plastic enclosures. By allowing the manipulation and study of an enclosed ecosystem in a large volume (1300 m^3) over a period of several months, these experiments were intended to bridge the gap between laboratory studies of a few species at one or two trophic

levels and field investigations where it is difficult to follow a particular planktonic community over time.

In an experiment carried out during August, September and October of 1976, the effects of upwelling (through air bubbling) and adding carnivores (salmonid juveniles) to enclosures were investigated. An analysis of the results has been given by Sonntag and Parsons(1979). Of particular interest here is the behaviour of the community in the control bag (CEE5) which was not bubbled. After an initial phytoplankton bloom, the biomass of phytoplankton dropped to very low levels and remained relatively constant for the duration of the experiment. As both estimated zooplankton grazing rates and the average nitrate concentration in the enclosure remained very high during this period, Sonntag and Parsons(1979) concluded that feeding thresholds, or some sort of spatial refuge, were necessary to explain the persistence of phytoplankton at low, constant levels. In view of the implications for the general questions raised in Chapter 2, a closer analysis of the zooplankton-phytoplankton interaction in this enclosure seemed justified.

A systems-identification technique for estimating copepod population parameters has already been described in Chapter 4 and applied there, with some modifications, to time series of copepod densities by size class from O.S.P. This technique was originally tested on simulated data and on observations of copepod densities by life-history stage from a CEPEX enclosure (Parslow et al ,1979). The estimation procedure performed poorly on the CEPEX time series compared with simulated data. This was tentatively attributed either to higher noise levels than

expected in the CEPEX data, or to the variation over time of population parameters (mortality rates and stage residence times) in the CEPEX population.

The second explanation has serious implications for parameter estimation in general. These higher-level population parameters depend on physical and biological components of the environment (eg temperature,food,predators) and can be expected to vary over time in all but the most tightly regulated laboratory situations. The best that can be expected of a single estimate of a time-varying parameter is that it represent, in some sense, an average over time. The systems-identification technique mentioned above involves the least-squares fitting to the data of a dynamic model in which parameters are assumed to be constant over time. If this assumption is not met, there is no guarantee that parameter estimates will represent any sort of average over time. The highly non-linear nature of the procedure may in fact lead to nonsensical estimates, even negative stage residence times (Parslow et al , 1979).

Ideally one would like to estimate parameters which are constant over time . Where environmental conditions vary, it may still be reasonable to assume that the parameters which determine the individual's response to these conditions are constant over time. It was suggested by Parslow et al (1979) that a more detailed model of the functional and numerical response of copepods, driven by observed time series of food and predators, might be fitted to densities in life-history stages. Reservations were expressed concerning the feasibility of such a scheme in view of difficulties encountered with simpler

population models.

In this chapter, an attempt is made to estimate functional and numerical response parameters in a copepod growth model from time series of copepod densities in the CEPEX enclosure CEE5. These parameter estimates are used to address the question of copepod response to the low food densities in CEE5, both directly and by inserting them in a combined nutrient-phytoplankton-zooplankton model.

5.2 Estimation of Parameters in a Zooplankton Growth Model.

The data obtained from CEE5 which are used in this paper consist of time series of observations of

(a) phytoplankton carbon (0-20m average) by taxanomic group : centric diatoms, pennate diatoms, dinoflagellates, silicoflagellates and unidentified flagellates,

(b) Chlorophyll a and ^{14}C productivity by 4m layer,

(c) nitrate concentration by 4m layer,

(d) zooplankton (numbers/liter) as total nauplii, and copepodids identified to species and to one of the groups CI-III, CIV-V, or CVI.

The aim in this section is to use the observed phytoplankton concentrations to drive a model of zooplankton growth for each species and to obtain estimates of the parameters in the model by minimising the sum of squares of deviations between predicted and observed numbers of zooplankton in the above groups of life-history stages.

There are many forms which a model of zooplankton growth which predicts numbers in various life-history stages can take.

A discussion of parameter estimation via systems identification techniques in some simple models which do not take the effect of food concentration into account is given in Parslow et al (1979). When the effect of food concentration on growth is to be treated explicitly, as intended here, a choice must be made between a model which has as its underlying state variables the numbers in a weight or stage class and calculates the transfer rates between classes as a function of food density (eg Sonntag and Greve,1977) and one which follows the weight and abundance of age-classes and assigns them to life-history stages on the basis of weight, as in Landry's (1976) multi-cohort version of Steele's model. The former has the disadvantage that it tends to numerically smear the initial weight or stage distribution, while the latter does not allow for observed individual variation in growth rate (eg Paffenhoffer,1970). The latter model was used here, primarily because of its similarity to Steele's model which has provided much of the biological motivation for this study.

The model used here is based on day classes. For each day class i, introduced on day t_i, the density on day $t > t_i$ is denoted by $Z_i(t)$, and the individual weight by $W_i(t)$. These change with time according to

$$\dot{W}_i = f(W_i, P(t)) \qquad 5.1a$$

$$\dot{Z}_i = g(W_i, Z_i) \qquad 5.1b$$

The initial number in day class i, $Z_i(t_i)$, is obtained by assuming that adults do not increase in weight but convert their calculated daily weight increment into nauplii with an efficiency

X. If $W_1, \ldots, W_4$ represent the initial weights in the life-history stage groups NI-NVI, CI-CIII, CIV-CV and CVI respectively, the total numbers in each of these respective groups can be defined as

$$Y_J(t) = \sum_i Z_i(t) . \phi_J(W_i(t))$$

where

$$\phi_J(W) = \begin{cases} 1 & \text{for } W_J < W < W_{J+1} \\ 0 & \text{otherwise} \end{cases}$$

The functions f and g have been chosen to be as simple as possible. Assimilation is assumed to depend hyperbolically on food density P and a non-zero basal metabolic rate is also allowed. Steele(1974) assumed a $W^{0.7}$ law for both, partly on the basis of observations (eg Paffenhoffer,1970) and partly on general theoretical grounds. On the other hand, Paffenhoffer and Harris(1976) found no significant deviation from a $w^{1.0}$ law for ingestion by Pseudocalanus elongatus and, even in the case of Calanus helgolandicus, maximum growth rates per unit body weight increased up to NV and were more or less constant from NVI to CII. I have chosen here to make growth proportional to $w^{1.0}$ but to allow for variation in growth parameters across the groups of stages described above. (The same groups of life-history stages were distinguished by Paffenhoffer(1970) and Paffenhoffer and Harris(1976), facilitating the use of their results in analysis of the CEPEX data.) Thus,

$$f(W,P) = (Cn.P/(D+P) - F) . W$$

where Cn, D and F can depend on W through their stage dependence. Note that the parameter Cn represents the maximum ingestion rate C, reduced by both assimilation efficiency and any component of metabolic rate proportional to ingestion, so that Cn - F is the maximum exponential growth rate.

According to Sonntag and Parsons(1979), the mortality imposed on copepods due to predation was insignificant in CEE5 so that copepod losses were presumably due to 'natural mortality', possibly exacerbated by low food densities. As discussed in Chapter 2, comparatively little is known about the dependence of mortality rates on food conditions in copepods. A constant per capita mortality rate, θ, has been assumed here with the possiblity that θ may vary over stage groups being retained. The question of the dependence of θ on food conditions will be returned to in the discussion.

The phytoplankton data from CEE5 were used to drive the model. The observations in Fig 64 represent µg phytoplankton carbon/liter, averaged over the whole bag (0 - 20m), as estimated from cell counts. The average concentration falls to very low levels (less than 5 µg $C.l^{-1}$) after day 30. Unfortunately, the accuracy of these observations is called into question by other phytoplankton data from the enclosure. The observed concentrations of Chl a from day 30 on are too high to be consistent with the carbon estimates, yielding C:Chl a ratios as low as 6 µg C.µg Chl a^{-1} and generally less than 10 µg C.µg Chl a^{-1}. The estimates of ^{14}C productivity in the top 8m over the same period range as high as 10 µg $C.l^{-1}.hr^{-1}$ and average about 5 µg $C.l^{-1}.hr^{-1}$. These are based on 4hr incubations and, even

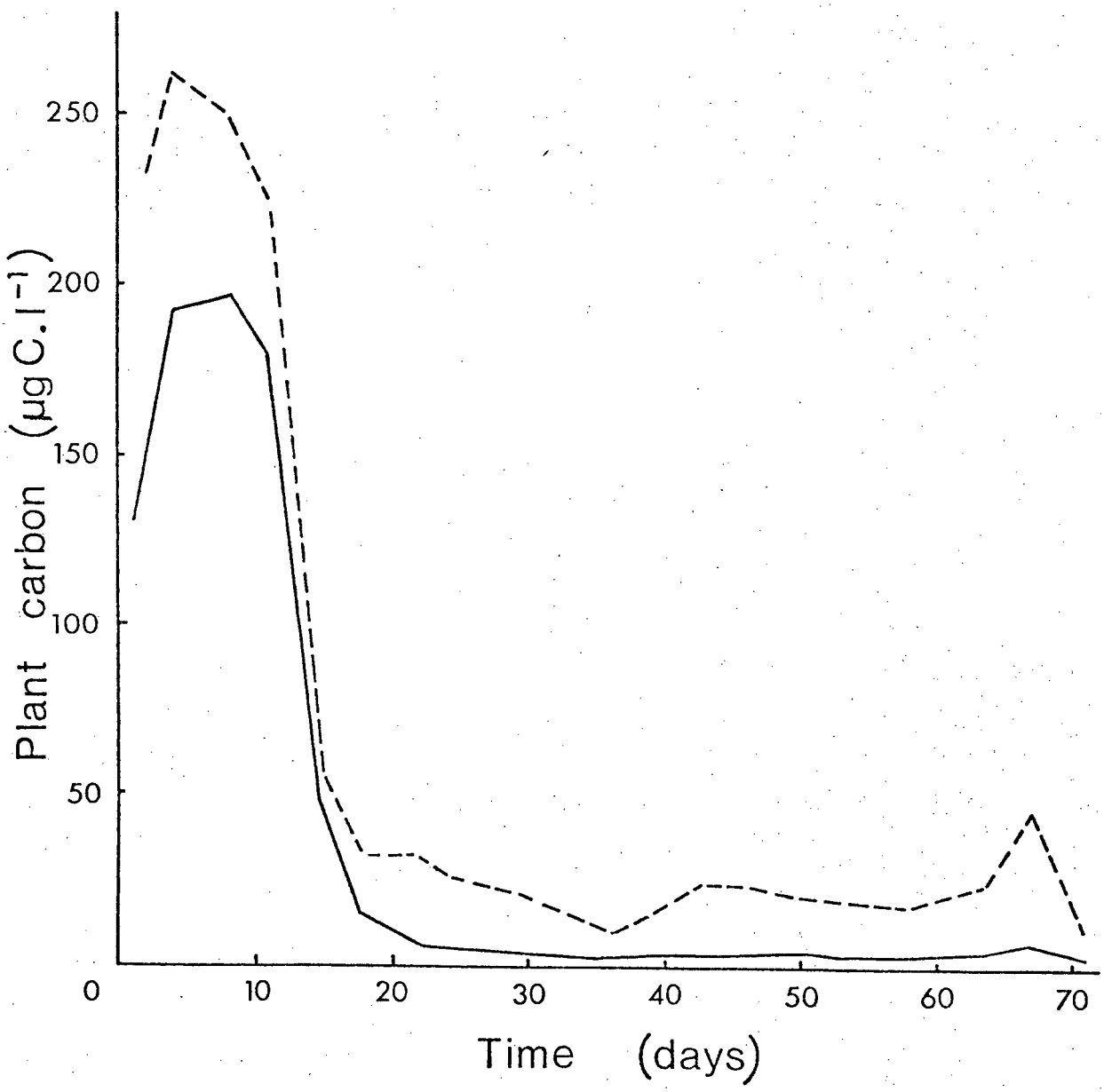

Figure 64. Phytoplankton carbon (0-20 m average) in CEE5 (solid line estimated from cell counts, dashed line represents corrected time stream used to drive estimation models).

allowing for an exponential increase in phytoplankton carbon during the incubations, when combined with the estimates of phytoplankton carbon from cell counts, they yield unreasonably high growth rates, of order 1 hr^{-1} and higher.

The ^{14}C and Chl a observations are consistent and both suggest that the estimated phytoplankton carbon is too low. Apart from the usual uncertainties associated with estimating carbon from cell counts (eg Mullin et al ,1966), the possibility that phytoplankton carbon has been underestimated is increased in this case by the fact that the phytoplankton over this period consisted almost entirely of small flagellates, so that preservation problems (Smetacek et al ,1980) may have led to an underestimate.

It will be assumed here that flagellate carbon is underestimated in Fig 64 by a factor of 5. This assumption results in corrected C : Chl a ratios after day 30 in the range 25 to 60 μg C.μg Chl a^{-1} with an average value of 37. The average growth rate in the top 8m over the same period has been estimated to be about 1.4 day^{-1} or 2 divisions per day, assuming that half the daily production occurs during the period of incubation (1000 to 1400 hrs).

Before the resulting time series of phytoplankton carbon can be used to drive the zooplankton growth model, the question of vertical variation in phytoplankton density must be addressed. The only guide to this vertical variation is the chlorophyll data, as carbon estimates are only available as a 0 to 20m average. The chlorophyll data have been used here as a rough guide to relative concentrations of phytoplankton carbon at

different depths, although the likelihood of variations in the C : Chl a ratio with depth is recognised. The early part of the experiment was characterized by an intense diatom bloom at the surface which sank out as a concentrated layer as nutrients became locally depleted. Thus, maximum local concentrations of phytoplankton over this period were much greater than the 0-20m average. However, it will be assumed here that zooplankton saw the average carbon concentration in the enclosure over this period as this was already high enough to achieve almost maximum growth so that increasing the available food density further would not significantly affect the conclusions reached here.

From day 22 on, Chl a concentrations are low and relatively uniform over the top 12m, decreasing slowly below this level, while phytoplankton growth rates are high (greater than 1 day^{-1}) in the top 8m but are much lower and apparently light limited below this depth. These high growth rates are apparently matched by high clearance rates on the part of the zooplankton (Sonntag and Parsons,1979). If these clearance rates were evenly distributed over the water column, the phytoplankton population below 8m would be subject to a very high net loss rate. This is inconsistent with the persistence of phytoplankton below 8m, given the small chlorophyll gradients and low mixing rates (Steele and Farmer,1977) observed in the enclosure. It is therefore assumed that, after day 22, grazing occurs predominantly in the top 8m and the concentration of phytoplankton carbon there, obtained using the average carbon for the enclosure and the variation of Chl a with depth, is used as available food. The time series of food density obtained in this

way and now used to drive the zooplankton model is also given in Fig 64.

While the aim here is to estimate parameters in the zooplankton model described above by fitting it to the time series of observations from CEE5, it is clear that not all the parameters can be estimated in this way. For example, the transition weights, W_J, must be specified as a characteristic of the species in question : their values determine the species size and the estimated growth rates. For each of the three principal zooplankton species present in the enclosure, I will therefore begin with a review of literature-established values for the parameters, indicating those which are well-established and those which are uncertain. The model will then be fitted to the data and the resulting parameter estimates discussed in terms of their relation to the literature values and the degree of confidence which the estimation procedure might lead us to place in them.

The objective fitting of the model to the data is made possible here by the application of the non-linear systems identification technique described in Benson(1978) and Parslow et al (1979). Briefly, the procedure involves making an initial guess at the parameter values and iteratively reducing the sum of squares of errors between predictions and observations using a non-linear optimisation algorithm. The Marquardt technique (Marquardt,1963) has been used here and its implementation in this case is relatively straight-forward with one exception. The model as described above uses weight thresholds to assign day classes to observed stage groups; that is

$$Y_J(t) = \sum_i Z_i(t).\phi_J(W_i(t))$$

where the ϕ_J, defined above, are step-functions. As a result, while $W_i(t)$ and $Z_i(t)$ are differentiable functions of the parameters through the system equations 5.1, the predicted densities in stage groups, $Y_J(t)$, are discontinuous functions of the parameters. The Marquardt technique requires that the derivatives of predictions with respect to parameters be calculated, and cannot be used under these circumstances. This problem has been overcome by replacing the step-functions ϕ_J by smooth functions ψ_J defined by

$$\psi_J(W) = (\mathrm{erf}(W-W_J)/(\sigma.W_J) - \mathrm{erf}(W-W_{J+1})/(\sigma.W_{J+1}))/2.$$

Here, σ is a small parameter which controls the spread of ψ_J about W_J and W_{J+1} (Fig 65). As σ approaches 0, $\psi_J(W)$ approaches $\phi_J(W)$. A value of $\sigma = 0.1$ was used here and found to allow reasonable convergence of the iterative scheme while leading to predictions, for a given set of other parameters, which were more or less indistinguishable from those obtained using thresholds.

5.3 Estimation results.

The application of the estimation scheme will now be discussed for each of the dominant copepod species in CEE5 in turn.

A Pseudocalanus minutus

This species has been the subject of a number of laboratory and field studies. (eg Parsons et al ,1969; Poulet,1973;

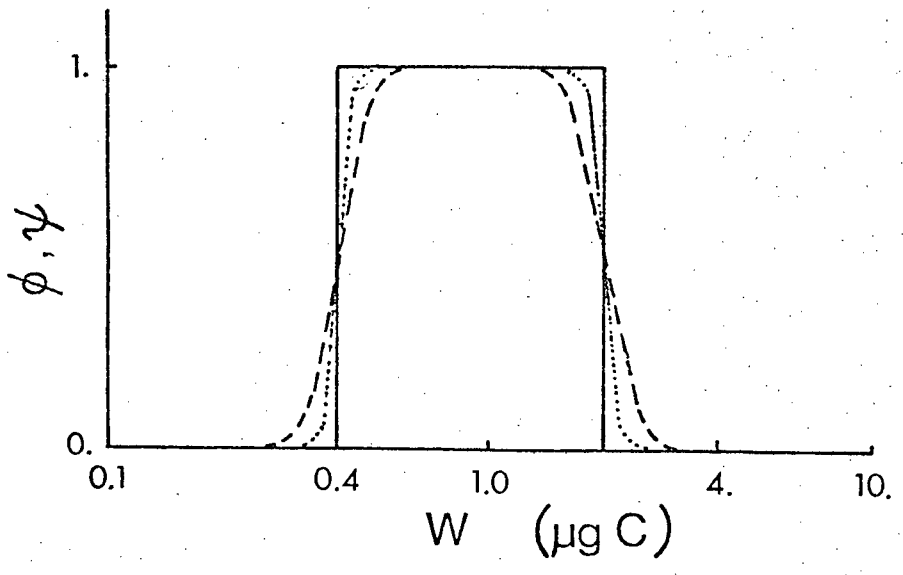

Figure 65. $\phi_J(W)$, $\psi_J(W)$ for W_J=0.4 µg C, W_{J+1}=2.0 µg C. (Solid line is $\phi_J(W)$, dashed line is $\psi_J(W)$ with σ = 0.2, dotted line is $\psi_J(W)$ with σ = 0.1.)

Ikeda,1976). However, most of these have dealt with behaviour over short time periods or only at late life-history stages. I have relied heavily here on the results of Paffenhoffer and Harris(1976) for another species, Pseudocalanus elongatus, based on long-term laboratory cultures. According to Frost(1979), the two species are quite similar.

The transition weights $W_1,\ldots,W_4$ have been taken from Paffenhoffer and Harris(1976) as 0.08, 0.4, 2.0 and 8.0 µg C/individual respectively. The first and last are in good agreement with values given by Frost(1979) for Pseudocalanus minutus. Maximum exponential growth rates (Cn-F in the model used here) were found to be significantly higher for stages CI to CIII than for other stages (about 0.3 day^{-1} compared with 0.18 day^{-1}). However, no significant overall relationship was found between ingestion per unit body weight and weight itself. Paffenhoffer and Harris cultivated P. elongatus at 4 different densities of a moderately sized diatom (Thalassiosira rotula, 20-22 µm diameter). While estimates of a half-saturation constant D could be obtained for any particular copepod weight from their graphs of clearance rate or ingestion rate versus body weight for each food density, the scatter in their data results in high uncertainty in estimates of D. For example, the graphs in Fig 66 are based on the same data set but one uses Paffenhoffer and Harris's regression lines through their clearance rate vs weight data while the other is based on their average ingestion rates per unit body weight for different food concentrations. The first yields a value for D less than 15 µg $C.l^{-1}$ (for an individual of 10 µg dry weight) while the second gives a value

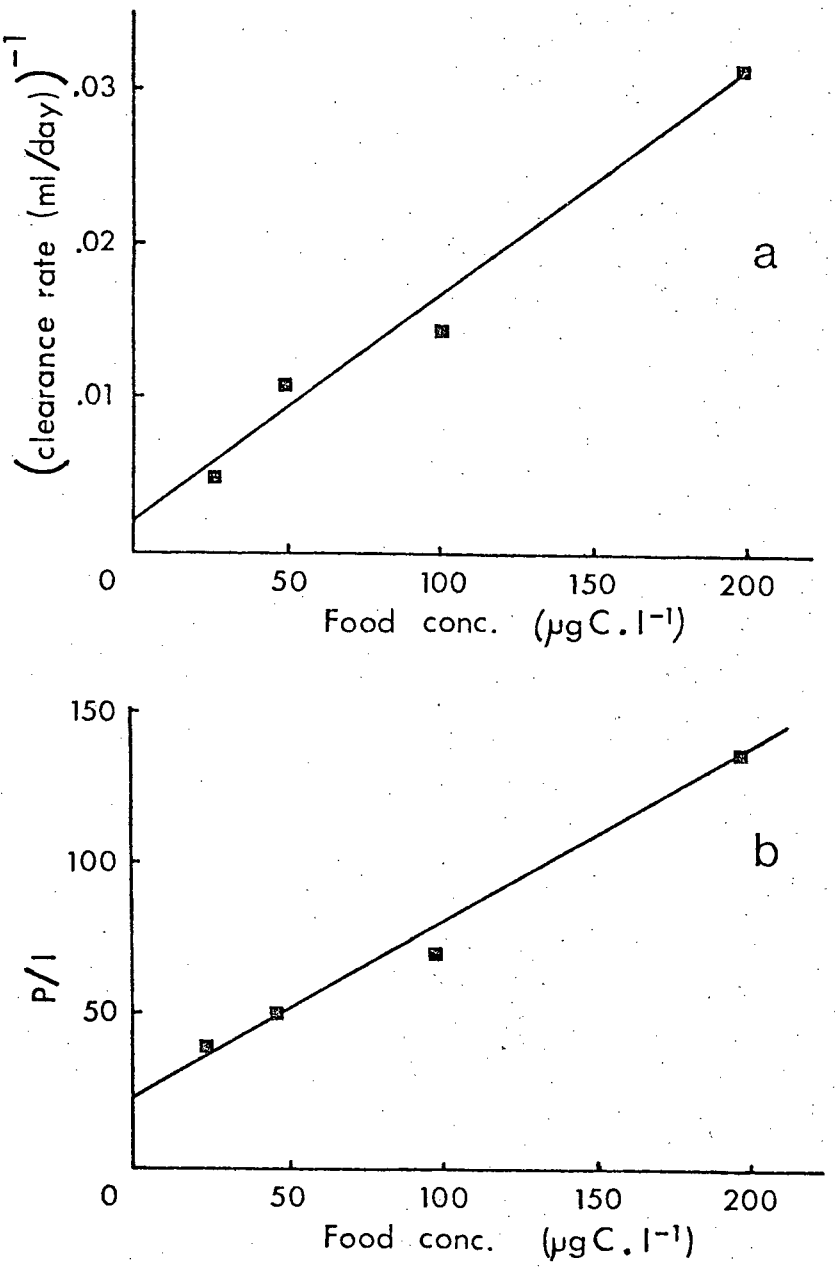

Figure 66. (a) (Clearance rate)$^{-1}$ vs food concentration (P) for 10 μg dry weight Pseudocalanus (from Fig 3, Paffenhoffer and Harris, 1976). Line : Ingestion = 0.69.P/(12.6+P) (μg C.day^{-1}).

(b) (Food concentration P)/(% body weight ingested per day) vs food concentration (Paffenhoffer and Harris,1976). Line: % body weight ingested per day = 181.P/(41.+P).

greater than 40 μg $C.l^{-1}$.

An estimate of basal metabolic rate in Pseudocalanus might be obtained from the data of Paffenhoffer and Harris by looking for a decrease in gross growth efficiency with decreasing food concentrations. Yet, their results suggest, if anything, an increase in gross growth efficiency down to the lowest food concentration they used. On the other hand, measurements of oxygen consumption by small copepods in the absence of food suggest basal metabolic rates as high as 0.04 to 0.11 day^{-1} (Marshall,1973; Ikeda,1977).

Paffenhoffer and Harris(1976) found that, at a food concentration of 115 μg $C.l^{-1}$, naupliar production could continue in P. elongatus for as long as 35 days, with average production over the first 15 days being about 4 per female per day (from their Fig 6). Under the assumptions of our model, such a production rate requires an efficiency X of 0.2 for females or 0.1 for a 50:50 male:female ratio.

The observations of densities of P. minutus in CEE5 are shown in Fig 67. An anomalous feature is the appearance of large numbers of adults on day 19 with no sign of any cohort in CI-III or CIV-V before this day. If the data were accurate, they would imply the passage of these individuals from NVI to CVI in less than 3 days which is quite impossible according to the results of Paffenhoffer and Harris(1976) and references cited therein. It will be assumed here that the adults observed in the enclosure were present from day 1 and that the earlier copepodite stages are due to the production of nauplii by adults during the initial phytoplankton bloom. Only the CI-III and CIV-V time series will

Figure 67. Observed densities of Pseudocalanus in CEE5. Error bars represent 95% confidence limits based on Poisson sub-sampling statistics.

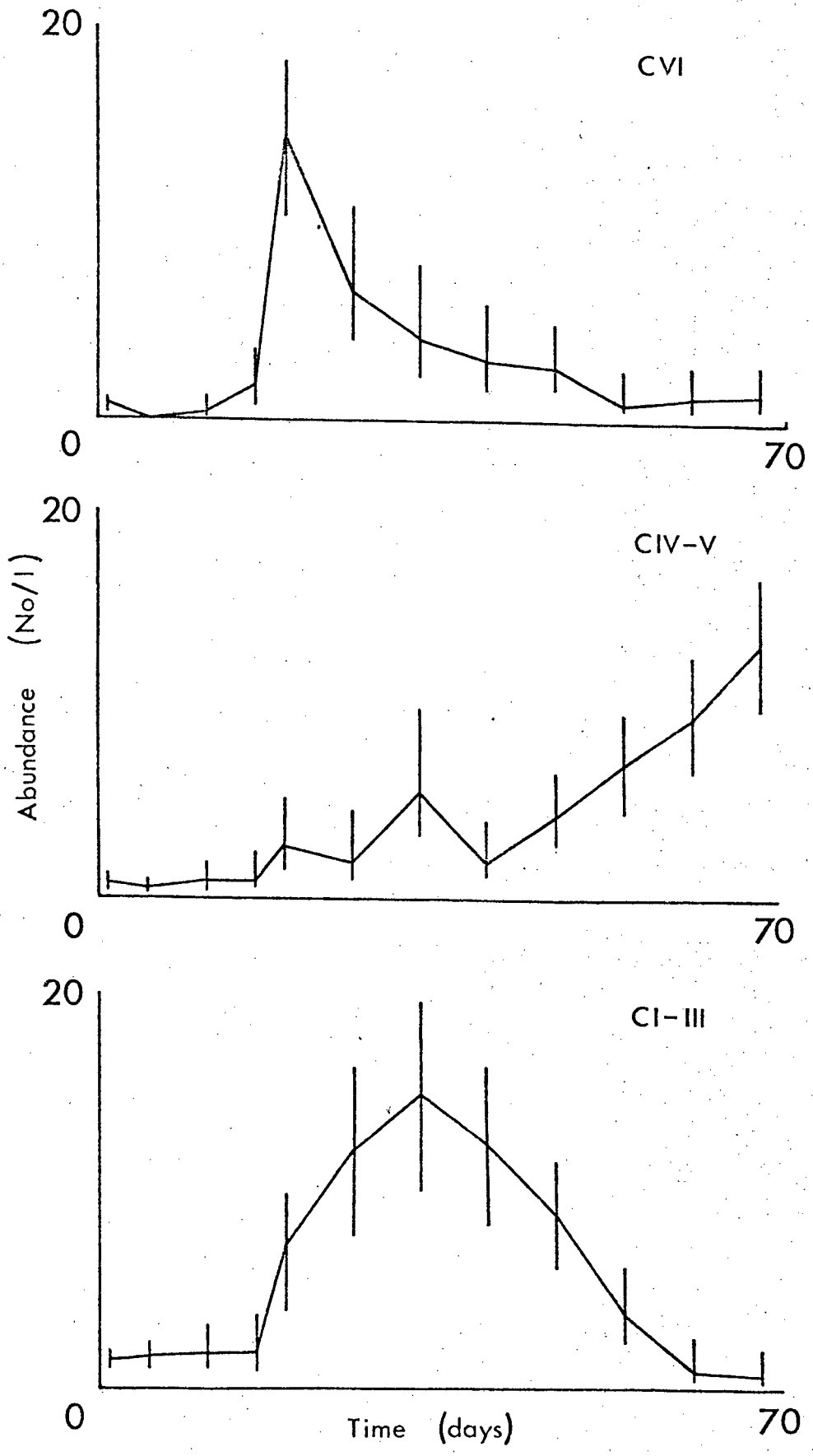
20
CVI
0
70
20
CIV-V
Abundance (No/l)
0
70
20
CI-III
0
Time (days)
70

be fitted.

The error bars drawn in Fig 67 and in the corresponding figures for the other species represent 95% confidence intervals based solely on the sub-sampling statistics. A relatively small proportion of the sample taken on each day was counted and the raw counts are assumed to be Poisson distributed with a mean fixed by the true concentration in the original sample. This does not take into account the degree to which concentrations in the pumped sample are representative of the populations in the enclosure; this question has been addressed by Lawson and Grice (1977).

The following parameters were not estimated but fixed on the basis of the references discussed above. The transition weights W_J were taken as 0.08, 0.4, 2.0 and 8.0 μg C/ind. The reproductive efficiency was taken as 0.1 but, as the initial number of reproductive adults was estimated, this did not fix the naupliar recruitment. The estimation results for P. minutus can be divided into two categories. The first were obtained by assuming that growth and mortality parameters were constant across stages. Some justification for this can be found in Paffenhoffer and Harris's ingestion data.

The initial trial with all parameters free converged very slowly. This slow convergence was due primarily to the inability of the model to distinguish between different values of the basal metabolic rate F on the basis of these observations. When F was fixed at each of three different values, 0.0, 0.03, 0.10, convergence was rapid and direct and a unique optimum with a low SSQ was obtained in each case. The three resulting parameter

sets and the corresponding SSQ are given as Trials 1, 2 and 3 in Table VIII; the predictions and observations for Trial 1 are given in Fig 68a. It can be seen from Table VIII that the lowest SSQ is obtained for F = 0.0 but that the increase in SSQ for F = 0.03 or F = 0.1 is very small. As F is increased, the technique maintains a good fit to the observations by increasing Cn and decreasing D. Note that the maximum exponential growth rate, Cn-F, is roughly constant as F changes (0.13 to 0.14 day^{-1}), but somewhat lower than that found by Paffenhoffer and Harris(1976). The principal effect of increasing F is to alter D but the values of D are all within the range calculated above from Paffenhoffer and Harris's data.

The second set of estimates was obtained by multiplying the growth rate for CI-III by a factor 1.7, following Paffenhoffer and Harris's observations of higher growth rates in these stages. The parameters Cn, D, θ, and the initial number of adults were again estimated for F = 0.0, 0.03 and 0.10 day^{-1}. As before, convergence was rapid and direct in all cases and the resulting parameter estimates and minimum SSQ are given as trials 4, 5 and 6 in Table VIII. The SSQ are slightly lower than for the first set (Table VIII,Fig 68b) and now decrease as F increases although the change with F is again small. The parameter Cn changes little with the introduction of the 1.7 growth factor and the major effect is a large increase in D. This behaviour is easy to understand as the growth of nauplii in the enclosure takes place primarily at high food concentrations, fixing the maximum growth rate, while the growth of CI-III takes place at low food concentrations, fixing the value of D.

Table VIII.

Final parameter estimates and corresponding SSQ errors for Pseudocalanus. (Subscripts 1...4 refer to stage groupings NI-VI, CI-III,CIV-V,CVI respectively. A '"' means that the parameter value is fixed at the value given for the stage group above; an asterisk means that the parameter value is fixed, not estimated.)

Parameters	Trials					
	1	2	3	4	5	6
Cn_1	.14	.16	.23	.16	.18	.24
Cn_2	"	"	"	.28	.30	.41
Cn_3	"	"	"	.16	.18	.24
Cn_4	"	"	"	"	"	"
D_1	34.	20.	9.9	72.	34.	16.
D_2	"	"	"	"	"	"
D_3	"	"	"	"	"	"
D_4	"	"	"	"	"	"
F_1	.00*	.03*	.10*	.00*	.03*	.10*
F_2	"	"	"	"	.05*	.17*
F_3	"	"	"	"	.03*	.10*
F_4	"	"	"	"	"	"
θ_1	.01	.01	.01	.01	.01	.01
θ_2	"	"	"	"	"	"
θ_3	"	"	"	"	"	"
θ_4	"	"	"	"	"	"
Init. adults	1.84	1.85	1.86	1.93	1.94	1.88
SSQ	74.	75.	77.	66.	63.	60.

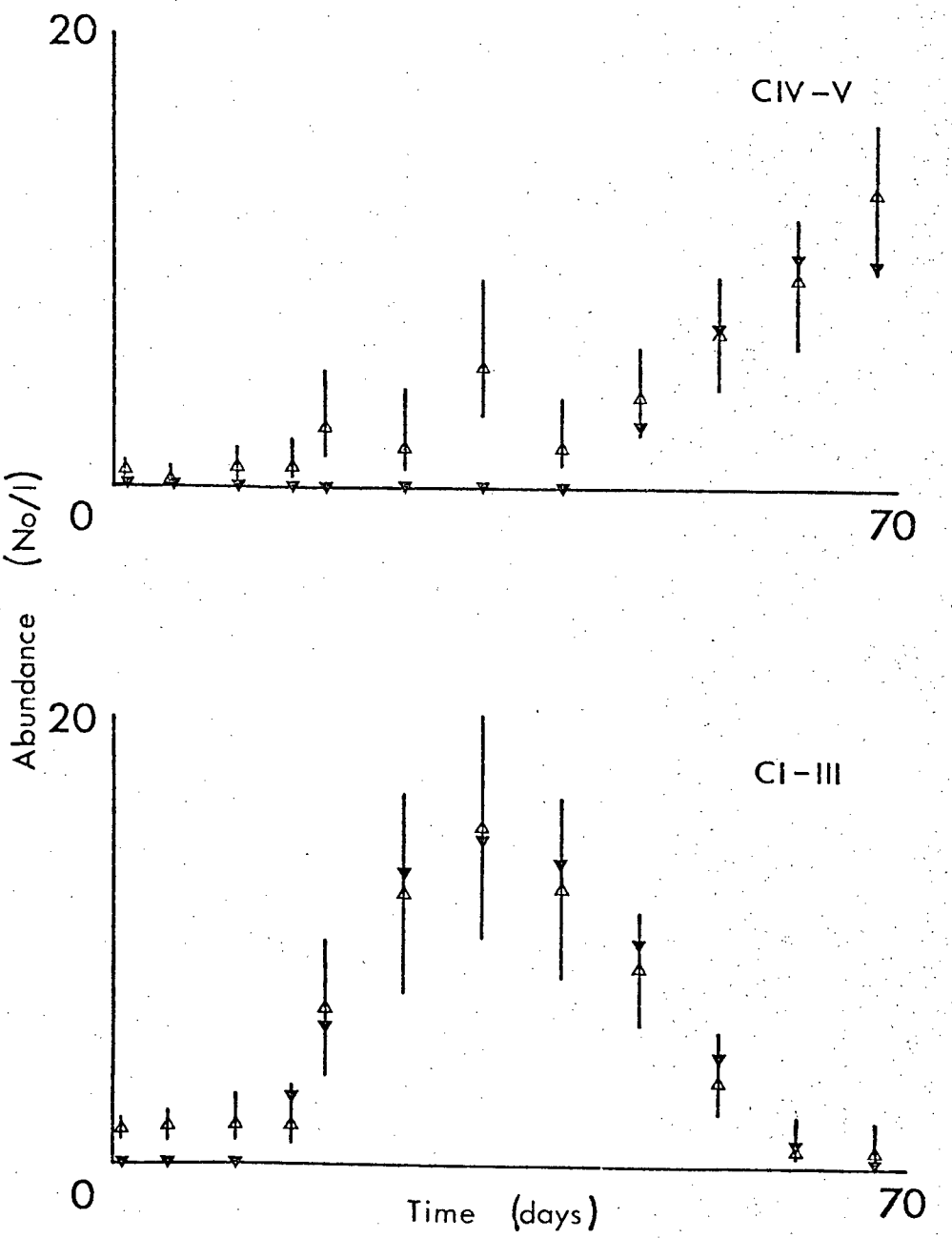

Figure 68a. Comparison of predictions (solid symbols) and observations (open symbols) for Pseudocalanus (trial 1).

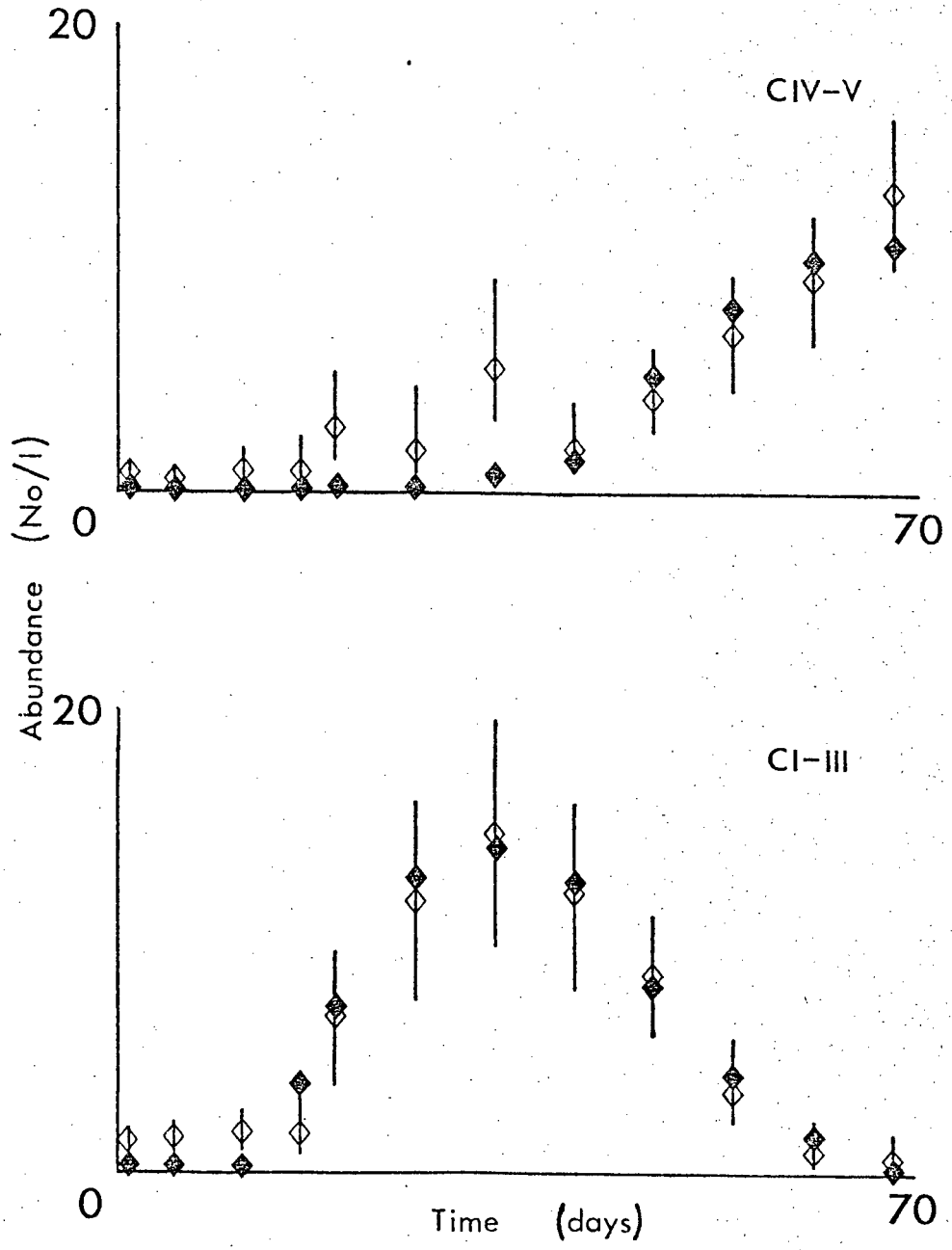

Figure 68b. Comparison of predictions (closed symbols) and observations (open symbols) for Pseudocalanus (trial 6).

The estimated initial number of adults required to produce the cohort is relatively constant across all trials, lying between 1.78 and 1.96 per liter. This estimate is of course inversely proportional to the assumed efficiency of production, X. The low value of Θ is also worthy of comment. There appears to have been little or no increase in mortality rate as a result of the low food concentrations. Note that this mortality rate has been assumed constant across stages and is really determined by observations of CI-V. It is entirely possible that mortality rates of nauplii in the enclosure were higher than those of copepodids, as found by Paffenhoffer and Harris(1976) in laboratory cultures, but without observations on Pseudocalanus nauplii alone, it is impossible to estimate a naupliar mortality rate.

B Calanus pacificus

Calanus pacificus (helgolandicus) is the largest of the three dominant calanoid copepods in CEE5. It has been the subject of a large number of laboratory and field studies (Paffenhoffer,1970,1971,1976; Mullin and Brooks,1970; Frost,1972,1975,1979; Runge,1980), being one of the best-studied of marine pelagic copepods.

The transition weights W_J have been taken from Paffenhoffer(1971) as 0.1, 1.0, 10., 70. µg C per individual respectively. The fact that C. pacificus grows through a much greater weight range than P. minutus in roughly the same generation time has been commented on by Frost (1979) and the maximum exponential growth rates reported by Paffenhoffer(1976) explain this, being 0.41, 0.41, 0.33 and 0.2 for nauplii, CI-III,

CIII-V and CV to young adult respectively. These are almost twice those found for P. elongatus.

This large ratio of adult to naupliar weight is also reflected in the fecundity of C. pacificus females which maintained a production rate of about 40 eggs per female per day over 40 to 50 days at high food concentrations (Paffenhoffer,1976). Under the assumptions of the model, a reproductive efficiency of about 0.28 for females or a value of X of 0.14 for a 1:1 sex ratio is required to produce this fecundity.

The results of Paffenhoffer(1970,1971) and Frost(1972) emphasize the dependence of the half-saturation constant, D, on the type and particularly the size of the phytoplankton cells offered as food. Paffenhoffer's (1970,1971) long-term culture studies were designed to look at the effect of food type rather than food density on growth, but when two concentrations of one food type (50 and 100 $\mu g\ C.l^{-1}$ of the diatom Lauderia borealis) were used, clearance rates per unit body weight were only about 1.2 times as high at the lower density, suggesting that D for ingestion is rather large. Frost's (1972) grazing experiments using adult females also suggested rather high values of D ranging from about 50 to 150 $\mu g\ C.l^{-1}$. (Frost's data were fitted to a rectilinear rather than a curvilinear functional response but the two models could not be distinguished statistically (Mullin et al ,1975) and it is exceedingly unlikely that they could be distinguished on the basis of the time series fitted here. I have therefore continued to use the curvilinear form for consistency.) Runge(1980) found higher clearance rates and

consequently lower values for D in C. pacificus than Frost reported, although he indicates that these may have been due to pretreatment effects. His results suggest values of D as low as 15 μg $C.l^{-1}$ for the largest cell size used. If average exponential growth rates over NI to CIV are calculated from the data of Mullin and Brooks(1970), the results (Table IX) suggest that D for growth lies well below 19 μg $C.l^{-1}$ for Gymnodinium and below 49 μg $C.l^{-1}$ for Thalassiosira. It is again impossible to estimate basal metabolic rates from the laboratory culture results as gross growth efficiency appears to decrease rather than increase with increasing food concentration (Mullin and Brooks,1970). Estimates of oxygen consumption by late stages of copepods in the size range of C. pacificus suggest low respiration rates of order 0.03 day^{-1} (Marshall,1973; Ikeda,1977). Mortality rates in culture were found to be markedly dependent on food density (Paffenhoffer,1970) and to be highest for nauplii. There is a possible complication in the CEPEX enclosures as the late stages of C. pacificus are strong vertical migrators in the wild (Mullin and Brooks,1970) and may not be able to survive in the enclosures at any food concentration.

The time series of observed C. pacificus densities in CEE5 are shown in Fig 69. Adults were not observed after day 1. In attempting to fit the model to this data set, the transitional weights were set at 0.1, 1., 10. and 70. μg C/ind. and the efficiency X at 0.14. Again the initial number of adults present was estimated and adults were assumed to produce eggs for only 4 days as they were not observed on day 5.

Table IX.

Exponential growth rates for *Calanus* over NI to CIV at 12°C and different concentrations of *Gymnodinium* and *Thalassiosira* (calculated from Table 3 and Fig 2, Mullin and Brooks, 1970).

Gymnodinium						
Food concentration ($\mu g\ C.l^{-1}$)	19.	23.	54.	78.	271.	318.
Growth rate (day^{-1})	.24	.19	.26	.30	.33	.33

Thalassiosira						
Food concentration ($\mu g\ C.l^{-1}$)	49.	63.	165.	205.	750.	750.
Growth rate (day^{-1})	.25	.25	.29	.31	.31	.34

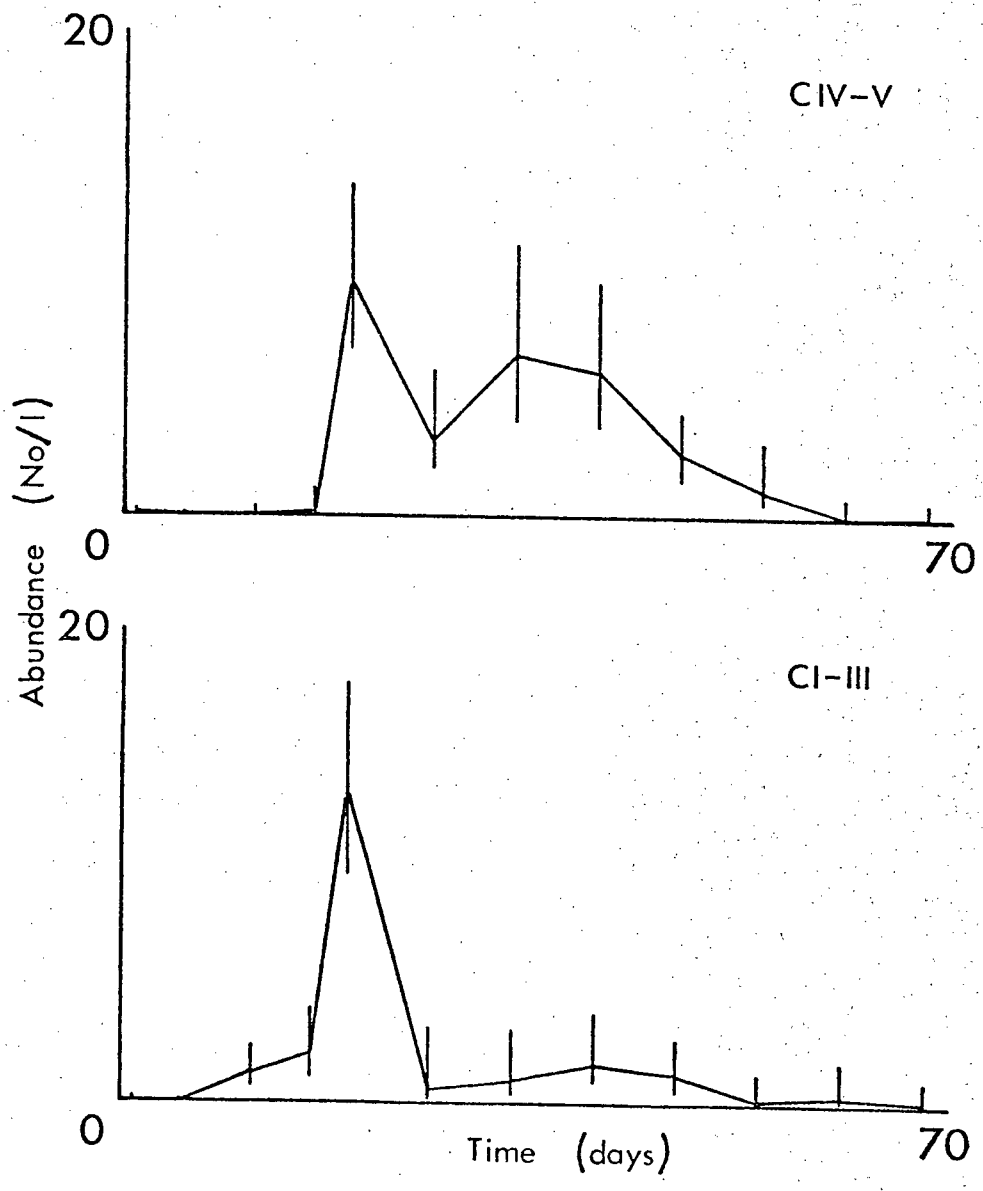

Figure 69. Observed densities of Calanus in CEE5.

(Error bars as in Fig 67.)

In the initial trial, growth rates in NI-VI, CI-III, CIV-V and CVI were assumed to follow a fixed ratio 1:1:0.8:0.5 and the half-saturation constant, D, was assumed to be constant across stages. The resulting best fit was rather unrealistic; in particular, adults appeared from day 47 on. To prevent this, the half-saturation constant D for CIV-V was increased to a high level of 100 $\mu g\ C.l^{-1}$. This rather ad hoc action was based on the observation that the phytoplankton population when CIV-V were present consisted of small flagellates for which, on the basis of Frost's (1972) results, the late stages of C. pacificus might be expected to have low clearance rates. However, any change in the growth parameters of stages CIV-V which prevented them from reaching CVI would result in equally good agreement between predictions and observations.

With the new value of D_{IV-V}, the algorithm converged rapidly to the parameter set and SSQ given in trial 1, Table X. The final SSQ is rather high and the comparison of predictions and observations in Fig 70a shows why: the model is unable to reproduce the sharp coincident rise in CI-III and CIV-V on day 19 and compromises with a smaller and earlier increase in CI-III and a later increase in CIV-V. The parameter estimates of Cn and D are lower than the literature values discussed above. As in the case of Pseudocalanus, the SSQ is entirely insensitive to the value of the basal metabolic rate F; when F is fixed at 0.0 or 0.08, the same SSQ is obtained, (trials 2 and 3, Table X). Higher values of F are compensated for by increases in Cn and slight decreases in D.

The reason for the comparatively poor fit here is that the

Table X.

Final parameter estimates and corresponding SSQ errors for Calanus.

(Subscripts 1...4, '"' and '*' as in Table VIII.)

Parameters	Trials							
	1	2	3	4	5	6+	7+	8+
Cn_1	.26	.24	.32	.18	.20	.26	.25	.24
Cn_2	"	"	"	.31	.34	"	.43	.41
Cn_3	.21	.19	.26	.14	.16	.21	.20	.19
Cn_4	.13	.12	.16	.09	.10	.13	.12	.12
D_1	9.5	10.6	7.3	0.0	10.0*	8.6	0.0	10.0*
D_2	"	"	"	"	"	"	"	"
D_3	100.*	100.*	100.*	100.*	100.*	100.*	100.*	100.*
D_4	9.5	10.6	7.3	0.0	10.0*	8.6	0.0	10.0*
F_1	.020	.000*	.080*	.020*	.015	.023	.022	.000
F_2	"	"	"	"	.024	"	.037	.000
F_3	.016	.000*	.064*	.016*	.012	.018	.018	.000
F_4	.010	.000*	.040*	.010*	.007	.012	.011	.000
θ_1	.030	.030	.030	.054	.047	.056	.107	.081
θ_2	"	"	"	"	"	"	"	"
θ_3	"	"	"	"	"	"	"	"
θ_4	"	"	"	"	"	"	"	"
Init. adults	.23	.23	.23	.84	.60	.62	2.3	1.2
SSQ	195.	195.	195.	130.	152.	124.	75.	86.

\+ In these trials, observations on day 16 were ignored.

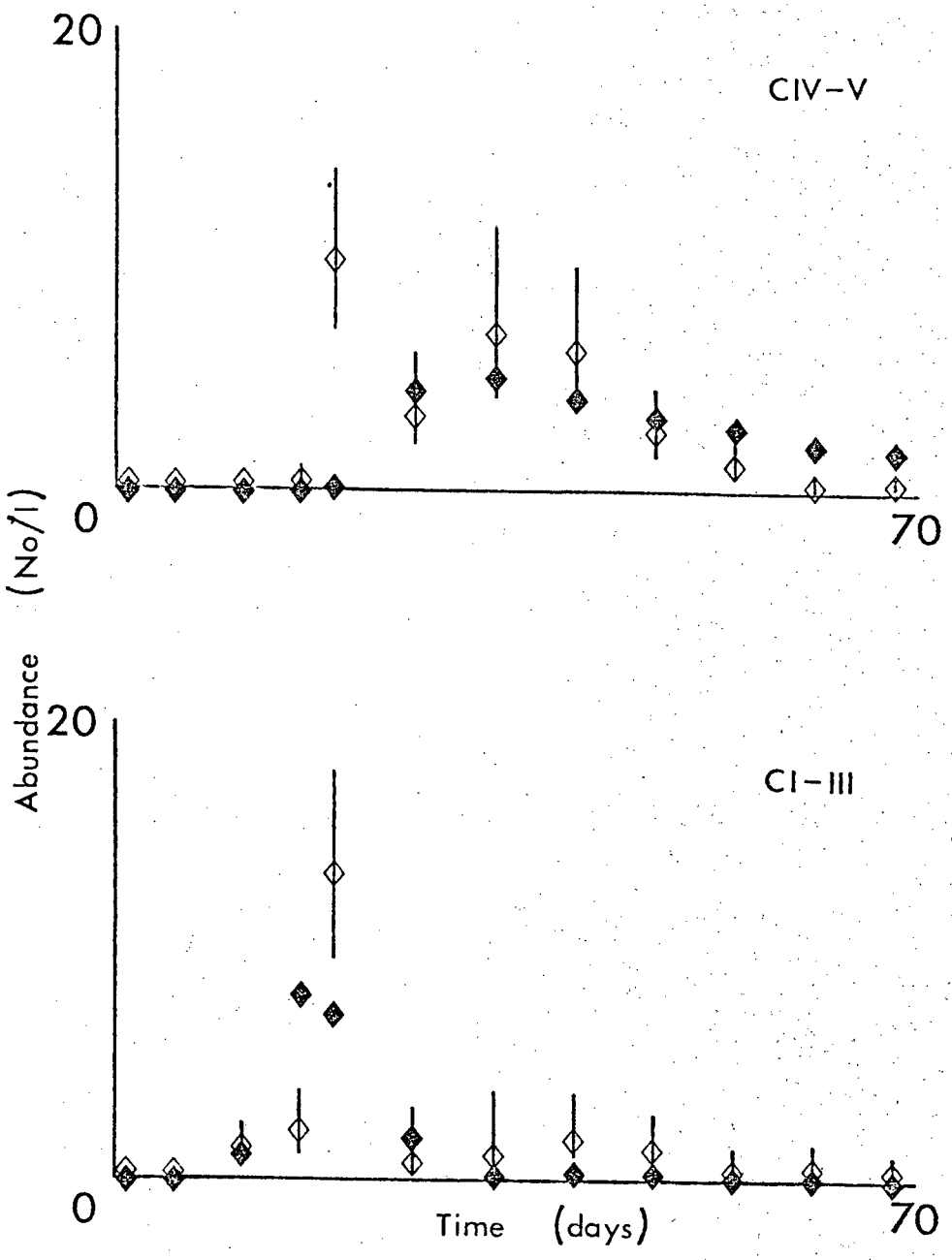

Figure 70a. Comparison of predictions (solid symbols) and observations (open symbols) for Calanus (trial 1).

observations are inconsistent with the known growth characteristics of C. pacificus . The data suggest that, over a period of apparently high food density, C. pacificus nauplii took more than 16 days to reach CI, yet almost half of these reached CIV by day 19 at lower food concentrations. This is impossible if growth rates in NI-VI are as high as those in CI-III at the same food concentrations. In fact, an individual reaching CIV from NVI in 3 days would have to grow at an exponential rate exceeding 0.77 day^{-1}, almost twice the maximum reported from laboratory cultures with abundant food.

If we are prepared to concede a higher maximum growth rate in CI-III than in NI-VI, a considerably better fit can be obtained. For example, if the factor 1.7 for CI-III over NI-VI, used for Pseudocalanus, is introduced, a considerable reduction in minimum SSQ is possible (trial 4, Table X). It can be seen from Fig 70b that the resulting increase in growth rate during CI-III has allowed the model to eliminate the early increase in CI-III and to match the peak density on day 19 more closely. The model is still unable to produce an increase in CIV-V by day 19, not surprisingly, and the algorithm forces D towards zero in an effort to do so. A similar fit, with a somewhat higher SSQ, can be obtained with D frozen at 10 μg $C.l^{-1}$ (trial 5, Table X). The final value of Cn implies a maximum growth rate for NI-NVI of 0.16 day^{-1} and for CI-III of 0.27 day^{-1}, still well below the maximum found by Paffenhoffer(1976).

Unless we are willing to allow unreasonably high growth rates for stages CI-III, the model must either predict an increase in CI-III before day 19 or an increase in CIV-V after

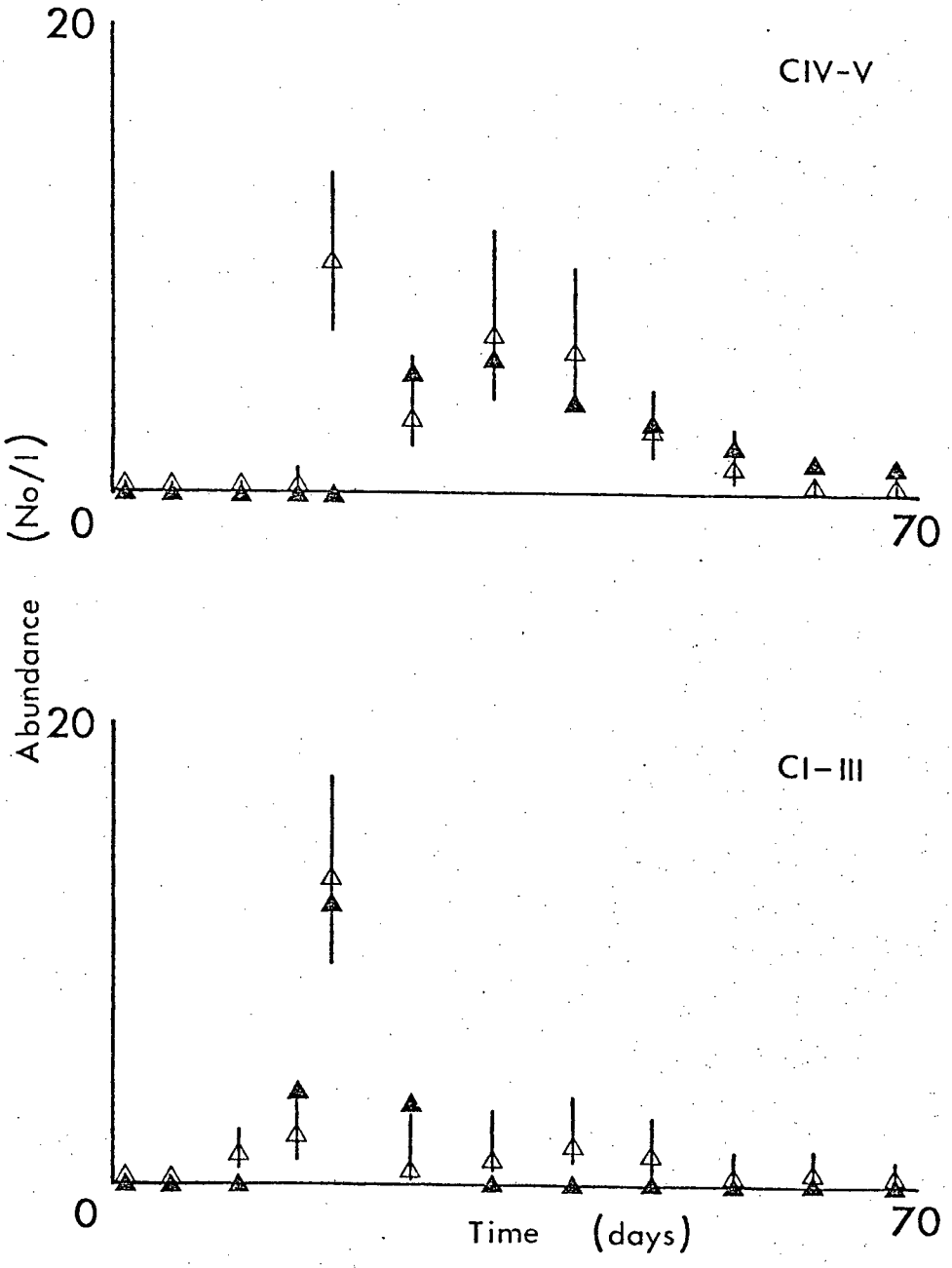

Figure 70b. Comparison of predictions (solid symbols) and observations (open symbols) for Calanus (trial 4).

day 19. Faced with the entire set of observations, the algorithm 'chooses' to do the latter. However, the observation of low CI-III on day 16 may be more open to question as a sample of part of the bag was lost. In trial 6, the observations on day 16 are omitted and the 1:1 ratio between maximum growth rates in NI-VI and CI-III is returned to. The model is still unable to achieve an increase in CIV-V by day 19 (Fig 70c). To do so, nauplii must still take at least 11 days to reach CI-III and less than 8 days subsequently to reach CIV-V, at lower food concentrations. Reintroducing the factor 1.7 and neglecting the observations on day 16 allows for the first time an increase in CIV-V on day 19 (Fig 70d) and a significant reduction in SSQ (trial 7, Table X). Again the algorithm tends to make D zero; on freezing D at 10 μg $C.l^{-1}$, a similar fit with a slightly higher SSQ can be obtained (trial 8, Table X). The maximum growth rates for NI-VI and CI-III from trial 8 are 0.24 and 0.41 day^{-1} respectively. The former is, of course, low but the second agrees rather well with the maximum rates reported by Paffenhoffer(1976).

We are therefore led to the following conclusions. It is impossible for the growth model to reproduce the observations of C. pacificus without using much higher growth rates than are reasonable. To make sense of the data, it must be assumed that either the low observation of CI-III on day 16 or the high observation of CIV-V on day 19 is incorrect. In either case, a higher maximum growth rate in CI-III than in NI-VI and a low value of D is necessary to fit the remaining observations closely.

Especially in the later trials where the early rise in CIV-V

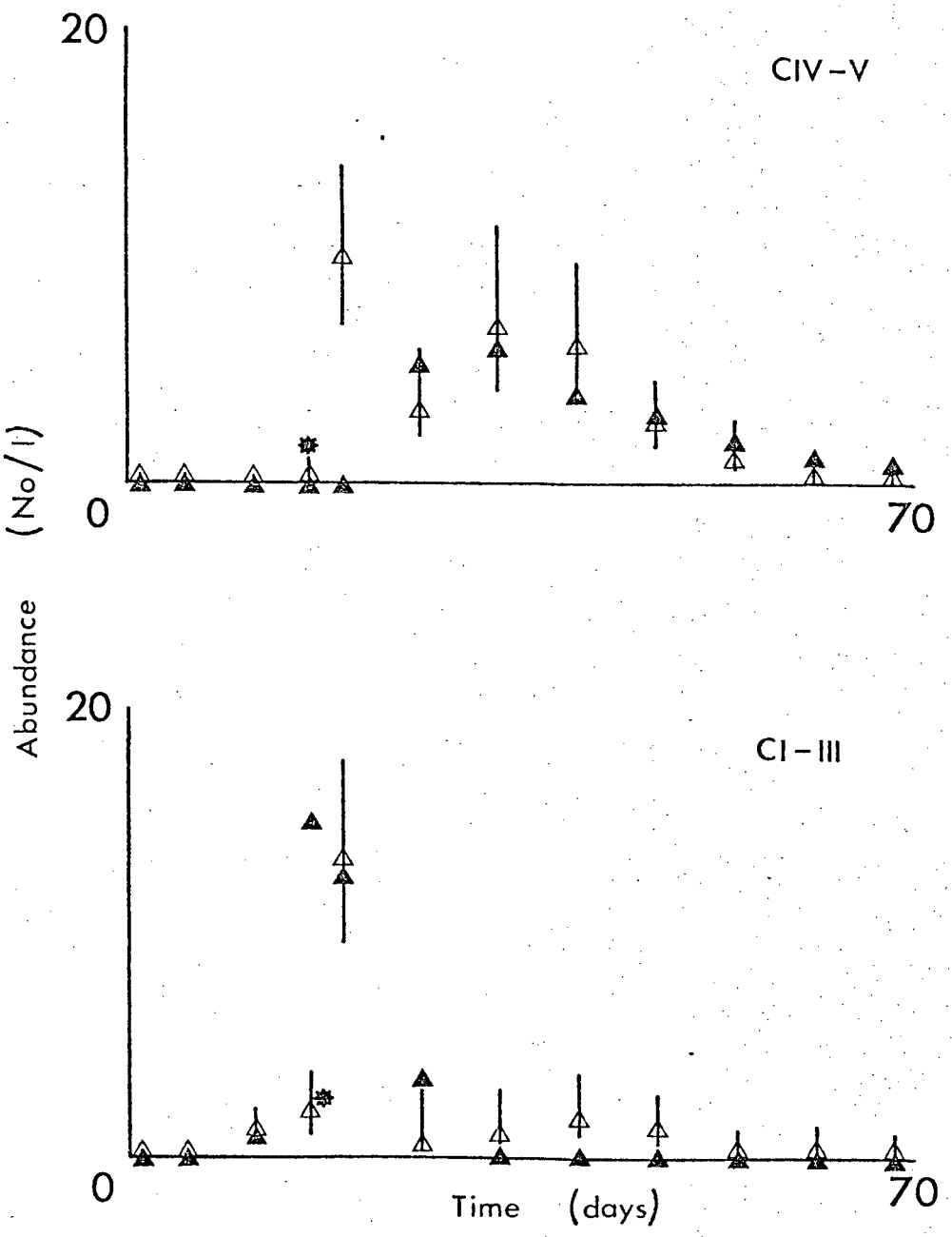

Figure 70c. Comparison of predictions (solid symbols) and observations (open symbols) for Calanus (trial 6). (* this observation not fitted.)

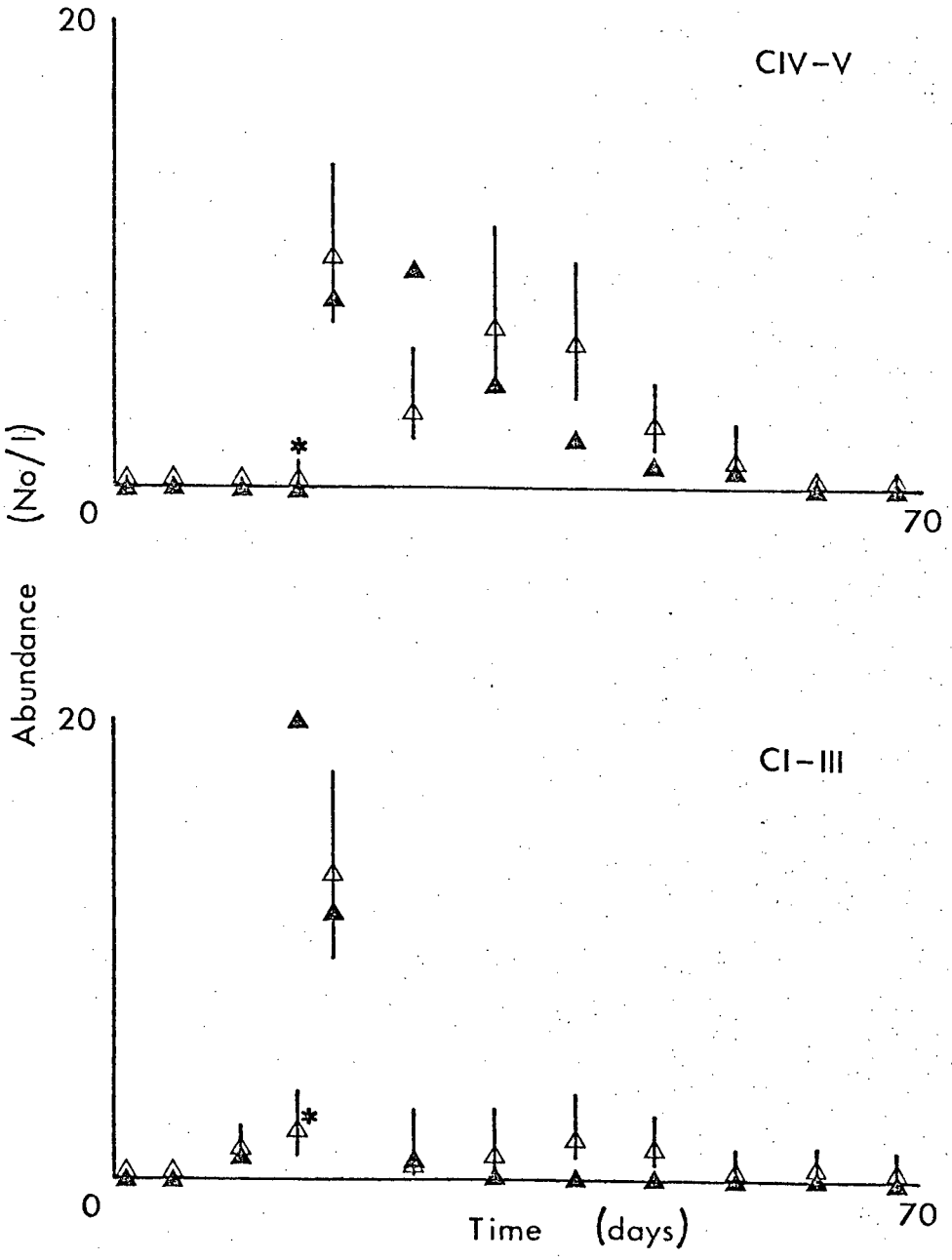

Figure 70d. Comparison of predictions (solid symbols) and observations (open symbols) for Calanus (trial 7). (* this observation was not fitted.)

is reproduced, a very high mortality rate (0.08 day^{-1}) is estimated. This is required to explain the rapid decrease in copepodite densities after day 19. The mortality rate has been assumed constant across stages but, as noted for Pseudocalanus, it is impossible to estimate mortality rates during the naupliar stages without observations of C. pacificus nauplii. In fact, there may be reasons to suspect lower mortality rates for nauplii. The copepodids, especially CIV-V, were exposed to low densities of small phytoplankton cells and Paffenhoffer's (1970) results suggest that this may have led to increased mortality rates. Attempts to migrate vertically in a shallow enclosure could also have contributed to higher mortality rates in the copepodids. Finally, the number of initial adults required to produce the cohort in trials 7 and 8 is several times that observed in CEE5 on day 1 : this number could be reduced without affecting the fit to the copepodids by decreasing the naupliar mortality rate.

C Paracalanus parvus

The third species here, Paracalanus parvus, is the smallest of the three and comparatively little is known of its feeding and growth dynamics. The major source of information known to the author is a recent laboratory and field study of feeding and egg production by adult females of Paracalanus (Checkley,1980). The weights of adult females and eggs have been taken from this study as 3.0 and 0.02 µg C/ind respectively. The transition weights for NVI to CI and CIII to CIV are not known and have been guessed to be 0.1 and 0.6 µg C/ind, roughly in keeping with the pattern of growth in the other two species. Paracalanus is intermediate

between Pseudocalanus and Calanus in terms of the ratio of adult female weight to weight of egg, but in maximum exponential growth rate, it appears to match or exceed Calanus pacificus, having an exceedingly short generation time of as little as 14 days (Sonntag and Parslow,1980). This corresponds to a maximum average exponential growth rate of 0.36 day^{-1}. The pattern of growth rate over stages is unknown.

The fecundity of Paracalanus females in response to food supply has been well studied by Checkley(1980), who found maximum rates of production of order 50 eggs/female day, again matching those of C. pacificus, although the duration of breeding in Paracalanus is unknown. The daily egg production represents more than 0.3 of the female body weight per day as compared with less than 0.1 for Pseudocalanus and Calanus. An efficiency X equal to 1.0 for females or 0.5 for a 1:1 sex ratio in adults is required in the model to reproduce this high fecundity.

Checkley found a consistent half-saturation constant for egg production of about 4 $\mu gN.l^{-1}$ or about 20 to 40 $\mu g\ C.l^{-1}$ depending on the C:N ratio of the phytoplankton. This was obtained for a diatom (Thalassiosira) and extrapolating it to the flagellates in CEE5 or to stages other than adult females might be difficult to justify. He also reported very low basal metabolic rates, about 0.01 day^{-1}, based on the relationship between ingestion and egg production. His 95% confidence interval for this parameter was rather wide, however, allowing values up to 0.12 day^{-1}. In a study of respiration in zooplankton, Ikeda(1977) found oxygen consumption by Paracalanus to drop to about 0.02 $\mu l.hr^{-1}$ after 3 days of starvation, giving

a 'basal' metabolic rate of about 0.08 day^{-1}. However, both ammonia excretion and dry weight loss suggested lower values, less than 0.03 day^{-1}.

While 'natural' mortality rates for Paracalanus have not been reported, Checkley emphasized the lack of lipid reserves in this small copepod and found that females could survive starvation for an average of 5 days only. Some sort of mortality response to low food densities might therefore be reasonably expected.

The time series of observed densities of Paracalanus copepodids in CEE5 are shown in Fig 71. The total density of nauplii in all species is also given in Fig 72. The transition weights W_J were set at 0.02,0.1,0.6 and 3.0 µg C respectively and the reproductive efficiency fixed at 0.5 as discussed above. A new feature of the Paracalanus data is that considerable numbers of adults are present later in the experiment; to prevent the production of nauplii by these adults in numbers much greater than those observed, it was found necessary to set the parameters controlling adult fecundity so that nauplii production ceased after about day 30. This was accomplished by setting Cn, D and F for adults equal to 0.4 day^{-1}, 80 µg $C.l^{-1}$ and 0.08 day^{-1} respectively. The fit to the data is more or less insensitive to the values taken by these parameters, provided they prevent late naupliar production, and they have been fixed rather than estimated.

In the initial series of trials, the observed cohort has been assumed to be due to an initial population of adults which produce nauplii beginning on day 1. In trial 1, all growth and

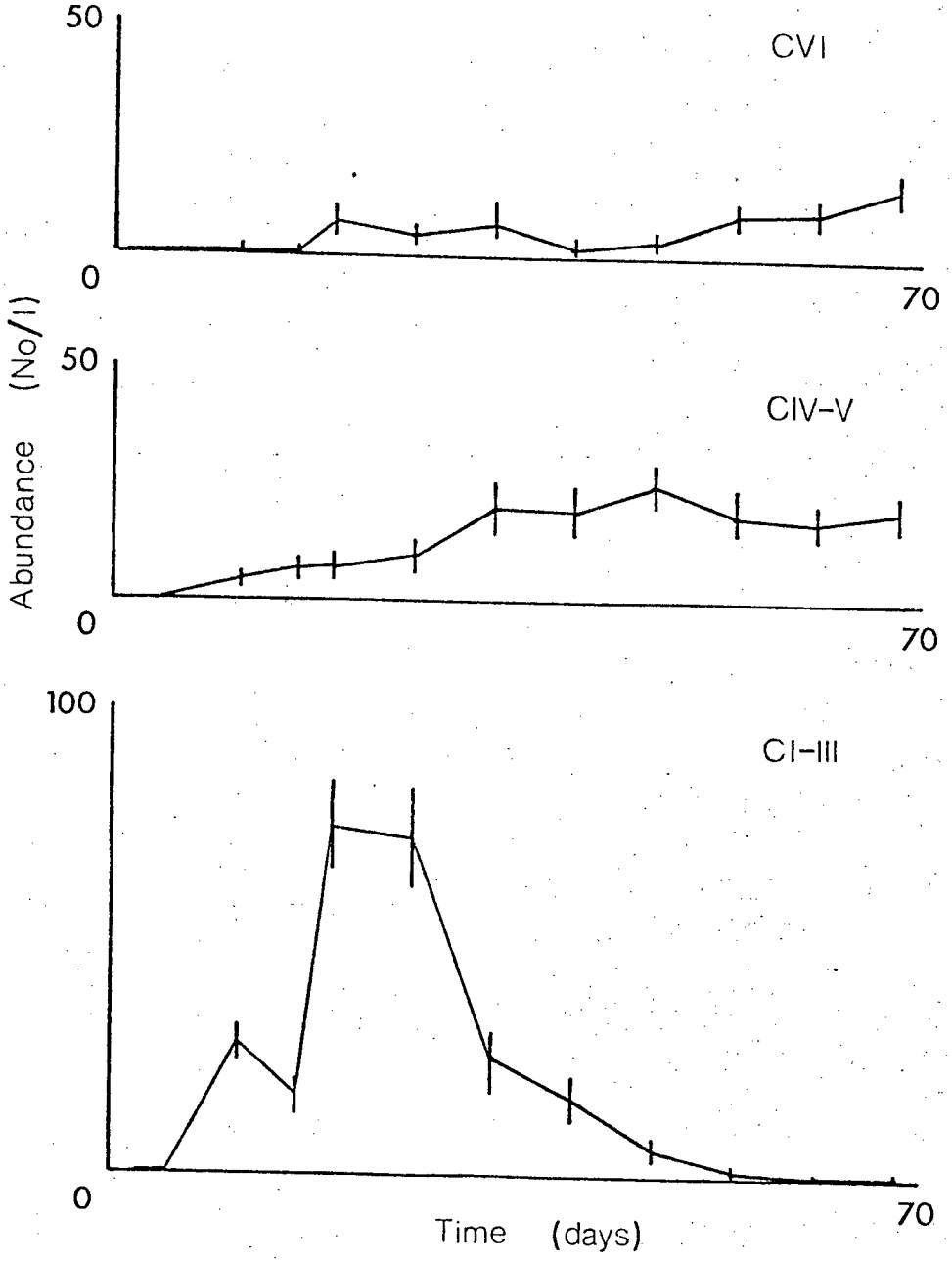

Figure 71. Observed densities of Paracalanus in CEE5. (Error bars as in Fig 67.)

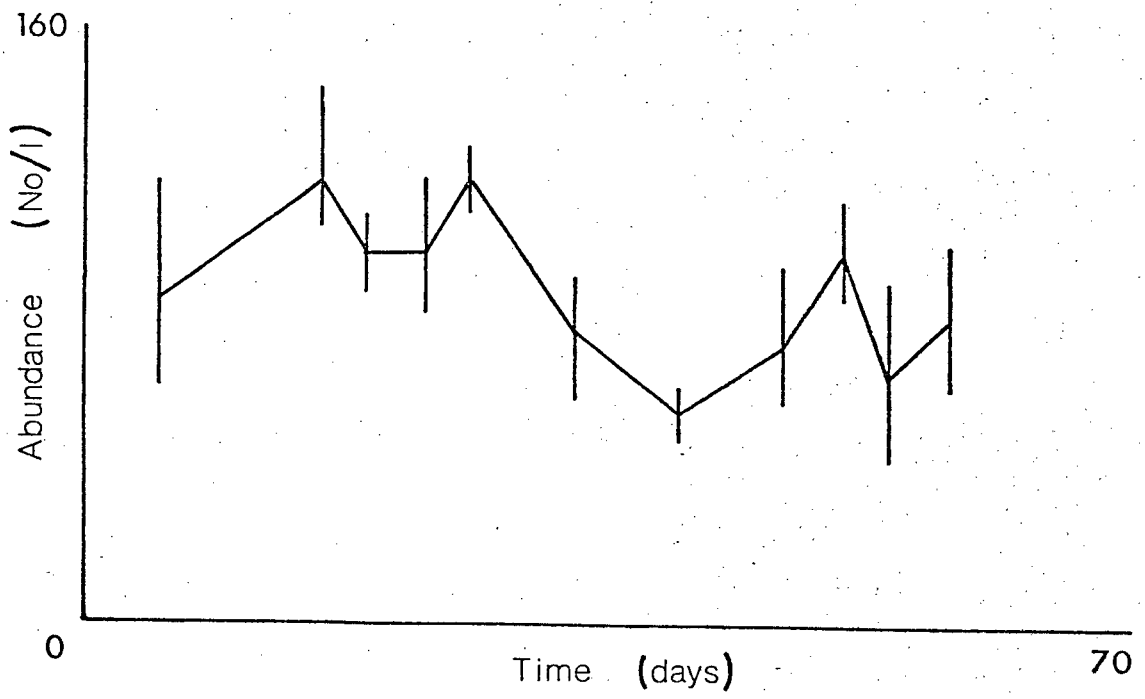

Figure 72. Observed densities of total nauplii in CEE5.

(Error bars as in Fig 67.)

mortality parameters were assumed to be constant over NI-CV. As in the case of Pseudocalanus, the rate of convergence was very slow and improved greatly when the basal metabolic rate, F, was frozen. The resulting best parameter estimates are given in Table XI. The SSQ is high and the reason can be seen in Fig 73a; the dip in CI-III on day 16 cannot be reproduced by the model which smooths out the rise in CI-III and cuts off the peak. The early increases in CIV-VI are ignored entirely by the model.

The observations on day 16 were questioned during the analysis of the C. pacificus data. It is not surprising that the SSQ is reduced when these are ignored (trial 2, Table XI), but the fit to remaining observations is also much improved (Fig 73b), although the early CIV-VI observations are still ignored. While the predicted decrease in CIV-V densities after day 54 does not agree with observations, the latter indicate an increase in combined numbers of CIV-V and CVI after this day when the density in CI-III has dropped to near-zero; the model, which has to 'conserve' copepods, cannot reproduce this.

Another discrepancy in trial 2 is the predicted disappearance of nauplii after day 33, although total nauplii numbers are observed to remain high. As an excess of CI-III's is also predicted from day 33 on, it seems likely that nauplii are continuing to grow and reach CI-III in the model at food concentrations which prevent this in the enclosure. On increasing F for nauplii to 0.12 day^{-1} and allowing Cn for nauplii to vary independently of Cn for copepodids, a considerable reduction in minimum SSQ was achieved (trial 3, Table XI) with a much better fit to CI-III in particular (Fig

Table XI.

Final parameter estimates and corresponding SSQ errors for Paracalanus.

(Subscripts 1...4, '"', '*' and '+' as in Table X.)

Parameters	Trials			
	1	2+	3+	4
Cn_1	.22	.24	.36	.52
Cn_2	"	"	.34	.47
Cn_3	"	"	"	.36
Cn_4	.40*	.40*	.40*	.40*
D_1	20.	23.	61.	41.
D_2	"	"	"	41.
D_3	"	"	"	50.
D_4	80.*	80.*	80.*	80.*
F_1	.03*	.03*	.12*	.14*
F_2	"	"	.03*	.03*
F_3	"	"	"	"
F_4	.08*	.08*	.08*	.08*
θ_1	.039	.051	.037	.020
θ_2	"	"	"	.070
θ_3	"	"	"	"
θ_4	"	"	"	.020
Init adults	.80	1.27	1.95	.36 +4.60 juveniles.
SSQ	2660.	1137.	760.	1584.

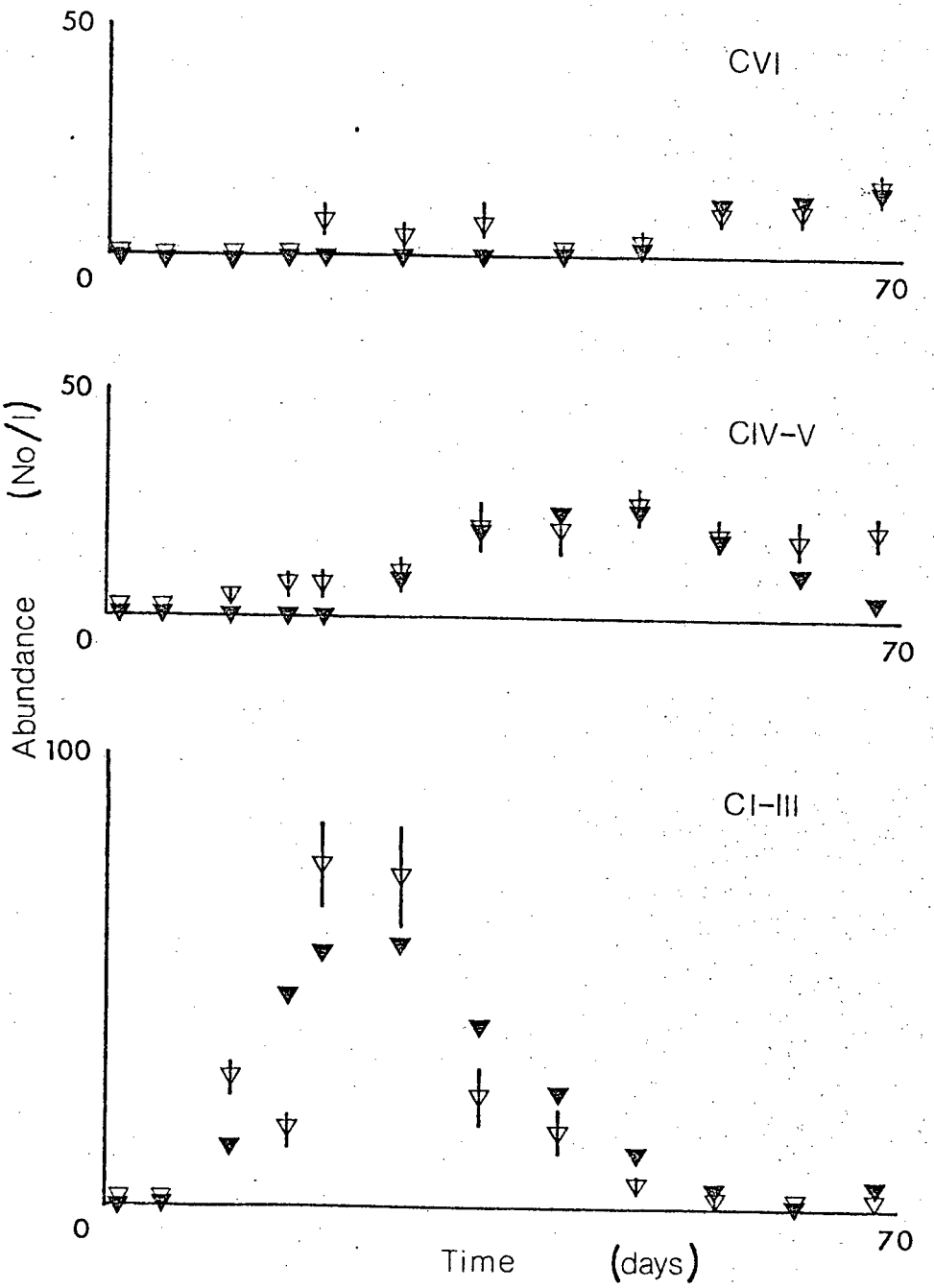

Figure 73a. Comparison of predictions (solid symbols) and observations (open symbols) for Paracalanus (trial 1).

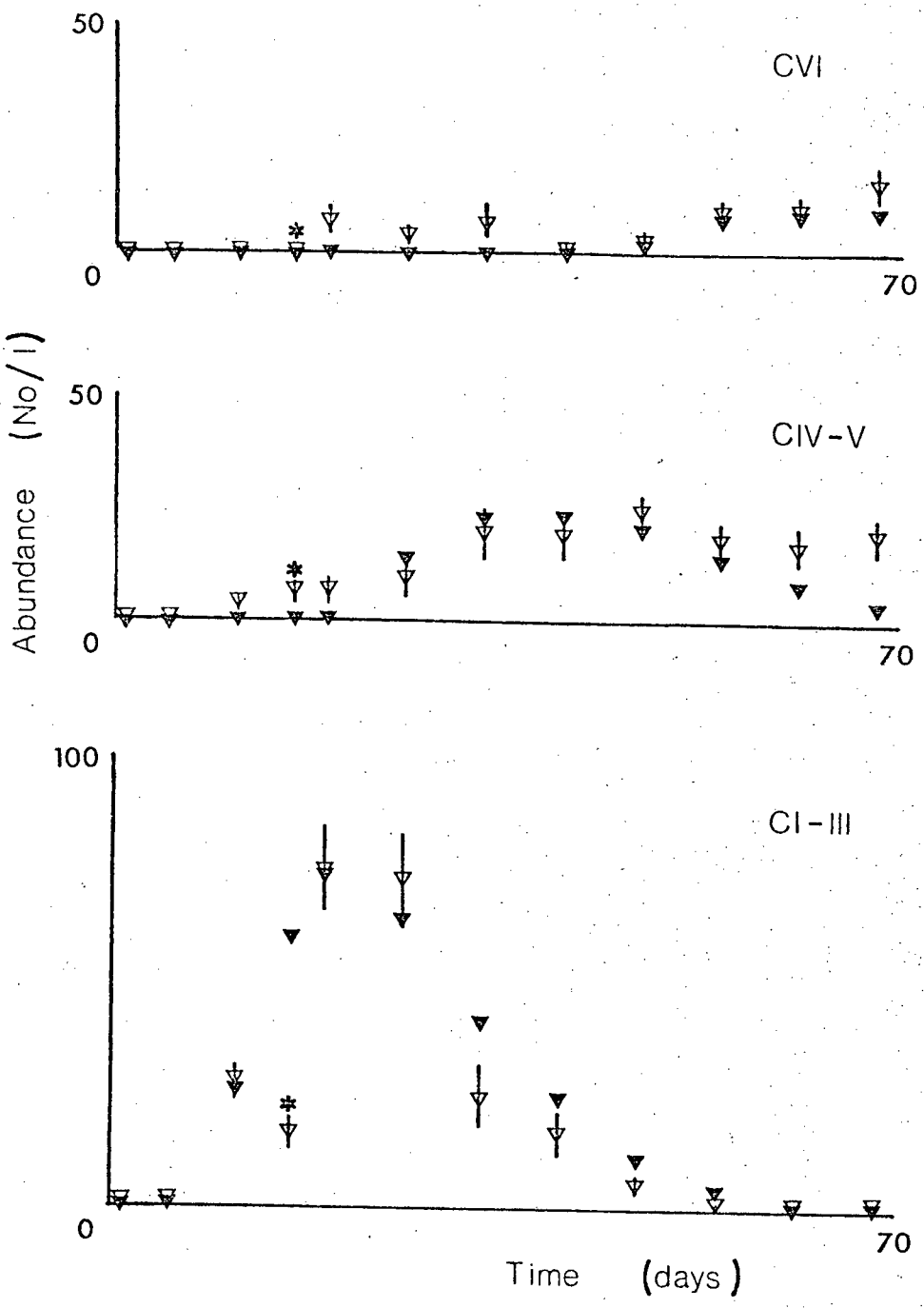

Figure 73b. Comparison of predictions (solid symbols) and observations (open symbols) for Paracalanus (trial 2).

73c). The resulting set of parameter estimates is characterized by much higher maximum growth rates and half-saturation constants for CI-V. The estimated maximum growth rate for nauplii is still low, however. As in the case of Pseudocalanus and Calanus, the minimum SSQ is more or less independent of the value of F chosen for CI-V although high values of F for NI-VI and CVI are necessary here to explain the observed naupliar densities.

A set of parameters which would allow the model to predict the early increases in CIV-V and CVI and still fit the later observations, on the basis of a single cohort starting on day 1, could not be found. However, the data set for Paracalanus differs from that for Pseudocalanus in that the early observations are consistent: an increase in CI-III on day 11 is followed by an increase in CIV-V on day 16 and an increase in CVI on day 19. This could be a case where the model's inability to allow variation in growth rate within a day class is at fault. Alternatively, especially if we are prepared to accept the low CI-III density on day 16 as genuine, it also seems plausible that the data represent 2 cohorts, one due to adults which reproduce for a short period starting on day 1 and the other due to copepodids on day 1 which mature and reproduce in time to give rise to the large CI-III peak observed on day 19. This is supported by the fact that the initial number of adults observed is low (0.1 ind/l) and increases to 0.8 ind/l by day 11.

The model was therefore changed to allow two initial day classes, one consisting of adults which produce eggs for 5 days and the other consisting of juveniles. The number of individuals in both initial day classes and the weight of individuals in the

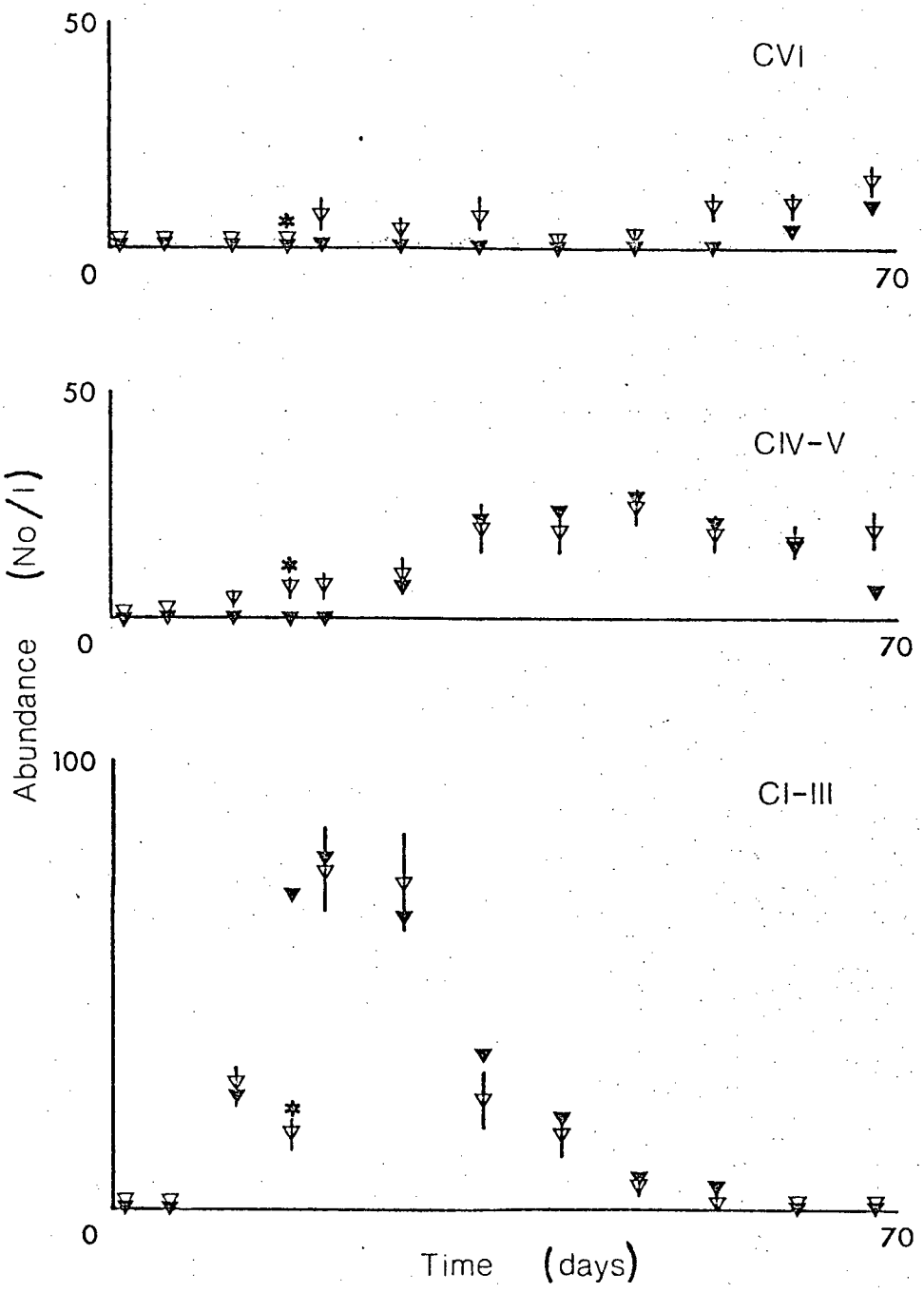

Figure 73c. Comparison of predictions (solid symbols) and observations (open symbols) for Paracalanus (trial 3).

juvenile day class were estimated along with growth and mortality parameters. The parameters controlling reproduction were the same as those used above. Convergence for this case was rather poor, however; the parameter set giving the lowest SSQ found is given in Table XI (trial 4) and the predicted and observed time series compared in Fig 70d. The SSQ obtained is not particularly low and the second increase in CI-III is not as steep as observed. Because of continued naupliar growth, the decrease in CI-III is also too slow and predicted naupliar densities are too low by day 50. The problem here is that the observed decrease in phytoplankton carbon after day 19 (Fig 64) is not great enough to permit a set of growth parameters which will allow the rapid naupliar growth necessary to reproduce the large increase in CI-III between day 16 and 19, while preventing naupliar growth into CI-III after day 30.

The parameter estimates obtained here involve considerable variation across stages; this is partly justified by the fact that all stages are now present over a range of food densities due to the two cohort assumption. The maximum growth rates (0.38,0.44,0.33) are higher than those found for a single cohort and in general agreement with the average rate calculated from the generation time. The values of D are rather similar for NI-CV and at the upper end of the range suggested for adult females feeding on diatoms by Checkley. High mortality rates in CI-VI are required to explain the low survival from CI-III to CIV-V to CVI. There is no evidence that the mortality rate for nauplii is as low as 0.02 day^{-1} except that the estimated sizes of the initial day classes are already rather high compared to

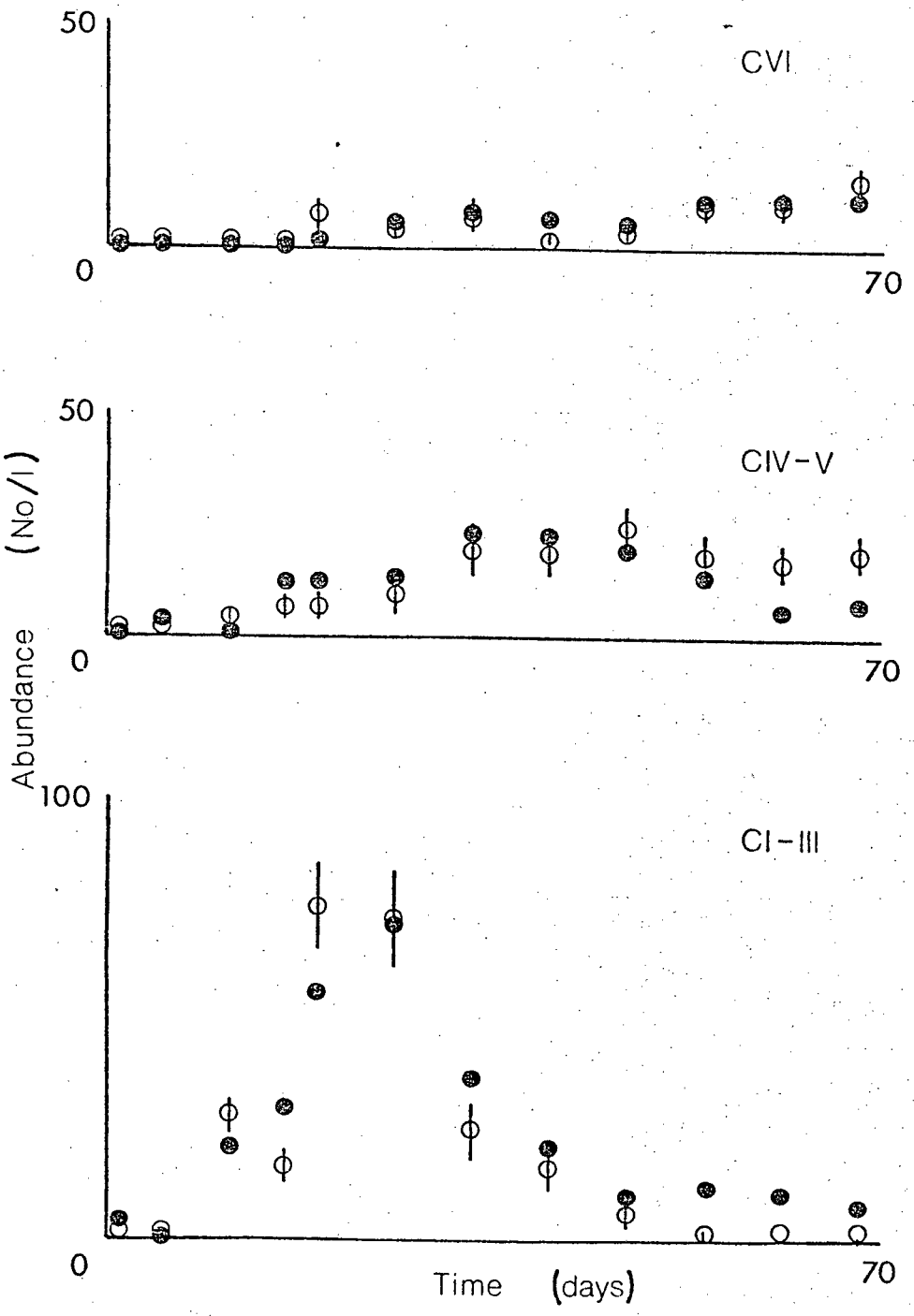

Figure 73d. Comparison of predictions (solid symbols) and observations (open symbols) for Paracalanus (trial 4).

observations and would need to be even higher if naupliar mortality rates were increased.

5.4 Stability of the Phytoplankton-Zooplankton Interaction.

In the preceding section, the phytoplankton dynamics were ignored, zooplankton parameters being estimated on the basis of observed phytoplankton concentrations. However, as noted by Sonntag and Parsons(1979), the phytoplankton-zooplankton interaction in the enclosure is also worthy of study. As a first step, we might ask what impact the zooplankton had on phytoplankton concentrations according to the estimated feeding parameters. The zooplankton model was therefore altered to allow all three zooplankton species to feed simultaneously on the observed phytoplankton and the total phytoplankton carbon ingested daily was calculated. This required the evaluation of an efficiency Ef which incorporated both the assimilation efficiency and any component of metabolic rate proportional to ingestion. Assimilation efficiency was taken as 0.7, following Steele(1974). In a later version of Steele's model, Landry used a combination of basal and ingestion-dependent metabolic rate. Combining his value for the latter with the assimilation efficiency of 0.7 yielded a value of Ef equal to 0.5.

For the period from day 30 on, when phytoplankton densities are low and relatively constant, the average calculated zooplankton ingestion is 24.9 $\mu g\ C.l^{-1}.day^{-1}$ compared with the calculated average daily production of 25.7 $\mu g\ C.l^{-1}$. This close agreement is probably fortuitous, given the crude assumptions made to convert ^{14}C observations to daily production and to

convert zooplankton growth to ingestion, but it does suggest that the grazing parameter estimates are at least in the right ball-park.

The question of the stability of the phytoplankton-zooplankton interaction remains. Simple predator-prey models (May,1974) indicate that an interaction between a prey which is growing exponentially in the absence of resource limitation and a predator which is feeding according to a hyperbolic (Type 2, Holling,1965) functional response will lead to unstable oscillations in the two populations. Given the high turnover rate of phytoplankton in CEE5, we would expect the system to break down very quickly.

As shown in Chapter 1, simple models also indicate that a stable equilibrium is possible if the predator possesses a threshold or type-3 functional response (Holling,1965). Sonntag and Parsons(1979) have suggested that a response of this type on the part of the zooplankton, or some sort of spatial refuge for the phytoplankton, could be responsible for the persistence at relatively constant levels of the phytoplankton in CEE5. A closer examination of the CEPEX data suggests an alternative explanation. While the average nitrate concentration in the enclosure remains high, the nitrate profiles show very low levels in the top 8m from day 30 on. There is a steep nutricline between 8 and 16m with greater than 16 μg at $NO_3^-.l^{-1}$ below this depth. The ^{14}C data indicate that most of the primary production is occurring in the top 8m and production below this depth appears to be light limited. It seems possible that the behaviour observed in the enclosure could be analogous to that

described in chapter 2 for Steele's model following nutrient depletion, with the nutrient flux into the upper layer limiting phytoplankton growth and thereby stabilizing the phytoplankton-zooplankton interaction.

The calculated daily respiration by zooplankton in the combined run discussed above was 12.5 $\mu g\ C.l^{-1}$. Assuming that 0.4 of this is recycled as nutrient (Steele,1974), a net nutrient influx of approximately 20 μg C(equivalent).$l^{-1}.day^{-1}$ into the top 8m is required to meet the demands of phytoplankton growth. The nutrient gradient from 8 to 16m is approximately 2 mg $at.m^{-4}$ or 200 mg $C(eq).m^{-4}$ (assuming a C:N ratio of 7:1). A diffusion rate of 1 $m^2.day^{-1}$ would maintain a flux of 200 mg $C(eq).m^{-2}.day^{-1}$ into the upper layer, providing 25 mg $C(eq).m^{-3}$ (ie 25 $\mu g\ C(eq).l^{-1}$) over the 8m depth per day. Steele and Farmer(1977) report mixing rates for the enclosures of 0.05 to 0.26 $cm^2.sec^{-1}$ or approximately 0.4 to 2.2 $m^2.day^{-1}$, so that the observed nutrient gradient and diffusion rates are certainly compatible with the calculated demand.

To test the stability of the proposed nutrient-phytoplankton zooplankton interaction, nutrient and phytoplankton components were added to the zooplankton model, following the formulation of Steele(1974). The nutrient and phytoplankton equations are:

$$\dot{R} = -A.R.P/(B+R) + V.(R0-R) + U.res(P)$$

$$\dot{P} = A.R.P/(B+R) - ing(P)$$

where res(P) and ing(P) represent total zooplankton respiration and ingestion rates as calculated by the combined zooplankton

model using the estimated feeding parameters and the predicted phytoplankton concentration P. In fact, no attempt has been made to model the sinking out of the diatom bloom or the change in species composition from diatoms to silicoflagellates to flagellates. This was avoided by driving the zooplankton model with observed phytoplankton densities up to day 30. The phytoplankton and nutrient dynamics were then switched on with the observed value of P (17.87 $\mu g\ C.l^{-1}$) and a low value of R (20 $\mu g\ C(eq).l^{-1}$) as initial conditions.

The parameters used in the phytoplankton-nutrient equations were largely determined by the observations discussed above. As in-situ phytoplankton growth rates have been calculated to be about 1.4 day^{-1}, supposedly under conditions of nutrient limitation, the maximum growth rate was chosen to be higher. A value of A equal to 2 day^{-1}, or about 3 $div.day^{-1}$ was taken as a reasonable maximum at this temperature. The half-saturation constant for growth has been taken as 5 $\mu g\ C(eq).l^{-1}$ or 0.05 $\mu g\ at.NO_3^-.l^{-1}$; this is rather low although lower values have been reported (Goldman and McCarthy,1978). It is needed to explain growth rates up to 0.75.A at the low nutrient concentrations observed in the top 8m. The values of V and RO were chosen so as to provide a nutrient flux of 20 $\mu g\ C(eq).l^{-1}.day^{-1}$ into the top 8m and U was taken as 0.4 following Steele(1974).

It can be seen from Fig 74 that the system behaves in a stable manner after day 30 as expected on the basis of the qualitative analysis of Chapter 2. The oscillation resulting from the initial phytoplankton and nutrient concentrations damps out and approximately 20 μg phytoplankton carbon.l^{-1} are

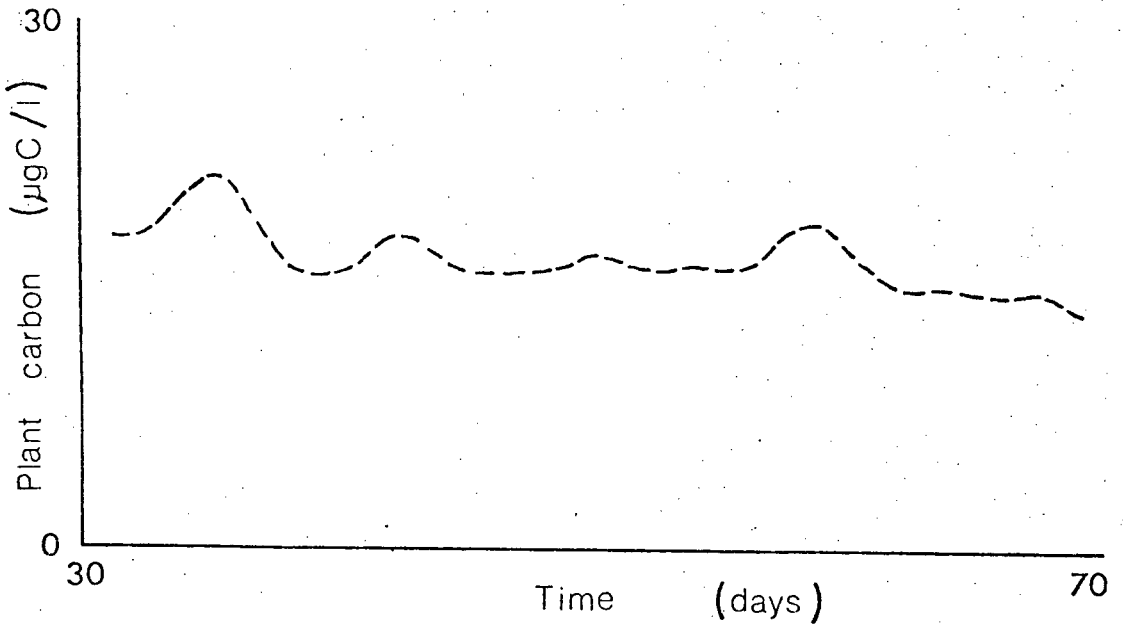

Figure 74. Predicted phytoplankton concentration in CEE5 after day 30.

maintained for the remaining 40 days. The zooplankton ingestion rate also stays relatively constant at about 25 μg $C.l^{-1}.day^{-1}$. In view of this, it is not surprising that the predicted zooplankton time series based on predicted and on observed phytoplankton carbon were very similar.

5.5 Conclusions.

The parameter estimation technique presented here appears to hold considerable promise as a tool for the investigation of zooplankton growth dynamics. It is hoped that a discussion of its performance on this data set, particularly in terms of the reliability of parameter estimates and its dependence on the data, will serve as a guide to the types of experiments and data of most value in the estimation of such parameters.

An obvious factor affecting the reliability of estimates is observation error. As noted above, the confidence limits placed on observations in Fig 67,69,71 and 72 are based on the statistics of sample splitting; that is, on the actual number of individuals counted. It is rather interesting that the strategy employed in counting these samples, a commonly practised one of counting approximately the same total number of individuals from each sample, results in an irregular distribution of observation errors over time. This is because the number of individuals counted for any particular group of stages and species depends not only on its absolute abundance but also on its abundance relative to other stages or species.

These confidence limits do not take into account the degree to which the pumped samples are representative of the enclosure

and, in this regard, the anomalous features of the Pseudocalanus and Calanus time series are particularly troubling. These time series could not be explained except by ignoring or assuming very large errors in one or several observations. This is an ad hoc procedure and introduced an unsatisfactory degree of ambiguity into the data analysis.

Where the distribution of observation errors is known, the local Jacobian evaluated in the Marquardt algorithm can be used to give approximate confidence limits for the parameter estimates (Benson,1978). While the irregular distribution of observation erros discussed above could be allowed for by minimising a weighted sum of squares of errors, the uncertainties introduced by anomalous features in the data make any such approach questionable and I have been content here to give some indication of the sensitivity of the SSQ to variations in certain parameters. Where sampling errors are better understood, perhaps in smaller-scale laboratory experiments, a more rigorous statistical approach to parameter uncertainty may be justified. Even if observation errors were minimized, certain ambiguities in parameter values would remain. The data, after all, represent only a single time series of observations of phytoplankton and zooplankton numbers. Some obvious sources of ambiguity are listed here in the hope that they will suggest more informative experimental designs or types of data to be collected.

In all cases, except for Paracalanus nauplii and adults, it was not possible to establish any preference between zero and rather high basal metabolic rates. This might be accomplished at even lower food densities but it seems likely that direct

information on the weights of individuals as well as life-history stage densities may be necessary.

The estimation of half-saturation constants for growth depends of course on a variation in food density over time. This variation coincided here with the progression of the cohorts through life history stages, so that it was necessary to assume some fixed pattern of variation of growth parameters with weight or stage in order to estimate their absolute value. This assumption can be avoided only if each stage is exposed to a range of food densities which would require several generations.

There was some tendency here for confusion between the size of initial recruitment and mortality rates, as has been found for simpler models (Parslow et al,1979). This confusion would have been reduced if nauplii had been identified to species and egg production had been estimated.

The effect of food particle size and quality on zooplankton ingestion rates has not been paid the respect it deserves here (Mullin and Brooks,1970; Paffenhoffer,1970; Frost,1972; Poulet,1973). In general, estimating a single half-saturation constant for ingestion when phytoplankton composition is varying is likely to be misleading. In CEE5, the change in species composition from diatoms to silico-flagellates to flagellates coincided with the change from high carbon concentrations to low, so that separate half-saturation constants for different food types could not have been estimated. The half-saturation constants obtained were determined primarily by behaviour at low food densities and should therefore apply to ingestion of flagellates.

Both in terms of reducing observation errors and in terms of manipulating food density and composition, smaller-scale laboratory experiments may be of more immediate use in estimating zooplankton parameters. Perhaps the most exciting prospect involves the maintenance of continuous cultures of phytoplankton and zooplankton (Droop and Scott,1979) and the investigation of both equilibrium and transient behaviour as has been done for phytoplankton and nutrients (eg Caperon and Meyer,1972). In an approach of this type, the estimation technique could be used for experimental design as well as data analysis. By studying the technique's ability to estimate parameters from predicted timestreams, those manipulations of the experimental system allowing greatest discrimination between parameters could be chosen. Features neglected in the model used here, such as the variation of growth rate across individuals in the same day class (Paffenhoffer,1970), the variation of weights at particular life history stages with nutritional status (Mullin and Brooks,1970; Paffenhoffer and Harris,1976) and changes in sex ratio with food quality and quantity (Paffenhoffer,1970), might also be usefully included and parameterised in an interactive study of this type.

Ultimately, however, the conclusions drawn from laboratory studies have to be tested in the field. The traditional approach has been to construct a simulation model, insert parameter values obtained in the laboratory and see if the field observations are reproduced. If the observations and predictions are judged to agree, it may be concluded that the laboratory values apply in the field, although one has no indication as to how good a test the field data represent. (Perhaps the predictions are

completely insensitive to changes in certain parameters or combinations of parameters). If the observations and predictions disagree and it is suspected that changes in parameter values may be responsible, this approach leaves no alternative to 'tuning' the simulation model by altering parameters until agreement is obtained. Again there is no indication as to whether other parameter sets might do as well. The non-linear estimation technique offers a fresh approach to these problems. At best, where observation errors are well understood, confidence limits may be placed on parameter estimates and laboratory and field estimates compared statistically. At worst, the technique of freezing certain parameters and estimating others can be used, as it has been here, to indicate whether discrimination between parameter values on the basis of the data is possible.

The persistence of phytoplankton in CEE5 at low, constant levels has been explained here as a result of nutrient limitation, without any need for grazing thresholds or spatial refugia. Again this does not prove that grazing thresholds do not exist; just that they are not necessary to explain this data set. A comparison of the stability properties of the zooplankton model and the nutrient-phytoplankton-zooplankton model does raise some interesting questions concerning parameter estimation. Here, I chose to estimate zooplankton parameters by driving the zooplankton model with the observed phytoplankton concentrations. It could be argued that I should have fitted a nutrient-phytoplankton-zooplankton model to the full data set, especially in view of the uncertainties concerning the true level of phytoplankton carbon discussed earlier.

Apart from the numerical practicality of such a scheme, which would require the simultaneous estimation of parameters for all species of zooplankton, its results could be different in the following qualitative sense. When the zooplankton model is driven by the observed phytoplankton density, predicted weights depend exponentially on grazing parameters. At low food concentrations, increasing Cn or decreasing D will lead to a corresponding increase in exponential growth rate, and a large increase in individual weight after sufficient time has elapsed. In the combined nutrient-phytoplankton-zooplankton model, provided the equilibrium at low nutrient concentration is maintained, phytoplankton production and total zooplankton ingestion are fixed by the nutrient flux. Changes in D across species will not change predicted ingestion or growth rates but will change the equilibrium value of phytoplankton carbon. With nutrient flux fixed, the most direct way to affect growth rates would be through the growth gross efficiency; that is, through metabolic rates. A very different pattern of parameter discrimination might be expected.

There is another interesting aspect to the behaviour of the nutrient based model. An equilibrium with phytoplankton growth limited by nutrient levels is only possible provided the maximum phytoplankton growth rate, A, exceeds the zooplankton clearance rate. The value of A used here, 2 day^{-1}, is probably close to the maximum possible for phytoplankton at this temperature (Eppley,1972). The calculated zooplankton clearance rates, both on observed and predicted phytoplankton populations, are relatively constant at about 1.4 day^{-1} from day 30 on, in spite

of the fact that Paracalanus individuals, for example, undergo a 5 to 10 fold increase in weight and ingestion rate over the same period. It is only the high mortality rates estimated for Paracalanus and Calanus copepodids which keep the total zooplankton clearance rate low enough to allow the equilibrium to persist.

The source of these high mortality rates is not known. If carnivores are not important (Sonntag and Parsons,1979), the possibility that they were caused by low food densities seems plausible, especially in view of Paffenhoffer's (1970) and Checkley's(1980) results. The fact that low mortality rates were estimated for Pseudocalanus may seem inconsistent, but is in fact encouraging, since Paffenhoffer and Harris (1976) found no marked increase in mortality rates in Pseudocalanus elongatus at low food densities in culture. It was speculated in Chapter 2 that over-depletion of phytoplankton during a transient approach to a stable,nutrient-limited equilibrium might be prevented by a zooplankton mortality response to low food densities. Although no explicit dependence of mortality rate on nutritional status was assumed in the models used here, the estimation results and the behaviour of the nutrient based model suggest that the ecosystem in the CEE5 enclosure may well have constituted an example of this phenomenon.

Chapter 6

DIFFUSION, SINKING AND GROWTH OF PHYTOPLANKTON.

6.1 Introduction.

Laboratory studies of well-mixed phytoplankton cultures continue to yield more detailed knowledge of the dependence of growth rate on conditions of nutrients, light and cell history (Droop,1974; Goldman and McCarthy,1978). However, in considering natural phytoplankton populations in the oceans, one must recognise that the population is distributed in space and that physical growth processes such as turbulent mixing and sinking may be as important as in-situ growth rates. To model these physical processes precisely is no simple matter; the study of turbulent mixing alone is a challenging task, by no means complete. Moreover, recent studies (Marra,1978a,b) point to even more subtle interactions between mixing and past-history effects on the light-dependence of growth rates.

Nevertheless, certain highly simplified approaches to modelling phytoplankton populations have enjoyed considerable success. An example is Sverdrup's critical depth model (Sverdrup,1953), in which phytoplankton are assumed to be uniformly mixed throughout a mixed layer of depth z_M. Under the further assumptions that respiration is independent of depth and production is proportional to light intensity, Sverdrup derived the criterion for net growth $z_M < z_{cR}$, where

$$z_{cR} /(1-\exp(-k.z_{cR})) = I_e /(k.I_c) \ .$$

Here I_e is the average photosynthetically active radiation (P.A.R.) penetrating the surface and I_c is the compensation light intensity. This criterion was successfully applied by Sverdrup to data from Weathership M in the Atlantic and has since been found to explain other data sets (eg Parsons and LeBrasseur,1968).

Another simple approach to modelling the depth distribution of phytoplankton was devised by Riley,Stommel and Bumpus(1949), who considered the steady-state profiles which result when a phytoplankton population is subject to a constant (eddy) diffusion rate K and constant sinking rate w with growth rate varying as a step-function of depth. These authors also obtained steady-state profiles using numerical techniques under more realistic assumptions concerning the variation with depth of growth rate, diffusion, sinking and grazing. Numerical simulation has become more popular with the advent of computers (Riley et al obtained their numerical solutions with the help of a slide rule), and a number of numerical models treating phytoplankton, nutrients and possibly herbivores as functions of depth and time have been developed (eg Winter et al ,1975; Jamart et al ,1977; Wrobleski,1977).

The same degree of interest has not been shown in extending the analytic results of Sverdrup or Riley et al . Numerical models have tended towards increased detail and realism; the resulting complexity is not conducive to obtaining analytic solutions. However this complexity also means that the dependence of solutions on the structural assumptions and the particular parameter values used can be investigated only in a

limited sense, using sensitivity analysis. Analytic solutions of approximate or simplified models can provide useful insights into the behaviour of these more complicated numerical models, as well as explain field observations. In this chapter, a modest start is made by extending the results of Sverdrup to non-uniform mixed layers and non-zero sinking rates, and those of Riley et al to a more realistic dependence of growth rate on depth.

6.2 Review of a Simple Model.

The concentration of phytoplankton is taken to be a function $P(z,t)$ of depth z, measured vertically downwards from the surface $z=0$, and time t. Phytoplankton cells are subject to eddy diffusivity $K(z)$, sink at rate $w(z)$ and grow at rate $\mu(z)$, yielding the partial differential equation:

$$\frac{\partial P}{\partial t} = \frac{\partial}{\partial z}\left(K.\frac{\partial P}{\partial z}\right) - \frac{\partial}{\partial z}(w.P) + \mu(z).P \qquad 6.1$$

(Riley et al ,1949). The boundary conditions are $K\partial P/\partial z = w.P$ at $z=0$ (zero flux through the surface) and $P \to 0$ as $z \to \infty$. Growth rate is assumed to be a function of depth only; in particular, nutrient-limitation is not considered and any effect of phytoplankton density on the extinction coefficient and hence light availability is ignored. These simplifications are consistent with a discussion of the onset of the spring bloom, as in Sverdrup (1953), or of a region in which nutrients are abundant and the phytoplankton concentration is kept low by grazing, as appears to be the case in the Sub-Arctic Pacific.

As mentioned above, Riley et al (1949) considered the case

of K,w constant and $\mu(z)$ a step function:

$$\mu(z) = \begin{cases} \mu - d & 0 < z < z_g \\ -d & z > z_g \end{cases} \qquad 6.2$$

and looked for steady-state solutions only. Before proceeding, it is convenient at this point to introduce non-dimensionalized variables $\tau = \mu_s.t$, $S = z.(\mu_s/K)^{0.5}$. When these are substituted into 6.1, using the form of $\mu(z)$ given in 6.2 and the assumption K,w constant, the equation

$$\frac{\partial P}{\partial \tau} = \frac{\partial^2 P}{\partial S^2} - 2.\omega.\frac{\partial P}{\partial S} + \begin{cases} (1-\delta).P & 0 < S < S_g \\ -\delta.P & S > S_g \end{cases} \qquad 6.3$$

is obtained. The non-dimensional parameters ω, S_g and δ are given by

$$\omega = w/(2.(\mu_s.K)^{0.5}) \ , \quad \delta = d/\mu_s \ , \quad S_g = z_g.(\mu_s/K)^{0.5}.$$

The boundary conditions are

$$\partial P/\partial S = 2.\omega.P \text{ at } S = 0 \text{ and } P \to 0 \text{ as } S \to \infty .$$

The steady-state solution of Riley et al can be given a more general significance by treating the steady-state solution as a special case of a general eigenvalue problem; that is, by seeking solutions of 6.3 of the form

$$P(S,\tau) = \exp(\lambda.\tau).p(S) \ .$$

Then p satisfies the ordinary differential equation (ODE)

$$0 = p'' - 2.\omega.p' + \begin{cases} 1-(\delta+\lambda).p & 0 < S < S_g \\ -(\delta+\lambda).p & S > S_g \end{cases} \qquad 6.4$$

Thus, the problem reduces to solving two second-order linear ODE's with constant coefficients in the regions $0 < S < S_g$, $S > S_g$, subject to the boundary conditions $p'(0) = 2.\omega.p(0)$, $p \to 0$ as $S \to \infty$, and the requirement that p,p' be continuous at $S = S_g$.

This problem is easily solved; an indirect method is followed here as it will prove useful in the more difficult problem treated later. Letting $p(S)=\exp(\omega.S)h(S)$ and substituting in 6.4 gives:

$$0 = h'' + \begin{cases} (1 - \omega^2 - (\delta+\lambda)).h & 0 < S < S_g \\ -(\omega^2 + (\delta+\lambda)).h & S > S_g \end{cases} \qquad 6.5$$

It can easily be shown that a solution to 6.5 satisfying all boundary and continuity conditions is possible only if $\delta+\lambda > 0$, $1-\omega^2-(\delta+\lambda) > 0$ and is given by:

$$h(S) = \begin{cases} C.(\cos(a.(S - S_g)) - b.\sin(a.(S - S_g))/a) & 0 < S < S_g \\ C.\exp(-b.(S - S_g)) & S > S_g \end{cases}$$

where $a = (1-\omega^2-(\delta+\lambda))^{0.5}$, $b = (\omega^2+\delta+\lambda)^{0.5}$. The non-

dimensional growth rate λ must satisfy the eigen-condition:

$$\tan(a.S_g) = a.(\omega+(1-a^2)^{0.5})/(a^2-\omega.(1-a^2)^{0.5}) \qquad 6.6$$
$$= f(a)$$

A graph of f(a) vs a is shown in Figure 75. Only values of a in the interval $(0,(1-\omega^2)^{0.5})$ correspond to permissable values of $\delta+\lambda$. Depending on the value of S_g, there may be no solution, one solution or many solutions of 6.6 in this interval. In the latter case, only that solution corresponding to the smallest value of a or the largest value of $\lambda+\delta$ is of interest here.

By solving the eigen-condition 6.6 numerically, a contour plot of the largest solution $\lambda+\delta$ as a function $\Lambda(\omega, S_g)$ of non-dimensional sinking rate and depth of positive growth has been generated (Fig 76). Two interpretations are possible for this figure. For given $\delta < \Lambda(\omega,S_g)$, $\lambda = \Lambda(\omega,S_g)-\delta$ is the maximum sustainable growth rate of a population subject to these conditions and, after a sufficient increase in the population, the vertical profile of the population should be closely approximated by the corresponding eigensolution, $p(S)$. On the other hand, if steady-state solutions are of interest, it can be concluded that a non-dimensional loss rate of $\delta = \Lambda(\omega,S_g)$ is necessary for a steady-state solution and that the vertical profile in this steady-state is given by $p(S)$.

The reduction in the number of free parameters by non-dimensionalisation has allowed a simple, complete graphical representation of relevant solutions of 6.6 (Fig 76). The consideration of some approximate solutions of 6.6 in certain

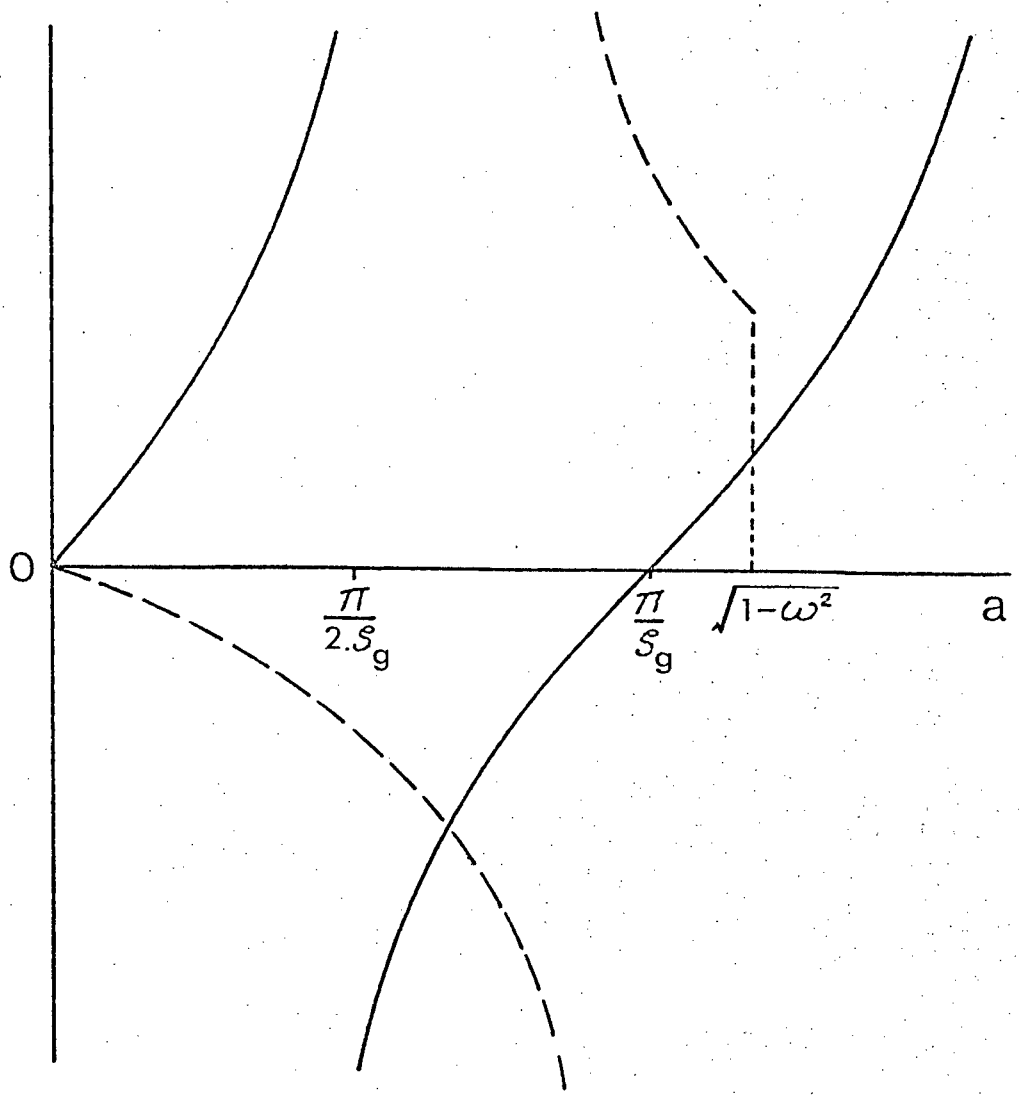

Figure 75. An illustration of the eigencondition 6.6 showing graphs of $\tan(a.\mathcal{S}_g)$ (solid line) and f(a) (dashed line).

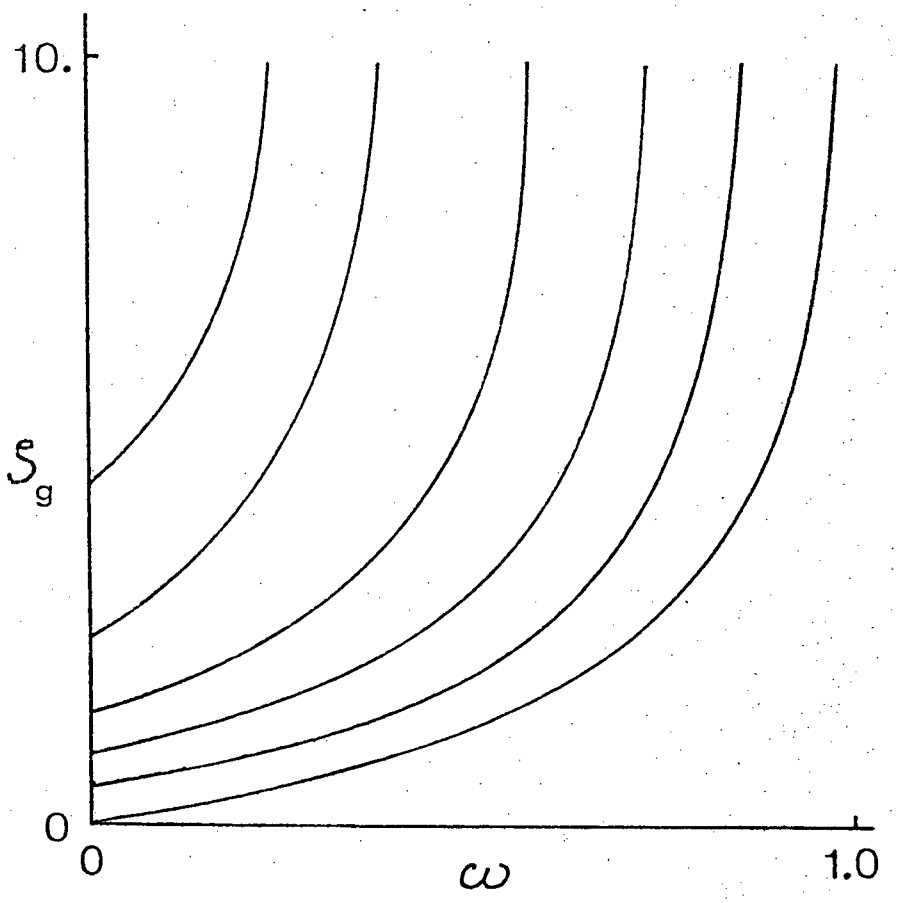

Figure 76. Contour plot of the function $\Lambda(\omega, S_g)$.

limiting cases is quite revealing of the balance of physical and biological processes involved. For $S_g << 1$, relevant solutions of 6.6 exist only for $2.\omega < S_g$ and are given approximately by

$$\lambda + \delta = S_g^2 - 2.\omega.S_g$$

Now $S_g = z_g.(\mu_s/K)^{0.5}$, so $S_g << 1$ corresponds to high mixing rates. The population is almost uniform within the growth layer and is mixed over depths much greater than z_g (Fig 77a). For zero sinking rate, the population declines exponentially below z_g with characteristic depth $K/(\mu_s.z_g)$. The predicted gross growth rate, $\mu_s.(\lambda + \delta) = \mu_s.z_g.(\mu_s.z_g)/K$ is just the ratio of production ($\mu_s.z_g.p(0)$) to total integrated biomass ($K.p(0)/(\mu_s.z_g)$). If the population were uniformly mixed over a layer of depth $K/(\mu_s.z_g)$, a sinking rate w would result in a loss rate $w.z_g.\mu_s/K$, or a non-dimensional loss rate $2.\omega.S_g$, which is just the correction term for sinking obtained from 6.6.

For $S_g >> 1$, the time scale for mixing over the growth layer is long compared with the growth time scale and the population can be expected to vary markedly with depth within this layer. The approximation of 6.6 depends on ω. If $\omega=0$ (or $\omega << 1/S_g$), $(a.S_g) \approx \pi/2$ and

$$\lambda + \delta \approx 1 - (\pi/(2.S_g))^2.$$

If $\omega = O(1/S_g)$ or greater,

$$\lambda + \delta \approx 1 - \omega^2 - \pi^2/S_g^2.$$

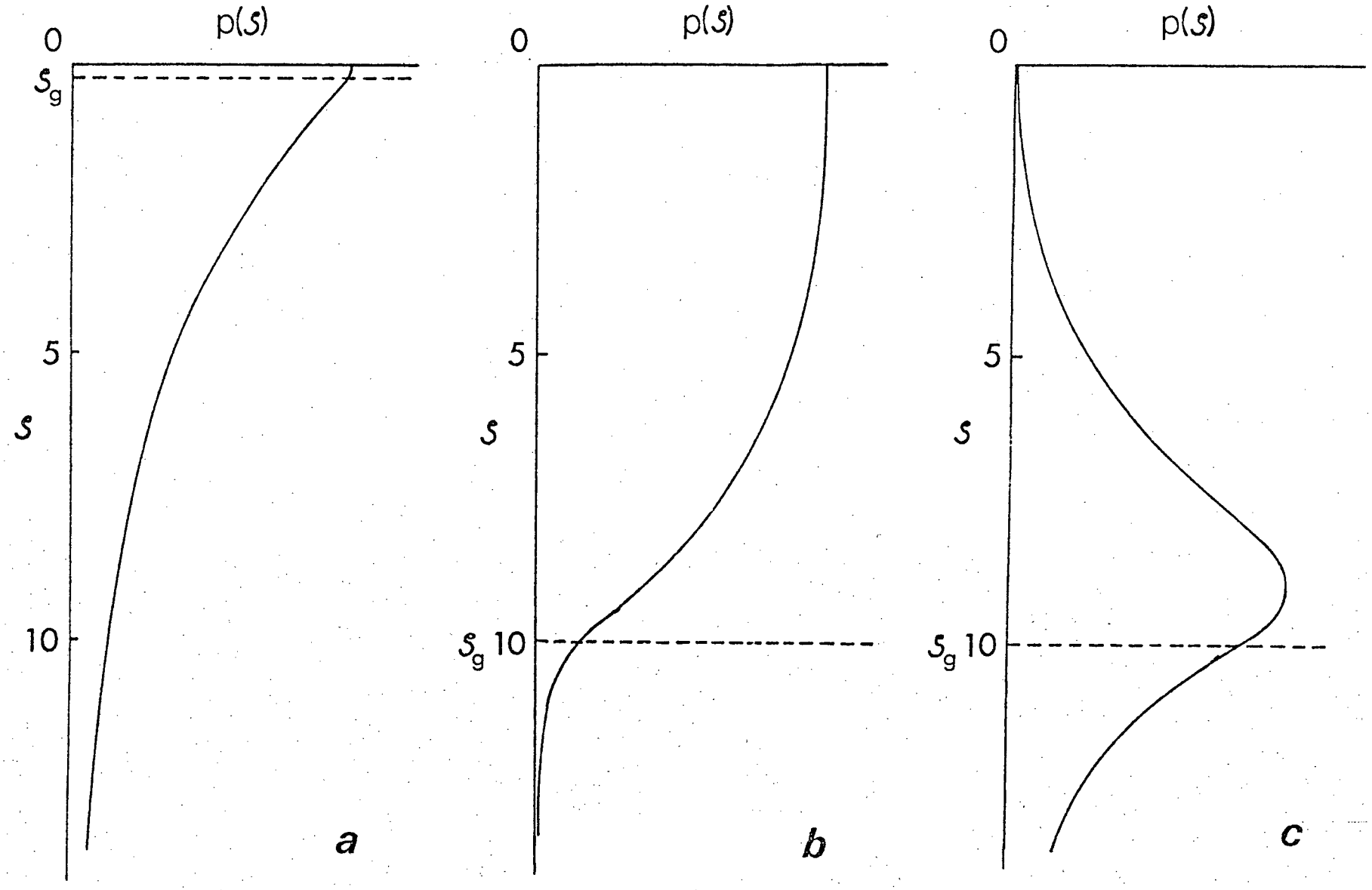

Figure 77. Characteristic profiles p($\mathcal{S}$). (a) $\mathcal{S}_g$=0.2, ω=0. (b) $\mathcal{S}_g$=10, ω=0. (c) $\mathcal{S}_g$=10, ω=0.5.

These two cases corrrespond to different depth profiles. For $\omega=0$, maximum biomass occurs at the surface (Fig 77b) and growth is reduced only by diffusive losses. In dimensional terms,

$$\mu + d = \mu_s - \pi^2.K/(4.z_g^2),$$

so diffusive losses decrease with K. For $\omega=O(1)$, there is a pronounced sub-surface maximum (Fig 77c). The dimensional growth equation is

$$\mu_s + d = \mu_s - w^2/(4.K) - \pi^2.K/(z_g^2)$$

There are several interesting features of this equation. The sinking loss term does not depend on w/z_g, as it would for a uniformly mixed layer. This is because the sub-surface layer has a thickness of order (K/w) and the sinking loss rate is determined by w/(K/w). The appearance of the diffusion rate K in both sinking and mixing terms emphasizes its dual role in determining population growth rates. Increasing K reduces sinking losses but increases mixing losses from the euphotic zone. The overall effect of changing K depends on the relative importance of these two losses.

The existence of pronounced sub-surface maxima in solutions for large s_g and moderate ω is rather interesting. It was noted by Riley et al (1949), who used it to explain observed sub-surface maxima. It is not clear, however, to what extent this property is the result of the rather unrealistic step-function form used to approximate $\mu(z)$. This question will be answered in

the next section, where an analytic solution is obtained for a more realistic form of $\mu(z)$.

6.3 A More Realistic Model.

The step-function form for $\mu(z)$ was presumably chosen by Riley et al to allow for simple analytic solutions while maintaining the general property of higher growth rates near the surface. This form is now replaced by Sverdrup's (1953) assumption that production at each depth is proportional to the mean light intensity at that depth. There are several advantages to making this assumption here. The assumption may be quite realistic under low surface light intensities (for a detailed discussion, see Sverdrup(1953)). The results obtained by using it represent a direct extension of Sverdrup's critical depth criterion to the case of finite diffusion rate and non-zero sinking rate. Finally, it represents in some sense the opposite extreme to the step-function form, since more realistic production profiles involving saturation or inhibition at the surface (Steele,1962) are intermediate between these two.

Under Sverdrup's assumption, assuming a constant extinction coefficient k for light, $\mu(z)$ takes the form:

$$\mu(z) = \mu_s . \exp(-k.z) - d$$

Non-dimensionalizing as before, equation 6.1 becomes:

$$\frac{\partial P}{\partial \tau} = \frac{\partial^2 P}{\partial S^2} - 2.\omega . \frac{\partial P}{\partial S} + (\exp(-2.S/\beta) - \delta).P$$

where the new non-dimensional parameter β is given by $\beta = 2.(\mu_s/K)^{0.5}/k$. As before, eigensolutions of the form $P = \exp(\lambda.\tau + \omega.S).h(S)$ are sought, with $h(S)$ satisfying

$$h'' + (\exp(-2.S/\beta) - (\lambda + \delta + \omega^2)).h = 0 \qquad 6.7$$

and boundary conditions: $h'(0) = \omega.h(0)$, $\exp(\omega.S).h(S) \to 0$ as $S \to \infty$. The solution to 6.7 can be obtained by means of a change of independent variable. Letting $y = \beta\exp(-S/\beta)$, $h(S) = H(y)$ and substituting in 6.7 yields

$$y^2.H'' + y.H' + (y^2 - \beta^2.(\lambda + \delta + \omega^2)).H = 0 \qquad 6.8$$

Equation 6.8 is Bessel's equation of order $\nu = \beta.(\lambda + \delta + \omega^2)^{0.5}$. Provided $\lambda + \delta + \omega^2$ is positive, the solution can be written as:

$$H = C_1.J_\nu(y) + C_2.Y_\nu(y).$$

The boundary conditions on $H(y)$ are:

$$\exp(\omega.S).h(S) = y^{\omega.\beta}.H(y) \to 0 \text{ as } S \to \infty \text{ or } y \to 0.$$
$$H'(\beta) = -\omega.H(\beta)$$

The first boundary condition implies that $C_2 = 0$, since Y_ν behaves like $y^{-\nu}$ as $y \to 0$. As J_ν behaves like y^ν as $y^\nu \to 0$, this boundary condition is satisfied provided $\nu > \omega.\beta$; that is, provided $\lambda + \delta > 0$.

The second boundary condition produces the eigen-condition:

$$J'_\nu(\beta) = -\omega . J_\nu(\beta) \quad . \qquad 6.9$$

Only values of β such that $J_\nu(y)>0$ for $0 < y < \beta$ correspond to positive and therefore meaningful population profiles. A sketch of $J_\nu(y)$ and $J'_\nu(y)$ is given in Fig 78. If j'_ν denotes the first zero of $J'_\nu(y)$, it is clear from Fig 78 that β must exceed j'_ν. It is a property of Bessel functions that $j'_\nu > \nu$, so that the condition $\beta > \nu$ or $\lambda+\delta+\omega^2 < 1$ must be satisfied in order to obtain a meaningful solution. This was also a necessary condition for the step-function profile.

Equation 6.9 can be solved numerically to obtain $\lambda+\delta$ as a function $\Lambda'(\omega,\beta)$. A contour plot of Λ' is given in Fig 79. Again, further insight into the physical processes underlying the condition 6.9 and Fig 79 results if some limiting cases are considered. For $\beta << 1$, the Taylor expansion for J_ν in a neighbourhood of the origin can be used to obtain the approximate solution

$$\lambda+\delta = (\beta/2)^2 - 2.\omega.(\beta/2)$$

This is identical to the approximate solution for the step-function growth profile if S_g is equated to $\beta/2$. The agreement is simply explained on physical grounds. For S_g or β very small, the population is mixed over depths large compared with those associated with change in growth. As explained earlier, the growth rate is determined by the ratio of integrated production to integrated biomass. As biomass is more or less constant over depths of order z_g or $1/k$, total production is the

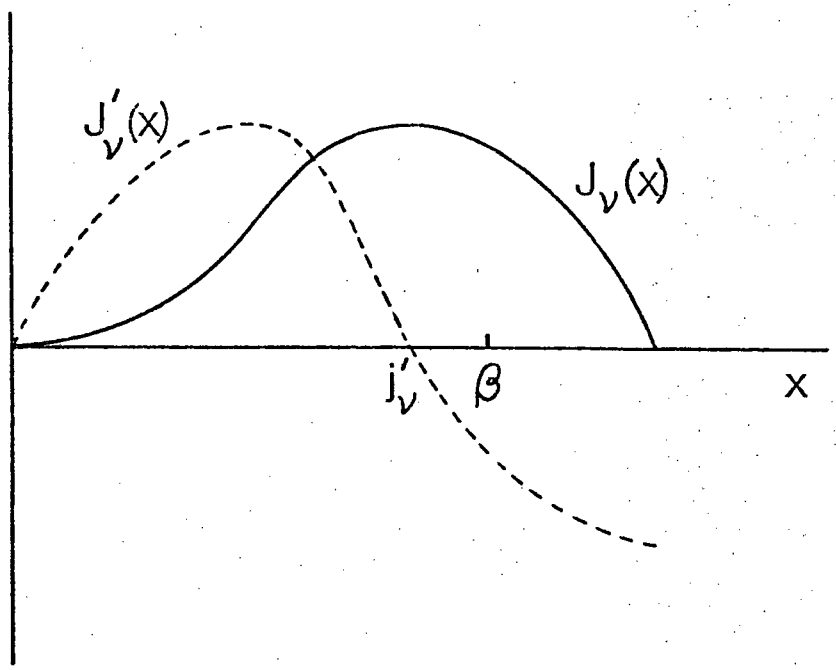

Figure 78. An illustration of the eigencondition 6.9, showing graphs of the functions $J_\nu(x)$, $J'_\nu(x)$.

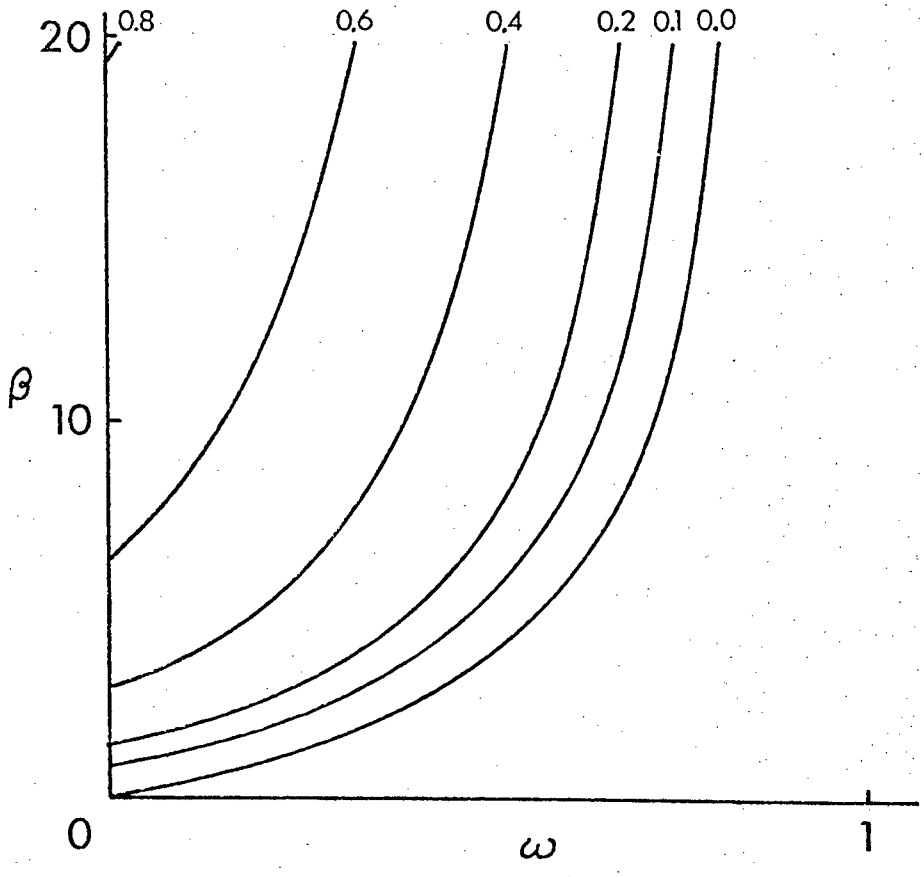

Figure 79. Contour plot of the function $\Lambda^1(\omega,\beta)$

same under the two growth laws when $z_g = 1/k$, or $S_g = \beta/2$.

An approximate treatment of the other limiting case, $\beta >> 1$, is rather more complicated for the exponential growth law. An asymptotic expansion of $J_\nu(y)$ for large ν, y with $y \approx \nu$ is needed. This can be derived by applying the method of steepest descent to an integral representation of the Bessel function (Sommerfeld,1949). Using this expansion, it can be shown that, to leading order in $(1/\beta)$,

$$\lambda + \delta = 1 - \omega^2 - \text{constant}.\beta^{-2/3}.$$

The 'mixing loss' term decreases like $\beta^{-2/3}$ as β increases. This is much slower than the corresponding term (const. S_g^{-2}) for the step-function growth profile. The eigen-solution $p(S)$ is given by

$$p(S) = \exp(\omega.S).J_\nu(\beta.\exp(-S/\beta)).$$

For ν large, $J_\nu(y)$ decreases as y increases towards the first zero over an interval of width $O(\beta^{1/3})$. The subsurface maximum in $p(S)$ therefore occurs at a depth S^* of order $\beta^{1/3}$ and the exponential growth law results in a reduction of growth rate in the biomass layer by a factor $\exp(-2.S^*/\beta)$ which is approximately $1-2.S^*/\beta$ or $1-\text{constant}.\beta^{-2/3}$. The slower increase in $\lambda+\delta$ as β increases can be seen by comparing Fig 79 with Fig 76.

An example of the sub-surface maxima which occur for large β and ω is given in Figure 80. The sub-surface maxima found by

Riley et al (1949) are not the result of choosing an unrealistic dependence of growth rate on depth. It is intriguing that such pronounced sub-surface maxima are possible for a fairly realistic growth profile in the absence of nutrient depletion and vertical variation in mixing and sinking rates.

The contour plot of Λ^1 (Fig 79) can be used in the same manner as Sverdrup's critical depth criterion. In fact, $\delta = d/\mu_s$ also equals I_c/I_e since growth rate is assumed to be proportional to light intensity. For given δ, the contour $\Lambda'(\omega,\beta) = \delta$ divides those regions of (ω,β) space where continued growth of the population is possible from those where it is not. Since ω and β are both proportional to $K^{-0.5}$, increasing the stability of the water column (decreasing K) moves (ω,β) outward along a straight line through the origin in Fig 79. Provided $\omega > 0$, the result is always an increase in growth rate followed by a decrease. This reversible effect of diffusion rate on population growth rate was commented on earlier and can be appreciated by considering two extreme situations. If K is very high, the population will be mixed more or less uniformly through a depth exceeding Sverdrup's critical depth and positive growth will be impossible, regardless of ω. On the other hand, if K is zero, the population must inevitably sink out, regardless of growth rate.

6.4 Effect of a Mixed Layer.

A direct comparison of the above results with Sverdrup's is not possible since his model is based on the assumption of a uniformly-mixed layer, not a semi-infinite layer with finite

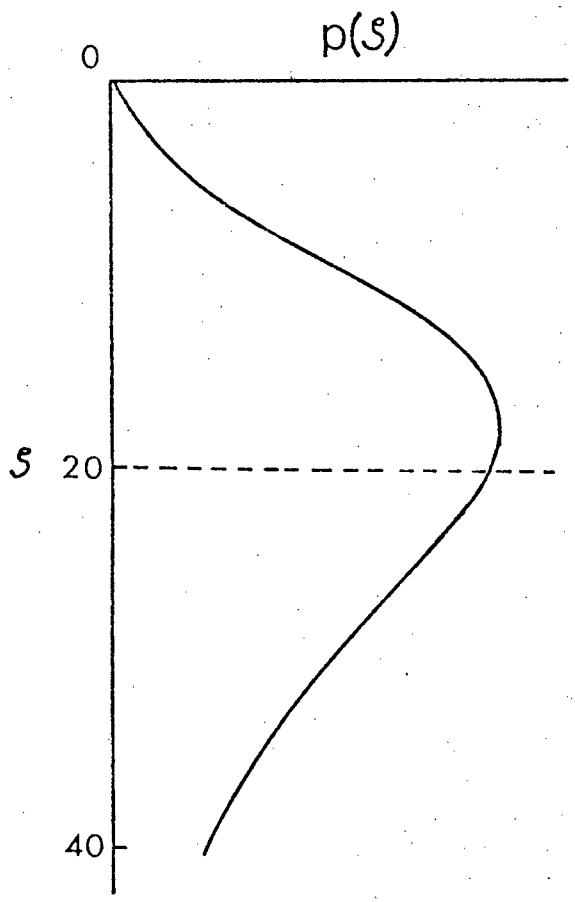

Figure 80. Characteristic phytoplankton profile for $\omega = 0.7$, $\beta = 20$.

diffusion rate. It is relatively simple to introduce a finite mixed layer into the model discussed above. Within the constraints of the eddy diffusion assumption and a desire for analytic solutions, this can be accomplished by making the diffusion coefficient K a step-function of z :

$$K(z) = \begin{cases} K & 0 < z < z_M \\ K.\epsilon & z > z_M \end{cases}$$

where ϵ is small, corresponding to low mixing rates below the mixed layer. This problem can be solved in a similar manner to that used with the growth step-function in the first section; that is, by obtaining solutions in $0 < z < z_M$, $z > z_M$ and using continuity of concentration and flux across $z = z_M$. The continuity of flux condition becomes

$$\frac{\partial P}{\partial z}(z_M^-) = \epsilon . \frac{\partial P}{\partial z}(z_M^+)$$

involving a discontinuity in the gradient of P at $z = z_M$.

Recent measurements of mixing rates in the thermocline have yielded low values, of order 1 $cm^2.sec^{-1}$ or less (Osborn,1980), so that ϵ is very small. The limiting case $\epsilon = 0$ is treated here; Sverdrup's results can be regarded as a limiting case of the results obtained in this way with $K \to \infty$ and $\omega = 0$. For $\epsilon = 0$, the problem for $z < z_M$ reduces to:

$$\frac{\partial P}{\partial t} = K . \frac{\partial^2 P}{\partial z^2} - w. \frac{\partial P}{\partial z} + (\mu_s.\exp(-k.z)-d).P \qquad 6.10$$

with boundary conditions:

$$\frac{\partial P}{\partial z} = w.P \text{ at } z=0 \text{ and } \frac{\partial P}{\partial z} = 0 \text{ at } z=z_M.$$

Eigensolutions corresponding to non-dimensional growth rate can be obtained from 6.10 by proceeding as in the previous section. They take the form:

$$p(\mathcal{S}) = \exp(\omega.\mathcal{S}).(J_\nu(y) + C_3.Y_\nu(y))$$

where $y = \beta.\exp(-\mathcal{S}/\beta)$ and
$C_3 = (J'_\nu(\beta) + \omega.J_\nu(\beta))/(Y'_\nu(\beta) + \omega.Y_\nu(\beta))$.
The eigen-condition for $\nu = \beta.(\lambda + \delta + \omega^2)^{0.5}$ is now rather complicated:

$$(y_M.J'_\nu(y_M) - \beta.\omega.J_\nu(y_M))/(y_M.Y'_\nu(y_M) - \beta.\omega.Y_\nu(y_M)) = (J'_\nu(\beta) + \omega.J_\nu(\beta))/(Y'_\nu(\beta) + \omega.Y_\nu(\beta)) \qquad 6.11$$

The constant $y_M = \beta.\exp(-\xi/2)$ where the new non-dimensional parameter ξ equals $k.z_M$ and has a direct physical interpretation as $\exp(-k.z_M)$ is the ratio of light intensity at the bottom of the mixed layer to that at the surface. As before, the equation 6.11 can be solved numerically to obtain $\lambda + \delta$ as a function Λ^2 of ξ, ω and β. The results of the previous section for a semi-infinite layer can be recovered in the limit $\xi \to \infty$.

It is of interest here to compare the results implicit in 6.10 and 6.11 with those predicted by Sverdrup for the uniformly-mixed layer. This comparison is facilitated by the introduction

of a new non-dimensional parameter $\Omega = 4.\omega/\beta = k.w/\mu_s$, a measure of the relative magnitude of sinking loss rate from the euphotic zone and growth rate. The function $\lambda + \delta = \Lambda^3(\xi, \Omega, \beta)$ can be obtained from the function $\Lambda^2(\xi, \omega, \beta)$ defined above. Of the parameters ξ, Ω, β, only β depends on the diffusion rate K and the effect of changing the diffusion rate can be demonstrated by a series of contour plots of $\lambda + \delta$ vs Ω, ξ for different values of β.

The contour plot for a uniformly-mixed layer is obtained by a simple extension of Sverdrup's theory. The average growth rate in a uniformly mixed layer of depth z is, by simple integration,

$$\mu_s.(1-\exp(-k.z_M))/(k.z_M) - d$$

A sinking rate w imposes an additional loss rate equal to w/z_M. On dividing by μ_s, the non-dimensional population growth rate becomes :

$$\lambda = (1-\exp(-k.z_M))/(k.z_M) - d/\mu_s - w/(\mu_s.z_M)$$

Substituting for ξ, Ω and δ, this becomes

$$\lambda + \delta = (1-\exp(-\xi)-\Omega)/\xi \qquad 6.12$$

Contour plots of $\lambda+\delta$ vs Ω,ξ for $\beta = 0$ (from (6.12)) and $\beta =$ 1,3,10 (from (6.11)) are shown in Figure 81.

The dependence of $\lambda + \delta$ on β, Ω and ξ again reflects the dual role of mixing whenever sinking is present. In the case

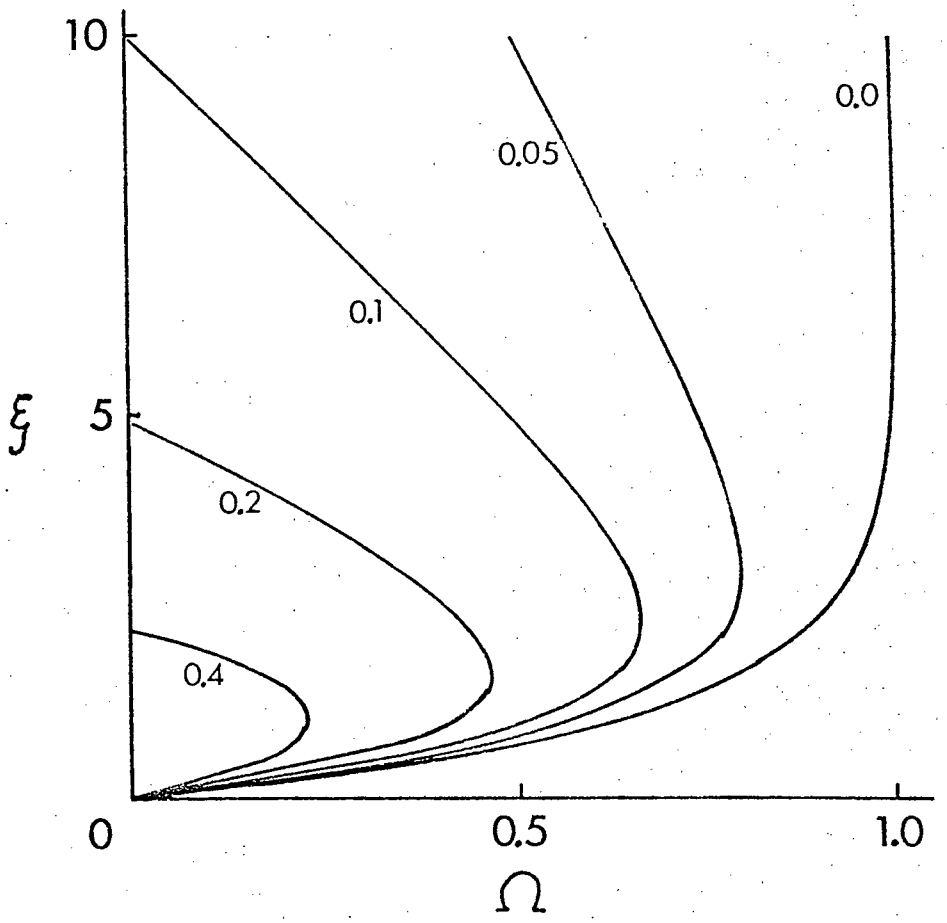

Figure 81a. Contour plot of the function $\mathcal{A}^3(\Omega, \xi)$ for $\beta = 0$.

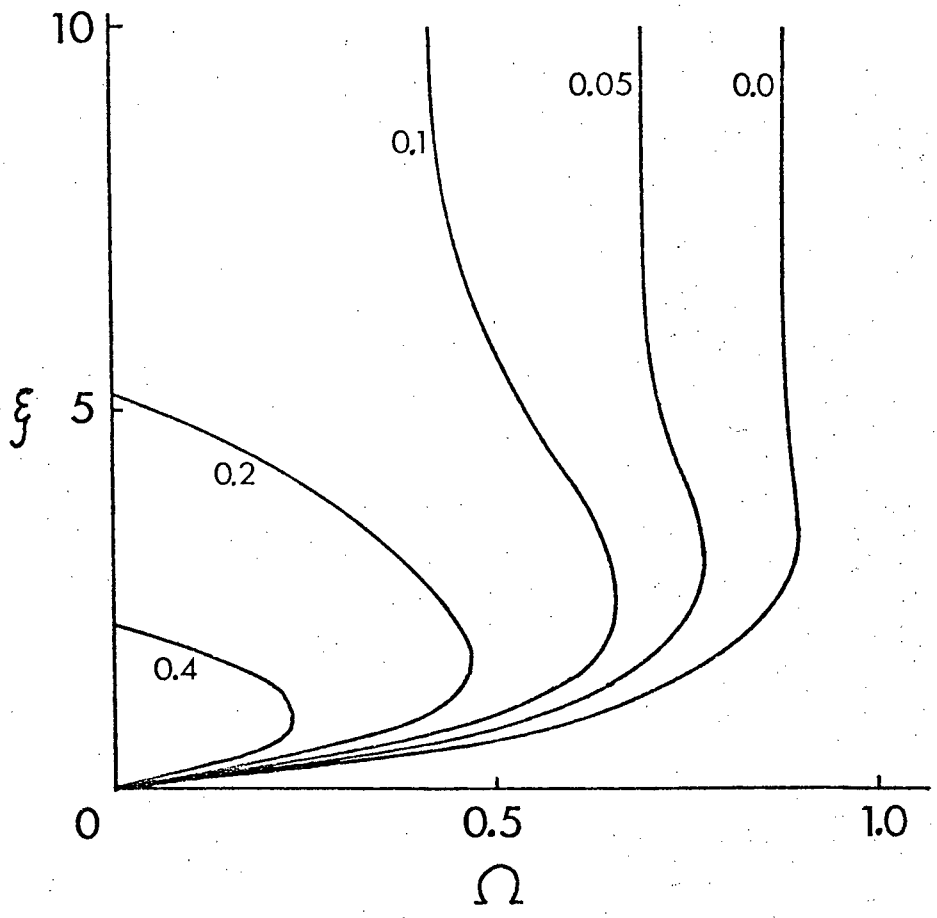

Figure 81b. Contour plot of the function $\Lambda^3(\Omega, \xi)$ for $\beta=1$.

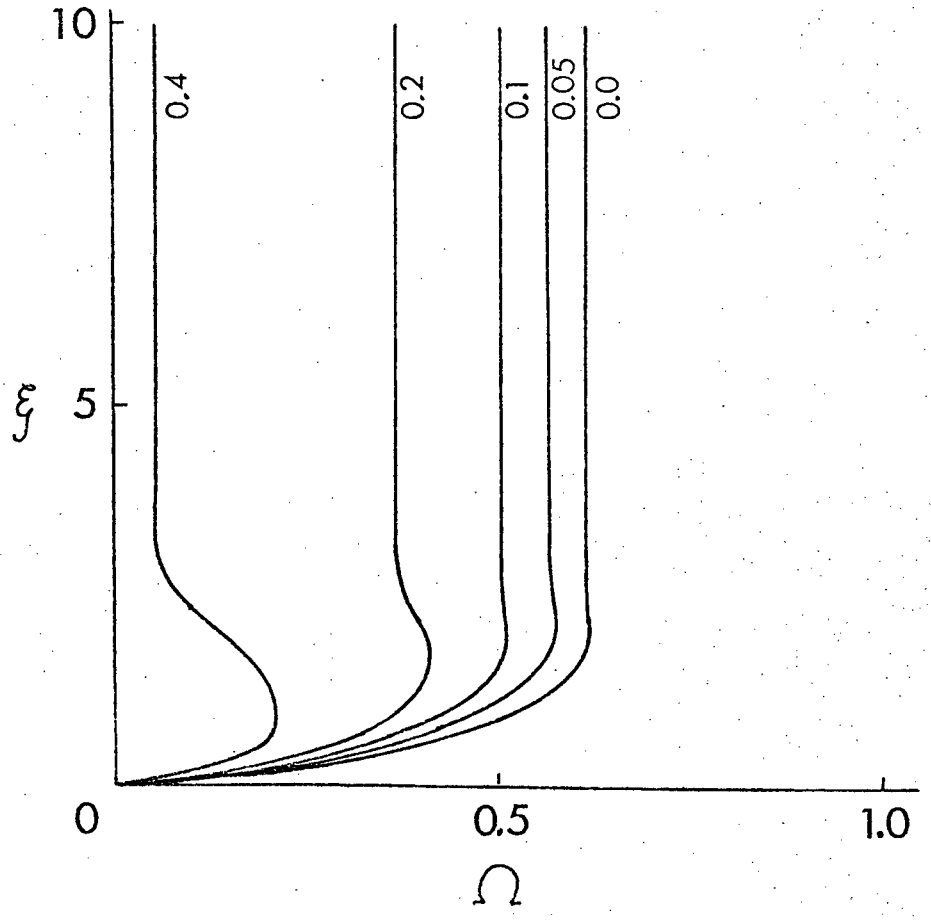

Figure 8lc. Contour plot of the function $\Lambda^3(\Omega,\xi)$ for $\beta=3$.

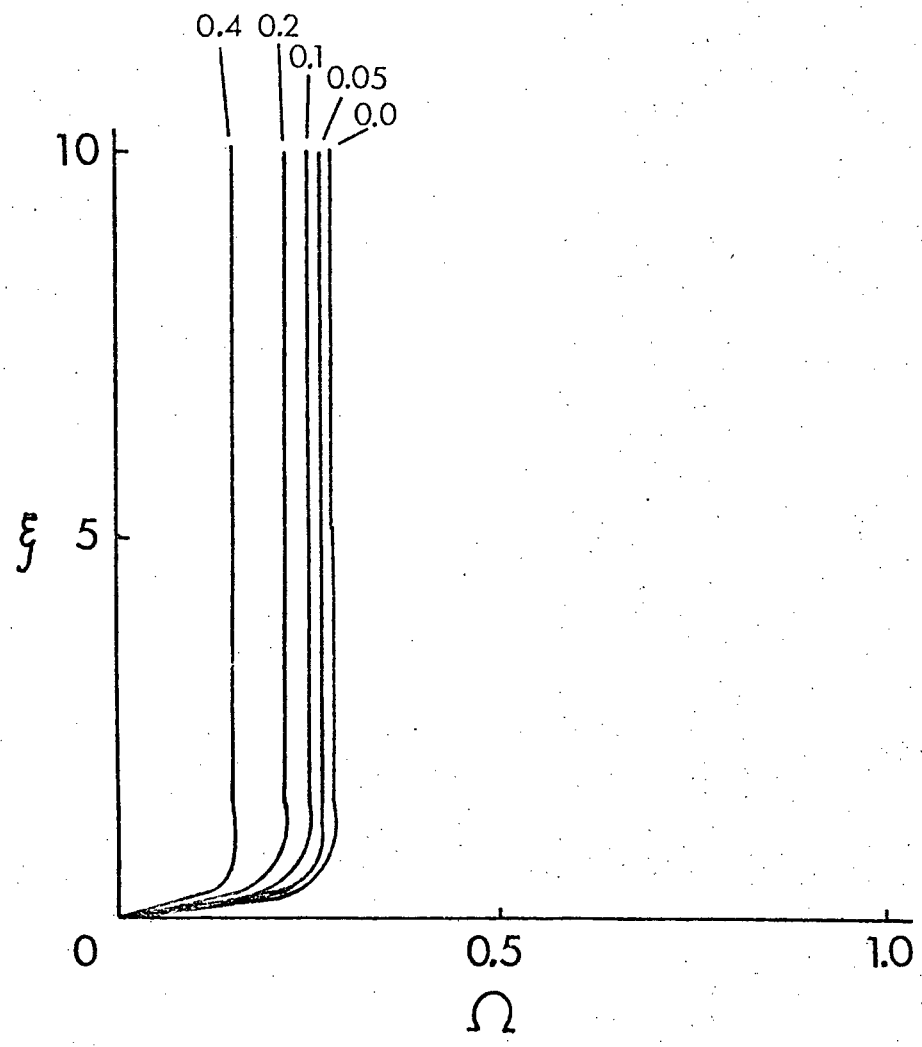

Figure 81d. Contour plot of the function $\Lambda^3(\Omega, \xi)$ for β=10.

β=0, for $\Omega > 0$, decreasing ξ by decreasing z_M results first in an increase in $\lambda+\delta$ as mixing below the euphotic zone decreases and then in a decrease in $\lambda+\delta$ as the loss rate due to sinking out of the mixed layer increases (Fig 81a). For ξ large, the effect of decreasing mixing rate or increasing β is to increase $\lambda+\delta$ for Ω small and decrease $\lambda+\delta$ for Ω large (Fig 81a,b,c,d). In the first case, losses from the euphotic zone due to mixing outweigh losses due to sinking; in the second case, the converse is true.

For β=1, the time scale for mixing over the light penetration depth (1/k) is of the same order as the doubling time of the phytoplankton at the surface but departures from the uniform mixed layer theory occur only at large values of $\xi = k.z_M$ (Fig 81b). For β large, significant departures from the uniformly-mixed layer theory occur at moderate values of ξ. In fact, for β=10, the dependence of $\lambda+\delta$ on Ω is the same for $\xi > 1$ as that derived in the semi-infinite layer theory ($\xi \to \infty$). It can be concluded from Fig 81 that the uniform mixed layer is a good approximation unless the time scale of mixing over the 'mixed layer' is much greater than the minimum doubling time of the phytoplankton. This will occur when $S_M = z_M.(\mu_s/K)^{0.5}$ (=2.ξ .β) is large. The semi-infinite layer theory then becomes a good approximation except for a limited region where ξ is small.

6.5 A General Necessary Condition for Growth.

It was noted earlier that the condition $\lambda+\delta+\omega^2 < 1$ is necessary for a solution for both step-function and exponential

versions of $\mu(z)$, although it was derived from rather different eigen-conditions. A simpler and more general derivation is possible from the differential equation itself. Consider a general version of equation 6.4 :

$$p'' - 2.\omega.p' + (q(\mathcal{S}) - \lambda - \delta).p = 0$$

where it is assumed that the time scale used in non-dimensionalizing is the inverse of the maximum growth rate, so that $q(\mathcal{S}) \leq 1$. Letting $p(\mathcal{S}) = \exp(\omega.\mathcal{S}).h(\mathcal{S})$ as before gives

$$h'' + (q(\mathcal{S}) - (\omega^2 + \lambda + \delta)).h = 0$$

If $\lambda + \delta + \omega^2 > 1$, $q(\mathcal{S}) - (\lambda + \delta + \omega^2) < 0$ for all $\mathcal{S}$ and $h'' > 0$ for all $\mathcal{S}$. The zero-flux boundary condition at $\mathcal{S}=0$ means that $h'(0) > 0$. Since $h'(0) > 0$ and h' increases with $\mathcal{S}$, h increases for all $\mathcal{S}$ and neither the condition $\exp(\omega.\mathcal{S}).h \rightarrow 0$ as $\mathcal{S} \rightarrow \infty$ for a semi-infinite layer, nor the condition $h'(\mathcal{S}_M) = -\omega.h(\mathcal{S}_M)$ for the finite mixed layer discussed in the previous section, can be met. Thus, the requirement $\lambda + \delta + \omega^2 < 1$ represents quite a general condition on populations subject to diffusion and sinking; in particular, if ω (= $w/(2.(K.\mu_S)^{0.5})$) > 1, continued net population growth, or a steady-state population, is not possible.

6.6 Discussion.

As mentioned in the introduction, this chapter has been aimed at a better understanding of the processes of diffusion,

sinking and growth and their interactive effect on phytoplankton growth rates and vertical distribution, rather than an explanation of a specific set of data. The question of the relevance of this theory to real phytoplankton populations remains and is addressed here by considering three related questions:

(a) to what extent do the assumptions and approximations involved in the theory (when compared to what is known of real populations or what is assumed in more complex numerical models) invalidate the conclusions?

(b) are the parameter ranges for which interesting results are predicted by the theory likely to be encountered in the oceans?

(c) do predictions of the theory correspond at least qualitatively to phenomena observed in the oceans?

The assumptions underlying the models discussed here have already been mentioned. Those underlying the last model will now be discussed in more detail as the most general and realistic. The physical structure of the water column is represented by an upper mixed layer bounded below by a thermocline across which no mixing occurs. This latter assumption was justified earlier on the basis of recent measurements of very low diffusion rates in the thermocline. A more probable source of error is the assumption that turbulent mixing within the mixed layer can be represented by a constant eddy diffusion coefficient, K. Mixing in the surface layers of the ocean appears to be a much more complicated affair, being characterized by transient periods of wind-mixing and stratification through heating in the summer and

by convective mixing and wind storms in the winter (Denman,1972). The lack of a better alternative, and its widespread use in numerical models (Winter et al ,1975; Jamart et al ,1977) are considered to justify the use of the diffusion approximation here.

The assumptions made regarding growth rate and its dependence on depth are the same as those made by Sverdrup (1953) and much of the discussion there is still valid. However a number of phenomena such as photoinhibition (Steele,1962), light adaptation (Jorgansen,1969) and short-term vs long-term responses (Marra,1978a,b) are now better understood. In view of these effects, the predictions of the model must be viewed with some caution, especially in the case of very small mixing rates.

The question of phytoplankton sinking rates is also a complex one. The assumption of a constant, positive sinking rate has to be suspect for motile phytoplankters such as flagellates and some dinoflagellates. Even for non-motile phytoplankters such as pelagic diatoms, a non-zero sinking rate in the presence of plentiful nutrient is not clearly established. Positive sinking rates have usually been observed (Smayda,1970), and have been used in previous models (Jamart et al ,1977; Parsons and Takahashi,1973), but under some conditions zero or even positive buoyancy in diatoms has been reported (Smayda,1970).

Both the biological and physical parameters involved in the model can range over at least an order of magnitude and the non-dimensional parameters appearing in the theory have a correspondingly large range. If μ_s is assumed to be close to the maximum growth rate of phytoplankton, values of about 0.5 to 1

day^{-1} are appropriate (Chan,1978). Sinking rates for healthy cells may range from 0 to 5m/day (Smayda,1970) with lower values of less than 1.0 m/day being appropriate for smaller cells at high nutrient concentrations. Extinction coefficients in the ocean can vary from <0.04 m^{-1} in clear ocean water to >0.5 m^{-1} in turbid coastal water (Jerlov,1968). The corresponding range of Ω ($=k.w/\mu_s$) is 0 to 5. Taking w=0.5 m/day and reasonably clear water ($k < 0.25$,say) gives a range for Ω of 0.025 to 0.25, the region of interest in Figure 81.

Mixed layer depths in the ocean can vary from a few meters in highly stratified regions to over 100 metres in the open ocean in some seasons. Although large values of k tend to occur in coastal waters where z_M is small, $\xi = k.z_M$ can range from <1 to >10.

The correct value for K is as uncertain in most cases as the diffusion approximation itself. In a numerical model, Jamart et al (1977) use values of 10 to 40 $cm^2.sec^{-1}$ or about 100 to 400 $m^2.day^{-1}$ for the mixed layer in the open ocean off Oregon. Much smaller values may be appropriate in sheltered, enclosed waters and values as low as 1 to 5 $m^2.day^{-1}$ were recorded in 10m diameter experimental enclosures in Saanich Inlet (Steele et al ,1977). With the values of k and μ_s given above, values of β ranging from <0.05 to >20 are possible.

The ranges of parameters in nature appear to be sufficient to cover the complete range of behaviours found in the analysis of the model. The chapter is concluded by examining the implications of the theory with regard to two specific points. The first concerns Riley et al 's (1949) derivation of a

pronounced sub-surface maximum. It has been shown that this phenomenon is still possible with an exponential production profile for large β, say $\beta > 10$. But if the values of K used by Jamart et al are characteristic of most oceanic mixed layers, values of $\beta > 4$ will not occur, even in the clearest ocean water, and it follows that pronounced deep chlorophyll maxima due solely to a balance between diffusion and sinking do not seem likely in oceanic mixed layers. In fact, observed deep chlorophyll maxima are found below a mixed layer which is usually nutrient depleted, and current explanations rely on this (Jamart et al ,1977). However, the existence of subsurface maxima due solely to a balance between sinking, diffusion and growth, without nutrient depletion, is still at least theoretically possible in sheltered waters.

The second point is concerned with the usefulness of the extension of Sverdrup's spring bloom condition to include diffusion and sinking. It was noted that significant changes to the uniform mixed layer theory occur only when $S_M (= z_M . (\mu_S / K)^{0.5})$ is large. If values for K of 100 to 400 $m^2.day^{-1}$ are used, large values of S_M will be obtained only for deep mixed layers, of order 100m. If these diffusion rates can be used in the deep mixed layers which are present in the open Pacific and Atlantic before the spring bloom , significant corrections to Sverdrup's criterion may be required. These situations correspond to the region of β of order 1 and large ξ in Figure 81. Again, larger values of β can occur in sheltered waters and the correction to Sverdrup's theory may also be significant there, despite the shallower mixed layers.

CHAPTER 7

MATHEMATICAL ANALYSIS OF DEEP CHLOROPHYLL MAXIMA.

7.1 Introduction.

Observations of deep chlorophyll maxima have been reported from the Indian Ocean (Saijo,1973), the Atlantic Ocean and Gulf of Mexico (Hobson and Lorenzen,1972; Steele,1964), and the Pacific Ocean (Anderson,1972). Thse maxima appear to be a widespread and predictable feature of oceans at middle and low latitudes. For an extensive review of this phenomenon the reader is referred to Jamart et al (1977).

Explanations of the phenomenon have ranged in structure from simple hypotheses such as the collection of sinking cells at pycnoclines to sophisticated numerical models incorporating multiple hypotheses (Jamart et al ,1977). Both the physical and chemical properties of the water column and the physiological attributes of the phytoplankton have been appealed to. The former include vertical variations in density, temperature, turbulent mixing, light intensity and nutrient concentration while the latter include the dependence of phytoplankton growth, sinking rate and chlorophyll content on light intensity, nutrient concentration and temperature.

One of the earliest mathematical treatments, due to Riley, Stommel and Bumpus (1949), has been discussed and expanded upon in the previous chapter. It was shown there that pronounced subsurface maxima can be generated in the absence of both nutrient limitation and vertical variation in sinking or mixing rates, but that this required eddy diffusion rates lower than

those usually attributed to oceanic mixed layers. In fact, the subsurface maxima explained by Riley et al were associated with two conditions shared by most other observations of this phenomenon. They tend to be found below the mixed layer (often in or below a seasonal thermocline), (Anderson,1972; Steele,1964) and to occur when nutrient levels in the mixed layer are very low, the maximum itself often coinciding with a pronounced nutricline (Venrick,McGowan and Mantyle,1973). This has resulted in a view of the deep chlorophyll maximum as a 'nutrient trap' (Anderson,1969; Anderson, Parsons and Stephens,1969; Venrick et al ,1973), a view which is supported by the simulation results of Jamart et al (1977).

Some theoretical discussion has been prompted by the relation of the maximum to the compensation depth. Steele and Yentsch (1960) pointed out that the nature of the conservation equation for phytoplankton requires that the maximum concentration must occur above the compensation depth, provided that sinking rate and diffusion rate are constant with depth. However, while maxima are often found below the 1% light level traditionally used to estimate compensation depth (Parsons et al ,1977), recent discussions of adaptation to low light intensity (Winter et al ,1975) have suggested that the 1% light level is an underestimate of compensation depth and there now appears to be a consensus that deep chlorophyll maxima consist of actively-growing, shade-adapted cells (Eppley et al ,1973).

In this section, a theoretical treatment of deep chlorophyll maxima based on coupled equations for phytoplankton and nutrients is given. Although the effects of vertical variation in

diffusion and sinking rates are considered, the emphasis is on the phytoplankton-nutrient interaction and the nutrient-trap hypothesis. The analysis is intended to give general insights into the phenomenon of the deep chlorophyll maximum and the dependence of attributes such as the depth and concentration of the maximum on physical and biological parameters. In this regard, it can be regarded as complementary to the detailed, rationalistic numerical modelling approach taken by Jamart et al (1977), which aimed at explaining a particular set of observations.

7.2 A Phytoplankton-Nutrient Model.

A simple physical structure will be considered first to allow concentration on the phytoplankton-nutrient interaction. A semi-infinite water column is considered with a constant eddy diffusion rate K. The phytoplankton concentration P(z,t) and nutrient concentration N(z,t), both functions of depth z and time t, are subject to diffusion. Phytoplankton also sink at rate w and grow at a rate $\mu(z,N)$ which is dependent on depth (through light intensity) and nutrient concentration. They are also subject to a loss rate d (day^{-1}) due to both respiration and grazing. The appropriate equation, given K and w constant, is:

$$\frac{\partial P}{\partial t} = K.\ \frac{\partial^2 P}{\partial z^2} - w.\ \frac{\partial P}{\partial z} + (\mu(z,N)-d).P \qquad 7.1a$$

If phytoplankton and nutrient concentrations are expressed in the same units, each unit of phytoplankton production corresponds to a unit of nutrient uptake. Some fraction U of the phytoplankton

loss rate d, corresponding to respiration and part of the grazing losses, will be rapidly recycled as nutrient so that the conservation equation for nutrients becomes:

$$\frac{\partial N}{\partial t} = K.\ \frac{\partial^2 N}{\partial z^2} - (\mu(z,N)-d.U).P \qquad 7.1b$$

Boundary conditions at the surface, z=0, are given by the zero-flux condition:

$$K.\ \frac{\partial P}{\partial z} - w.P = 0\ ,\quad \frac{\partial N}{\partial z} = 0 \qquad \text{at } z=0.$$

Boundary conditions at $z = \infty$ turn out to be more problematical and their discussion is postponed for a little.

These equations represent a pair of coupled non-linear second-order partial differential equations and the prospects for obtaining a general solution in closed form are not good. Progress is made by a series of simplications and approximations based on the mathematical form of 7.1 and on the observed properties of chlorophyll maxima in nature. First, the observation that deep chlorophyll maxima are widespread and persistent phenomena (Venrick et al ,1973), which change on time scales of months, much longer than those of phytoplankton growth, allows us to look for steady-state solutions of 7.1 which satisfy:

$$K.P'' - w.P' + (\mu(z,N)-d).P = 0 \qquad 7.2a$$

$$K.N'' - (\mu(z,N)-U.d).P = 0 \qquad 7.2b$$

The problem is reduced to that of solving coupled ordinary

differential equations. The equations are still non-linear and further approximation will be necessary to obtain solutions in closed form, but the problem of defining boundary conditions at $z = \infty$ must be addressed first. By combining 7.2a and 7.2b and integrating twice, the nutrient concentration at depth z can be written as:

$$N(z) = N(0) - P(0) + P(z) + (w/K).\int_o^z P(s).ds + (d.(1-U)/K).\int_o^z\int_o^u P(s).ds.du$$

As long as $U < 1$, the last term is unbounded as $z \rightarrow \infty$, making it impossible for N(z) to satisfy any physically reasonable boundary condition there. The physical basis of this problem is simple: provided $U < 1$, there is a net loss from the combined phytoplankton-nutrient pool which must be balanced by diffusion from below. Since the diffusive flux of nutrient upward through any depth z is $K\partial N/\partial Z$, this term must approach some positive, non-zero value as $z \rightarrow \infty$ to balance the total loss of nutrient in the water column above.

Of course, nutrient concentrations do not increase in this fashion in the ocean and there are a number of processes omitted from this simple model which account for it. In reality, the net loss from the phytoplankton-nutrient pool discussed above enters a number of other pools ranging from particulate and dissolved detritus to higher trophic levels. Much of this nutrient is eventually returned to the inorganic pool by processes varying greatly in spatial distribution and time scale, and that which is lost to sedimentation or terrestrial predators is replaced by

coastal runoff or sources such as nitrogen fixation. All these processes making up the large-scale nutrient cycle of the oceans (Parsons and Harrison,1981) maintain a constant deep nutrient concentration despite short-term fluctuations in the upper layers. There is no point in introducing these processes into the simple model as they involve a vast range of time scales, some of which, particularly those of detrital pools, are still controversial (Menzel,1974; Ichikawa and Nishizawa,1975).

A simple alternative, used by Jamart et al (1977), is to fix the nutrient concentration at some finite depth z_L, well below the chlorophyll maximum, at a high 'deep-water' value, N_L. On the time scale of a few months over which deep chlorophyll maxima persist, this is a reasonable condition, in keeping with observations, although processes other than those represented in 7.2 are needed to explain it.

We now seek an approximate steady-state solution to 7.2 corresponding to a deep chlorophyll maximum. It was noted in the introduction that these maxima are typically found in the vicinity of a nutricline, below a region of nutrient depletion. This suggests that the water column may be divided into two regions: an upper layer in which nutrient concentrations are low and growth is nutrient-limited, and a lower region in which nutrients are plentiful and growth is light-limited. This approach is facilitated by using a limiting factor or Liebig approach to the interaction of light and nutrients (Droop,1977) :

$$\mu(z,N) = \min(\mu_1(z),\mu_2(N))$$

where, for simplicity, growth is assumed to depend linearly on light and nutrient concentration separately :

$$\mu_1(z) = \mu_s.\exp(-k.z),\ \mu_2(N) = \mu_s.N/N_R\ .$$

Then, corresponding to the two regions described above, there exist some depth z_T and nutrient concentration $N_T = N_R\exp(-k.z_T)$ such that, for $z > z_T$, $N > N_T$ and $\mu(z,N)=\mu_1(z)$, while for $z < z_T$, $N < N_T$ and $\mu(z,N)=\mu_2(N)$. It is convenient at this point to non-dimensionalize by scaling time and depth as in the previous section:

$$S = z.(\mu_s/K)^{0.5}\ ,\quad S_T = z_T.(\mu_s/K)^{0.5}\ ,\quad S_L = z_L.(\mu_s/K)^{0.5}\ ,$$
$$\tau = \mu_s.t\ ,\quad \omega = w/(2.(\mu_s.K)^{0.5})\ ,\quad \beta = 2.(\mu_s/K)^{0.5}/k\ .$$

On substituting in 7.2, we obtain for $S < S_T$:

$$P'' - 2.\omega.P' + (N/N_R - \delta).P = 0$$
$$N'' - (N/N_R - U.\delta).P = 0 \qquad 7.3a$$

and for $S > S_T$:

$$P'' - 2.\omega.P' + (\exp(-2.S/\beta) - \delta).P = 0$$
$$N'' - (\exp(-2.S/\beta) - U.\delta).N = 0 \qquad 7.3b$$

with boundary conditions:

$$P'(0) = 2.\omega.P(0)\ ,\ N'(0) = 0\ ,\ P \to 0 \text{ as } S \to \infty\ ,\ N(S_L) = N_L\ ,$$

and P, N, P' and N' continuous at $S = S_T$.

The boundary conditions on N and P may now appear inconsistent since N is only defined on $(0, S_L)$, but the equation governing P is independent of N for $S > S_T$, so that a solution for P can be defined on $(0, \infty)$ and the boundary condition $P \to 0$ as $S \to \infty$ applied. (Jamart et al used the boundary condition $P'(S_L) = 0$ but this assumption of zero diffusive flux of phytoplankton across $S = S_L$ is inconsistent with their boundary condition $N(S_L) = N_L$ which implies a diffusive flux of nutrient across the same depth. The results of the previous chapter do suggest that, for S_L sufficiently large, their boundary condition on the phytoplankton will produce similar results to mine).

The system 7.3b is linear and the solution for P was obtained in the previous chapter:

$$P = P_T.\exp(\omega.(S - S_T)).J_\nu(\beta.\exp(-S/\beta))/J_\nu(\beta.\exp(-S_T/\beta)) \qquad 7.4$$

where $\nu = \beta.(\omega^2 + \delta)^{0.5}$. Integrating the equation for N twice gives:

$$N = N_T + N'(S_T).(S - S_T) + \int_{S_T}^{S}\int_{S_T}^{u} (\exp(-2.s/\beta) - U.\delta).P(s).ds.du .$$

The boundary condition $N(S_L) = N_L$ represents a condition linking N_T, $N'(S_T)$, N_L and P_T.

For $S < S_T$, the problem is still non-linear and an approximate solution must be found. The approach taken here is suggested by recent evidence that phytoplankton can take up

nutrients and grow rapidly at very low nutrient concentrations (eg Goldman and McCarthy,1978); that is, that N_R is very small. If in particular $N_R << P_T$, define

$$n = N/N_R \ , \ n_T = N_T/N_R \ (= \exp(-k.z_T)) \ , \ p = P/P_T \ , \ \varepsilon^2 = N_R/P_T .$$

Substitution in the equations 7.3a gives:

$$p'' - 2.\omega.p' + (n-\delta).p = 0$$
$$n'' - (n-U.\delta).p/\varepsilon^2 = 0. \qquad 7.5$$

An exact outer solution of 7.5, satisfying the surface boundary condition, is

$$p^\circ = C_1.\exp(\omega.\zeta).(\cosh(a.\zeta) + \omega.\sinh(a.\zeta)/a)$$
$$n^\circ = U.\delta \qquad 7.6$$

where $a = (\omega^2+(1-U).\delta)^{0.5}$. However, this solution cannot satisfy the boundary condition $n(\zeta_T) = n_T$, so we must look for an inner or boundary layer solution by writing

$$p = p^\circ(\zeta)+p^i(\xi) \ , \ n = n^\circ(\zeta)+n^i(\xi)$$

where $\xi = (\zeta - \zeta_T)/\varepsilon$. Substituting for p,n in 7.5 gives :

$$p^i'' - 2.\varepsilon.\omega.p^i' + \varepsilon^2.(n^i-(1-U).\delta).(p^\circ(\zeta_T + \varepsilon.\xi)+p^i) = 0$$
$$n^i'' - n^i.(p^\circ(\zeta_T+\varepsilon.\xi)+p^i) = 0 \qquad 7.7$$

We now expand p^i and n^i in powers of ε :

$$p^i = p^i_o(\xi) + \varepsilon.p^i_1(\xi) + \ldots \quad , \quad n^i = n^i_o(\xi) + \varepsilon.n^i_1(\xi) + \ldots$$

To order ε^o, 7.7 becomes :

$$p^i_o{}'' = 0 \quad , \quad n^i_o{}'' - n^i_o.(p^o(S_T) + p^i_o) = 0.$$

Using the conditions p^i_o, $n^i_o \to 0$ as $\xi \to -\infty$ yields $p^i_o = 0$, $n^i_o = C_2.\exp(\xi)$. Collecting terms of order ε^1 in 7.7 gives :

$$p^i_1{}'' - 2.\omega.p^i_o{}' = 0$$
$$n^i_1{}'' - n^i_1.p^o(S_T) - n^i_o.p^o{}'(S_T).\xi = 0$$

and the matching conditions p^i, $n^i \to 0$ as $\xi \to -\infty$ imply that $p^i_1 = 0$, $n^i_1 = C_2.p^o{}'(S_T).\exp(\xi).(\xi^2 - \xi)/4$. Thus, to order ε^1, the solution for $S < S_T$ is :

$$P(S) = P_T.\exp(\omega.S).C_1.(\cosh(a.S) + \omega.\sinh(a.S)/a)$$

$$N(S) = N_R.U.S + C_2.\exp(\xi).(1 + \varepsilon.p^o{}'(S_T).(\xi^2 - \xi)/4)$$

To complete the solution, the continuity conditions for P, N, dP/dS, dN/dS must be satisfied at $S = S_T$. The continuity condition for P, N is simply a matter of defining the constants C_1, C_2 so that $P(S_T -) = P_T$, $N(S_T -) = N_T$. For $S < S_T$,

$$dP/dS = P_T.(dp^o/dS + (1/\varepsilon).(dp^i_o/d\xi + \varepsilon.dp^i_1/d\xi + O(\varepsilon^2))$$
$$= P_T.dp^o/dS + O(\varepsilon^2) \qquad 7.8$$

so that, to order ε^o, the continuity condition for dP/dS at $S =$

S_T becomes :

$$(a.\sinh(a.S_T)+\omega.\cosh(a.S_T))/(\cosh(a.S_T)+\omega.\sinh(a.S_T)/a)$$
$$+\exp(-S_T/\beta).J_\nu'(\beta.\exp(-S_T/\beta))/J_\nu(\beta.\exp(-S_T/\beta)) = 0 \qquad 7.9$$

For $S < S_T$,

$$dN/dS = N_R.(dn^\circ/dS + (1/\varepsilon).(dn_\circ^!/d\xi + \varepsilon.dn_1^!/d\xi + O(\varepsilon^2))$$
$$= P_T.\varepsilon^2.((n_T - U.\delta)/\varepsilon + dn_1^r/d\xi) \text{ , so}$$

$$N'(S_T) = \varepsilon.P_T.(\exp(-2.S_T/\beta) - U.\delta) + O(\varepsilon^2)$$

Substituting in equation 7.4 for $N(S)$, $S > S_T$, gives :

$$N = \varepsilon^2.P_T.\exp(-2.S_T/\beta) + \varepsilon.P_T.(\exp(-2.S_T/\beta) - U.\delta).(S - S_T)$$
$$+\int_{S_T}^{S}\int_{S_T}^{u} (\exp(-2.s/\beta) - U.\delta).P(s).ds.du$$

so, for S_L large, the boundary condition at $S = S_L$ becomes :

$$N = \int_{S_T}^{S_L}\int_{S_T}^{u} (\exp(-2.s/\beta) - U.\delta).P(s).ds.du + O(\varepsilon) \qquad 7.10$$

On collecting these results together then, we have a solution to order ε° in $0 < S < S_L$ of the form :

$$P = P_T.\exp(\omega.(S - S_T).(\cosh(a.S) + \omega.\sinh(a.S)/a)$$
$$/ (\cosh(a.S_T) + \omega.\sinh(a.S_T)/a) \qquad \text{for } S < S_T$$
$$P = P_T.\exp(\omega.(S - S_T)).J_\nu(\beta.\exp(-S/\beta))/J_\nu(\beta.\exp(-S_T/\beta))$$
$$\text{for } S > S_T$$

$$N = N_R.(U.\delta + \exp(-(2.\mathcal{S}_T/\beta) - U.\delta).\exp((\mathcal{S} - \mathcal{S}_T)/\varepsilon) \quad \text{for } \mathcal{S} < \mathcal{S}_T$$

$$N = N_R.\exp(-2.\mathcal{S}_T/\beta) + \varepsilon.P_T.(\exp(-2.\mathcal{S}_T/\beta) - U.\delta).(\mathcal{S} - \mathcal{S}_T) + \int_{\mathcal{S}_T}^{\mathcal{S}}\int_{\mathcal{S}_T}^{u} (\exp(-2.s/\beta) - U.\delta).P(s).ds.du \quad \text{for } \mathcal{S} > \mathcal{S}_T, \qquad 7.11$$

with $\mathcal{S}_T$ determined by equation 7.9 and P_T determined by equation 7.10.

This approximate solution, although algebraically complicated, has a simple physical interpretation. Phytoplankton have been assumed to be able to take up nutrient and grow at near maximum rates at very low nutrient concentrations. As a result, the layer where phytoplankton growth rate actually varies with nutrient concentration (and the governing equations are nonlinear) is thin compared with mixing length scales, the nutrient concentration being rapidly reduced by phytoplankton uptake within this layer to the equilibrium level $N_R.U.\delta$ at which uptake is balanced by nutrient recycling. When this layer is thin enough, it has a negligible influence on the distribution of phytoplankton which, to first order, is obtained by matching the outer solution ($N = N_R.U.\delta$) above the layer with the light-limited solution below. In particular, the depth and shape of the phytoplankton maximum is determined to this approximation by the light-limited kinetics and grazing and respiration losses, as almost all net growth occurs in the light-limited region. Decreasing the grazing rate will tend to deepen the phytoplankton maximum as a smaller growth rate is then needed to balance grazing losses. The nutrient concentration in deep water, N_L, does not affect the depth or shape of the maximum but does

determine the amount of phytoplankton present. The details of the dependence of phytoplankton growth rate on nutrient concentration have a negligible influence on the phytoplankton distribution and abundance, provided the basic approximation remains valid.

7.3 Effect of a Mixed Layer.

As most deep maxima are found below a mixed layer, the assumption of a constant diffusion rate in the above discussion is rather unrealistic. The simplest way to introduce a mixed layer is to use a step-function form for the dependence of diffusion rate on depth :

$$K(z) = \begin{cases} Q.K & z < z_M \\ K & z > z_M \end{cases}$$

where Q is a large constant. We are interested in the case $z_M < z_T$, that is, in phytoplankton maxima below the mixed layer. Provided $(\mathcal{S}_T - \mathcal{S}_M)/\mathcal{E}$ is large enough, the previous analysis can be applied with only one change; namely that the outer solution in the region $\mathcal{S} < \mathcal{S}_T$ must be solved in the two layers $\mathcal{S} < \mathcal{S}_M$ and $\mathcal{S} > \mathcal{S}_M$ with continuity of p°, n° at $\mathcal{S} = \mathcal{S}_M$ and the flux conditions: $Q.p^{\circ\prime}(\mathcal{S}_M^-) = p^{\circ\prime}(\mathcal{S}_M^+)$ and $Q.n^{\circ\prime}(\mathcal{S}_M^-) = n^{\circ\prime}(\mathcal{S}_M^+)$. The solution is:

$$N = N_R.U.\mathcal{S} \quad \text{for} \quad \mathcal{S} < \mathcal{S}_T$$

$$P = C_4.\exp(\omega.\mathcal{S}/Q).(\cosh(a_M.\mathcal{S}) + \omega.\sinh(a_M.\mathcal{S})/(a_M.Q))$$

$$\text{for} \quad \mathcal{S}_M > \mathcal{S} \ ,$$

$$P = \exp(\omega.(\mathcal{S} - \mathcal{S}_M).(C_5.\cosh(a.(\mathcal{S} - \mathcal{S}_M)) + C_6.\sinh(a.(\mathcal{S} - \mathcal{S}_M)))$$

$$\text{for } \mathcal{S}_M < \mathcal{S} < \mathcal{S}_T ,$$

where $a_M = (\omega^2 + (1-U).\delta.Q)^{0.5}/Q$, $a = (\omega^2 + (1-U).\delta)^{0.5}$ as before, and the continuity conditions give:

$$C_5 = C_4.\exp(\omega.\mathcal{S}_M/Q).(\cosh(a_M.\mathcal{S}_M) + \omega.\sinh(a_M.\mathcal{S}_M)/(a_M.Q))$$

$$C_6 = C_4.\exp(\omega.\mathcal{S}_M/Q).(a_M.Q/a).(\sinh(a_M.\mathcal{S}_M) + \omega.\cosh(a_M.\mathcal{S}_M)/(a_M.Q))$$

The constant C_4 is determined by $P(\mathcal{S}_T) = P_T$.
This solution is rather complicated and can be simplified considerably if the diffusion rate in the mixed layer is high enough. For Q sufficiently large or, more accurately, $\mathcal{S}_M/Q$ sufficiently small, the outer solution can be approximated by :

$$P = P(\mathcal{S}_M) \qquad \text{for } \mathcal{S} < \mathcal{S}_M$$

$$P = P(\mathcal{S}_M).\exp(\omega.(\mathcal{S} - \mathcal{S}_M).(\cosh(a.(\mathcal{S} - \mathcal{S}_M)) + (\omega + (1-U).\delta.\mathcal{S}_M).\sinh(a.(\mathcal{S} - \mathcal{S}_M))/a) \qquad \text{for } \mathcal{S}_M < \mathcal{S} < \mathcal{S}_T$$

7.12

where, as before, the condition $P(\mathcal{S}_T) = P_T$ determines $P(\mathcal{S}_M)$.

From 7.12, $P'(\mathcal{S}_M^+) = 2.\omega.P(\mathcal{S}_M^+) + (1-U).\delta.\mathcal{S}_M.P(\mathcal{S}_M^+)$ and this has a simple physical interpretation. For Q sufficiently large, the mixed layer becomes uniformly mixed with phytoplankton concentration $P(\mathcal{S}_M)$ and nutrient concentration $N_R.U.\delta$. There is a resultant local loss rate $(1-U).\delta$ for phytoplankton in this layer, or total loss rate of $(1-U).\delta.\mathcal{S}_M.P(\mathcal{S}_M)$ in the mixed layer. If a steady state is to be maintained, this loss must be balanced by a net flux upwards through $\mathcal{S} = \mathcal{S}_M$ which is given by

$P'(\mathcal{S}_M^+) - 2.\omega.P(\mathcal{S}_M^+)$.

7.4 Effect of Nutrient Dependent Sinking rates.

The dependence of phytoplankton sinking rates on nutrient concentration was associated with deep chlorophyll maxima by Steele (1960). A recent discussion is given by Jamart et al (1977). The quantitative details of this dependence have not yet been fully uncovered by experiment. In fact, even the direction of the relationship has been called into question by recent experiments (P. J. Harrison and P. Bienfang,pers. comm.). The traditional increase in sinking rate with nutrient depletion is assumed here and it is simplest to associate this effect with nutrient limitation of growth. In the context of a chlorophyll maximum solution, with nutrient limited growth for $\mathcal{S} < \mathcal{S}_T$, $N < N_T$, and light-limited growth for $\mathcal{S} > \mathcal{S}_T$, $N > N_T$, it seems reasonable to take

$$w(z) = \begin{cases} w \text{ (constant)} & \text{for } N > N_T \\ w.(1+X.(1-N/N_T)) & \text{for } N < N_T \end{cases}$$

as a first approximation. The form of the solution for $\mathcal{S} > \mathcal{S}_T$ is unchanged. For $\mathcal{S} < \mathcal{S}_T$, equation 7.5 becomes

$$p'' - 2.\omega.(1+X(1-n/n_T)).p' + 2.\omega.X.p.n'/n_T + (n-\delta).p = 0$$
$$n'' - (n-U.\delta).p/\varepsilon^2 = 0 \qquad 7.13$$

The outer solution to 7.13 is given by

$$n^\circ = U.\delta$$

$$p^\circ = C_7.\exp(\omega_1.(\mathcal{S} - \mathcal{S}_T)).(\cosh(a_1.\mathcal{S}) + \omega_1.\sinh(a_1.\mathcal{S})/a_1)$$

where $a_1 = (\omega_1^2 + (1-U).\delta)^{0.5}$ and $\omega_1 = \omega.(1+X.(1-U.\delta/n_T))$. As before, an inner solution is sought by writing $p = p^\circ + p^i(\xi)$ where $\xi = (\mathcal{S} - \mathcal{S}_T)/\varepsilon$. Expanding p^i, n^i in powers of ε and substituting in 7.12, we get as before, to order ε°:
$p_\circ^i = 0$, $n_\circ^i = (n_T - U.\delta).\exp(\xi)$. However, to order ε^1, the equation for p^i becomes :

$$d^2p_1^i/d\xi^2 + 2.\omega.X.(1-U.\delta/n_T).\exp(\xi) = 0,$$

with solution :

$$p_1^i = 2.\omega.X.(1-U.\delta/n_T).(1-\exp(\xi)).$$

For $\mathcal{S} < \mathcal{S}_T$, neglecting terms of order ε^1 or smaller, we have :

$$P = P_T.\exp(\omega_1.(\mathcal{S} - \mathcal{S}_T).C_7.(\cosh(a_1.\mathcal{S}) + \omega.\sinh(a_1.\mathcal{S})/a_1))$$
$$dP/d\mathcal{S} = P_T.(dp^\circ/d\mathcal{S} + (1/\varepsilon).(dp_\circ^i/d\xi + \omega.dp_1^i/d\xi + \ldots))$$
$$= P_T.(dp^\circ/d\mathcal{S} - P_T.2.\omega.X.(1-U.\delta./n_T).\exp((\mathcal{S} - \mathcal{S}_T)/\varepsilon)$$

At $\mathcal{S} = \mathcal{S}_T$, $P = P_T$ implies that

$$C_7 = (\cosh(a_1.\mathcal{S}_T) + \omega_1.\sinh(a_1.\mathcal{S}_T)/a_1)^{-1}$$

and

$$P'(\mathcal{S}_T^-) = P_T.dp^\circ/d\mathcal{S}(\mathcal{S}_T) - P_T.2.\omega.X.(1-U.\delta/n_T) \qquad 7.14$$

Comparing 7.14 with the equivalent formula in the case of

constant sinking rate (equation 7.8), and recalling that the solution for $S > S_T$ has the same form in both cases, it can be seen that, to zeroth order in ε, the only effect of variable sinking rate is the additional term $-P_T.2.\omega.X.(1-U.\delta/n_T)$ which appears in the continuity condition for dP/dS at $S = S_T$. But this term is just equal to $-P_T.2.(\omega_1 - \omega)$ and again there is a simple interpretation. Just as in the case of growth rate, the layer over which sinking rate varies with nutrient concentration is thin enough that the zeroth order solution for P is obtained by matching the outer solution for $S < S_T$, where $N = U.\delta.N_R$ and $w=w_1$, to the solution for $S > S_T$. The additional term which appears in the continuity condition for dP/dS at $S = S_T$ ensures compliance with the physical requirement that the vertical flux $dP/dS - 2.\omega.P$ be continuous at $S = S_T$.

The full solution for the case of nutrient-dependent sinking rate can be obtained from the solution for constant sinking rate, 7.11, by substituting ω_1, a_1 in the formula for $P(S)$, $S < S_T$, and replacing equation 7.9 for S_T by

$$0 = \omega - \omega_1 + (a_1.\sinh(a_1.S_T) + \omega_1.\cosh(a_1.S_T)) \\ /(\cosh(a_1.S_T) + \omega_1.\sinh(a_1.S_T)/a_1) \\ + \exp(-S_T/\beta).J_\nu'(\beta.\exp(-S_T/\beta))/J_\nu(\beta.\exp(-S_T/\beta))$$

7.5 Discussion.

The contour plot of S_T/β vs ω,β for $\delta=0.1$ and $U=0.5$ (Fig 82) was obtained by solving equation 7.9 numerically and serves to illustrate a number of features of the approximate solution. As we might expect, increasing ω with β fixed produces a decrease in S_T/β : growth must occur at higher light

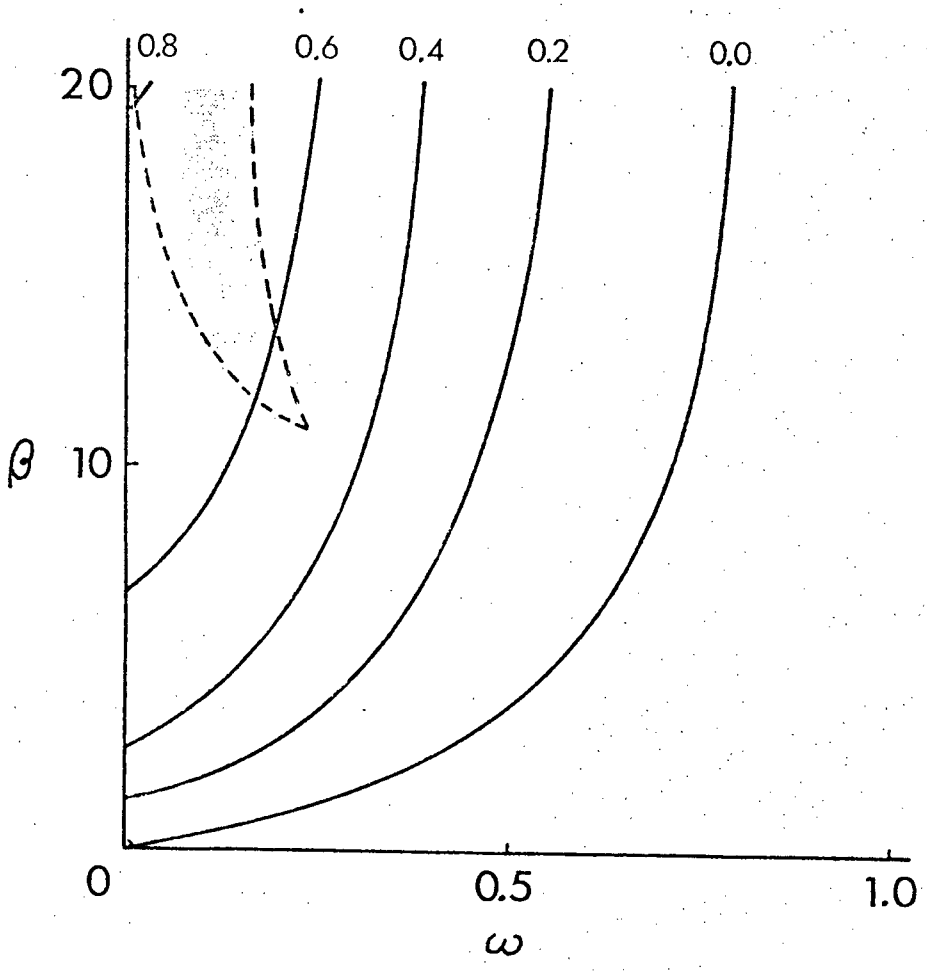

Figure 82. Contour plot of $\mathcal{S}_T/\beta$ vs ω,β for $\delta=0.1$. The shaded region corresponds to $P_T/P(0) > 20.$, $P_{max}/P_T < e$.

intensities to compensate for increased sinking losses. Increasing β with ω fixed increases not only S_T but also S_T/β ; this is due to the decreased importance of sinking losses from the euphotic zone. Note that the $S_T/\beta = 0$ contour is identical to the $\lambda+\delta = 0$ contour in Fig 79. This is just the set of values of (ω,β) for which a purely light-limited steady-state is possible.

Three examples of steady-state phytoplankton profiles predicted by 7.11 are given in Figure 83. The first is typical of profiles for small ω and β. As found in chapter 6, phytoplankton concentration varies slowly with depth and there is no pronounced subsurface maximum for β small. For β and ω both large, Fig 83b, S_T/β is small and almost all the increase in P occurs below $S = S_T$. This situation is close to the purely light-limited chlorophyll maxima found in the previous section and is of little interest here as $P_T << P_{MAX}$ (the peak phytoplankton concentration) and the condition $P_T >> N_R$, required for the approximate solution to be valid, is unlikely to be fulfilled.

The profile in Figure 83c, corresponding to large β and small ω can be regarded as a typical example of the 'nutrient trap' chlorophyll maximum sought here. Note that almost all the increase in P with depth occurs above S_T. The region in the (ω,β) plane corresponding to solutions of this type has been defined roughly by the conditions $P_T/P(0) > 20$ and $P_{MAX}/P_T < e$ (shaded area in Fig 82). The region is relatively small and even in this region $S_T/\beta < 1$ which means that the zone of nutrient-limited growth cannot extend below the depth at which the light

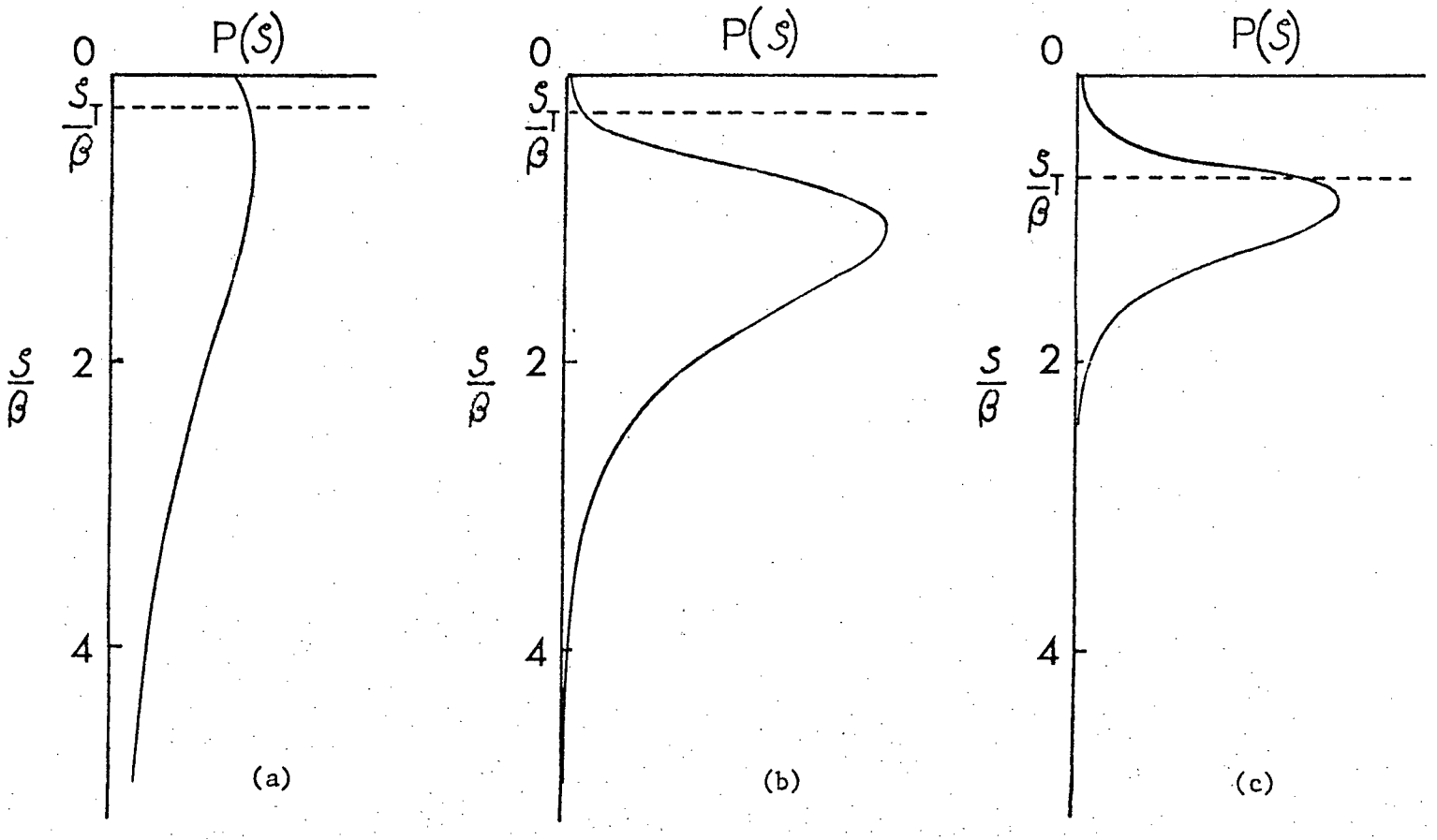

Figure 83. Characteristic profiles $P(S)$ vs S/β for $\delta=0.1$ and (a) $\beta=2.$, $\omega=0.1$, (b) $\beta=2.$, $\omega=0.5$ and (c) $\beta=20.$, $\omega=0.1$.

intensity is reduced to 10% of its surface value. This is not surprising as, for δ =0.1, the depth of 10% suface light intensity corresponds to zero net phytoplankton growth and, as Steele and Yentsch (1960) have pointed out, when diffusion and sinking rates are constant, the chlorophyll maximum must occur above this depth.

To explain deeper chlorophyll maxima, a smaller value of δ is needed and this requires a more careful examination of our assumed growth law for phytoplankton. The net growth rate of phytoplankton has been assumed to have the form :

$$\mu_{net} = \mu_s.(\min(\exp(-k.z) , N/N_R) - \delta)$$

where $d = \mu_s.\delta$ is the combined loss rate due to respiration and grazing. If μ_s is less than or equal to the true maximum growth rate of the phytoplankton (μ_{MAX}), δ is probably of order 0.1, even in the absence of grazing (Ryther,1956). However, for a shade-adapted population at low light intensity and high nutrient concentration, the gross growth rate will be $\mu = \alpha.I/V$ where α is the photosynthetic efficiency (mg C.mg Chl $a^{-1}.ly^{-1}$) and V is the C:Chl a ratio. If $I = I_o.\exp(-k.z)$, then $\mu_s = \alpha.I_o/V$ and μ_s need not be an attainable growth rate. For example, a value of α =1 (Hameedi,1977; Chan,1978) and V = 20 (Anderson <u>et al</u>,1969) together with a surface light intensity of 200 ly/day produces a value for μ_s of 10 day^{-1}. Since the maximum growth rate achieved in a solution of the form 7.11 is $\mu_T = \mu_s.\exp(-k.z_T)$, the solution will still be biologically meaningful provided z_T is large enough to make $\mu_T < \mu_{MAX}$.

The non-dimensional parameters β, ω and δ all involve the parameter μ_S which was used to scale time. Since μ_S may be an order of magnitude greater than μ_{MAX}, it is preferable to introduce a new set of non-dimensional parameters using μ_{MAX} to scale time. If $\Theta = \mu_{MAX}/\mu_S$, the rescaled parameters

$$\beta^* = \beta.\Theta^{0.5}, \quad \omega^* = \omega.\Theta^{-0.5} \text{ and } \quad \delta^* = \delta/\Theta$$

are independent of μ_S. The effect of shade adaptation on deep chlorophyll maxima can be seen by decreasing Θ while keeping β^*, ω^* and δ^* fixed. On setting $\varphi = S/\beta$ (=k.z/2), $\varphi_T = S_T/\beta$, equation 7.11 for the phytoplankton profile and equation 7.9, which determines S_T, can be rewritten in terms of β^*, ω^*, and δ^* as:

$$P(\varphi)/P_T = \exp(\omega^*.\beta^*.(\varphi-\varphi_T)).(\cosh(a^*.\varphi)+\beta^*.\omega^*.\sinh(a^*.\varphi)/a^*) \\ /(\cosh(a^*.\varphi)+\beta^*.\omega^*.\sinh(a^*.\varphi)/a^*) \quad \text{for } \varphi < \varphi_T,$$

$$P(\varphi)/P_T = \exp(\omega^*.\beta^*.(\varphi-\varphi_T).J_\nu(\beta^*.\Theta^{-0.5}.\exp(-\varphi)) \\ /J_\nu(\beta^*.\Theta^{-0.5}.\exp(-\varphi_T)) \quad \text{for} \quad > \quad . \qquad 7.15$$

$$0 = (a^*.\sinh(a^*.\varphi)+\omega^*.\beta^*\cosh(a^*.\varphi_T)) \\ /(\cosh(a^*.\varphi_T)+\beta^*.\omega^*.\sinh(a^*.\varphi_T)/a^*) \\ + \beta^*.\Theta^{-0.5}.\exp(-\varphi_T).J_\nu'(\beta^*.\Theta^{-0.5}.\exp(-\varphi_T)) \\ /J_\nu(\beta^*.\Theta^{-0.5}.\exp(-\varphi_T)) \qquad 7.16$$

where $a^* = \beta^*.(\omega^{*2}+(1-U).\delta^*)^{0.5}$, $\nu = \beta^*.(\omega^{*2}+\delta^*)^{0.5}$ are independent of Θ. The cases of interest are those with $P_T >> P(0)$ or $a^*.\varphi_T >> 1$. Then for φ of order φ_T, $\cosh(a^*.\varphi)$ and $\sinh(a^*.\varphi)$ can be approximated by $\exp(a^*.\varphi)/2$ and equations

7.15 and 7.16 become approximately

$$P(\varphi)/P_T = \exp(\omega^*.\beta^*.(\varphi - \varphi_T)).\exp(a^*.(\varphi - \varphi_T)) \quad \text{for } \varphi < \varphi_T$$

$$P(\varphi)/P_T = \exp(\omega^*.\beta^*.(\varphi - \varphi_T)).J_\nu(\beta^*.\exp(-(\varphi - \varphi_T)-(\varphi_T - \varphi_c))) / J_\nu(\beta^*.\exp(-(\varphi_T - \varphi_c))) \quad \text{for } \varphi > \varphi_T \qquad 7.17$$

$$\beta^*.\exp(-(\varphi_T - \varphi_c).J'_\nu(\beta^*.\exp(-(\varphi_T - \varphi_c)))/J_\nu(\beta^*.\exp(-(\varphi_T - \varphi_c))) + a^* = 0 \qquad 7.18$$

Here, φ_c is defined by $\exp(-2.\varphi_c) = \Theta$ and can be interpreted as the non-dimensional increase in the compensation depth due to shade-adaptation.

Equation 7.18 determines a value of $\varphi_T - \varphi_c$ which is independent of Θ, while equation 7.17 determines $P(\varphi)/P_T$ as a function of $\varphi - \varphi_T$ and $\varphi_T - \varphi_c$ only. Thus, in the case of pronounced deep chlorophyll maxima due to nutrient limitation, the effect of increasing shade adaptation is to increase the depth of nutrient depletion by an amount equal to the increase in compensation depth, and to translate the phytoplankton profile by the same amount while preserving its shape. An example is given in Fig 84 where the profile from Fig 83c with $\Theta = 1$ is reproduced along with a corresponding profile with $\Theta = 0.1$. In Fig 85, the contour plot of Fig 82 has been replotted as $\varphi_T - \varphi_c$ vs β^*, ω^* and the corresponding plot for $\Theta = 0.1$ superimposed. For β^* large, the condition $a^*.\varphi_T >> 1$ is fulfilled and the contours are almost coincident, as predicted by 7.18.

The introduction of a mixed layer of depth $z_M < z_T$ resulted in an algebraically complicated form for $P(S)$, $S < S_T$, which

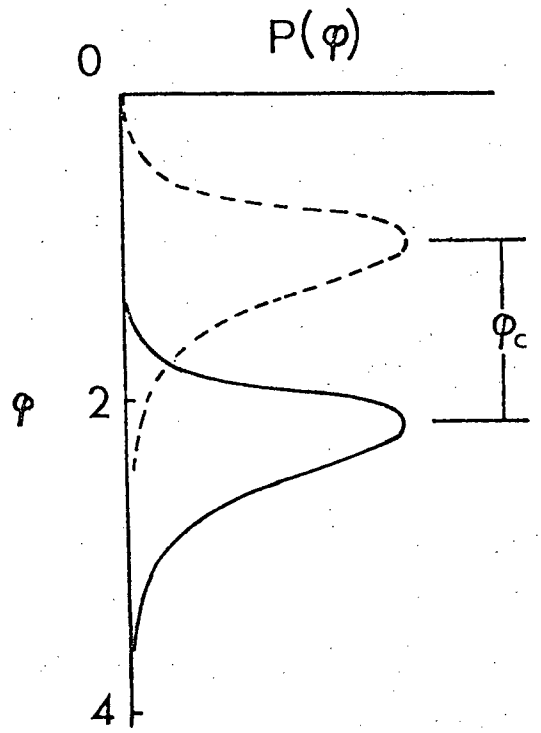

Figure 84. Phytoplankton profiles $P(\varphi)$ vs φ for $\beta^* = 20.$, $\omega^* = 0.1$ and $\delta^* = 0.1$. Dashed line corresponds to $\theta = 1.$, solid line to $\theta = 0.1$.

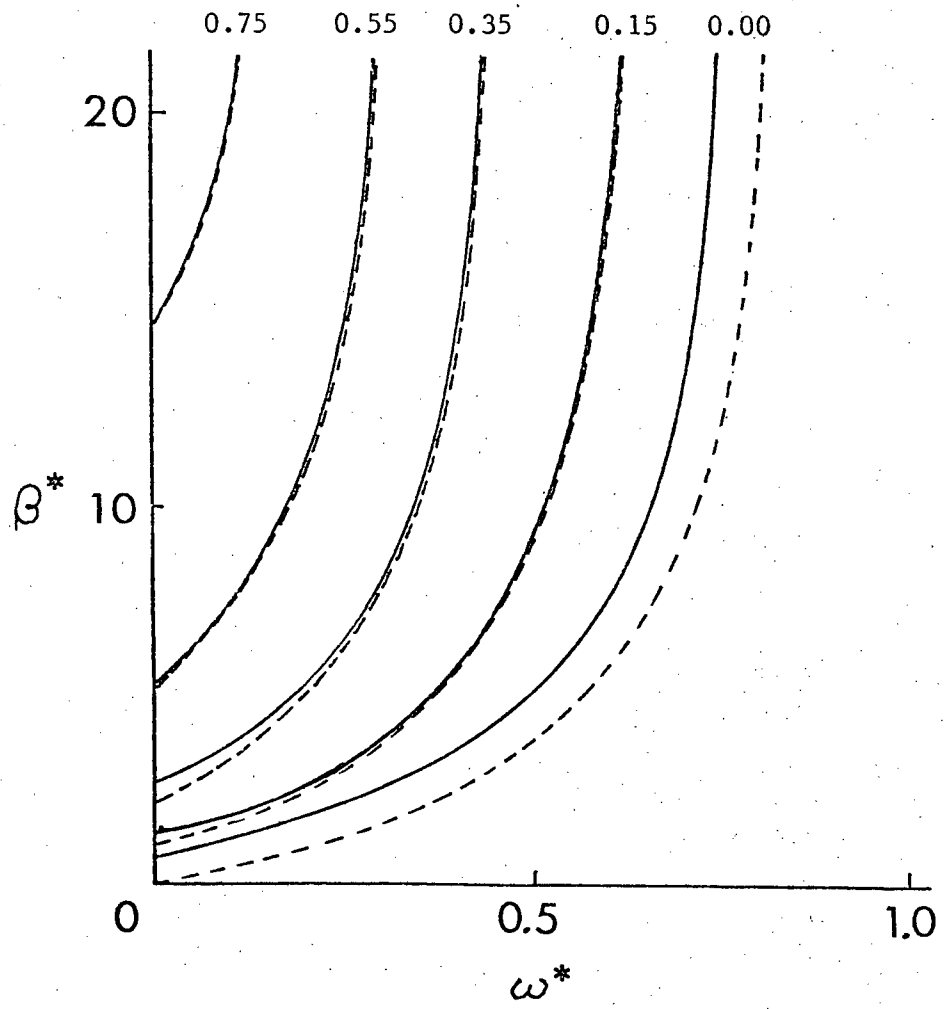

Figure 85. Contour plots of $\varphi_T - \varphi_c$ vs β^*, ω^* for δ^* = 0.1. Dashed line corresponds to θ = 1., solid line to θ = 0.1.

was simplified in the limit of a uniform mixed layer to that given in equation 7.12. The corresponding equation for δ_T, rewritten in terms of the new non-dimensional parameters defined above, is

$$a^*.\sinh(a^*.(\varphi_T-\varphi_M))+F.\cosh(a^*.(\varphi_T-\varphi_M)) \Big/ (\cosh(a^*.(\varphi_T-\varphi_M))+F.\sinh(a^*.(\varphi_T-\varphi_M)/a^*) + \beta^*.\Theta^{-0.5}.\exp(-\varphi_T).J_v'(\beta^*.\exp(-(\varphi_T-\varphi_c))) \Big/ J_v(\beta^*.\exp(-(\varphi_T-\varphi_c))) = 0 \qquad 7.19$$

where $F = \beta^*.\omega^* + \beta^{*2}.(1-U).\delta^*.\varphi_M$. In the cases of interest here, namely pronounced subsurface maxima with $P_T >> P(0)$ and $P_T \approx P_{MAX}$, it must be true that $a^*.(\varphi_T - \varphi_M) >> 1$, and the first term in 7.19 can be approximated by a^* as in equation 7.18. In these cases, the presence of the mixed layer has a negligible effect on the depth of nutrient depletion z_T, or on the phytoplankton profile below z_T. Its principal role is to allow the realistic use of a small diffusion rate or large value of in the region below the mixed layer and thereby to permit solutions with pronounced maxima. The high mixing rate within the mixed layer also prevents a decrease in P to unrealistically low levels at the surface, which can occur if a uniformly low diffusion coeffient is assumed.

The effect of introducing a nutrient-dependent sinking rate on the depth of nutrient-depletion can be seen in Fig 86 where contour plots of φ_T vs ω^* and β^* for $\delta^* = 0.1$, $\Theta = 0.1$ and $w_1/w = 1$ and 5 are given. It can be seen that the only marked

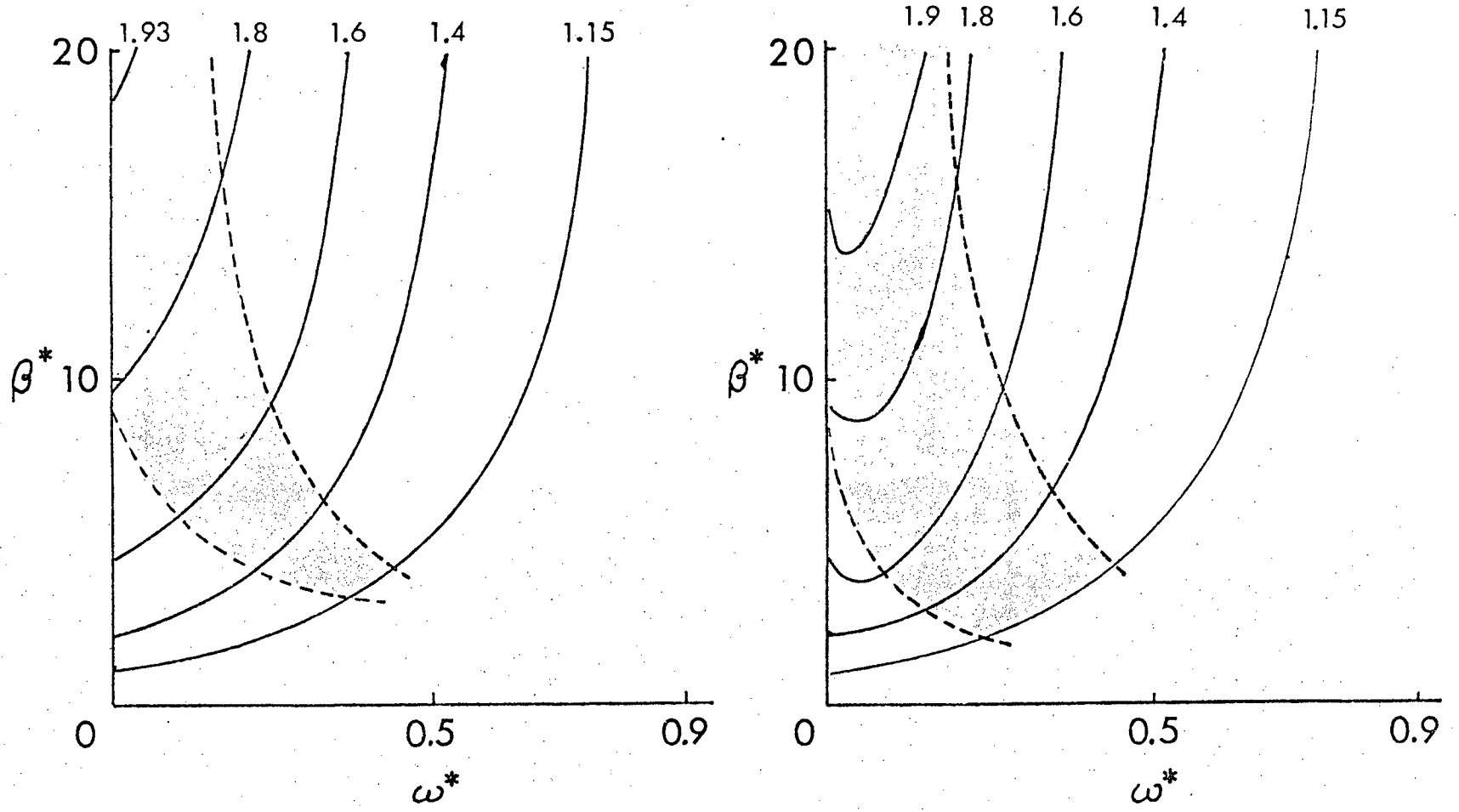

Figure 86. Contour plots of φ_T vs β^*, ω^* for $\delta^* = 0.1$, $\theta = 0.1$. (a) $w_1 = w$. (b) $w_1 = 5.w$.

effect on φ_T is a slight deepening of the nutrient-depleted zone at small values of ω. This is due to a more rapid reduction in P above z_T, so that a lower net production is required in the light-limited region to balance the net loss in the nutrient depleted zone. As before, the region in (ω^*, β^*) space corresponding to $P_T/P(0) > 20$ and $P_{MAX}/P_T < e$ has been indicated. This region, which corresponds to pronounced subsurface maxima of the 'nutrient trap' type, is extended to smaller values of ω^*, β^* by the introduction of a nutrient-dependent sinking rate. This result is not surprising as the greater sinking rate above $z=z_T$ means a rapid increase in P(z) with depth, thus increasing the ratio $P_T/P(0)$.

To conclude, a comparison between the assumptions and predictions of this theory and the numerical model of Jamart et al (1977) is presented. As noted in the introduction, two quite different approaches to modelling sub-surface maxima are involved. The intention here has been to provide qualitative insight into the roles of diffusion, sinking and growth in a general class of deep chlorophyll maxima, while Jamart et al attempted (quite successfully) to represent as accurately as possible the processes involved in the formation and maintenance of subsurface maxima in a particular, well-studied system. If their model is accepted as a faithful copy of reality, a comparison of the two treatments should reveal some of the limitations and strengths of the simpler analytic theory presented here.

The detailed numerical model incorporates many features of the biological and physical systems which have been neglected in

the simpler model. Two nutrient state variables, representing nitrate and ammonia, are defined there and comparatively complex submodels are used for the uptake and recycling of nutrients. The chemical composition (C:Chl a and C:N ratios) of the phytoplankton is allowed to vary and to affect the dependence of growth rate on nutrient concentration and light intensity. The diffusion coefficient and respiration and grazing losses all vary with depth and a grazing threshold is also employed. Finally, the numerical model is not analyzed for steady-state solutions. Instead, the development of the chlorophyll maximum is simulated over time and the importance of this to their results is stressed by Jamart et al (1977).

By comparison, the assumptions of the simple analytic model treated here seem rather crude and there may seem to be little point in comparing the predictions of the two models. Nonetheless, there are a number of reasons to hope for agreement in such a comparison. Jamart et al state of their simulation that : 'the net rates of change often represent a delicate balance between large contributions of opposite sign', which suggests that the numerical solution may be close to steady-state much of the time. Furthermore, at least in the case of pronounced deep chlorophyll maxima of the 'nutrient trap' type, the results presented here indicate that the depth of nutrient depletion and the phytoplankton profile are largely independent of the details of nutrient uptake kinetics, provided half-saturation constants for nutrient uptake are low enough. They depend primarily on the light-dependence of growth rate at low light intensities, the magnitude of grazing and respiration

losses in the vicinity of the chlorophyll maximum and diffusion and sinking rates in the same region, all of which may be represented fairly accurately in the simple model.

Inspection of Jamart et al 's Fig 10 shows that a pronounced deep chlorophyll maximum of the type studied here, with $P_{MAX} >> P(0)$, is predicted by the numerical simulation only towards the end of the simulated period (their Figure 10d). The parameters required for the simple model have been derived from their counterparts in the numerical model at this time. The diffusion rate below the mixed layer is 0.5 $cm^2.sec^{-1}$, the sinking rate in the presence of abundant nutrient is 0.5 $m.day^{-1}$, the extinction coefficient for light is 0.075 m^{-1} and the loss rate (dominated by grazing pressure) is approximately 0.2$\cdot day^{-1}$. The value corresponding to μ_s in the numerical model increases slowly with depth, and an intermediate value of 10 day^{-1} is used here. The resulting phytoplankton profile, as predicted by equations 7.9 and 7.11, is compared with the simulation result in Fig 87. The reasonable agreement supports the argument of the previous paragraph that the biologically simple model studied here captures the essential processes which affect the depth and shape of deep chlorophyll maxima of the 'nutrient trap' type.

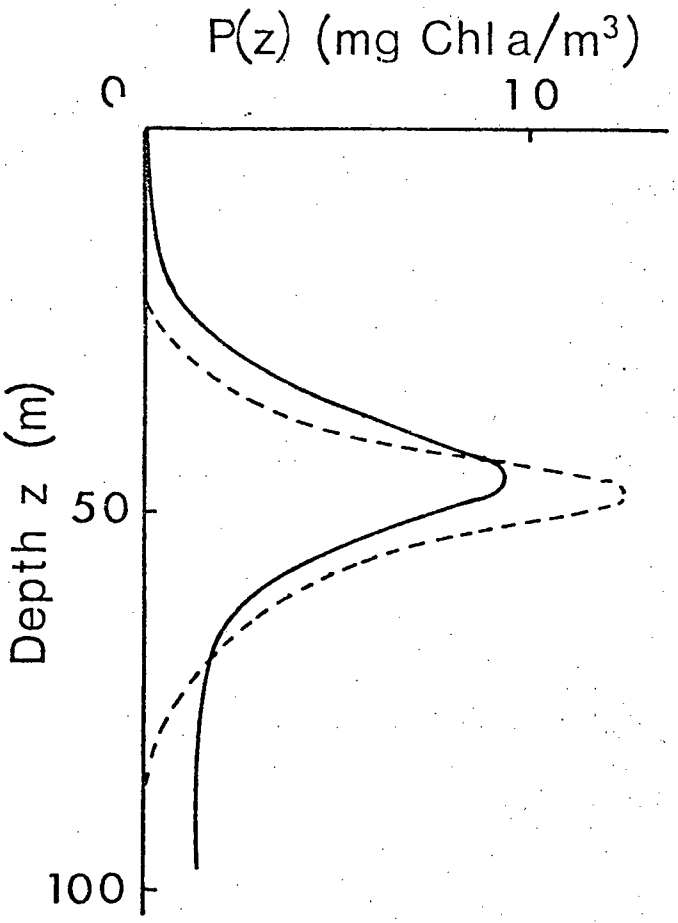

Figure 87. Comparison of phytoplankton profiles predicted by complex simulation model (solid line, from Fig 10d, Jassby et al, 1977) and by asymptotic analysis (dashed line).

CHAPTER 8

CONCLUDING REMARKS.

A rather diverse set of problems in theoretical marine ecology has been addressed in the preceding chapters. This short final chapter is not simply a summary of the contributions made in each problem area, chapter by chapter. A general approach to the problems of theoretical ecology which has been used throughout the thesis was outlined in the preface. An attempt is made here to assess the success or failure of this approach in each problem area.

The first aspect of the approach which was emphasized in the preface was the use of qualitative and approximate techniques to understand the behaviour of complex simulation models. Chapter 2 constitutes the most straightforward example of this approach and it may be worth repeating the principal conclusions of that chapter. An approximate analysis, based on separation of time scales, was applied to a complex simulation model taken from the literature. The importance of parameter interactions in determining model behaviour, and the consequent limitations of standard sensitivity analyses, were emphasized. Stable cyclic solutions under conditions of nutrient limitation in the absence of thresholds were discovered by using the qualitative analysis. (These were not found in previous numerical studies.) Their discovery allowed a distinction between problems associated with modelling the spring bloom transient and those associated with stability during the summer, which was not only of intrinsic interest, but also suggested a broader conceptual approach to the question of grazing response to low food concentrations.

The asymptotic analysis of Chapters 6 and 7 involved rather more sophisticated and complicated mathematics, although the underlying models were in many ways conceptually simpler. The aim in these chapters was more general: to understand the interplay of phytoplankton growth rates, respiration rates and sinking velocities and the environmental factors of light extinction coefficients, mixed layer depths, mixing rates above and below the thermocline and nutrient dynamics in determining phytoplankton vertical distribution and growth. The technique of non-dimensionalization served to reduce the parameter space to manageable dimensions. The specific numerical results, presented as contour plots, may be useful for quick assessment of particular real-world situations. The qualitative understanding of interactions which was achieved is perhaps more valuable. Examples include the dual role of diffusion when sinking is present, the roles of nutrient and light limitation in determining the depth and structure of the 'nutrient-trap' sub-surface maximum and the effects of changes in the ratio μ_S/μ_{MAX}, in the mixed layer depth and in the nutrient-dependence of sinking on the depth and shape of the sub-surface maximum. This qualitative understanding in turn makes it possible to find real-world situations where the simpler model provides a good approximation, as in the comparison with simulation model results in Chapter 7.

The role of qualitative analysis in the study of the O.S.P. ecosystem is not as clear because there are really two types of questions addressed there. There are mathematical questions of the type addressed in Chapters 2,6 and 7: to uncover

the possible range of behaviours of any particular model of the O.S.P. ecosystem. There are also biological questions concerning the correct assumptions for a model of the O.S.P. ecosystem. Given the present gaps in our biological knowledge, as discussed in Chapters 3 and 4, all the models discussed must be regarded as speculative. In these circumstances, the use of a combination of simple models in Chapter 1, and the insights into more complex models gained in Chapter 2, has allowed a larger number of possible models to be explored more fully than would have been possible with simulation alone. This modelling study of O.S.P., prompted by the consideration of the weathership time series, must be regarded as an intermediate step, valuable only to the extent that the biological questions raised are addressed by experimental or field studies.

The second aspect of the approach emphasized in the preface was the use of non-linear optimisation techniques to estimate biologically meaningful parameters in dynamic models from time series of observations. These techniques were used principally in Chapters 4 and 5. The statistical techniques used in Chapter 3 were more or less conventional, although to my knowledge the procedure used to separate seasonal and annual effects in 'gappy' data in Section 3.2 is original. In both Chapter 4 and Chapter 5, use of the systems-identification technique was hindered by deficiencies in the data. This raises the question of whether these estimation procedures are sufficiently robust to handle real-world data. In neither case were the data collected with parameter estimation in mind. Suggestions such as improving size class resolution and collecting deep samples are made in Chapter

4. If these are followed, time series will be produced which should allow much more reliable parameter estimates. The estimation problem considered in Chapter 5 is more ambitious and it may be that, at this level of complexity, rigorous and reliable parameter estimates will be possible only for data collected under the tightly controlled conditions of small-scale laboratory enclosures. However, its usefulness in Chapter 5 in ultimately addressing the biological questions of feeding thresholds, nutrient limitation and starvation mortality suggests that the technique, used less rigorously, may provide a valuable tool for the heuristic interpretation of field data.

BIBLIOGRAPHY

Anderson, G. C. 1969. Subsurface chlorophyll maximum in the north-east Pacific Ocean. Limnol. Oceanogr. 14: 386-391.

Anderson, G. C. 1972. Aspects of marine phytoplankton studies near the Columbia River, with special reference to a subsurface chlorophyll maximum. Pages 219-240 in A. T. Pruter and D. L. Alverson, ed. The Columbia River Estuary and Adjacent Ocean Waters: Bioenvironmental Studies. Univ. of Washington Press, Seattle.

Anderson, G. C., T. R. Parsons and K. Stephens. 1969. Nitrate distribution in the Subarctic North-east Pacific Ocean. Deep-Sea Res. 16: 329-334.

Antia, N. J., C. D. McAllister, T. R. Parsons, K. Stephens and J. D. H. Strickland. 1963. Further measurements of primary production using a large-volume plastic sphere. Limnol. Oceanogr. 8: 166-183.

Bannister, T. T. 1974. A general theory of steady-state phytoplankton growth in a nutrient-saturated mixed layer. Limnol. Oceanogr. 19: 13-30.

Bannister, T. T. 1979. Qualitative description of steady-state, nutrient-saturated algal growth, including adaptation. Limnol. Oceanogr. 24: 76-96.

Banse, K. 1974. On the interpretation of data for the carbon-to-nitrogen ratio of phytoplankton. Limnol. Oceanogr. 19: 695-699.

Barnes, H. 1952. The use of transformations in marine biological statistics. J. Cons. Int. Explor. Mer. 18: 61-71.

Bazykin, A. D. 1974. Structural and dynamical stability of model predator-prey systems. Publication R-3-R. Institute of Resource Ecology, Univ. of British Columbia.

Beardall, A. and I. Morris. 1976. The concept of light intensity adaptation in marine phytoplankton: some experiments with Phaeodactylum tricornatum. Mar. Biol. 37: 377-387.

Benson, M. W. 1978. Numerical parameter estimation in differential equations. Ph.D. Thesis. Univ. of British Columbia, Vancouver.

Brauer, F. and A. C. Soudack. 1979. Constant-rate stocking of predator-prey systems. M.R.C. Tech. Summ. Rept. 1962. Univ. of Wisconsin.

Buckingham, S. L. 1978. Functional responses and feeding strategies of fresh-water filter-feeding zooplankton. Ph. D. Thesis. Univ. of British Columbia, Vancouver.

Burris, J. E. 1977. Photosynthesis, photorespiration and dark respiration in eight species of algae. Mar. Biol. 30: 371-379.

Caperon, J. and J. Meyers. 1972. Nitrogen-limited growth of marine phytoplankton II. Uptake kinetics and their role in nutrient-limited growth of phytoplankton. Deep-Sea Res. 19: 619-632.

Chan, A. T. 1978. Comparative physiological study of marine diatoms and dinoflagellates in relation to irradiance and cell size. Ph. D. Thesis. Univ. of Washington, Seattle.

Checkley, D. M. (Jr). 1980. The egg production of a marine planktonic copepod in relation to its food supply: laboratory studies. Limnol. Oceanogr. 25: 430-446.

Cushing, D. H. 1959. The seasonal variation in oceanic production as a problem in population dynamics. J. Cons. Int. Explor. Mer. 24: 455-464.

Cushing, D. H. 1976. Biology of fish in the pelagic community. Pages 317-340 in D. H. Cushing and J. J. walsh, eds. Ecology of the Seas. W. B. Saunders Co., Toronto.

Denman, K. L. 1972. The response of the upper ocean to meteorological forcing. Ph. D. Thesis. Univ. of British Columbia, Vancouver.

Dodimead, A. J., F. Favorite and T. Hirano. 1963. Review of oceanography of the Subarctic Pacific region. Int. N. Pac. Fish. Comm. Bull. 13: 1-195.

Droop, M. R. 1977. An approach to quantitative nutrition of phytoplankton. J. Protozool. 24: 528-532.

Droop, M. R. and J. M. Scott. 1978. Steady-state energetics of a planktonic herbivore. J. Mar. Biol. Ass. U. K. 58: 749-772.

Eppley, R. W. 1972. Temperature and phytoplankton growth in the sea. Fish. Bull. 70: 1063-1085.

Eppley, R. W., E. H. Renger, E. L. Venrick and M. M. Mullin. 1973. A study of plankton dynamics and nutrient cycling in the central gyre of the North Pacific Ocean. Limnol. Oceanogr. 18: 534-551.

Evans, G. T. 1978. Biological effects of vertical-horizontal interactions. in J. H. Steele, ed. Spatial Pattern in Plankton Communities. Plenum Press.

Favorite, F., A. J. Dodimead and K. Nasu. 1976. Oceanography of the Subarctic Pacific region, 1960-71. Int N. Pac. Fish. Comm. Bull. 33: 1-187.

Frost, B. W. 1972. Effects of size and concentration of food particles on the feeding behaviour of the marine planktonic copepod Calanus helgolandicus. Limnol. Oceanogr. 17: 805-815.

Frost, B. W. 1975. A threshold feeding behaviour in Calanus pacificus. Limnol. Oceanogr. 20: 263-266.

Frost, B. W. 1979. The inadequacy of body size as an indicator of niche in the zooplankton. Preprint.

Frost, B. W. and L. E. McCrone. 1974. Vertical distribution of zooplankton and myctophid fish at Canadian Weather Station P with description of a new multiple net trawl. Proc. Int. Conf. Engineering Ocean. Envir., Inst Elect. Electron. Engineers.

Fulton, J. D. Laboratory zooplankton atlas for the Strait of Georgia. Laboratory Manual, Dept. Oceanography, Univ. of British Columbia, Vancouver.

Fulton, J. D. 1973. Some aspects of the life history of Calanus plumchrus in the Strait of Georgia. J. Fish. Res. Bd. Can. 30: 811-815.

Fulton, J. D. 1978. Seasonal and annual variations of net zooplankton at Ocean Station P, 1965-1976. Can. Fish. Mar. Serv. Data Rept. 49.

Goldman, J. C. and J. J. McCarthy. 1978. Steady-state growth and ammonium uptake of a fast-growing marine diatom. Limnol. Oceanogr. 23: 695-703.

Greenspan,H.P. 1969. Applied Mathematics at M.I.T.

Grice, D. G., M. R. Reeve, P. Koeller and D. W. Menzel. 1977. The use of large-volume (1300m^3) transparent, enclosed sea-surface

water columns in the study of stress on plankton ecosystems. Helgol. wiss Meer. 30: 118-133.

Hameedi, M. J. 1977. Changes in specific photosynthetic rate of oceanic phytoplankton from the North-east Pacific Ocean. Helgol. wiss. Meer. 30: 62-75.

Harbison, G. R. and V. L. McAlister. 1979. The filter-feeding rates and particle retention efficiencies of three species of Cyclosalpa (Tunicata, Thaliacea). Limnol. Oceanogr. 875-892.

Harris, R. P. and G. A. Paffenhoffer. 1976. Feeding, growth and reproduction of the marine planktonic copepod Temora longicornis muller. J. Mar. Biol. Ass. U.K. 56: 675-690.

Harris, R. P., M. R. Reeve, G. D. Grice, G. T. Evans, V. R. Gibson, J. R. Beers and B. K. Sullivan. 1980. Trophic interactions and production processes in natural zooplankton communities in enclosed water columns. in Symposium on Enclosed Marine Experimental Ecosystems (in press).

Harris, G. P. and B. B. Piccinin. 1977. Photosynthesis by natural populations. Arch. Hydrobiol. 80: 405-457.

Heath, W. A. 1977. The ecology and harvesting of euphausiids in the Strait of Georgia. Ph. D. Thesis. Univ. of British Columbia, Vancouver.

Heinrich, A. K. 1962. The life histories of plankton animals and seasonal cycles of plankton communities in the oceans. J. Cons. Int. Explor. Mer. 27: 15-24.

Hilborn, R. 1975. The effect of spatial heterogeneity on the persistence of predator-prey interactions. Theor. Pop. Biol. 8: 346-355.

Hobson, L. A. and C. J. Lorenzen. 1972. Relationships of chlorophyll maxima to density structure in the Atlantic Ocean and Gulf of Mexico. Deep-Sea Res. 19: 297-306.

Holling, C. S. 1959. The components of predation as revealed by a study of small-mammal predation of the European pine sawfly. The Can. Entomol. 91: 293-320.

Holling, C. S. 1965. The functional response of predators to prey density and its role in mimicry and population regulation. Mem. Entomol. Soc. Can. 45: 1-60.

Ichikawa, T. and S. Nishizawa. 1975. Particulate organic carbon and nitrogen in the eastern Pacific Ocean. Mar. Biol. 29: 129-138.

Ikeda, T. 1972. Chemical composition and nutrition of zooplankton in the Bering Sea. Pages 433-442 in A. Y. Takenouti, ed. Biological Oceanography of the Northern North Pacific Ocean. Idemitsu Shoten, Tokyo.

Ikeda, T. 1976. The effect of laboratory conditions on the extrapolation of experimental measurements to the ecology of marine zooplankton. I Effect of feeding condition on the respiration rate. Bull. Plankton Soc. Jap. 23: 1-10.

Ikeda, T. 1977. The effect of laboratory conditions on the extrapolation of experimental measurements to the ecology of marine zooplankton. IV Changes in respiration and excretion rates of boreal zooplankton species maintained under fed and starved conditions. Mar. Biol. 41: 241-252.

Ishimaru, T. and T. Nemoto. 1977. Distribution of phytoplankton. Pages 76-77 in A. Hattori, ed. Preliminary Report of the Hakuho Maru Cruise KH-75-4. Ocean. Res. Inst., Univ. of Tokyo.

Jamart, B. M., D. F. Winter, K. Banse, G. C. Anderson and R. K. Lam. 1977. A theoretical study of phytoplankton growth and nutrient distribution in the Pacific Ocean off the North-western U.S. coast. Deep-Sea Res. 24: 733-773.

Jassby, A. D. and T. Platt. 1976. Mathematical formulation of the relationship between photosynthesis and light for phytoplankton. Limnol. Oceanogr. 21: 540-547.

Jerlov, N. G. 1968. Optical Oceanography. Elsevier, N.Y. 194 pp.

Jorgansen, E. G. 1969. The adaptation of plankton algae IV light adaptation in different algal species. Physiol. Plant. 22: 1307-

1315.

Kendall, M. G. 1973. Time-series. Griffin, London. 197pp.

Kierstead, H. and L. B. Slobodkin. 1953. The size of water masses containing plankton blooms. J. Mar. Res. 12: 141-147.

Kopell, N. and L. N. Howard. 1973. Plane wave solutions to reaction-diffusion equations. Studies in Appl. Math. 52: 291-328.

Krause, E.P. and A. G. Lewis. 1979. Ontogenetic migration and the distribution of Eucalanus bungi (Copepoda; Calanoida) in British Columbia inlets. Can. J. Zool. 57: 2211-2222.

Kuhn, T. S. 1970. The Structure of Scientific Revolutions. 2nd ed. Univ. of Chicago Press, Chicago. 210pp.

Lam, R. K. and B. W. Frost. 1976. Model of copepod filtering responses to changes in size and concentration of food. Limnol. Oceanogr. 21: 490-500.

Landry, M. R. 1976. The structure of marine ecosystems: an alternative. Mar. Biol. 35: 1-7.

Lawson, T. J. and G. D. Grice. 1977. Zooplankton sampling variability: controlled ecosystem pollution experiments. Bull. Mar. Sci. 27: 80-84.

LeBrasseur, R. J. 1965. Seasonal and annual variations of net zooplankton at Ocean Station P 1956-64. Fish. Res. Bd. Can. Manuscr. Rept. Ser. (Oceanogr. Limnol.) 202 153pp.

LeBrasseur, R. J. 1969. Predator-prey relationships in the epipelagic zone of the North-East Pacific Ocean. Ph. D. THesis. Univ of Glasgow.

LeBrasseur, R. J. and O. D. Kennedy. 1972. Microzooplankton in coastal and oceanic areas of the Pacific Subarctic water mass: a preliminary report. Pages 355-366 in A. Y. Takenouti, ed. Biological Oceanography of the Northern North Pacific Ocean. Idemitsu Shoten, Tokyo.

Lorenzen, M. W. 1980. Use of chlorophyll-Secchi disk relationships. Limnol. Oceanogr. 25: 371-372.

Lotka, A. J. 1925. Elements of physical biology. Williams and Morris, Baltimore. (Reissued as Elements of Mathematical Biology by Dover, 1956.)

Ludwig, D., D. D. Jones and C. S. Holling. 1978. Qualitative analysis of insect outbreak systems: the spruce budworm and forest. J. Anim. Ecol. 47: 315-332.

McAllister, C. D. 1961. Zooplankton studies at Ocean Weather Station 'P' in the North-east Pacific Ocean. J. Fish. Res. Bd. Can. 18: 1-29.

McAllister, C. D. 1963. Measurements of diurnal variation in productivity at Ocean Station P. Limnol. Oceanogr. 8: 289-292.

McAllister, C. D. 1969. Aspects of estimating zooplankton production from phytoplankton. J. Fish. Res. Bd. Can. 26: 199-220.

McAllister, C. D. 1972. Estimates of the transfer of primary production to secondary production at Ocean Station P. Pages 575-580 in A. Y. Takenouti, ed. Biological Oceanography of the Northern North Pacific Ocean. Idemitsu Shoten, Tokyo.

McAllister, C. D., T. R. Parsons and J. D. H. Strickland. 1960. Primary productivity at Station 'P' in the North-east Pacific Ocean. J. Cons. Int. Explor. Mer. 25: 240-259.

Madin, L. P. 1974. Field observations on the feeding behaviour of salps (Tunicata: Thaliacea). Mar. Biol. 25: 143-148.

Manly, B. F. J. 1974. Estimation of stage-specific survival rates and other parameters for insect populations developing through several stages. Oecologia 15: 277-285.

Marlowe, C. J. and C. B. Miller. 1975. Patterns of vertical distribution and migration of zooplankton at Ocean Station 'P'. Limnol. Oceanogr. 20: 824-844.

Marquardt, D. W. 1963. An algorithm for least-squares estimation

of non-linear parameters. J. Soc. Indust. Appl. Math. 11: 431-441.

Marra, J. 1978a. Effect of short-term variations in light intensity on photosynthesis of a marine phytoplankter: a laboratory study. Mar. Biol. 46: 191-202.

Marra, J. 1978b. Phytoplankton photosynthetic response to vertical movement in a mixed layer. Mar. Biol. 46: 203-208.

Marshall, S. M. 1973. Respiration and feeding in copepods. Adv. Mar. Biol. 11: 57-120.

May, R. M. 1974. Stability and complexity in model ecosystems. 2nd ed. Princeton Univ. Press, Princeton.

May, R. M. 1975. Biological populations obeying difference equations: stable points, stable cycles and chaos. J. Theor. Biol. 49: 511-524.

Mayzaud, P. and S. A. Poulet. 1978. The importance of the time factor in the trophic relationships between herbivorous copepods and naturally-occurring particulate matter. Limnol. Oceanogr. 23: 1144-1154.

McCarthy, J. J. and J. C. Goldman. 1979. Nitrogenous nutrition of marine phytoplankton in nutrient-depleted waters. Science 203: 670-672.

Megard, R. O., J. C. Settles, H. A. Boyer and W. S. Combs, Jr. 1980. Light, Secchi disks and trophic states. Limnol. Oceanogr. 25: 373-377.

Menzel, D. W. 1974. Primary productivity, dissolved and particulate organic matter and the sites of oxidation of organic matter. in E. G. Goldberg, ed. The Sea, Vol 6. Wiley, N.Y.

Miyake, M. 1979. Oceanographic observations at stations along the triangular grids during the mixed layer experiment August 1, 1978. Vol 84c. Pac. Mar. Sci. Rept. 79-2 191pp.

Monthly Radiation Summary. Can. Meteorol. Branch, Toronto.

Mosteller, F. and J. W. Tukey. 1977. Data Analysis and Regression. A Second Course in Statistics. Addison-Wesley, Reading. 588pp.

Mullin, M. M., P. R. Sloan and R. W. Eppley. 1966. Relationship between carbon content, cell volume and area in phytoplankton. Limnol. Oceanogr. 11: 307-311.

Mullin, M. M. and E. R. Brooks. 1970a. The effect of concentration of food on body weight, cumulative ingestion, and rate of growth of the marine copepod Calanus helgolandicus. Limnol. Oceanogr. 15: 748-755.

Mullin, M. M. and E. R. Brooks. 1970b. Growth and metabolism of

two planktonic copepods as influenced by temperature and type of food. Pages 74-95 in J. H. Steele, ed. Marine Food Chains. Oliver and Boyd, Edinburgh.

Mullin, M. M., E. F. Stewart and F. J. Fuglister. 1975. Ingestion by planktonic grazers as a function of concentration of food. Limnol. Oceanogr. 20: 259-262.

Myers, J. and J. Graham. 1971. The photosynthetic unit in Chlorella measured by repetitive short flashes. Plant. Physiol. 48: 282-286.

Nemoto, T. 1957. Foods of baleen whales in the N. Pacific. Sci. Repts. Whale Res. Inst. 12: 33-89.

Osborn, T. R. 1980. Estimates of the local rate of vertical diffusion from dissipation measurements. J. Phys. Oceanogr. 10: 83-89.

Paffenhoffer, G. A. 1970. Cultivation of Calanus helgolandicus under controlled conditions. Helgol. wiss Meer. 20: 346-359.

Paffenhoffer, G. A. 1971. Grazing and ingestion rates of nauplii, copepodids and adults of the marine planktonic copepod, Calanus helgolandicus. Mar. Biol. 11: 286-298.

Paffenhoffer, G. A. 1976. Feeding, growth and food conversion of the marine planktonic copepod Calanus helgolandicus. Limnol.

Oceanogr. 21: 39-50.

Paffenhoffer, G. A. and R. P. Harris. 1976. Feeding, growth and reproduction of the marine planktonic copepod Pseudocalanus elongatus boeck. J. Mar. Biol. Ass. U. K. 56: 327-344.

Paffenhoffer, G. A. and Harris, R. P. 1979. Laboratory culture of marine holozooplankton and its contribution to studies of marine planktonic food webs. Adv. Mar. Biol. 16: 211-308.

Parslow, J., N. C. Sonntag, and J. B. L. Matthews. 1979. Technique of systems identification applied to estimating copepod population parameters. J. Plankton Res. 1: 137-151.

Parsons, T. R. 1965. A general description of some factors governing primary production in the Strait of Georgia, Hecate Strait and Queen Charlotte Sound, and the N. E. Pacific Ocean. Fish. Res. Bd. Can. Manuscr. Rept. Ser. (Oceanogr. Limnol.) 198.

Parsons, T. R. 1972. Size fractionation of primary producers in the Subarctic Pacific Ocean. Pages 275-278 in A. Y. Takenouti, ed. Biological Oceanography of the Northern North Pacific Ocean. Idemitsu Shoten, Tokyo.

Parsons, T. R., R. J. LeBrasseur and J. D. Fulton. 1967. Some observations of the dependence of zooplankton grazing on the cell size and concentration of phytoplankton blooms. J Oceanogr. Soc. Japan. 23: 10-17.

Parsons, T. R. and R. J. LeBrasseur. 1968. A discussion of some critical indices of primary and secondary production for large-scale ocean surveys. Calif. Mar. Res. Comm. CalCOFI Rept. 12: 54-63.

Parsons, T. R., R. J. LeBrasseur, J. D. Fulton and O. D. Kennedy. 1969. Production studies in the Strait of Georgia II. Secondary production under the Fraser River plume, February to May, 1967. J. Exp. Mar. Biol. Ecol. 3: 39-50.

Parsons, T. R. and G. C. Anderson. 1970. Large-scale studies of primary production in the North Pacific Ocean. Deep-Sea Res. 17: 765-776.

Parsons, T. R. and M. Takahashi, M. 1973. Environmental control of phytoplankton cell size. Limnol. Oceanogr. 18: 511-515.

Parsons, T. R., M. Takahashi and B. Hargreaves. 1977. Biological Oceanographic Processes. 2nd ed. Pergamon Press. 332pp.

Parsons, T. R. and P. J. Harrison. 1981. Nutrient cycling in aquatic ecosystems. Marine environments. in W. H. Ruhland, ed. Encyclopaedia of Plant Physiology (New Series) Vol. C. Springer-Verlag, Heidelburg.

Platt, T. 1972. Local phytoplankton abundance and turbulence. Deep-Sea Res. 19: 183-187.

Platt, T., K. L. Denman and A. D. Jassby. 1975. The mathematical representation and prediction of phytoplankton productivity. Can. Fish. Mar. Serv. Res. Dev. Tech. Rept. 523. 110 pp.

Poulet, S. A. 1973. Grazing of Pseudocalanus minutus on naturally-occurring particulate matter. Limnol. Oceanogr. 18: 564-572.

Riley, G. A., H. Stommel and D. F. Bumpus. 1949. Quantitative ecology of the plankton of the western North Atlantic. Bull. Bingham Oceanogr. Coll. 12: 1-169.

Runge, J. A. 1980. Effects of hunger and season on the feeding behaviour of Calanus pacificus. Limnol. Oceanogr. 25: 134-145.

Ryther, J. H. 1956. The measurement of primary production. Limnol. Oceanogr. 1: 72-84.

Saijo, Y. 1973. The formation of the chlorophyll maximum in the Indian Ocean. Pages 171-173 in B. Zeitzschel and S. A. Gerlach, eds. The Biology of the Indian Ocean. Springer-Verlag, Heidelburg.

Sanger, G. A. 1972. Fisheries potentials and estimated biological productivity of the Subarctic Pacific region. in A. Y. Takenouti, ed. Biological Oceanography of the Northern North Pacific Ocean. Idemitsu Shoten, Tokyo.

Segel, L. A. and J. L. Jackson. 1972. Dissipative structure: an explanation and an ecological example. J. Theor. Biol. 37: 545-559.

Sekiguchi, H. 1975. Seasonal and ontogenetic vertical migrations in some common copepods in the northern region of the North Pacific. Bull. Fac. Fish., Mie Univ. 2: 29-38.

Semina, H. J. 1958. Types of areas in the neritic zone in the boreal region of the Pacific. C. R. Acad. Sci. U.R.S.S. 118: 1194-1196. (quoted from Heinrich, 1962).

Semina, H. J. 1960. The influence of vertical circulation on the phytoplankton in the Bering Sea. Int. Rev. Hydrobiol. 45: 1-10.

Smayda, T. J. 1970. The suspension and sinking of phytoplankton in the sea. Oceanogr. Mar. Biol. Ann. Rev. 8: 353-414.

Smayda, T. J. and B. Mitchell-Innes. 1974. Dark survival of autotrophic, planktonic marine diatoms. Mar. Biol. 25: 195-202.

Smetacek, V., B. Von Bodungen, B. Knoppers, H. Neubert, F. Pollehne and B. Zeitzschel. 1980. Shipboard experiments on the effect of vertical mixing on natural plankton populations in the central Baltic Sea. Ophelia. (in press).

Sommerfeld, A. 1949. Partial differential equations in physics. Academic Press,N.Y. 335pp.

Sonntag, N. C. and W. Greve. 1977. Investigation of the impact of mercury on enclosed water columns using a zooplankton simulation model. J. Fish. Res. Bd. Can. 34: 2295-2307.

Sonntag, N. C. and T. R. Parsons. 1979. Mixing an enclosed 1300m³ water column: effects on the planktonic food web. J. Plankton Res. 1: 85-102.

Sonntag, N. C. and J. Parslow. 1980. Technique of systems identification applied to estimating copepod production. (submitted manuscr.)

Steele, J. H. 1962. Environmental control of photosynthesis in the sea. Limnol. Oceanogr. 7: 137-150.

Steele, J. H. 1964. A study of production in the Gulf of Mexico. J. Mar. Res. 22: 211-221.

Steele, J. H. 1974a. The Structure of Marine Ecosystems. Harvard Univ. Press, Cambridge. 128pp.

Steele, J. H. 1974b. Stability of plankton ecosystems. Pages 179-191 in M. B. Usher and M. H. Williamson, eds. Ecological Stability. Chapman and Hall.

Steele, J. H. 1976a. The role of predation in ecosystem models. Mar. Biol. 35: 9-11.

Steele, J. H. 1976b. Patchiness. Pages 98-115 in D. H. Cushing and J. J. Walsh, eds. The Ecology of the Seas. W. B. Saunders Co., Philadelphia.

Steele, J. H. and C. S. Yentsch. 1960. The vertical distribution of chlorophyll. J. Mar. Biol. Ass. U. K. 39: 217-226.

Steele, J. H. and I. E. Baird. 1961. Relations between primary production, chlorophyll and particulate carbon. Limnol. Oceanogr. 6: 68-78.

Steele, J. H. and D. W. Menzel. 1962. Conditions for maximum primary production in the mixed layer. Deep-Sea Res. 9: 39-49.

Steele, J. H. and M. M. Mullin. 1977. Zooplankton Dynamics. Pages 857-890 in E. D. Goldberg, I. n. McCave, J. J. O'Brien and J. H. Steele, eds. The Sea Vol 6 Marine Modelling. Wiley-Interscience, N.Y.

Steele, J. H. and B. W. Frost. 1977. The structure of plankton communities. Phil. Trans. Roy. Soc. London. B. 280: 485-534.

Steele, J. H., D. M. Farmer and E. W. Henderson. 1977. Circulation and temperature structure in large marine enclosures. J. Fish. Res. Bd. Can. 34: 1095-1104.

Steeman Nielson, E. 1975. Marine Photosynthesis: with special emphasis on the ecological aspects. Elsevier, N. Y. 141pp.

Steeman Nielsen, E. and T. S. Park. 1964. On the time course in adapting to low light intensities in marine phytoplankton. J. Cons. Int. Explor. Mer. 29: 19-24.

Stephens, K. 1966. Primary production data from the N. E. Pacific Ocean January 1964 to December 1965. Fish. Res. Bd. Can. Manuscr. Rept. Ser. (Oceanogr. and Limnol.) 209.

Stephens, K. 1968. Primary production data from the N. E. Pacific Ocean January 1966 to December 1967. Fish. Res. Bd. Can. Manuscr. Rept. Ser. 957.

Stephens, K. 1970. Primary production data from the N. E. Pacific Ocean January 1968 to December 1969. Fish. Res. Bd. Can. Manuscr. Rept. Ser. 1123.

Stephens, K. 1977. Primary productivity data from weatherships occupying Ocean Station 'P' 1969 to 1975. Can. Fish. Mar. Serv. Data Rept. 38.

Sullivan, B. K. 1980. In situ feeding behaviour of Sagitta elegans and Eukrohnia hamata (Chaetognatha) in relation to the vertical distribution of prey at Ocean Station 'P'. Limnol. Oceanogr. 25: 317-326.

Sverdrup, H. U. 1953. On conditions for the vernal blooming of phytoplankton. J. Cons. Int. Explor. Mer. 18: 287-295.

Tabata, S. 1965. Variability of oceanographic conditions at Ocean Station 'P' in the N. E. Pacific Ocean. Trans. Roy. Soc. Can. Ser. IV. 3: 367-418.

Taguchi, S. and H. Ishii. 1972. Shipboard experiments on respiration, excretion and grazing of Calanus cristatus and C. plumchrus (Copepoda) in the northern North Pacific. Pages 419-432 in A. Y. Takenouti, ed. Biological Oceanography of the Northern North Pacific Ocean, Idemitsu Shoten, Tokyo.

Takahashi, M. and T. R. Parsons. 1972. Maximization of the standing stock and primary productivity of marine phytoplankton under natural conditions. Indian J. Mar. Sci. 1: 61-62.

Taylor, F. J. R. and R. E. Waters. 1980. Spring phytoplankton in the Subarctic Pacific Ocean. Mar. Biol. (in press).

Turing, A. M. 1972. The chemical basis of morphogenesis. Phil. Trans. Roy. Soc. London. B. 237: 37-72.

Turpin, D. 1980. Processes in nutrient based phytoplankton ecology. Ph. D. Thesis. Univ of British Columbia, Vancouver.

Turpin, D., Harrison, P. and J. Parslow. 1980. On limiting nutrient- patchiness and phytoplankton growth - a conceptual approach. (Submitted manuscript.)

Venrick, E. L. 1971. Recurrent groups of diatom species in the N.

Pacific. Ecology 52: 614-625.

Venrick, E. L., J. A. McGowan and A. W. Mantyla. 1973. Deep maxima of photosynthetic chlorophyll in the Pacific Ocean. Fish. Bull. 71: 41-52.

Vinogradov, M. E. 1968. Vertical distribution of the oceanic zooplankton. Nauka House, Moscow. (Russian.) Israel Program for Sci. Transl., Jerusalem, 1970.

Weizenbaum, J. 1976. Computer Power and Human Reason. W. H. Freeman Co., N. Y. 300pp.

Wickett, P. W. 1967. Ekman transport and zooplankton concentration in the North Pacific Ocean. J. Fish. Res. Bd. Can. 24: 581-594.

Winberg, G. C. 1968. Methods for the estimation of production of aquatic animals. (transl. by A. Duncan, 1971.) Adv. Ecol. Res. Acad. Press, London. 175pp.

Winter, D. F., K. Banse and G. C. Anderson. 1975. The dynamics of phytoplankton blooms in Puget sOund, a fjord in the northwestern United States. Mar. Biol. 29: 139-176.

Wrobleski, J. S. 1977. A model of phytoplankton plume formation during variable Oregon upwelling. J. Mar. Res. 35: 357-394.

Yentsch, C. S. and Ryther, J. H. 1957. Short-term variations in phytoplankton chlorophyll and their significance. Limnol. Oceanogr. 2: 140-142.